Last Compiled November 28, 2021

The Soft-Collinear Effective Theory

Christian W. Bauer (LBL) and Iain W. Stewart (MIT)

TASI Lecture Notes 2013 and 2014

&

Iain W. Stewart (MIT)

EFT course 8.851 and edX course 8.EFTx
SCET Lecture Notes
2013

(The original version of these notes were typeset by Mobolaji Williams.)

PDF version:
http://courses.edx.org/c4x/MITx/8.EFTx/asset/notes_scetnotes.pdf

Abstract

Contents

1 Lecture Notes Introduction **5**

2 Introduction to SCET **6**
2.1 What is SCET? . . . 6
2.2 Light-Cone Coordinates . . . 7
2.3 Momentum Regions: SCET I and SCET II . . . 9

3 Ingredients for SCET **15**
3.1 Collinear Spinors . . . 15
3.2 Collinear Fermion Propagator and ξ_n Power Counting . . . 18
3.3 Power Counting for Collinear Gluons and Ultrasoft Fields . . . 18
3.4 Collinear Wilson Line, a first look . . . 19

4 SCET Lagrangian **22**
4.1 $\mathrm{SCET_I}$ Quark Lagrangian . . . 22
4.2 Wilson Line Identities . . . 31
4.3 $\mathrm{SCET_I}$ Collinear Gluon and Ultrasoft Lagrangians . . . 32
4.4 Feynman Rules for Collinear Quarks and Gluons . . . 33
4.5 $\mathrm{SCET_{II}}$ Lagrangian . . . 34
4.6 Rules for Combining Label and Residual Momenta in Amplitudes . . . 35

5 Symmetries of SCET **39**
5.1 Spin Symmetry . . . 39
5.2 Gauge Symmetry . . . 40
5.3 Reparamterization Invariance . . . 43
5.4 Discrete Symmetries . . . 46
5.5 Extension to Multiple Collinear Directions . . . 47

6 Factorization from Mode Separation **48**
6.1 Ultrasoft-Collinear Factorization . . . 48
6.2 Wilson Coefficients and Hard Factorization . . . 51
6.3 Soft-Collinear Factorization . . . 52
6.4 Mixed, hard, collinear and soft factorization **[Strong overlap]** . . . 54
6.5 Operator Building Blocks . . . 57
6.6 Helicity Operator Building Blocks . . . 59
6.7 Convolutions in $\mathrm{SCET_I}$ and $\mathrm{SCET_{II}}$ **[First Pass]** . . . 62

7 Wilson Coefficients and Hard Dynamics **62**
7.1 $b \to s\gamma$, SCET Loops and Divergences . . . 63
7.2 $e^+e^- \to$ 2-jets, SCET Loops . . . 69
7.3 Summing Sudakov Logarithms . . . 73
7.4 RGE solution to higher orders . . . 76

8 Power correction in SCET **78**
8.1 Power Counting Formula for $\mathrm{SCET_I}$ **[Needs Cutting down]** . . . 78

8.2 Power Suppressed SCET_I Lagrangians [**Check Words, Add Ghosts**] . . . 81
8.3 Power Counting Formula for SCET_II [**Empty**] . . . 83

9 SCET for e^+e^- Collider Observables **83**
9.1 Kinematics, Expansions, and Regions . . . 83
9.2 Factorization: Hard, Jet and Soft functions [**fix notation**] . . . 84
9.3 Perturbative Results [**fix notation**] . . . 87
9.4 Results with Resummation . . . 88

10 Deep Inelastic Scattering [Draft Needs Work] **89**
10.1 DIS Factorization: Hard and Parton Distributions . . . 89
10.2 Renormalization of PDF . . . 94

11 SCET for pp Collider Observables [Needs Lots of Work] **96**
11.1 Kinematics . . . 96
11.2 Inclusvive Drell-Yan: $pp \to Xl^+l^-$ . . . 97
11.3 Threshold Drell-Yan: $pp \to Xl^+l^-$ . . . 97
11.4 Beam thrust in Drell-Yan: $pp \to Xl^+l^-$ . . . 98
11.5 pp Jet Factorization:: Hard, Beam, Jet, Soft Functions . . . 99

12 More SCET_I Applications (Remove) **99**
12.1 $B \to X_s\gamma$ [**Remove?**] . . . 99

13 SCET II **101**
13.1 Deriving SCET_II operators by using SCET_I . . . 101
13.2 Rapidity Divergences [**EMPTY**] . . . 102

14 SCET_II Applications **102**
14.1 $\gamma^*\gamma \to \pi^0$ [**Remove?**] . . . 102
14.2 $B \to D\pi$ [**Needs Work**] . . . 102
14.3 Massive Gauge Boson Form Factor & Rapidity Divergences [**Empty**] . . . 104
14.4 p_T Distribution for Higgs Production & Jet Broadening [**Remove**] . . . 104

A $\mathcal{L}_{\text{SCET}}$ and SCET Feynman rules **105**
A.1 Summary of Notation for Derivatives . . . 105
A.2 Massless and Massive SCET at Leading Power . . . 105
A.3 Massless SCET at Subleading Power . . . 107
A.4 Subleading Heavy-to-Light Currents . . . 109

B Wilson line Identities and Feynman Rules **112**

C Mathematical Identities **114**
C.1 Loop Integral Formula . . . 114
C.1.1 Loop Integral Tricks . . . 114
C.1.2 Parameter Integrals . . . 115
C.1.3 d-dimensional Integrals . . . 115
C.2 One Loop SCET Integrals . . . 116
C.3 Useful Function Identities . . . 116
C.4 Convolution identities . . . 117

C.5 Laplace transform Identities . . . 119
C.6 Plus functions from Imaginary parts . . . 120

D QCD Summary **121**
D.1 Fields and Feynman Rules . . . 121
D.2 QCD β-Function . . . 122
D.3 QCD Cusp Anomalous Dimensions . . . 122

E General All-Orders Resummation Formula **123**
E.1 Simple multiplicative RGE . . . 123
E.2 RGE with a Convolution . . . 124

F Hard, Jet, Beam, and Soft Functions **125**
F.1 Hard Functions, q and g Form Factors . . . 126
F.2 Jet Function . . . 129
F.3 b-quark Shape Function . . . 133
F.3.1 Shape Function at Fixed Order . . . 133
F.3.2 Shape Function RGE . . . 133
F.4 Hemisphere Soft function . . . 133
F.5 Beam Functions . . . 135
F.6 Parton Distribution Function . . . 139
F.7 Convolution of Soft and Jet Functions . . . 141

G More on the Zero-Bin [Remove?] **142**
G.1 0-bin subtractions with a 0-bin field Redefinition . . . 142
G.2 0-bin subtractions for phase space integrations . . . 142

H Spinor Relations with a different representation **143**

1 Lecture Notes Introduction

These notes provide reading material on the Soft-Collinear Effective Theory (SCET). They are intended to cover the material studied in the second half of my effective field theory graduate course at MIT. A complete hand written version of the notes I used when teaching this course in 2013 can be found at:

http://http://www2.lns.mit.edu/$\tilde{\text{i}}$ains/talks/SCET_Lectures_Stewart_2013.pdf

These latex notes will also appear as part of TASI lecture notes and a review article with Christian Bauer.

Familiarity will be assumed with various basic effective field theory (EFT) concepts, including power counting with operator dimensions, the use of field redefinitions, and top-down effective theories. Also the use of dimensional regularization for scale separation, the equivalences and differences with Wilsonian effective field theory, and the steps required to carry out matching computations for Wilson coefficients. A basic familiarity with heavy quark effective theory (HQET), the theory of static sources, is also assumed. In particular, familiarity with HQET as an example of a top-down EFT where we simultaneously study perturbative corrections and power corrections, and for understanding reparameterization invariance. These topics were covered in the first half of the EFT course.

A basic familiarity with QCD as a gauge theory will also be assumed. Given that SCET is a top-down EFT, we can derive it directly from expanding QCD and integrating out offshell degrees of freedom. This familiarity should include concepts like the fact that energetic quarks and gluons form jets, renormalization and renormalization group evolution for nonabelian gauge theory, and color algebra. Also some basic familiarity with the role of infrared divergences is assumed, namely how they cancel between virtual and real emission diagrams, and how they otherwise signal the presence of nonperturbative physics and the scale $\Lambda_{\rm QCD}$ as they do for parton distribution functions.

Finally it should be remarked that later parts of the notes are still a work in progress (particularly sections marked at the start as ROUGH which being around chapter 8). This file will be updated as more parts become available. Please let me know if you spot typos in any of chapters 1-7. The notes also do not yet contain a complete set of references. Some of the most frequent references I used for preparing various topics include:

1. Degrees of freedom, scales, spinors and propagators, power counting: [1, 2, 3]
2. Construction of $\mathcal{L}_{\rm SCET}$, currents, multipole expansion, label operators, zero-bin, infrared divergences: [2, 4, 5]
3. $\rm SCET_I$, Gauge symmetry, reparameterization invariance: [4, 6, 7]
4. Ultrasoft-Collinear factorization, Hard-Collinear factorization, matching & running for hard functions: [1, 2, 4, 6]
5. DIS, SCET power counting reduces to twist, renormalization with convolutions: [8, 9]
6. $\rm SCET_{II}$, Soft-Collinear interactions, use of auxillary Lagrangians, power counting formula, rapidity divergences: [6, 3, 10, 5, 11]
7. Power corrections, deriving $\rm SCET_{II}$ from $\rm SCET_I$: [12, 13, 10]

2 Introduction to SCET

2.1 What is SCET?

The Soft-Collinear Effective Theory is an effective theory describing the interactions of soft and collinear degrees of freedom in the presence of a hard interaction. We will refer to the momentum scale of the hard interaction as Q. For QCD another important scale is $\Lambda_{\rm QCD}$, the scale of hadronization and nonperturbative physics, and we will always take $Q \gg \Lambda_{\rm QCD}$.

Soft degrees of freedom will have momenta $p_{\rm soft}$, where $Q \gg p_{\rm soft}$. They have no preferred direction, so each component of $p^\mu_{\rm soft}$ for $\mu = 0, 1, 2, 3$ has an identical scaling. Sometimes we will have $p_{\rm soft} \sim \Lambda_{\rm QCD}$ so that the soft modes are nonperturbative (as in HQET for B or D meson bound states) and sometimes we will have $p_{\rm soft} \gg \Lambda_{\rm QCD}$ so that the soft modes have components that we can calculate perturbatively.

Collinear degrees of freedom describe energetic particles moving preferrentially in some direction (here motion collinear to a direction means motion near to but not exactly along that direction). In various situations the collinear degrees of freedom may be the constituents for one or more of

- energetic hadrons with $E_H \simeq Q \gg \Lambda_{\rm QCD} \sim m_H$,
- energetic jets with $E_J \simeq Q \gg m_J = \sqrt{p_J^2} \gg \Lambda_{\rm QCD}$.

Both the soft and collinear particles live in the infrared, and hence are modes that are described by fields in SCET. Here we characterize infrared physics in the standard way, by looking at the allowed values of invariant mass p^2 and noting that all offshell fluctuations described by SCET degrees of freedom have $p^2 \ll Q^2$. Thus SCET is an EFT which describes QCD in the infrared, but allows for both soft homogeneous and collinear inhomogeneous momenta for the particles, which can have different dominant interactions. The main power of SCET comes from the simple language it gives for describing interactions between hard $\leftrightarrow$ soft $\leftrightarrow$ collinear particles.

Phenomenologically SCET is useful because our main probe of short distance physics at Q is hard collisions: $e^+e^- \to$ stuff, $e^-p \to$ stuff, or $pp \to$ stuff. To probe physics at Q we must disentangle the physics of QCD that occurs at other scales like $\Lambda_{\rm QCD}$, as well as at the intermediate scales like m_J that are associated with jet production. This process is made simpler by a separation of scales, and the natural language for this purpose is effective field theory. Generically in QCD a separation of scales is important for determining what parts of a process are perturbative with $\alpha_s \ll 1$, and what parts are nonperturbative with $\alpha_s \sim 1$. For some examples this is fairly straightforward, there are only two relevant momentum regions, one which is perturbative and the other nonperturbative, and we can separate them with a fairly standard operator expansion. But many of the most interesting hard scattering processes are not so simple, they involve either multiple perturbative momentum regions, or multiple nonperturbative momentum regions, or both. In most cases where we apply SCET we will be interested in two or more modes in the effective theory, such as soft and collinear, and often even more modes, such as soft modes together with two distinct types of collinear modes.

Part of the power of SCET is the plethora of processes that it can be used to describe. Indeed, it is not really feasible to generate a complete list. New processes are continuously being analyzed on a regular basis. Some example processes where SCET simplifies the physics include

- inclusive hard scattering processes: $e^-p \to e^-X$ (DIS), $p\overline{p} \to Xl^+l^-$ (Drell-Yan), $pp \to HX$, ... (either for the full inclusive process or for threshold resummation in the same process)

- exclusive jet processes: dijet event shapes in $e^+e^- \to$ jets, $pp \to H +$ 0-jets, $pp \to W +$ 1-jet, $e^-p \to e^- +$ 1-jet, $pp \to$dijets, ...
- exclusive hard scattering processes: $\gamma^*\gamma \to \pi^0$, $\gamma^* p \to \gamma^{(*)} p'$ (Deeply Virtual Compton), ...
- inclusive B-decays: $B \to X_s\gamma$, $B \to X_u \ell\bar{\nu}$, $B \to X_s \ell^+\ell^-$
- exclusive B-decays: $B \to D\pi$, $B \to \pi\ell\bar{\nu}_\ell$, $B \to K^*\gamma$, $B \to \pi\pi$, $B \to K^*K$, $B \to J/\psi K$, ...
- Charmonium production: $e^+e^- \to J/\psi\, X$, ...
- Jets in a Medium in heavy-ion collisions

Some of these examples combine SCET with other effective theories, such as HQET for the B-meson, or NRQCD for the J/ψ.

Before we dig in, it is useful to stop and ask **What makes SCET different from other EFT's?** Put another way, what are some of the things that make it more complicated than more traditional EFTs? Or another way, for the field theory afficionato, what are some of the interesting new techniques I can learn by studying this EFT? A brief list includes:

- We will integrate off-shell modes, but not entire degrees of freedom. (This is analogous to HQET where low energy fluctuations of the heavy quark remain in the EFT.)
- Having multiple fields that are defined for the same particle

  $$\xi_n = \text{collinear quark field}, \qquad q_s = \text{soft quark field}$$

  which are required by power counting and to cleanly separate momentum scales.
- In traditional EFT we sum over operators with the same power counting and quantum numbers. In SCET some of these sums are replaced by convolutions, $\sum_i C_i \mathcal{O}_i \to \int d\omega C(\omega)\mathcal{O}(\omega)$.
- λ, the power counting parameter of SCET, is not related to the mass dimensions of fields
- Various Wilson Lines, which are path-ordered line integrals of gauge fields, P $\exp[ig\int ds n\cdot A(ns)]$, play an important role in SCET. Some appear from integrating out offshell modes, others from dynamics in the EFT, and all are related to the interesting gauge symmetry structure of the effective theory.
- There are $1/\epsilon^2$ divergences at 1-loop which require UV counterterms. This leads to explicit $\ln(\mu)$ dependence in anomalous dimensions related to the so-called cusp anomalous dimensions, and to renormalization group equations whose solutions sum up infinite series of Sudakov double logarithms, $\sum_k a_k[\alpha_s \ln^2(p/Q)]^k$.

2.2 Light-Cone Coordinates

Before we get into concepts, which should decide on convenient coordinates. To motivate our choice, consider the decay process $B \to D\pi$ in the rest frame of the B meson. This decay occurs through the exchange of a W boson mediating $b \to c\bar{u}d$, along with a valence spectator quark that starts in the B and ends up in the D meson. We are concerned here with the kinematics. Aligning the π with the $-\hat{z}$ axis it is easy to work out the pion's four momentum for this two-body decay,

$$p_\pi^\mu = (2.310\,\text{GeV}, 0, 0, -2.306\,\text{GeV}) \simeq Q n^\mu\,, \tag{2.1}$$

where $n^\mu = (1,0,0,-1)$ in a $0,1,2,3$ basis for the four vector. Here $n^2 = 0$ is a light-like vector and $Q \gg \Lambda_{\rm QCD}$. This pion has large energy and has a four-momentum that is close to the light-cone. With a slight abuse of language we will often say that the pion is moving in the direction n (even though we really mean the direction specified by the $1,2,3$ components of n^μ). The natural coordinates for particles whose energy is much larger than their mass are light-cone coordinates.

We would like to be able to decompose any four vector p^μ using n^μ as a basis vector. But unlike cartesian coordinates the component along n will not be $n \cdot p$, since $n^2 = 0$. If we want to describe the components (we do) then we will need another auxillary light-like vector $\bar{n}$. The vector n has a physical interpretation, we want to describe particles moving in the n direction, whereas $\bar{n}$ is simply a devise we introduce to have a simple notation for components.

Thus we start with light-cone basis vectors n and $\bar{n}$ which satisfy the properties

$$n^2 = 0, \qquad \bar{n}^2 = 0, \qquad n \cdot \bar{n} = 2\,, \tag{2.2}$$

where the last equation is our normalization convention. A standard choice, and the one we will most often use, is to simply take $\bar{n}$ in the opposite direction to n. So for example we might have

$$n^\mu = (1,0,0,1)\,, \qquad\qquad \bar{n}^\mu = (1,0,0,-1) \tag{2.3}$$

Other choices for the auxillary vector work just as well, e.g. $n^\mu = (1,0,0,1)$ with $\bar{n}^\mu = (3,2,2,1)$, and later on this freedom in defining $\bar{n}$ will be codified in a reparameterization invariance symmetry. For now we stick with the choice in Eq. (2.3).

It is now simple to represent standard 4-vectors in the light-cone basis

$$p^\mu = \frac{n^\mu}{2}\bar{n}\cdot p + \frac{\bar{n}^\mu}{2} n\cdot p + p_\perp^\mu \tag{2.4}$$

where the $\perp$ components are orthogonal to both n and $\bar{n}$. With the choice in Eq. (2.3), $p_\perp^\mu = (0, p^1, p^2, 0)$. It is customary to represent a momentum in these coordinates by

$$p^\mu = (p^+, p^-, \vec{p}_\perp) \tag{2.5}$$

where the last entry is two-dimensional, and the minkowski $p_\perp^2$ is the negative of the euclidean $\vec{p}_\perp^{\,2}$ (ie. in our notation $p_\perp^2 = -\vec{p}_\perp^{\,2}$). Here we have also defined

$$p^+ = p_+ \equiv n\cdot p\,, \qquad\qquad p^- = p_- \equiv \bar{n}\cdot p. \tag{2.6}$$

As indicated the upper or lower $\pm$ indices mean the same thing.

Using the standard $(+---)$ metric, the four-momentum squared is

$$p^2 = p^+p^- + p_\perp^2 = p^+p^- - \vec{p}_\perp^{\,2}\,. \tag{2.7}$$

We can also decompose the metric in this basis

$$g^{\mu\nu} = \frac{n^\mu\bar{n}^\nu}{2} + \frac{\bar{n}^\mu n^\nu}{2} + g_\perp^{\mu\nu}\,. \tag{2.8}$$

Finally we can define an antisymmetric tensor in the $\perp$ space by $\epsilon_\perp^{\mu\nu} = \epsilon^{\mu\nu\alpha\beta}\bar{n}_\alpha n_\beta/2$.

2.3 Momentum Regions: SCET I and SCET II

Lets continue with our exploration of the $B \to D\pi$ decay with the goal of identifying the relevant quark and gluon degrees of freedom (d.o.f.) for designing an EFT to describe this process. We'll then do the same for a process with jets.

There are different ways of finding the relevant infrared degrees of freedom. We could characterize all possible regions giving rise to infrared singularities at any order in perturbation theory using techniques like the Landau equations, and then determine the corresponding momentum regions. We could carry out QCD loop calculations using a technique known as the method of regions, where the full result is obtained by a sum of terms that enter from different momentum regions. Then by examining these regions we could hypothesize that there should be corresponding EFT degrees of freedom for those regions that appear to correspond to infrared modes that should be in the EFT. (Either of these approaches may be useful, but note that when using them we must be careful that the degrees of freedom are appropriate to our true physical situation, and do not contain artifacts related to our choice of perturbative infrared regulators that are not present in the true nonperturbative QCD situation.) Instead, our approach in this section will be based solely on physical insight of what the relevant d.o.f. are, from thinking through what is happening in the hard scattering process we want to study. More mathematical checks that one has the right d.o.f. are also desirable, and we will talk about some examples of how to do this later on. This falls under the ruberic of not fully trusting a physics argument without the math that backs it up, and visa versa.

For $B \to D\pi$ in the rest frame of the B, the constituents of the B meson are the nearly static heavy b quark, and the soft quarks and gluons with momenta $\sim \Lambda_{\rm QCD}$, ie. just the standard degrees of freedom of HQET. Since $|\vec{p}_D| = 2.31\,\text{GeV} \sim m_D = 1.87\,\text{GeV}$ the constituents of the D meson are also soft and described by HQET. The pion on the other hand is highly boosted. We can derive the momentum scaling of the pion constituents by starting with the $(+,-,\perp)$ scaling of

$$p^\mu \sim (\Lambda_{\rm QCD}, \Lambda_{\rm QCD}, \Lambda_{\rm QCD}) \qquad \text{for constituents in the pion rest frame,}$$

and then by boosting along $-\hat{z}$ by an amount $\kappa = Q/\Lambda_{\rm QCD}$. The boost is very simple with light cone coordinates, taking $p^- \to \kappa p^-$ and $p^+ \to p^+/\kappa$. Thus

$$p_c^\mu \sim \Big(\frac{\Lambda_{\rm QCD}^2}{Q}, Q, \Lambda_{\rm QCD}\Big) \tag{2.9}$$

for the energetic pions constituents in the B rest frame. This scaling describes the typical momenta of the quarks and gluons that bind into the pion moving with large momentum $p_\pi^\mu = (0, Q, 0) + \mathcal{O}(m_\pi^2/Q)$, as in

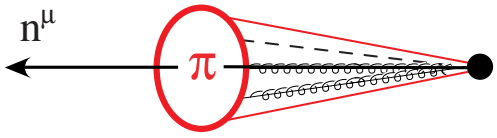

The important fact about Eq. (2.9) is that

$$p_c^- \gg p_c^\perp \gg p_c^+ \,. \tag{2.10}$$

Whenever the components of p_c^μ obey this hierarchy we say it has a **collinear** scaling. Its convenient to describe this collinear scaling with a dimensionless parameter by writing

$$p_c^\mu \sim Q(\lambda^2, 1, \lambda) \tag{2.11}$$

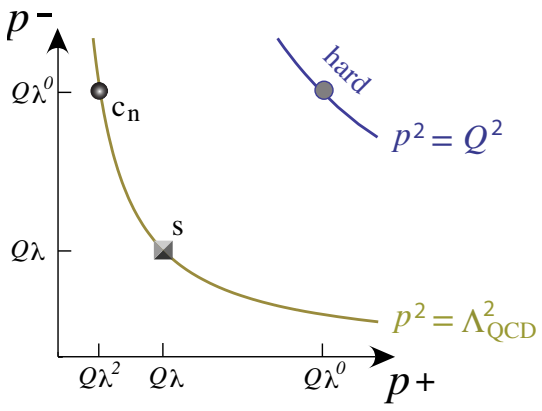

Figure 1: SCET$_{\rm II}$ example. Relevant degrees of freedom for $B \to D\pi$ with an energetic pion in the B rest frame.

where $\lambda \ll 1$ is a small parameter. This result is generic. For our $B \to D\pi$ example we have $\lambda = \Lambda_{\rm QCD}/Q$.[1] This λ will be the power counting parameter of SCET. With this notation we can also say how the soft momenta of constituents in the B and D meson scale,

$$p_s^\mu \sim Q(\lambda, \lambda, \lambda)\,. \tag{2.12}$$

Thus we see that we need both soft and collinear degrees of freedom for the $B \to D\pi$ decay.

It is convenient to represent the degrees of freedom with a picture, as in Fig. 1. This picture has some interesting features. Unlike simpler effective theories SCET requires at least two variables to describe the d.o.f. The choice of p^- and p^+ as the axis here suffices since the $\perp$-momentum satisfies $p_\perp^2 \sim p^+p^-$ and hence does not provide additional information. The hyperbolas in the figures are lines of constant $p^2 = p^+p^-$. The labelled spots indicate the relevant momentum regions. We have included a hyperbola and a spot for the hard region where $p^2 \sim Q^2$, but these are the modes that are actually integrated out when constructing SCET. (For $B \to D\pi$ they are fluctuations of order the heavy quark masses.) On the $p^2 \sim \Lambda_{\rm QCD}^2$ hyperbola in Fig. 1 we have two types of nonperturbative modes, collinear modes c_n for the pion constituents, and soft modes s for the B and D meson constituents. Since these modes live at the same typical invariant mass p^2 we need another variable, namely p^-/p^+, to distinguish them. This variable is related to the rapidity, Y, since $e^{2Y} = p^-/p^+$. Put another way, we need both of the variables p^+ and p^- to define the modes for the EFT.

The example in Fig. 1 is what is known as an SCET$_{\rm II}$ type theory. Its defining characteristic is that the soft and collinear modes in the theory have the same scaling for p^2, they live on the same hyperbola. This type of theory turns out to be appropriate for a wide variety of different processes and hence we give it the generic name SCET$_{\rm II}$. Essentially this version of SCET is the appropriate one for hard processes which produce energetic identified hadrons, what we earlier called exclusive hard scattering and exclusive B-decays.

[1] Please do not be confused into thinking that you need to assign a precise definition to λ. It is only used as a scaling parameter to decide what operators we keep and what terms we drop in the effective field theory, so any definition which is equivalent by scaling is equally good. In the end any predictions we make for observables do not depend on the numerical value of λ. The only time we need a number for λ is when making a numerical estimate for the size of the terms that are higher order in the power expansion which we've dropped.

When looking at Fig. 1 we should interpret the collinear degrees of freedom as living mostly in a region about the c_n spot and the soft degrees of freedom as living mostly in a region about the s spot. An obvious question is what determines the boundary between these degrees of freedom. In a Wilsonian EFT the answer would be easy, there would be hard cutoffs that carve out the regions defined by these modes. But hard cutoffs break symmetries. For SCET the cutoffs must be "softer regulators" so as to not to break symmetries like Lorentz invariance and gauge invariance. Dimensional regularization is one regulator that can be used for this purpose. If we were only trying to distinguish modes with the invariant mass p^2 then the dim.reg. scale parameter μ would suffice for the cutoff between UV and IR modes, and we would be set to go. But in SCET we also need to distinguish modes in another dimension, μ does not suffice to separate or distinguish the s and c_n modes of Fig. 1. We will see how to do this later on without spoiling any symmetries. In general it will require a combination of subtractions that localize the modes in the regions shown in the figure, as well as additional cutoff parameters. The bottom line is that the physical picture in Fig. 1 for where the modes live is the correct one to think about for the purpose of power counting. But when integrating over loop momenta in a virtual diagram involving one of these modes we integrate over all values with a soft regulator to avoid breaking symmetries.

Lets consider a second example involving QCD jets. Jets are collimated sprays of hadrons produced by the showering process of an energetic quark or gluon as it undergoes multiple splittings. The splitting is enhanced in the forward direction by the presence of collinear singularities. The simplest process is $e^+e^- \to$ dijets, which at lowest order is the process $e^+e^- \to \gamma^* \to q\bar{q}$ with each of the light quarks q and $\bar{q}$ forming a jet. Let q^μ be the momentum of the γ^*, then in the center-of-momentum frame (CM frame) $q^\mu = (Q, 0, 0, 0)$ and sets the hard scale. If there are only two jets in the final state then by momentum conservation they will be back-to-back along the horizontal $\hat{z}$ axis:

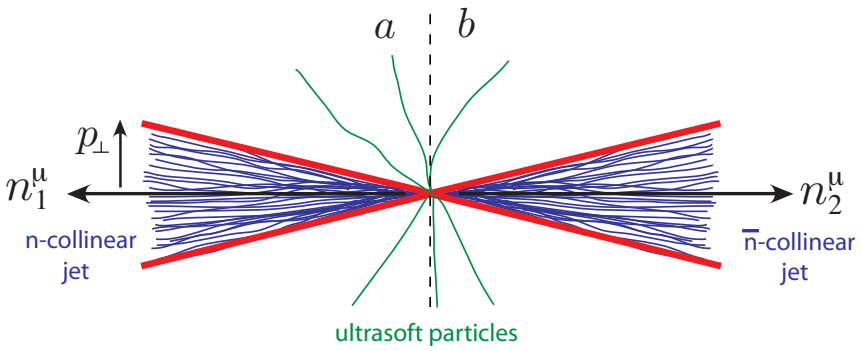

The $x-y$ plane defines two hemispheres a and b, and we consider a process with one jet in each of them. The energy in each hemisphere is $Q/2$ and is predominantly carried by the collimated particles in the jets. To describe the degrees of freedom we need two collinear directions. We align n_1^μ with the direction of the first jet and n_2^μ with the second. (These directions can be defined by using a jet algorithm to determine the particles inside a jet, or indirectly from the process of calculating a jet event shape like thrust.)

Lets first consider the energetic constituents of the n_1-jet. Since these constituents are collimated they have a $\perp$-momentum that is parametrically smaller than their large minus momentum, $p_\perp \sim \Delta \ll p^- \sim Q$. In order that we have a jet of hadrons and not a single hadron or small number of hadrons we must have $\Delta \gg \Lambda_{\rm QCD}$. Thus the jets constituents have $(+,-,\perp)$ momenta with respect to the axes $n_1 = (1, -\hat{z})$ and $\bar{n}_1 = (1, \hat{z})$ that have a collinear scaling

$$p_{n_1}^\mu \sim \Big(\frac{\Delta^2}{Q}, Q, \Delta\Big) = Q(\lambda^2, 1, \lambda)\,. \tag{2.13}$$

As usual the scaling of the $+$-momentum is determined by noting that we are considering fluctuations about $p^2 = 0$, so $p^+ \sim p_\perp^2/p^-$. Here the power counting parameter is $\lambda = \Delta/Q \ll 1$. Note that the jet

constituents have the same scaling as the constituents of a collinear pion, but carry larger offshellness p^2. If we make Δ so large that $\Delta \sim Q$ then we no longer have a dijet configuration, and if we make Δ so small that $\Delta \sim \Lambda_{\rm QCD}$ then the constituents will bind into one (or more) individual hadrons rather than the large collection of hadrons that make up the jet. Another way to characterize the presence of the jet is through the jet-mass m_J^2, since a jet will have $Q^2 \gg m_J^2 \gg \Lambda_{\rm QCD}^2$. For our example here we can make use of the a-hemisphere jet-mass,

$$m_{J_a}^2 \equiv \Big(\sum_{i\in a} p_i^\mu\Big)^2 \sim p_{n_1}^+ p_{n_1}^- \sim \Delta^2 \ll Q^2\,. \tag{2.14}$$

For the constituents of the n_2-jet we simply repeat the discussion above, but with particles collimated about the direction, $n_2 = \bar n_1 = (1,\hat z)$. A choice that makes this simple is $\bar n_2 = n_1 = (1,-\hat z)$, since then we can simply take the n_1-jet analysis results with $+ \leftrightarrow -$. Using the same $(+,-,\perp)$ components as for the n_1-jet we then have

$$p_{n_2}^\mu \sim \Big(Q, \frac{\Delta^2}{Q}, \Delta\Big) = Q(1,\lambda^2,\lambda)\,. \tag{2.15}$$

Again a measurement of the b-hemisphere jet-mass can be used to ensure that there is only one jet in that region jet-mass,

$$m_{J_b}^2 \equiv \Big(\sum_{i\in b} p_i^\mu\Big)^2 \sim p_{n_2}^+ p_{n_2}^- \sim \Delta^2 \ll Q^2\,. \tag{2.16}$$

Finally in jet processes there are also soft homogeneous modes that account for soft hadrons that appear between the collimated jet radiation (as well as within it). The precise momentum of these degrees of freedom depends on the observable being studied, and the restrictions it imposes on this radiation. In our $e^+e^- \to$ dijets example we can consider measuring that $m_{J_a}^2$ and $m_{J_b}^2$ are both $\sim \Delta^2$. In this case the homogeneous modes are "ultrasoft" with momentum scaling as

$$p_{us}^\mu \sim \Big(\frac{\Delta^2}{Q}, \frac{\Delta^2}{Q}, \frac{\Delta^2}{Q}\Big) = Q(\lambda^2,\lambda^2,\lambda^2)\,. \tag{2.17}$$

To derive this we consider the restrictions that $m_{J_a}^2 \sim \Delta^2$ imposes on the observed particles, noting in particular that with a collinear and ultrasoft particle in the a-hemisphere we have

$$(p_{n_1} + p_{us})^2 = p_{n_1}^2 + 2p_{n_1}\cdot p_{us} + p_{us}^2 \sim \Delta^2\,. \tag{2.18}$$

The term $2p_{n_1}^- \cdot p_{us} = p_{n_1}^- p_{us}^+$ plus higher order terms, so $p_{us}^+ \sim \Delta^2/p_{n_1}^- \sim \Delta^2/Q$, which is the ultrasoft momentum scale given in Eq. (2.17). Any larger momentum for p_{us}^+ is forbidden by the hemisphere mass measurement. The scaling of the other ultrasoft momentum components then follows from homogeneity.

If we draw the degrees of freedom, then for the double hemisphere mass distribution measurement of $e^+e^- \to$ dijets in the p^+-p^- plane we find Fig. 2. Again we have labelled hard modes with momenta $p^2 \sim Q^2$ that are integrated out in constructing the EFT (here they correspond to virtual corrections at the jet production scale). In the low energy effective theory we have two types of collinear modes c_n and $c_{\bar n}$, one for each jet, which live on the $p^2 \sim \Delta^2$ hyperbola. Finally the ultrasoft modes live on a different hyperbola with $p^2 \sim \Delta^4/Q^2$. The collinear and ultrasoft modes all have $p^2 \lesssim Q^2\lambda^2$ and are degrees of freedom in SCET, while modes with $p^2 \gg Q^2\lambda^2$ are integrated out. When we are in a situation like this one, where the collinear and homogeneous modes live on hyperbolas with parametrically different scaling for p^2, then the resulting SCET is known as an $\rm SCET_I$ type theory. Note that the c_n and us modes have

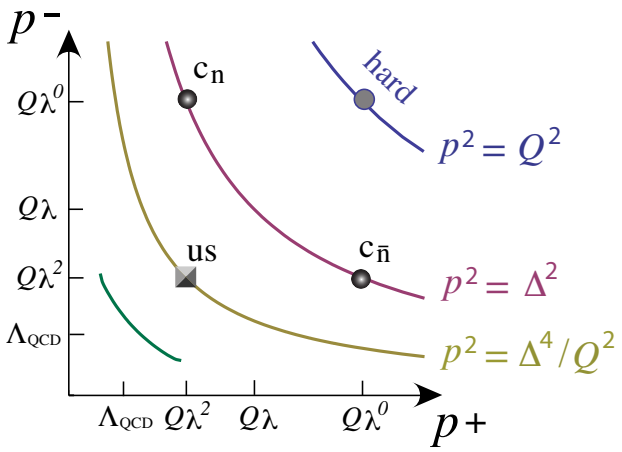

Figure 2: SCET$_{\rm I}$ example. Relevant degrees of freedom for dijet production $e^+e^- \to$ dijets with measured hemisphere invariant masses $m^2_{J_a}$ and $m^2_{J_b}$.

p^+ momenta of the same size, whereas the $c_{\bar{n}}$ and us modes have p^- momenta of the same size. The names collinear and ultrasoft denote the fact that these modes live on different hyperbolas.[2] Once again these degrees of freedom capture regions of momentum space, which are centered around the spots indicated and each of them extend into the infrared.

It is important to note in this dijet example that $\Delta^4/Q^2 \gtrsim \Lambda^2_{\rm QCD}$, so in general the nonperturbative ultrasoft modes can live on an even smaller hyperbola $p^2 \sim \Lambda^2_{\rm QCD}$ than the perturbative contributions from ultrasoft modes that have $p^2 \sim \Delta^4/Q^2$. An additional $p^2 \sim \Lambda^2_{\rm QCD}$ hyperbola is shown in green in Fig. 2. If $\Delta^4/Q^2 \sim \Lambda^2_{\rm QCD}$ then the yellow and green hyperbolas are not distinguishable by power counting, and hence are equivalent. If on the other hand we are in a situation where $\Delta^4/Q^2 \gg \Lambda^2_{\rm QCD}$ then when we setup the SCET$_{\rm I}$ theory both the perturbative ultrasoft modes with $p^2 \sim \Delta^4/Q^2$ and the nonperturbative ultrasoft modes with $p^2 \sim \Lambda^2_{\rm QCD}$ will be part of our single ultrasoft degree of freedom. This is convenient because we can first formulate the $\Delta/Q \ll 1$ expansion with the c_n, $c_{\bar{n}}$ and us d.o.f., and only later worry about making another expansion in $Q\Lambda_{\rm QCD}/\Delta^2 \ll 1$ to separate the two types of ultrasoft modes that would live on the yellow and green hyperbolas.

If we compare Fig. 1 and Fig. 2 we see that it is the relative behaviour of the collinear and soft/ultrasoft modes that determine whether we are in an SCET$_{\rm I}$ or SCET$_{\rm II}$ type situation. (There are also SCET$_{\rm II}$ examples which involve jets with $\perp$ measurements rather than jet masses, and we will meet these later on in Section 14.3 and 14.4.) Much of our discussion will be devoted to studying these two examples of SCET, since they are already quire rich and cover a wide variety of processes. In general however one should be aware that a more complicated process or set of measurements may well require a more sophisticated pattern of degrees of freedom. For example, we could have soft or collinear modes on more than one hyperbola, or might require modes with a new type of scaling. Indeed, this is not even uncommon, the collider physics example of $pp \to$ dijets in the CM frame requires both SCET$_{\rm II}$ type collinear modes for the incoming protons, and SCET$_{\rm I}$ type collinear modes for the jets. Nevertheless, after having studied both SCET$_{\rm I}$ and SCET$_{\rm II}$ we will see that often these more complicated processes do not really require additional formalism, but rather simply require careful use of the tools we have already developed in studying SCET$_{\rm I}$

[2] In certain situations in the literature to use the names hard-collinear and soft to denote the same thing, and we will find occasion to explain why when discussing how SCET$_{\rm I}$ can be used to construct SCET$_{\rm II}$.

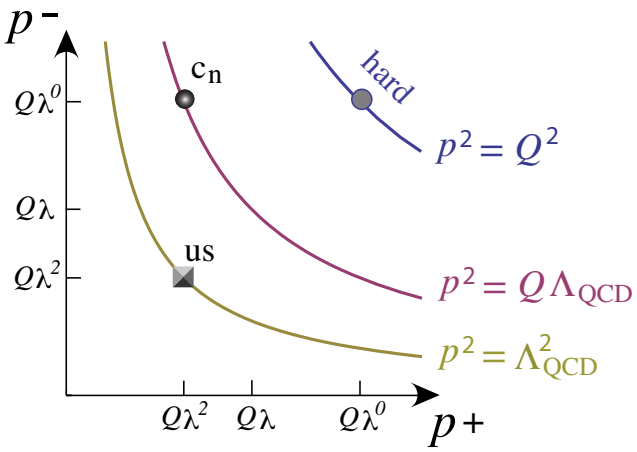

Figure 3: Another SCET_I example. Relevant degrees of freedom for $B \to X_s\gamma$ in the endpoint region.

and SCET_II.

A comment is also in order about the frame dependence of our degrees of freedom. In both of our examples we found it convenient to discuss the degrees of freedom in a particular frame (the B rest frame, or e^+e^- CM frame). Typically there is a natural reference frame to think about the analysis of a process, but of course the final result describing the dynamics of a process will actually not be frame dependent. Thus it is natural to ask what the d.o.f. and corresponding momentum regions would look like in a different frame. A simple example to discuss is a boost of the entire process along the $\hat{z}$ axis. All the modes then slide along their hyperbolas (since p^2 is unchanged). The important point is that the relative size of momenta of different d.o.f. is unchanged by this procedure: the p^+ momenta of collinear and ultrasoft modes in SCET_I will be the same size even after the boost, and the p^+ momentum of a soft particle will always be larger than the p^+ momentum of a collinear particle in SCET_II. In $B \to D\pi$ such a boost can take us to the pion rest frame, where its constituents are now soft, and the constituents of the B and D are now boosted. Some components of the SCET analysis may look a bit different if we use different frames, but the final EFT results for decay rates and cross sections will obey the expected overall boost relations. In general it is only the relative scaling of the momenta of various degrees of freedom that enter into expansions and the final physical result. The relative placement of the spots for our d.o.f. in SCET_I and SCET_II is not affected by the $\hat{z}$ boost.

Before finishing our discussion of d.o.f. we consider one final example. For the purpose of studying SCET_I it is useful to have an example with one jet rather than two, so the d.o.f. become simply c_n and us. This can occurs for the process $B \to X_s\gamma$ or for $B \to X_u e\bar{\nu}$. The underlying processes here are the flavor changing neutral current proess $b \to s\gamma$ or the semileptonic decay $b \to ue\bar{\nu}$. For these inclusive decays we sum over any collection of hadronic s tates X_s or X_u that can be produced from the s or u quark. In the B rest frame, the total energy of the γ or $(e\bar{\nu})$ is $E = (m_B^2 - m_X^2)/(2m_B)$ and ranges from 0 to $(m_B^2 - m_{H_\text{min}}^2)/(2m_B)$ where m_{H_min} is the smallest appropriate hadron mass, either $m_{H_\text{min}} = m_{K^*}$ or m_π for X_s or X_u respectively. An interesting region to consider for the application of SCET is

$$\Lambda_\text{QCD}^2 \ll m_X^2 \ll Q^2 = m_B^2 \tag{2.19}$$

where the photon or $(e\bar{\nu})$ recoils against a jet of hadrons which are the constituents of X. For $B \to X_s\gamma$ the picture is (double line being the b-quark, yellow lines are soft particles, and red lines are collinear particles):

mode	fields	p^μ momentum scaling	physical objects
n_j-collinear	ξ_{n_j}, $A^\mu_{n_j}$	$(n_j{\cdot}p, \bar{n}_j \cdot p, p_{\perp j}) \sim Q(\lambda^2, 1, \lambda)$	collinear virtual/real radiation in jet or hadron in $\hat{n}_j$ direction
soft	ψ_s, A^μ_s	$p^\mu \sim Q(\lambda, \lambda, \lambda)$	soft virtual/real radiation
ultrasoft	ψ_{us}, A^μ_{us}	$p^\mu \sim Q(\lambda^2, \lambda^2, \lambda^2)$	ultrasoft virtual/real radiation
Glauber	–	$p^\mu \sim Q(\lambda^a, \lambda^b, \lambda)$ with $a+b<2$	forward scattering potential
hard	–	$p^2 \gtrsim Q^2$	hard scattering

Table 1: Infrared momentum regions and the corresponding quark and gluon fields in SCET (taken from Ref. [**?**]). Here $n_j^\mu = (1, \hat{n}_j)$, Q is the scale of the hard interaction, and $\lambda \ll 1$ is a dimensionless power counting parameter.

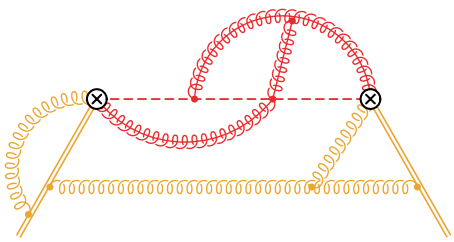

Here the jet mass is also the mass of the hadronic final state, and the situation which dominates the phenomenology has $m_X^2 \sim Q\Lambda_{\rm QCD}$. We have collinear modes for the jet, and ultrasoft modes with $p_{us}^2 \sim \Lambda_{\rm QCD}^2$ which are the constituents of the B meson for this inclusive decay. Often the region where $m_X^2 \ll Q^2$ is known at the endpoint region since $E \sim m_B/2 - \Lambda_{\rm QCD}$ and hence is close to the physical endpoint $E = m_B/2$. (The case $m_X^2 \sim Q^2$ is then known as the local OPE region where the traditional HQET operator product expansion analysis suffices.) The picture of the modes for this case are shown in Fig. 3, and indeed yield an example of an SCET$_{\rm I}$ theory with only one collinear mode.

3 Ingredients for SCET

Our objective in this section is to expand QCD and formulate collinear and ultrasoft degrees of freedom. In doing so, we will derive power counting expressions for operators and see what form the quark Lagrangian takes in a SCET theory.

3.1 Collinear Spinors

We begin our exploration by considering the expansion in the collinear limit of Dirac spinors $u(p)$ for particles and $v(p)$ for antiparticles. The relevant collinear spinors are obtained by considering the expansion in momentum components, but the final result decomposes each QCD spinor into just two types of terms rather than an infinite expansion.

It is useful to consider spinors of definite chirality

$$u^\pm(p) = \frac{1 \pm \gamma_5}{2}\, u(p)\,, \qquad v^\pm(p) = \frac{1 \pm \gamma_5}{2}\, v(p)\,. \tag{3.1}$$

Adopting the Dirac representation

$$\gamma^0 = \begin{pmatrix} 1 & 0 \\ 0 & -1 \end{pmatrix}, \quad \gamma^i = \begin{pmatrix} 0 & \sigma^i \\ -\sigma^i & 0 \end{pmatrix}, \quad \gamma_5 = \begin{pmatrix} 0 & 1 \\ 1 & 0 \end{pmatrix}, \tag{3.2}$$

a convenient set of solutions for the full Dirac equations $\not{p}\,u(p)=0$ and $\not{p}\,v(p)=0$ are then

$$u^+(p)=v^-(p)=\frac{1}{\sqrt{2}}\begin{pmatrix}\sqrt{p^-}\\ \sqrt{p^+}e^{i\phi_p}\\ \sqrt{p^-}\\ \sqrt{p^+}e^{i\phi_p}\end{pmatrix},\qquad u^-(p)=v^+(p)=\frac{1}{\sqrt{2}}\begin{pmatrix}\sqrt{p^+}e^{-i\phi_p}\\ -\sqrt{p^-}\\ -\sqrt{p^+}e^{-i\phi_p}\\ \sqrt{p^-}\end{pmatrix}, \tag{3.3}$$

where here

$$p^\pm=p^0\mp p^3\,,\qquad \exp(\pm i\phi_p)=\frac{p^1\pm ip^2}{\sqrt{p^+p^-}}\,, \tag{3.4}$$

and the onshell condition sets $p^2=p^+p^--(p^1)^2-(p^2)^2=0$. With this convention, which is also a common one in the spinor-helicity literature [14], the spinors for particles and antiparticles with opposite chirality are related.

For a collinear momentum $p^\mu=(p^0,p^1,p^2,p^3)$ we have $p^-\gg p^{1,2}\gg p^+$ so keeping the leading order term simply amounts to dropping the $\sqrt{p^+}$ terms in Eq. (3.3), which gives

$$u_n^\pm=v_n^\mp=\sqrt{\frac{p^-}{2}}\begin{pmatrix}\sigma^3\mathcal{U}^\pm\\ \mathcal{U}^\pm\end{pmatrix}, \tag{3.5}$$

where $\mathcal{U}^+=\begin{pmatrix}1\\0\end{pmatrix}$ and $\mathcal{U}^-=\begin{pmatrix}0\\1\end{pmatrix}$. From this analysis we see that in the collinear limit both quark and antiquarks remain as relevant degrees of freedom (and indeed, there is no suppression for pair creation from splitting). We also see that both spin components remain in each of the spinors. The same result can be obtained by applying a projection operator. Recalling our default definitions of $n^\mu=(1,0,0,1)$ and $\bar n^\mu=(1,0,0,-1)$, we can calculate their contractions with the gamma matrix,

$$\not{n}=\gamma_0-\gamma_3=\begin{pmatrix}\mathbb{1}&-\sigma^3\\ \sigma^3&-\mathbb{1}\end{pmatrix},\qquad \not{\bar n}=\gamma_0+\gamma_3=\begin{pmatrix}\mathbb{1}&\sigma^3\\ -\sigma^3&-\mathbb{1}\end{pmatrix}. \tag{3.6}$$

We can then define the projection operators

$$P_n=\frac{\not{n}\not{\bar n}}{4}=\frac{1}{2}\begin{pmatrix}\mathbb{1}&\sigma^3\\ \sigma^3&\mathbb{1}\end{pmatrix},\qquad P_{\bar n}=\frac{\not{\bar n}\not{n}}{4}=\frac{1}{2}\begin{pmatrix}\mathbb{1}&-\sigma^3\\ -\sigma^3&\mathbb{1}\end{pmatrix}, \tag{3.7}$$

which satisfy $P_n^2=P_n$, $P_{\bar n}^2=P_{\bar n}$. From $\{\gamma^\mu,\gamma^\nu\}=2g^{\mu\nu}$ we also have the completeness relation

$$P_n+P_{\bar n}=\frac{\not{n}\not{\bar n}}{4}+\frac{\not{\bar n}\not{n}}{4}=\mathbb{1}\,. \tag{3.8}$$

Note that only the explicit matrix formulas depend on the explicit choice for n and $\bar n$, whereas formulas like Eq. (3.8) only use $n^2=\bar n^2=0$ and $n\cdot\bar n=2$. The results for the collinear spinors in Eq. (3.5) can now be obtained as a projection from the full theory spinors using the projector P_n as

$$P_n u^\pm(p)=u_n^\pm\,,\qquad P_n v^\pm(p)=v_n^\pm\,. \tag{3.9}$$

The other projector, $P_{\bar n}$ projects out precisely the small spinor components proportional to $\sqrt{p^+}$ in Eq. (3.3). Therefore the expansion of the full theory spinor $u^\pm$ contains just two terms, a large term from $P_n u^\pm$ and a smaller term from $P_{\bar n}u^\pm$.

Since $P_n^2 = P_n$ we also have projection relations for the collinear spinors alone

$$P_n u_n = \frac{\not{n}\bar{\not{n}}}{4} u_n = u_n, \qquad P_n v_n = \frac{\not{n}\bar{\not{n}}}{4} v_n = v_n. \tag{3.10}$$

Finally, noting that $\not{n} P_n = 0$ since $\not{n}^2 = n^2 = 0$ we have the following relations

$$\not{n} u_n = 0\,, \qquad \not{n} v_n = 0\,. \tag{3.11}$$

These can be recognized as the leading term in the equations of motion $\not{p} u(p) = \not{p} v(p) = 0$ when expanded in the collinear limit. The bottom line regarding the presence of collinear spinors is that when a hard interaction produces a collinear fermion or antifermion it will be the components obeying the spin relations in Eqs. (3.11) and (3.10) that appear at leading order.

A useful set of projection operator identities can easily be derived from $n^2 = 0$, $\bar{n} \cdot n = 2$, and/or hermitian conjugation $\gamma^{\mu\dagger} = \gamma^0 \gamma^\mu \gamma^0$:

$$P_n P_{\bar{n}} = 0\,, \qquad P_n P_n = P_n\,, \qquad P_n \bar{\not{n}} = P_{\bar{n}} \not{n} = 0\,, \qquad P_n \not{n} = \not{n}\,, \qquad P_{\bar{n}} \bar{\not{n}} = \bar{\not{n}}\,, \qquad P_n^\dagger = \gamma_0 P_{\bar{n}} \gamma_0\,. \tag{3.12}$$

None of these results depends on making the canonical back-to-back choice for $\bar{n}$. The last result is useful for the computation of $\bar{u}_n$ from $u_n = P_n u$, i.e.

$$\bar{u}_n = u_n^\dagger \gamma^0 = u^\dagger P_n^\dagger \gamma^0 = \bar{u}\, P_{\bar{n}}\,. \tag{3.13}$$

For example, we can use this result to sum over spins for the product of collinear spinors

$$\sum_{s=\pm} u_n^s \bar{u}_n^s = P_n \sum_{s=\pm} u^s \bar{u}^s P_{\bar{n}} = P_n \not{p} P_{\bar{n}} = \frac{\not{n}}{2}\, \bar{n} \cdot p\,. \tag{3.14}$$

For later purposes it will be useful to decompose the QCD Dirac field ψ into a field ξ_n that obeys these same spin relations. We write ψ in terms of two fields,

$$\psi = P_n \psi + P_{\bar{n}} \psi = \hat{\xi}_n + \varphi_{\bar{n}} \tag{3.15}$$

where we defined

$$\hat{\xi}_n = P_n \psi = \frac{\not{n}\bar{\not{n}}}{4} \psi\,, \qquad \varphi_{\bar{n}} = P_{\bar{n}} \psi = \frac{\bar{\not{n}}\not{n}}{4} \psi. \tag{3.16}$$

These fields satisfy the desired spin relations

$$\not{n} \hat{\xi}_n = 0\,, \qquad P_n \hat{\xi}_n = \xi_n\,, \qquad \bar{\not{n}} \varphi_{\bar{n}} = 0\,, \qquad P_{\bar{n}} \varphi_{\bar{n}} = \varphi_{\bar{n}}\,. \tag{3.17}$$

The label n on $\hat{\xi}_n$ reminds us that it obeys these relations and that we will eventually be expanding about the n-collinear direction. We also have the analog of Eq. (3.13)

$$\bar{\hat{\xi}}_n = \hat{\xi}_n^\dagger \gamma^0 = \psi^\dagger P_n^\dagger \gamma^0 = \overline{\psi}\, P_{\bar{n}}\,. \tag{3.18}$$

Note that here we denote the collinear field components with a hat, as in $\hat{\xi}_n(x)$, since there are still further manipulations that are required before we arrive at our final SCET collinear field $\xi_n(x)$. Nevertheless both $\hat{\xi}_n$ and ξ_n satisfy these spinor relations. Thus just like the relations for $\hat{\xi}_n$ or ξ_n we have the following relations for $\bar{\hat{\xi}}_n$ or $\bar{\xi}_n$:

$$\bar{\hat{\xi}}_n \not{n} = 0\,, \qquad \bar{\hat{\xi}}_n P_n = 0\,, \qquad \bar{\hat{\xi}}_n P_{\bar{n}} = \bar{\hat{\xi}}_n \frac{\bar{\not{n}}\not{n}}{4} = \bar{\hat{\xi}}_n\,. \tag{3.19}$$

In addition to our collinear decomposition of the Dirac spinors and field, we will also need spinors and quark fields for the ultrasoft degrees of freedom. However, since all ultrasoft momenta are homogeneous of order λ^2 and the scaling of momenta does not affect the corresponding components of the ultrasoft spinors, which are the same as those in QCD.

3.2 Collinear Fermion Propagator and ξ_n Power Counting

Having considered the decomposition of spinors in the collinear limit, we now turn to the fermion propagator in the collinear limit. Here $p^2 + i0 = \bar{n}\cdot p\, n\cdot p + p_\perp^2$, and since both of these terms are $\sim \lambda^2$ there is no expansion of the denominator of the propagator. We can however expand the numerator by keeping only the large $\bar{n}\cdot p$ momentum, as

$$\frac{i\not{p}}{p^2+i0} = \frac{i\not{n}}{2}\frac{\bar{n}\cdot p}{p^2+i0} + \ldots = \frac{i\not{n}}{2}\frac{1}{n\cdot p + \frac{p_\perp^2}{\bar{n}\cdot p} + i0\,\mathrm{sign}(\bar{n}\cdot p)} + \ldots \tag{3.20}$$

The fermion-gluon coupling will be proportional to $\bar{\not{n}}/2$ and hence will form a projector P_n when combined with the $\not{n}/2$ from the propagator. Therefore the displayed term in the propagator has overlap with our spinors u_n and v_n, just giving $P_n u_n = u_n$ etc. The fact that both $+i0$ and $-i0$ occur in the expanded propagator is a reflection of the fact that the lowest order SCET Lagrangian will contains both propagating particles ($\bar{n}\cdot p > 0$) and propagating antiparticles ($\bar{n}\cdot p < 0$).

The leading collinear propagator displayed in Eq. (3.20) should be obtained from a time-ordered product of the effective theory field, $\langle 0|T\hat{\xi}_n(x)\bar{\hat{\xi}}_n(0)|0\rangle$. At this point we can already identify the λ power counting for the field $\hat{\xi}_n$ by noting that if its propagator has the form in Eq. (3.20) then its action must be of the form

$$L_n^{(0)} = \int d^4x\, \mathcal{L}_n^{(0)} = \int \underbrace{d^4x}_{\mathcal{O}(\lambda^{-4})}\, \underbrace{\bar{\hat{\xi}}_n}_{\mathcal{O}(\lambda^a)}\, \frac{\bar{\not{n}}}{2}\big[\underbrace{in\cdot\partial + \ldots}_{\mathcal{O}(\lambda^2)}\big]\, \underbrace{\hat{\xi}_n}_{\mathcal{O}(\lambda^a)} \sim \lambda^{2a-2}\,. \tag{3.21}$$

Here we used the fact that $d^4x = \frac{1}{2}(dx^+)(dx^-)(d^2x_\perp) \sim (\lambda^0)(\lambda^{-2})(\lambda^{-1})^2 \sim \lambda^{-4}$ where the scaling for the coordinates x^μ follows from those for the collinear momenta by writing $x\cdot p_c = x^+p_c^- + x^-p_c^+ + 2x_\perp\cdot p_c^\perp$ and demanding that the terms in this sum are all $\mathcal{O}(1)$. In (3.21) we assigned $\hat{\xi}_n \sim \lambda^a$ with the goal of determining the value of a. To do this we take the standard approach of assigning a power counting to the leading order kinetic term in the action so that $L_n^{(0)} \sim \lambda^0$, which gives

$$\hat{\xi}_n \sim \xi_n \sim \lambda\,. \tag{3.22}$$

Even though we have not fully considered all the issues needed to define the SCET collinear field ξ_n, the further manipulations we will make in section 4 below will not effect its power counting, so we have also recorded here the fact that the SCET field $\xi_n \sim \lambda$. Note that this scaling dimension does not agree with the collinear quark fields mass dimension since $[\hat{\xi}_n] = [\xi_n] = 3/2$. This is simply a reflection of the fact that the SCET power counting for operators is not a power counting in mass dimensions. The observant reader will notice that the λ scaling of the collinear field is the same as its twist, and indeed the SCET power counting reduces to a (dynamic) twist expansion when the latter exists.

3.3 Power Counting for Collinear Gluons and Ultrasoft Fields

Similar to our procedure for the collinear fermion field, we can analyze the collinear gluon field A_n^μ in our n-collinear basis to determine the λ scaling of its components. This information is necessary to formulate the importance of operators in SCET. We begin by writing the full theory covariant gauge gluon propagator, but we label the fields as $A_n^\mu(x)$ to denote the fact that we will be considering a n-collinear momenta:

$$\int d^4x\, e^{ik\cdot x}\, \langle 0|\,\mathrm{T}A_n^\mu(x)A_n^\nu(0)\,|0\rangle = -\frac{i}{k^2}\left(g^{\mu\nu} - \tau\frac{k^\mu k^\nu}{k^2}\right) = -\frac{i}{k^4}\left(k^2 g^{\mu\nu} - \tau\, k^\mu k^\nu\right), \tag{3.23}$$

where τ is our covariant gauge fixing parameter. From our standard power counting result from the light-cone coordinate section, we know that $k^2 = k_+k_- + k_\perp^2 = Q^2\lambda^2$. So the $1/k^4$ on the RHS matches up with the scaling of the collinear integration measure

$$d^4x \sim \lambda^{-4} \sim \frac{1}{(k^2)^2} \tag{3.24}$$

Thus the quantity in the final parentheses in (3.23) must be the same order as the product of $A_n^\mu(x)A_n^\nu(0)$ fields. If both of the $\mu\nu$ indices are $\perp$ then both of the terms in these parantheses are $\sim \lambda^2$, so therefore we must have $A_{n\perp}^\mu \sim \lambda$. If one index is $+$ and the other $-$ then again both terms are the same size and we find $A_n^+A_n^- \sim \lambda^2$. To break the degeneracy we take both indices to be $+$, then $g^{++} = 0$, $(n\cdot k)^2 \sim \lambda^4$, so $A_n^+ \sim \lambda^2$ and $A_n^- \sim \lambda^0$. Other combinations also lead to this result, namely that the components of the collinear gluon field scales in the same way as the components of the collinear momentum

$$A_n^\mu \sim k^\mu \sim (\lambda^2, 1, \lambda). \tag{3.25}$$

This result is not so surprising considering that if we are going to formulate a collinear covariant derivative $D^\mu = \partial^\mu + igA^\mu$ with collinear momenta ∂^μ and gauge fields, then for each component both terms must have the same λ scaling. Indeed imposing this property of the covariant derivative is another way to derive Eq. (3.25).

The same logic can be used to derive the power counting for ultrasoft quark and gluon fields. Since the momentum $k_{us}^\mu \sim (\lambda^2, \lambda^2, \lambda^2)$ the measure on ultrasoft fields scales as $d^4x \sim \lambda^{-8}$. Also the result is now uniform for the components of A_{us}^μ. Once again we find that the gluon field scales like its momentum. For the ultrasoft quark we have the Lagrangian $\mathcal{L} = \bar\psi_{us} i\not{D}_{us}\psi_{us}$ with $iD_{us}^\mu = i\partial^\mu + gA_{us}^\mu \sim \lambda^2$. Therefore $\bar\psi_{us}\psi_{us} \sim \lambda^6$. All together we have

$$A_{us}^\mu \sim (\lambda^2, \lambda^2, \lambda^2)\,, \qquad\qquad \psi_{us} \sim \lambda^3\,. \tag{3.26}$$

For a heavy quark field that is ultrasoft the Lagrangian is $\mathcal{L}_{\rm HQET} = \bar h_v^{us} iv\cdot D_{us} h_v^{us}$ which is again linear in the derivative, so $h_v^{us} \sim \lambda^3$ as well.

For completeness we also remark that the power counting for momenta determines the power counting for states. For one-particle states of collinear particles (with a standard relativistic normalization):

$$\langle p'|p\rangle = 2p^0\delta^3(\vec p - \vec p\,') = p^-\delta(p^- - p'^-)\delta^2(\vec p^{\,\perp} - \vec p\,') \sim \lambda^{-2} \tag{3.27}$$

Thus the single particle collinear state has $|p\rangle \sim \lambda^{-1}$ for both quarks and gluons. Given the scaling of the collinear quark and gluon fields, this implies power counting results for the polarization objects. The collinear spinors $u_n \sim \xi_n|p\rangle \sim \lambda^0$ which is consistent with our earlier Eq. (H.3). For the physical $\perp$ components of polarization vectors for collinear gluons we also find $\epsilon_\perp^\mu \sim \lambda^0$.

Of particular importance in the result in Eq.(3.25) is the fact that $\bar n\cdot A_n = A_n^- \sim \lambda^0$, indicating that there is no λ supression to adding A_n^- fields in SCET operators. To understand the relevance of this result we consider in the next section an example of matching for an external current from QCD onto SCET.

3.4 Collinear Wilson Line, a first look

To see what impact there is to having a set of gauge fields $\bar n\cdot A_n \sim \lambda^0$ lets consider as an example the process $b \to ue\overline{\nu}$, where the b quark is heavy and decays to an energetic collinear u quark. This process has the advantage of only invoving a single collinear direction. This decay has the following weak current with QCD fields

$$J_{QCD} = \overline{u}\,\Gamma b \tag{3.28}$$

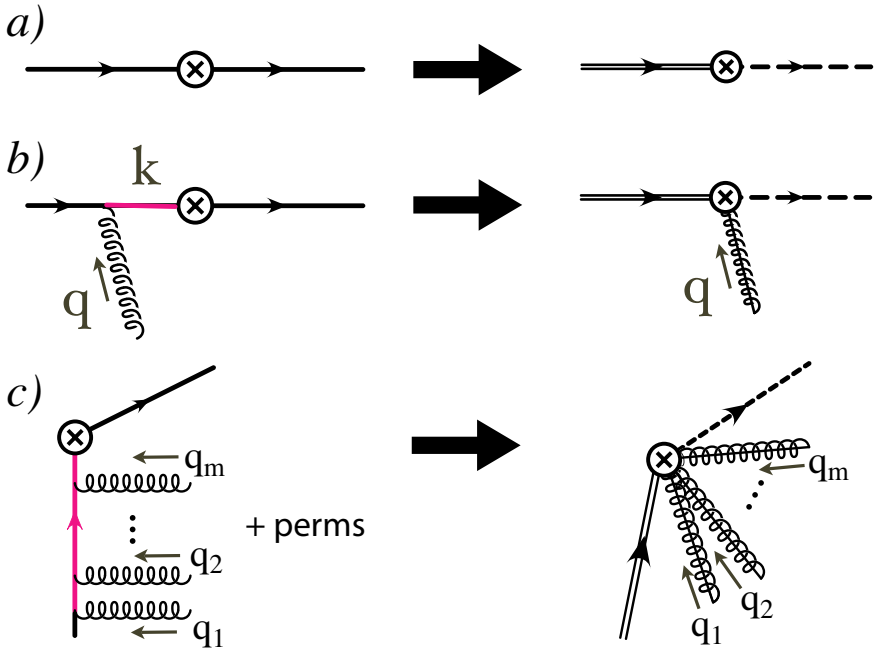

Figure 4: Tree level graphs for matching the heavy-to-light current. (Swap $q_m \to q_k$.)

where $\Gamma = \gamma^\mu(1-\gamma^5)$. Without gluons we can match this QCD current onto a leading order current in SCET by considering the heavy b field to be the HQET field h_v and the lighter u field by the SCET field ξ_n. This is shown in Fig. 4 part (a), where we use a dashed line for collinear quarks. The resulting SCET operator is

$$\bar{\xi}_n \Gamma h_v. \tag{3.29}$$

Next we consider the case where an extra A_n^- gluon is attached to the heavy quark. This process is shown in Fig.4 part (b) and leads to an offshell propagator, shown by the pink line, that must be integrated out when constructing the EFT. The full theory amplitude for this process is (replacing external spinors and polarization vectors by SCET fields):

$$\begin{aligned}
A_n^{\mu\,A}\,\bar{\xi}_n\Gamma\,\frac{i(\not{k}+m_b)}{k^2-m_b^2}\,igT^A\gamma_\mu h_v &= -g\Big(\frac{n^\mu}{2}\bar{n}\cdot A_n^A\Big)\,\bar{\xi}_n\Gamma\,\frac{[m_b(1+\not{v})+\not{q}]}{2m_b v\cdot q+q^2}T^A\gamma_\mu h_v \\
&= -g\bar{n}\cdot A_n^A\,\bar{\xi}_n\Gamma\left[\frac{m_b(1+\not{v})+\frac{\not{n}}{2}\bar{n}\cdot q}{m_b v\cdot n\,\bar{n}\cdot q}+\ldots\right]T^A\frac{\not{n}}{2}h_v \\
&= -g\bar{n}\cdot A_n^A\,\bar{\xi}_n\Gamma\left[\frac{\frac{\not{n}}{2}(1-\not{v})+v\cdot n}{v\cdot n\,\bar{n}\cdot q}+\ldots\right]T^A h_v \\
&= \bar{\xi}_n\Big(\frac{-g\,\bar{n}\cdot A_n}{\bar{n}\cdot q}\Big)\Gamma h_v
\end{aligned} \tag{3.30}$$

In the first equality we have used the fact that the incoming b quark carries momentum $m_b v^\mu$, that

$k = m_b v + q$ so that $k^2 - m_b^2 = 2m_b v\cdot q + q^2$, and that

$$A_n^\mu = \frac{n^\mu}{2}\underbrace{\bar n\cdot A_n}_{O(\lambda^0)} + \frac{\bar n^\mu}{2}\underbrace{n\cdot A_n}_{O(\lambda^2)} + \underbrace{A_\perp^\mu}_{O(\lambda)} \tag{3.31}$$

where we can keep only the $\sim\lambda^0$ term. In the second equality in Eq. (3.30) we have expanded the numerator and denominator of the propagator in λ and kept only the lowest order terms. Since $m_b v\cdot n\,\bar n\cdot q \sim Q^2\lambda^0$ we see that the propagator is offshell by an amount of $\sim Q^2$, and hence is a hard propagator that we must integrate out when constructing the corresponding SCET operator. In the third equality we use $\not{n}^2 = 0$ and pushed the $\not{n}$ through to the left. Noting that $(1-\not{v})h_v = 0$, the fourth equality gives the final leading order result from this calculation. Thus we we see that in SCET integrating out offshell hard propagators that are induced by $\bar n\cdot A_n$ gluons leads to an operator for the leading order current with one collinear gluon coming out of the vertex, pictured on the RHS of Fig. 4 part (b).

Inspecting the final result in Eq. (3.30) we see that, in addition to being a great simplification of the original QCD amplitude for this gluon attachments, it is indeed of the same order in λ as the result in Eq. (3.29). Indeed it straightforward to prove that the same $(-g\bar n\cdot A_n/\bar n\cdot q)$ result will be obtained if we replace the heavy quark by a particle that is not n-collinear, such as a collinear quark in a different direction n' where $n\cdot n' \gg \lambda^2$. The sum of collinear momenta in the n and n' directions will also be offshell, for example when we add two back-to-back collinear momenta $(p_n + p_{\bar n})^2 \sim \lambda^0$. In all these situations we find operators with additional $\bar n\cdot A_n \sim \lambda^0$ fields.

In summary, the off-shell quark has been integrated out and its effects have been parameterized by an effective operator. This was necessary because the virtual quark resulting from the interaction of a heavy quark or a n' collinear particle with a n-collinear gluon yields an off-shell momentum.

This result can be contrasted with what happens if we attach a single $\bar n\cdot A_n$ collinear gluon field to the light collinear u quark, as shown below:

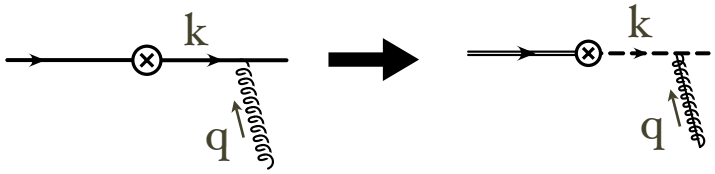

Calling the final u quarks momentum p we have $k^\mu = p^\mu - q^\mu$. However here since both p and q are n-collinear the propagator momentum k^μ also has n-collinear scaling. In particular $k^2 \sim \lambda^2$ and is not offshell, it instead represents a propagating mode within the effective theory. Thus this interaction is reproduced in SCET by a collinear propagator followed by a leading order Feynman rule that couples the $\bar n\cdot A_n$ field to the collinear quark. Thus this diagram corresponds to a time ordered product of the leading order SCET current $J^{(0)}$ with the leading order Lagrangian $\mathcal{L}_n^{(0)}$. If we attach more collinear gluons to the light u quark, the same remains true. We never get an offshell propagator that we have to integrate out when we have an interaction between n-collinear particles. Indeed we will also find that the components $n\cdot A_n$ and $A_n^\perp$ couple at leading order in T-products like the one shown above, so there is nothing special about the $\bar n\cdot A_n$ components for these diagrams.

Lets now consider the situation of multiple gluon emission from the heavy quark. In this case we again have offshell propagators, which are represented by the pink line in Fig. 4 part (c). By inspection, it is clear that the generalization from one gluon emission to k gluon emissions with momenta $q_1,\ldots,q_k$ and

propagators with momenta $q_1, q_1+q_2, \ldots, \sum_{i=1}^k q_i$ is reproduced by the field theory operator

$$\bar{\xi}_n \sum_{\text{perm}} \frac{(-g)^k}{k!} \left(\frac{\bar{n}\cdot A(q_k)\cdots \bar{n}\cdot A(q_1)}{[\bar{n}\cdot q_1][\bar{n}\cdot(q_1+q_2)]\cdots[\bar{n}\cdot\sum_{i=1}^k q_i]} \right) \Gamma h_v \tag{3.32}$$

Here the sum of permutations (perms) of the $\{q_1, \ldots, q_k\}$ momenta accounts for the fact that we must consider diagrams with crossed gluon lines on the LHS of Fig. 4 part (c). We also include the factor of $k!$ as a symmetry factor to account for the fact that all k gluon fields are localized and identical and may be contracted with any external gluon state. Finally, by summing over the number of possible gluon emissions, we can write the complete tree level matching of the QCD current to the SCET current,

$$J_{\text{SCET}} = \bar{\xi}_n W_n \Gamma\, h_v\,, \tag{3.33}$$

where

$$W_n = \sum_k \sum_{\text{perm}} \frac{(-g)^k}{k!} \left(\frac{\bar{n}\cdot A_n(q_k)\cdots \bar{n}\cdot A_n(q_1)}{[\bar{n}\cdot q_1][\bar{n}\cdot(q_1+q_2)]\cdots[\bar{n}\cdot\sum_{i=1}^k q_i]} \right). \tag{3.34}$$

Here W_n is the momentum space version of a Wilson line built from collinear A_n gluon fields. In position space the corresponding Wilson line is

$$W(0,-\infty) = \text{P}\exp\left(ig \int_{-\infty}^0 ds\, \bar{n}\cdot A_n(\bar{n}s) \right) \tag{3.35}$$

Here P is the path ordering operator which is required for nonabelian fields and which puts fields with larger arguments to the left e.g. $\bar{n}\cdot A_n(\bar{n}s)\,\bar{n}\cdot A_n(\bar{n}s')$ for $s > s'$.

In summary, we see that we have traded the field $\bar{n}\cdot A_n$ for the Wilson line $W_n[\bar{n}\cdot A_n]$. Also, including this Wilson line in our current operator makes our current gauge invariant, as we will show below in the Gauge Symmetry section. For a situation with n and n' collinear fields the same type of Wilson lines $W_n[\bar{n}\cdot A_n]$ are also generated in a manner that yields gauge invariant operators for each collinear sector.

4 SCET Lagrangian

In this section, we derive the SCET quark Lagrangian by analyzing and separating the collinear and usoft gluons, and momentum degrees of freedom. On the way to our final result we introduce the label operator which provide a simple method to separate large (label) momenta from small (residual) momenta.

4.1 SCET_I Quark Lagrangian

Lets construct the leading order SCET_I collinear quark Lagrangian. This desired properties that this Lagrangian must satisfy include

- Yielding the proper spin structure of the collinear propagator
- Contain both collinear quarks and collinear antiquarks
- Have interactions with both collinear gluons and ultrasoft gluons
- Yield the correct LO propagator for different situations without requiring additional expansions

- Should be setup so we do not have to revisit the LO result when formulating power corrections

To explain what is meant by the fourth point consider the propagator obtained when a collinear quark interacts with a collinear gluon

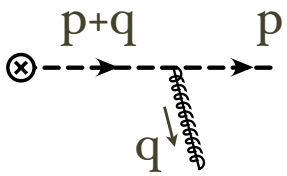

$$\propto \frac{\bar{n}\cdot(p+q)}{n\cdot(p+q)\,\bar{n}\cdot(p+q)+(p_\perp+q_\perp)^2+i0}\,.$$

Here both the momentum p and q appear on equal footing, and no momenta are dropped in the denominator. This can be contrasted with the leading propagator obtained when a collinear quark interacts with an ultrasoft gluon

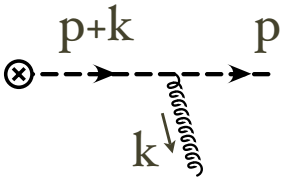

$$\propto \frac{\bar{n}\cdot p}{n\cdot(p+k)\,\bar{n}\cdot p+p_\perp^2+i0}\,.$$

Here the ultrasoft k^μ momentum is dropped for all components except $n\cdot k$ where it is the same size as the collinear momentum $n\cdot p$. The dropping of $k_\perp \ll p_\perp$ and $\bar{n}\cdot k \ll \bar{n}\cdot p$ corresponds to carrying out a multipole expansion for the interaction of the ultrasoft gluon with the collinear quark. The LO collinear quark propagator must be smart enough to give the correct leading order result without further expansions, irrespective of whether it later emits a collinear gluon or ultrasoft gluon.

We will achieve the desired collinear Lagrangian in several steps.

Step 1: Lagrangian for the larger spinor components

In this section we construct a Lagrangian for the field $\hat{\xi}_n$. It will satisfy the first two requirements in our bullet list.

We begin with the standard QCD lagrangian for massless quarks.

$$\mathcal{L}_{QCD} = \overline{\psi} i \not{D} \psi \tag{4.1}$$

Expanding ψ and D in our collinear basis gives us

$$\mathcal{L} = (\overline{\varphi}_{\bar{n}} + \overline{\hat{\xi}}_n)\left(\frac{\bar{\not{n}}}{2}\, in\cdot D + \frac{\not{n}}{2}\, i\bar{n}\cdot D + i\not{D}_\perp\right)(\varphi_{\bar{n}} + \hat{\xi}_n)\,. \tag{4.2}$$

We can simplify this result by using the projection matrix identities for the collinear spinor found in section 3.1. In particular, various terms vanish such as

$$\frac{\not{n}}{2}\, i\bar{n}\cdot D\hat{\xi}_n = 0\,, \qquad\qquad \overline{\varphi}_{\bar{n}}\frac{\bar{\not{n}}}{2}\, in\cdot D = 0 \tag{4.3}$$

by virtue of the analog of (3.19) for $\overline{\varphi}_{\bar{n}}$. Lastly, terms like

$$\overline{\hat{\xi}}_n i\not{D}_\perp \hat{\xi}_n = \overline{\hat{\xi}}_n i\not{D}_\perp P_n \hat{\xi}_n = \overline{\hat{\xi}}_n P_n i\not{D}_\perp \hat{\xi}_n = 0\,, \qquad\qquad \overline{\varphi}_{\bar{n}} i\not{D}_\perp \varphi_n = 0\,, \tag{4.4}$$

since $\bar{\xi}_n P_n = 0$ and $\bar{\varphi}_{\bar{n}} P_{\bar{n}} = 0$. These simiplifications leave us with the Lagrangian

$$\mathcal{L} = \overline{\hat{\xi}}_n \frac{\bar{\not{n}}}{2}\, in\cdot D\, \hat{\xi}_n + \overline{\varphi}_{\bar{n}} i\not{D}_\perp\, \hat{\xi}_n + \overline{\hat{\xi}}_n\, i\not{D}_\perp \varphi_{\bar{n}} + \overline{\varphi}_{\bar{n}} \frac{\not{n}}{2}\, i\bar{n}\cdot D\varphi_{\bar{n}}\,. \tag{4.5}$$

So far this is just QCD written in terms of the $\hat{\xi}_n$ and $\varphi_{\bar{n}}$ fields. However, the field $\varphi_{\bar{n}}$ corresponds to the spinor components which were subleading in the collinear limit. These spinor components will not show up in operators that mediate hard interactions at leading order. Therefore we will not need to consider a source term for $\varphi_{\bar{n}}$ in the path integral.[3] This means that we can simply perform the quadratic fermionic path integral over $\varphi_{\bar{n}}$. At tree level doing so is simply equivalent to imposing the full equation of motion for $\varphi_{\bar{n}}$. We find

$$\begin{aligned} 0 = \frac{\delta\mathcal{L}}{\delta\varphi_{\bar{n}}} \;:\qquad & \frac{\not{n}}{2}\, i\bar{n}\cdot D\varphi_{\bar{n}} + i\not{D}_\perp \xi_n = 0 \\ & i\bar{n}\cdot D\varphi_{\bar{n}} + \frac{\not{\bar{n}}}{2} i\not{D}_\perp \hat{\xi}_n = 0 \\ & \varphi_{\bar{n}} = \frac{1}{i\bar{n}\cdot D} i\not{D}_\perp \frac{\not{\bar{n}}}{2}\hat{\xi}_n\,, \end{aligned} \tag{4.6}$$

where the second line is obtained by multiplying the first by $\not{\bar{n}}/2$ on the left, and the plus sign in the last line comes from using $\not{\bar{n}} i\not{D}_\perp = -i\not{D}_\perp \not{\bar{n}}$. Plugging this result back into our Lagrangian, two terms cancel, and the other two terms give the Lagrangian for the $\hat{\xi}_n$ field

$$\mathcal{L} = \bar{\hat{\xi}}_n \left(in\cdot D + i\not{D}_\perp \frac{1}{i\bar{n}\cdot D} i\not{D}_\perp \right) \frac{\not{\bar{n}}}{2}\,\hat{\xi}_n\,. \tag{4.7}$$

The inverse derivative operator may look a little funny, but we can understand it in the same way we do for the operator $1/\hat{r}$ in quantum mechanics, namely by defining it through its eigenvalues, which in this case are in momentum space. Say we have the operator $\frac{1}{i\bar{n}\cdot\partial}$ acting on a field $\phi(x)$. Expressing this operation in momentum space gives

$$\frac{1}{i\bar{n}\cdot\partial}\phi(x) = \frac{1}{i\bar{n}\cdot\partial}\int d^4p e^{-ipx}\varphi(p) = \int d^4p e^{-ipx}\frac{1}{\bar{n}\cdot p}\varphi(p)\,, \tag{4.8}$$

and the eigenvalues $1/\bar{n}\cdot p$ define the inverse derivative operator.

Although we have a Lagrangian for $\hat{\xi}_n$ we are not yet done. In particular we have not yet separated the collinear and ultrasoft gauge fields, nor the corresponding momentum components. These remaining steps will be to

2. Separate the collinear and ultrasoft gauge fields.

3. Separate the collinear and usoft momentum components with a multipole expansion.

We then can expand in the fields and momenta and keep the leading pieces.

Step 2: Separate collinear and ultrasoft gauge fields

Recall that $A_n^\mu \sim (\lambda^2, 1, \lambda) \sim p_n^\mu$ and $A_n^\mu \sim (\lambda^2, \lambda^2, \lambda^2) \sim k_{us}^\mu$. Since $k_{us}^2 \ll p_n^2$ the ultrasoft gluons encode much longer wavelength fluctuations, so from the perspective of the collinear fields we can think of A_{us}^μ like a classical background field. In background field gauge we would write $A^\mu = Q^\mu + A_{cl}^\mu$ where Q^μ is the quantum gauge field and A_{cl}^μ is the classical background field that only appears on external lines. In general there is no need for a relationship between the full QCD gluon field A^μ and the SCET fields A_{us}^μ and A_n^μ, but if one exists then it does make matching computations much simpler. Based on the analogy

[3] At subleading order the coupling to the subleading components is introduced in operators via the combination involving ξ_n shown in the last line of Eq.(4.6), so there is still no reason to have a source term for $\varphi_{\bar{n}}$.

with a background gauge field you might not be too surprised to learn that a relation exists which encodes basic tree level matching

$$A^\mu = A_n^\mu + A_{us}^\mu + \cdots . \tag{4.9}$$

Here the ellipsis stand for additional terms involving Wilson lines which only will become relevant when we formulate power corrections, and hence will be ignorded for our leading order analysis here (they are given below in Eq.()). The interpretation of A_{us}^μ as a background field to ξ_n and A_n^μ will also prove useful when we derive the collinear gluon lagrangian and when we later consider gauge transformations in the theory.

Now, comparing the power counting between components of A_n^μ and A_{us}^μ, we find

$$\begin{aligned} \bar n\cdot A_n \sim \lambda^0 \gg \bar n\cdot A_{us} \sim \lambda^2 \\ A_{\perp\, n}^\mu \sim \lambda \gg A_{\perp\, us}^\mu \sim \lambda^2 \\ n\cdot A_n \sim \lambda^2 \sim n\cdot A_{us}. \end{aligned} \tag{4.10}$$

So we see that $A_{\perp\, us}^\mu$ and $\bar n\cdot A_{us}$ can be droped from our leading order analysis because in the combination $A_n^\mu + A_{us}^\mu$ they are always dominated by the collinear gluon term. Conversely, $n\cdot A_{us}$ cannot be dropped because it is of the same order as $n\cdot A_n$.

Step 3: The Multipole Expansion for Separating momenta

We want to find a way to isolate momenta that have different scaling with λ. Such a procedure is useful because it will allow us to formulate power corrections in a manner where operators give homogeneous contributions in λ order by order. For example, consider the denominator of the propagator of a quark with momentum $p_n + k_{us}$ expanded to keep the leading and first subleading terms

$$\begin{aligned} \frac{1}{(p_n+k_{us})^2} &= \frac{1}{(p_n^- + k_{us}^-)(p_n^+ + k_{us}^-) + (p_n^\perp + k_{us}^\perp)^2} \\ &= \frac{1}{p_n^-(p_n^+ + k_{us}^+) + p_n^{\perp\,2}} - \frac{2k_{us}^\perp\cdot p_n^\perp}{[p_n^-(p_n^+ + k_{us}^+) + p_n^{\perp\,2}]^2} + \ldots . \end{aligned} \tag{4.11}$$

By power counting, we see that the first term scales as λ^{-2} and the second term scales as λ^{-1}. Although the first term dominates the second, we need to be able to reproduce the second term at the level of the Lagrangian when higher order corrections are needed. Expressed more formally, we would like a systematic multipole expansion. Our desired expansion is similar to the one found in $E\&M$ which gives corrections to the electrostatic potential for a given charge distribution.

In position space the multipole expansion corresponds to expanding the long wavelength field, $A_{us}(x) = A_{us}(0) + x\cdot i\partial A_{us}(0) + \ldots$. To see what is going on here we can Fourier transform the operators (taking one-dimensional fields and ignoring indices for simplicity)

$$\begin{aligned} \int dx\ \bar\psi(x) A_{us}(0)\psi(x) &= \int dx \int dp_1\, dp_2\, dk\ e^{ip_1 x} e^{-ik(0)} e^{-ip_2 x}\ \bar\psi(p_1) A_{us}(k)\psi(p_2) \\ &= \int dp_1\, dp_2\, dk\ \delta(p_1 - p_2)\ \bar\psi(p_1) A_{us}(k)\psi(p_2). \end{aligned} \tag{4.12}$$

We see immediately that this corresponds to a 3-point Feynman rule where the small momentum k is ignored relative to the large momenta p_1 and p_2, and that total momentum is not conserved at the vertex. For the next order term we get

$$\int dx\ \bar\psi(x) x(i\partial A_{us})(0)\psi(x) = \int dp_1\, dp_2\, dk\ \delta'(p_1 - p_2)\ k\ \bar\psi(p_1) A_{us}(k)\psi(p_2). \tag{4.13}$$

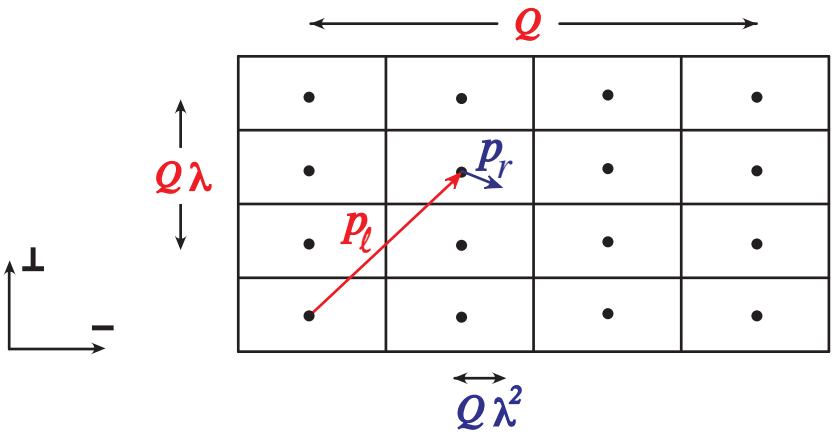

Figure 5: Grid to picture the separation of momenta into label and residual components.

Here the Feynman rule involves a $k\delta'(p_1 - p_2)$ and we must integrate by parts to obtain the multipole momentum conservation expressed by $\delta(p_1 - p_2)$. This integration by parts differentiates other parts of a diagram that carry this momentum, in particular the neighbouring propagators, which then would produce terms like the 2nd term in Eq. (4.11).

Since Feynman diagrams are almost always evaluated in momentum space it would be more convenient to have a multipole expansion formalism that avoids the step of going through position space. In the remainder of this section we will set up a formalism to achieve this. It will allow us to 1) simply derive the corresponding momentum space Feynman rules, 2) simplify the formulation of gauge transformations in the effective theory, and 3) incorporate the multipole expansion into propagators rather than vertices.

For the moment we only consider the quark part of the field $\hat{\xi}_n(x)$. We will add the anti-quark part later on. Computing the Fourier transform $\tilde{\xi}_n(p)$ of the quark part of our field we have

$$\tilde{\xi}_n(p) = \int d^4x\, e^{ip\cdot x}\, \hat{\xi}_n(x). \tag{4.14}$$

Now to separate momentum scales, we define our momentum p^μ to be a sum of a large momentum components p_ℓ^μ called the *label* momentum and a small momentum p_r^μ called the *residual* momentum.

$$\begin{aligned} p^\mu &= p_\ell^\mu + p_r^\mu \\ p_\ell^\mu &\sim Q(0, 1, \lambda) \\ p_r^\mu &\sim Q(\lambda^2, \lambda^2, \lambda^2) \end{aligned} \tag{4.15}$$

This decomposition is similar to the one found in HQET where the quark momentum is $p^\mu = m\, v^\mu + k^\mu$. Although at the end of the day all momenta will be continuous, it turns out that it is quite convenient for understanding the multipole expansion to interpret the p_ℓ as defining a grid of points, and the p_r as defining locations in the surrounding boxes. This expansion is only necessary for the p^- and $p^\perp$ momenta since there are no label p^+ momenta, so we have a grid as shown in Fig. 5 (for convenience we show only one of the $p_\perp^\mu$ components). Note that any momentum p^μ has a unique decomposition in terms of label and residual components. Since $p_\ell \gg p_r$ the spacing between grid points is always much larger than the spacing between points in a box. This setup has the advantage of allowing us to cleaning separate momentum scales in integrands, arranging things so every loop integrand is homogeneous in λ.

In practice the grid picture is a bit misleading, since actually the boxes are infinite and with momentum components (p_ℓ, p_r) we are really dealing with a product of continuous spaces $\mathbb{R}^3 \times \mathbb{R}^4/\mathcal{I}$ where $\mathcal{I}$ are a group of relations that remove redundancy order by order in λ. ($\mathcal{I}$ includes the set of RPI transformations that we will discuss later on.) Nevertheless it is very convenient to derive the rules for integrals on the label-residual space by working with a more familiar discrete label and continuous residual momentum picture, and then taking the continuum limit.

Thus if we are integrating the collinear momentum p over a certain region, we will write

$$\int d^4p \to \sum_{p_\ell \neq 0} \int d^4p_r \tag{4.16}$$

where we do not include $p_\ell = 0$ in the sum over all p_ℓ values, because $p_\ell = 0$ does not define a collinear momentum. Indeed the $p_\ell = 0$ bin corresponds to the ultrasoft modes. For an ultrasoft momentum p we simply have

$$\int d^4p \to \int d^4p_r \,. \tag{4.17}$$

With this momentum separation we can also label our fields by both components

$$\tilde{\xi}_n(p) \to \tilde{\xi}_{n,\,p_\ell}(p_r) \,. \tag{4.18}$$

We also have separate conservation laws for label and residual momenta

$$\int d^4x \; e^{i(p_\ell - q_\ell)\cdot x} \, e^{i(p_r - q_r)\cdot x} = \delta_{p_\ell, q_\ell} \; \delta^4(p_r - q_r)(2\pi)^4. \tag{4.19}$$

Every collinear field carries both label and residual momenta, they are both conserved at all vertices, but Feynman rules may depend on only one or the other of these components. For example, what was previously a nonconservation of momenta for an interaction between collinear and ultrasoft particles now becomes two separate conservations of momenta.

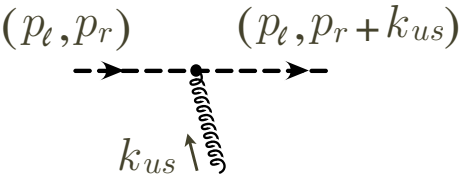

An example is shown in the figure above.

Finally, since all fields carry residual momenta the conservation law just corresponds to locality of the field theory with respect to the Fourier transformed variable $p_r \to x$. Therefore we transform the residual momenta back to position space to obtain our final collinear quark field

$$\xi_{n,p_\ell}(x) = \int \frac{d^4p_r}{(2\pi)^4} \, e^{-ip_r x} \, \tilde{\xi}_{n,\,p_\ell}(p_r) \,. \tag{4.20}$$

We will build operators using these fields. Altogether, the above steps allow us to rewrite our hatted collinear field $\hat{\xi}_n(x)$ as

$$\begin{aligned} \hat{\xi}_n(x) &= \int \frac{d^4p}{(2\pi)^4} \, e^{-ip\cdot x} \, \tilde{\xi}_n(p) = \sum_{p_\ell \neq 0} \int \frac{d^4p_r}{(2\pi)^4} \; e^{-ip_\ell \cdot x} e^{-ip_r \cdot x} \, \tilde{\xi}_{n,\,p_\ell}(p_r) \\ &= \sum_{p_l \neq 0} e^{-ip_\ell \cdot x} \, \xi_{n,\,p_\ell}(x) \,. \end{aligned} \tag{4.21}$$

We can identify several facts about label conservation for the field $\xi_{n,p_\ell}(x)$

- Interactions with ultrasoft gluons or quarks leave the label momenta of collinear fields conserved.
- Interactions with collinear gluons or quarks will change label momenta.
- The label n for the collinear direction is preserved by both ultrasoft and collinear interactions. Only a hard (external) interaction can couple fields with different collinear directions.

Now that we have separated momentum scales in our fields we would like to do the same with derivatives that act on these fields. Since $\xi_{n,\,p_\ell}(x)$ contains only residual momenta, we know that

$$i\partial_\mu \xi_{n,\,p_\ell}(x) \sim \lambda^2 \xi_{n,\,p_\ell}(x). \tag{4.22}$$

We also define a label momentum operator such that

$$\mathcal{P}^\mu \xi_{n,\,p_\ell}(x) \equiv p_\ell^\mu \xi_{n,\,p_\ell}(x). \tag{4.23}$$

Recall that $\mathcal{P}^\mu$ and p_ℓ^μ only contains the components $\overline{\mathcal{P}} \equiv \bar{n}\cdot\mathcal{P} \sim p_\ell^- \sim \lambda^0$ and $\mathcal{P}_\perp^\mu \sim p_\ell^{\perp\mu} \sim \lambda$. Therefore we have $n\cdot\mathcal{P} = 0$. Also

$$i\bar{n}\cdot\partial \ll \overline{\mathcal{P}}\,, \qquad\qquad i\partial_\perp^\mu \ll \mathcal{P}_\perp^\mu\,. \tag{4.24}$$

The main advantage of the label operator is that it provides a definite power counting for derivatives. It is also notationally friendly in that it removes the necessity of a label sum. We can see this by rewriting our field $\hat{\xi}_n(x)$ in terms of label momenta

$$\begin{aligned}\hat{\xi}_n(x) &= \sum_{p_\ell\neq 0} e^{-ip_\ell\cdot x}\,\xi_{n,p_\ell}(x) \\ &= e^{-i\mathcal{P}\cdot x}\sum_{p_\ell\neq 0}\xi_{n,p_\ell}(x) \\ &\equiv e^{-i\mathcal{P}\cdot x}\xi_n(x)\,.\end{aligned} \tag{4.25}$$

In the last line we defined $\xi_n(x) = \sum_{p_l\neq 0}\xi_{n,\,p_l}$. Since the label operator allows us to encode the phase factor involving label momenta as an operator, we can suppress the momentum labels on our collinear fields if there is no reason to make them explicit. For field products we have

$$\hat{\xi}_n(x)\hat{\xi}_n(x) = e^{-i\mathcal{P}\cdot x}\xi_n(x)\xi_n(x) \tag{4.26}$$

where the label operator acts on both fields. Consequently, conservation of label momenta is simply encoded by this phase factor and is manifest at the level of operators.

Lastly, we must deal with anti-particles and gluons. For the anti-particles, we expand our Dirac field into two parts

$$\begin{aligned}\psi(x) &= \int d^4p\,\delta(p^2)\theta(p^0)\big[u(p)a(p)e^{-ip\cdot x} + v(p)b^\dagger(p)e^{ip\cdot x}\big] \\ &= \psi^+(x) + \psi^-(x)\end{aligned} \tag{4.27}$$

we then associate each part with a collinear field and expand as a sum over label momenta.

$$\begin{aligned}\psi^+ \longrightarrow \hat{\xi}_n^+(x) &= \sum_{p_l\neq 0} e^{-ip_\ell\cdot x}\xi_{n,\,p_\ell}^+(x)\,, \\ \psi^- \longrightarrow \hat{\xi}_n^-(x) &= \sum_{p_\ell\neq 0} e^{ip_\ell\cdot x}\xi_{n,\,p_\ell}^-(x)\,,\end{aligned} \tag{4.28}$$

where both have a $\theta(p_\ell^0) = \theta(\bar{n}\cdot p_\ell)$. Because of charge conjugation symmetry it is convenient to combine the particle and anti-particle fields back into a single field. In order to do this we have to deal with the opposite signs for their phase. To do this we define

$$\xi_{n,\,p_\ell}(x) \equiv \xi^+_{n,\,p_\ell}(x) + \xi^-_{n,\,-p_\ell}(x) \tag{4.29}$$

where p_ℓ has either sign, but one picks out particles and one picks out antiparticles. Thus the action of the fields ξ_{n,p_ℓ} and $\bar{\xi}_{n,p_\ell}$ is that for

$$\begin{aligned} \bar{n}\cdot p_\ell > 0 \;:&\qquad \text{a particle is destroyed or created} \\ \bar{n}\cdot p_\ell < 0 \;:&\qquad \text{an antiparticle is created or destroyed} \end{aligned}$$

The sign convention for the label momentum is easy to remember since it is in the same direction as the fermion number flow. With this definition, we still define $\xi_n(x) = \sum_{p_\ell\neq 0}\xi_{n,p_\ell}(x)$ and write

$$\hat{\xi}_n(x) = e^{-i\mathcal{P}\cdot x}\xi_n(x)\,, \tag{4.30}$$

and all the manipulations we were making with particle fields carry through for the fields that have both particles and antiparticles. For collinear gluons, we proceed analogously to find

$$\hat{A}^\mu_n = \sum_{q_\ell\neq 0} e^{-iq_\ell\cdot x}A^\mu_{n,q_\ell} = e^{-i\mathcal{P}\cdot x}A^\mu_n(x) \tag{4.31}$$

where

$$A^\mu_n(x) = \sum_{q_\ell\neq 0} A^\mu_{n,\,q_\ell}. \tag{4.32}$$

Since the gluon field $A^\mu_n = A^{\mu A}_n T^A$ where $A^{\mu A}_n(x)$ is real we also have

$$[A^{\mu A}_{n,q_\ell}(x)]^* = A^{\mu A}_{n,-q_\ell}(x)\,. \tag{4.33}$$

Once again for $q^-_\ell > 0$ the field A_{n,q_ℓ} destroys a gluon, while for $q^-_\ell < 0$ it creates a gluon.

With our conventions the action of the label operator on a bunch of labelled fields is

$$\mathcal{P}^\mu(\phi^\dagger_{q_1}\phi^\dagger_{q_2}\cdots\phi_{p_1}\phi_{p_2}\cdots) = (p_1^\mu + p_2^\mu + \cdots - q_1^\mu - q_2^\mu - \cdots)(\phi^\dagger_{q_1}\phi^\dagger_{q_2}\cdots\phi_{p_1}\phi_{p_2}\cdots). \tag{4.34}$$

Thus it gives a minus sign when acting on daggered fields. It is also useful to note that if we differentiate an arbitrary collinear field $\hat{\phi}_n(x)$ that it yields

$$\begin{aligned} i\partial^\mu\hat{\phi}_n(x) &= i\partial_\mu\sum_{p\neq 0} e^{-ip\cdot x}\phi_{n,\,p}(x) \\ &= \sum_{p\neq 0} e^{-ip\cdot x}(\mathcal{P}^\mu + i\partial^\mu)\phi_{n,\,p}(x) \\ &= e^{-i\mathcal{P}\cdot x}(\mathcal{P}^\mu + i\partial^\mu)\phi_n(x). \end{aligned} \tag{4.35}$$

In the last line, we can suppress the exponent if we assume that label momenta are always conserved. Effectively, by introducing the label operator we have replaced the ordinary derivative operation by

$$i\partial^\mu\hat{\phi}_n(x) \to (\mathcal{P}^\mu + i\partial^\mu)\phi_n(x). \tag{4.36}$$

Final Result: Expand and put pieces together

At last, we may construct our final leading order Lagrangian. We begin with the result in Eq. (4.7). By introducing label operators, we can expand the derivative in powers of λ as

$$\begin{aligned} in\cdot D &= in\cdot\partial + gn\cdot A_n + gn\cdot A_{us} \\ iD_\perp &= \underbrace{(\mathcal{P}_\perp^\mu + gA_{n\perp}^\mu)}_{\sim\lambda} + \underbrace{(i\partial_\perp^\mu + gA_{\perp,\,us}^\mu)}_{\sim\lambda^2} + \cdots \\ i\bar n\cdot D &= \underbrace{(\overline{\mathcal{P}} + g\bar n\cdot A_n)}_{\sim\lambda^0} + \underbrace{(i\bar n\cdot\partial + g\bar n\cdot A_{us})}_{\sim\lambda^2} + \cdots \end{aligned} \tag{4.37}$$

where the ellipses again denote additional $\sim\lambda^2$ terms that can be dropped in our leading order analysis (but later on we will see are required by gauge symmetry when considering power suppressed operators). This allows us to write at leading power

$$\begin{aligned} iD^\mu &= i\partial_n^\mu + gA_n^\mu + \frac{\bar n^\mu}{2} gn\cdot A_{us} \\ &\equiv iD_n^\mu + \frac{\bar n^\mu}{2} gn\cdot A_{us} \\ &\equiv iD_{ns}^\mu\,, \end{aligned} \tag{4.38}$$

where the n-collinear derivative operator is

$$i\partial_n^\mu \equiv \overline{\mathcal{P}}\frac{n^\mu}{2} + \mathcal{P}_\perp^\mu + in\cdot\partial\frac{\bar n^\mu}{2}\,. \tag{4.39}$$

For later convenience we also define a collinear derivative including the leading ultrasoft gauge field

$$i\partial_{ns}^\mu \equiv i\partial_n^\mu + \frac{\bar n^\mu}{2} gn\cdot A_{us}\,. \tag{4.40}$$

Dropping the hat on the collinear quark fields and keeping only the lowest order terms, we have the following quark Lagrangian

$$\mathcal{L}_{n\xi}^{(0)} = e^{-ix\cdot\mathcal{P}}\;\bar\xi_n\Big(in\cdot D_{ns} + i\not{D}_{n\perp}\frac{1}{i\bar n\cdot D_n}i\not{D}_{n\perp}\Big)\frac{\bar{\not n}}{2}\,\xi_n\,, \tag{4.41}$$

Dropping the exponential factor that enforces label momentum conservation, we write the collinear quark Lagrangian in its final form

$$\boxed{\mathcal{L}_{n\xi}^{(0)} = \bar\xi_n\Big(in\cdot D_{ns} + i\not{D}_{n\perp}\frac{1}{i\bar n\cdot D_n}i\not{D}_{n\perp}\Big)\frac{\bar{\not n}}{2}\,\xi_n}\,, \tag{4.42}$$

Note the following interesting facts about this Lagrangian:

- Both terms with covariant derivatives in the $(\cdots)$ in $\mathcal{L}_{n\xi}^{(0)}$ are of order λ^2 so the leading order Lagrangian is order λ^4 (recalling that the fields scale as $\xi_n\sim\lambda$). Since for a Lagrangian with collinear fields $\int d^4x\sim\lambda^{-4}$ this gives us an action that is $\sim\lambda^0$ as desired. The superscript (0) on the Lagrangian denotes this power counting for the action.
- All fields are defined at x, and derivatives for this coordinate scale as $i\partial^\mu\sim\lambda^2$ so the action is explicitly local at the scale $Q\lambda^2$.

- The action is also local at the scale of $\mathcal{P}_\perp^\mu \sim Q\lambda$ since these derivatives occur in the numerator. It only has non-locality at the hard scale through the inverse $\overline{\mathcal{P}} \sim \lambda^0$. The fact that there is locality except at the hard scale is a key feature of $\mathrm{SCET_I}$. Some attempts to tweak the formalism described here, in order to simplify SCET, lead to actions that are non-local at the small scale $\sim \lambda^2$ because they integrate out some onshell particles, while leaving other onshell particles to be described by an action. We will avoid doing this, taking the attitude that low energy locality is a desired property for the effective field theory.

- The collinear Lagrangian above can be written by (re)introducing an auxiliary field φ_n

$$\mathcal{L}_{n\xi}^{(0)} = e^{-ix\cdot\mathcal{P}}\,\overline{\Xi}_n i\not{D}_{ns}\,\Xi_n\,, \qquad\qquad \Xi_n \equiv \begin{pmatrix} \xi_n \\ \varphi_{\bar n} \end{pmatrix}, \tag{4.43}$$

  since integrating out $\varphi_{\bar n}$ exactly reproduces Eq.(4.42). In the absence of the ultrasoft gluon field the covariant derivative D_{ns} is equal to the collinear derivative D_n, such that the Lagrangian is the same as the full QCD Lagrangian, with the only difference being that a particular direction n has been singled out. Thus, in situations where ultrasoft gluons don't matter, and one only considers a single direction n, the collinear Lagrangian can be replaced by the full QCD Lagrangian.

The computation of the propagator from $\mathcal{L}_{n\xi}^{(0)}$ is also greatly simplified without the need for any additional power counting. Specifically, Eq. (4.42) gives the collinear quark propagator

$$\frac{i\not{n}}{2}\frac{\bar n\cdot p_\ell}{(\bar n\cdot p_\ell)(n\cdot p_r)+(p_{\ell\perp})^2+i0}\,. \tag{4.44}$$

This gives the correct propagator in different situations without having to make further expansions. This is important to ensure that the leading order Lagrangian strictly give $\mathcal{O}(\lambda^0)$ terms, while subleading Lagrangians (and operators) will be responsible for power corrections. For example, if we have an interaction with an ultrasoft gluon then

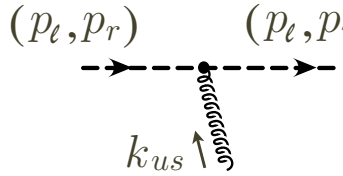

$$= \frac{i\not{n}}{2}\frac{\bar n\cdot p_\ell}{(\bar n\cdot p_\ell)(n\cdot p_r + n\cdot k_{us})+(p_{\ell\perp})^2+i0}\,, \tag{4.45}$$

while if we have an interaction with a collinear gluon then

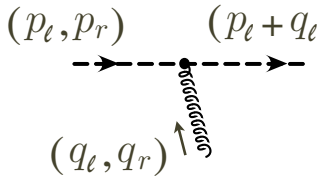

$$= \frac{i\not{n}}{2}\frac{(\bar n\cdot p_\ell + \bar n\cdot q_\ell)}{(\bar n\cdot p_\ell + \bar n\cdot q_\ell)(n\cdot p_r + n\cdot q_r)+(p_{\ell\perp}+q_{\ell\perp})^2+i0}\,. \tag{4.46}$$

4.2 Wilson Line Identities

With the label operator formalism there are several neat identities that we can derive for Wilson lines. In particular we can show that all occurences of the field $\bar n\cdot A_n$ can always be entirely replaced by the Wilson

line W_n. As an example we will show how this is done for the Lagrangian $\mathcal{L}^{(0)}_{n\xi}$. In position space the defining equations for a Wilson line are $W(x,x)=1$ and its equation of motion, which we can transform to momentum space

$$\begin{aligned} i\bar{n}\cdot D_x W(x,-\infty) &= 0 \qquad \text{(position space)} \\ &\Downarrow \text{Fourier Transform} \\ i\bar{n}\cdot D_n W_n &= (\overline{\mathcal{P}} + g\bar{n}\cdot A_n) W_n = 0\,. \end{aligned} \tag{4.47}$$

With this definition, the action of $i\bar{n}\cdot D_n$ on a product of W_n and some arbitrary operator is

$$\begin{aligned} i\bar{n}\cdot D_n(W_n\mathcal{O}) &= (\overline{\mathcal{P}} + g\bar{n}\cdot A_n) W_n\mathcal{O} \\ &= \big[(\overline{\mathcal{P}} + g\bar{n}\cdot A_n) W_n\big]\mathcal{O} + W_n\overline{\mathcal{P}}\mathcal{O} \\ &= W_n\overline{\mathcal{P}}\mathcal{O} \end{aligned} \tag{4.48}$$

So we have the operator equation

$$i\bar{n}\cdot D_n W_n = W_n\overline{\mathcal{P}} \tag{4.49}$$

and with $W_n^\dagger W_n = 1$ we have

$$i\bar{n}\cdot D_n = W_n\overline{\mathcal{P}}W_n^\dagger\,, \qquad\qquad \overline{\mathcal{P}} = W_n^\dagger i\bar{n}\cdot D_n W_n\,, \tag{4.50}$$

as operator identities. Since by collinear gauge invariance we can always group $\bar{n}\cdot A_n$ with $\overline{\mathcal{P}}$ to give $i\bar{n}\cdot D_n$, the first identity implies that we can always swap $\bar{n}\cdot A_n$ for the Wilson line W_n. Inverting these results also gives useful operator identities

$$\frac{1}{i\bar{n}\cdot D_n} = W_n\frac{1}{\overline{\mathcal{P}}}W_n^\dagger\,, \qquad\qquad \frac{1}{\overline{\mathcal{P}}} = W_n^\dagger\frac{1}{i\bar{n}\cdot D_n}W_n\,. \tag{4.51}$$

The first relation allows us to rewrite $\mathcal{L}^{(0)}_{n\xi}$ as

$$\mathcal{L}^{(0)}_{n\xi} = e^{-ix\cdot\mathcal{P}}\;\bar{\xi}_n\Big(in\cdot D_{ns} + i\not{D}_{n\perp}W_n\frac{1}{\overline{\mathcal{P}}}W_n^\dagger i\not{D}_{n\perp}\Big)\frac{\not{\bar{n}}}{2}\,\xi_n\,. \tag{4.52}$$

It is also useful to note that we can use the label operator to write a tidy expression for the Wilson line which is built from fields that carry both label and residual momenta:

$$W_n(x) = \Big[\sum_{\text{perms}}\exp\Big(\frac{-g}{\overline{\mathcal{P}}}\bar{n}\cdot A_n(x)\Big)\Big]\,. \tag{4.53}$$

4.3 SCET$_{\rm I}$ Collinear Gluon and Ultrasoft Lagrangians

To derive the collinear gluon Lagrangian, we treat usoft and collinear degrees of freedom separately by letting A^μ_{us} represent a background field with respect to A^μ_n. We begin with the gluon Lagrangian from QCD:

$$\mathcal{L} = \underbrace{-\frac{1}{2}\mathrm{Tr}\big\{G^{\mu\nu}G_{\mu\nu}\big\}}_{\text{Gauge Kinetic Term}} + \underbrace{\tau\mathrm{Tr}\{(i\partial_\mu A^\mu)^2\big\}}_{\text{Gauge Fixing Term}} + 2\underbrace{\mathrm{Tr}\big\{\bar{c}\,i\partial_\mu[iD^\mu,c]\big\}}_{\text{Ghost Term}} \tag{4.54}$$

where $G^{\mu\nu} = \frac{i}{g}[D^\mu, D^\nu]$. Here we are using a notation with fundamental color matrices, $G_{\mu\nu} = G^A_{\mu\nu} T^A$, $c = c^A T^A$, etc., and recall that $\mathrm{Tr}(T^A T^B) = T_F \delta^{AB} = \delta^{AB}/2$. Expanding the covariant derivative as we did in the quark sector we keep only the leading order terms. For a covariant derivative acting on collinear fields the leading order terms are

$$iD^\mu \to iD^\mu_{ns} \equiv \frac{n^\mu}{2}(\overline{\mathcal{P}} + g\bar{n}\cdot A_n) + (\mathcal{P}^\mu_\perp + gA^\mu_{\perp,n}) + \frac{\bar{n}^\mu}{2}(in\cdot\partial + gn\cdot A_n + gn\cdot A_{us}). \tag{4.55}$$

Recall that the field A^μ_{us} varys much more slowly than A^μ_n, so we can think of A^μ_{us} as a background field from the perspective of the collinear fields (even though it is a quantum field in its own right). The gauge fixing and ghost terms for the collinear Lagrangian should break the collinear gauge symmetry, but we do not want them to gauge fix the ultrasoft gluons, and hence they should be covariant with respect to the A^μ_{us} connection. Since by power counting only the $n\cdot A_{us}$ gluon can appear along with the collinear gluons A^μ_n, only this component is needed. Therefore we replace $i\partial^\mu \to i\partial^\mu_{ns}$ for all the ordinary derivatives in Eq. (4.54) where

$$i\partial^\mu_{ns} \equiv \frac{n^\mu}{2}\overline{\mathcal{P}} + \mathcal{P}^\mu_\perp + \frac{\bar{n}^\mu}{2} in\cdot\partial + \frac{\bar{n}^\mu}{2} gn\cdot A_{us}. \tag{4.56}$$

The resulting leading order collinear gluon Lagrangian is then

$$\boxed{\mathcal{L}^{(0)}_{ng} = \frac{1}{2g^2}\mathrm{Tr}\Big\{([iD^\mu_{ns}, iD^\nu_{ns}])^2\Big\} + \tau\mathrm{Tr}\Big\{([i\partial^\mu_{ns}, A_{n\,\mu}])^2\Big\} + 2\mathrm{Tr}\Big\{\bar{c}_n[i\partial_{ns\mu}, [iD^\mu_{ns}, c_n]]\Big\}.} \tag{4.57}$$

For the Langrangian with only ultrasoft quarks and ultrasoft gluons, at lowest order we simply have the QCD actions. Using a general covariant gauge for the ultrasoft gluon field we therefore can write

$$\boxed{\mathcal{L}^{(0)}_{us} = \overline{\psi}_{us} i\not{D}_{us}\psi_{us} - \frac{1}{2}\mathrm{Tr}\Big\{G^{\mu\nu}_{us}G^{us}_{\mu\nu}\Big\} + \tau_{us}\mathrm{Tr}\Big\{(i\partial_\mu A^\mu_{us})^2\Big\} + 2\mathrm{Tr}\Big\{\bar{c}_{us}\, i\partial_\mu iD^\mu_{us} c_{us}\Big\}},\tag{4.58}$$

where $iD^\mu_{us} = i\partial_\mu + A^\mu_{us}$. All the terms in $\mathcal{L}^{(0)}$ have a power counting of $\mathcal{O}(\lambda^8)$, but we subtract 8 for the ultrasoft measure d^4x which is why we label the Lagrangian as (0). Note that the choice of gauge fixing parameters τ and τ_{us} for the collinear and ultrasoft gluons are independent, which is related to the fact that there are independent gauge symmetries that define these connections.

All together this allows us to write down the full leading order $\mathrm{SCET_I}$ Lagrangian with a single set of quark and gluon collinear modes in the n direction, and quark and gluon ultrasoft modes,

$$\mathcal{L}^{(0)} = \mathcal{L}^{(0)}_{n\xi} + \mathcal{L}^{(0)}_{ng} + \mathcal{L}^{(0)}_{us}\,. \tag{4.59}$$

4.4 Feynman Rules for Collinear Quarks and Gluons

For convenience we summarize some of the Feynman rules that follow from the collinear quark and gluon Lagrangians. We do not show the purely ultrasoft interactions which are identical to those of QCD, nor do we show the purely collinear gluon interactions which are also identical to those of QCD.

The Feynman rules that follow from the leading order collinear quark Lagrangian are shown in Fig. 6 where each collinear line carries momenta (p, p_r) with label momenta $p^\mu = \bar{n}\cdot p\, n^\mu/2 + p^\mu_\perp$ and residual momentum p^μ_r. Only one momentum p or p' is indicated for lines where the Feynman rule depends only on the label momentum. For the collinear quark propagator we have contributions from both quarks and antiquarks which give:

$$\frac{i\not{n}}{2}\frac{\theta(\bar{n}\cdot p)}{n\cdot p_r + \frac{p_\perp^2}{\bar{n}\cdot p} + i0} + \frac{i\not{n}}{2}\frac{\theta(-\bar{n}\cdot p)}{n\cdot p_r + \frac{p_\perp^2}{\bar{n}\cdot p} - i0} = \frac{i\not{n}}{2}\frac{\bar{n}\cdot p}{\bar{n}\cdot p\, n\cdot p_r + p_\perp^2 + i0} \tag{4.60}$$

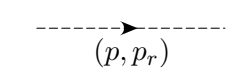

$$= \; i\,\frac{\bar{n}\!\!\!/}{2}\,\frac{\bar{n}\cdot p}{n\cdot p_r\,\bar{n}\cdot p + p_\perp^2 + i0}$$

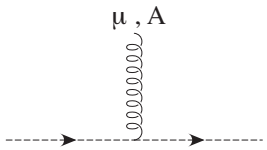

$$= ig\,T^A\,n_\mu\,\frac{\bar{n}\!\!\!/}{2}$$

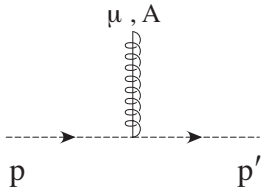

$$= ig\,T^A\left[n_\mu + \frac{\gamma_\mu^\perp p\!\!\!/_\perp}{\bar{n}\cdot p} + \frac{p\!\!\!/'_\perp \gamma_\mu^\perp}{\bar{n}\cdot p'} - \frac{p\!\!\!/'_\perp p\!\!\!/_\perp}{\bar{n}\cdot p\,\bar{n}\cdot p'}\bar{n}_\mu\right]\frac{\bar{n}\!\!\!/}{2}$$

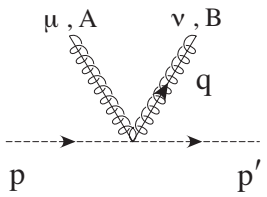

$$= \frac{ig^2\,T^A\,T^B}{\bar{n}\cdot(p-q)}\left[\gamma_\mu^\perp\gamma_\nu^\perp - \frac{\gamma_\mu^\perp p\!\!\!/_\perp}{\bar{n}\cdot p}\bar{n}_\nu - \frac{p\!\!\!/'_\perp\gamma_\nu^\perp}{\bar{n}\cdot p'}\bar{n}_\mu + \frac{p\!\!\!/'_\perp p\!\!\!/_\perp}{\bar{n}\cdot p\,\bar{n}\cdot p'}\bar{n}_\mu\bar{n}_\nu\right]\frac{\bar{n}\!\!\!/}{2}$$

$$+ \frac{ig^2\,T^B\,T^A}{\bar{n}\cdot(q+p')}\left[\gamma_\nu^\perp\gamma_\mu^\perp - \frac{\gamma_\nu^\perp p\!\!\!/_\perp}{\bar{n}\cdot p}\bar{n}_\mu - \frac{p\!\!\!/'_\perp\gamma_\mu^\perp}{\bar{n}\cdot p'}\bar{n}_\nu + \frac{p\!\!\!/'_\perp p\!\!\!/_\perp}{\bar{n}\cdot p\,\bar{n}\cdot p'}\bar{n}_\mu\bar{n}_\nu\right]\frac{\bar{n}\!\!\!/}{2}$$

Figure 6: Order λ^0 Feynman rules: collinear quark propagator with label p and residual momentum p_r, and collinear quark interactions with one soft gluon, one collinear gluon, and two collinear gluons respectively.

The Feynman rules between collinear gluons and ultrasoft gluons are shown in Fig. 7 with a collinear gluon in background field gauge that is ultrasoft covariant and specified by the parameter τ.

4.5 SCET$_{\rm II}$ Lagrangian

Define $i\partial_s^\mu = \frac{n^\mu}{2} i\bar{n}\cdot\partial + \frac{\bar{n}^\mu}{2} n\cdot\mathcal{P} + \mathcal{P}_\perp^\mu$ In SCET$_{\rm II}$ the scaling of the collinear and soft fields is given by

$$p_n \sim Q(1, \lambda^2, \lambda)\,, \qquad\qquad p_s \sim Q(\lambda, \lambda, \lambda)\,, \tag{4.61}$$

such that

$$p_n^2 \sim p_s^2 \sim Q^2\lambda^2\,. \tag{4.62}$$

However, the sum of a soft and collinear momentum scales as

$$p_n + p_s \sim Q(1, \lambda, \lambda) \quad \Rightarrow \quad (p_n + p_s)^2 \sim Q^2\lambda\,. \tag{4.63}$$

Since this combined momentum is more off-shell than the degrees of freedom in SCET$_{\rm II}$, there can be no coupling between collinear and soft fields in SCET$_{\rm II}$. Thus, the two Lagrangians completely decouple.

The leading order collinear Lagrangian is the same as the collinear Lagrangian in SCET$_{\rm I}$, with the only difference being that the coupling to the soft gluon is absent. This gives for the collinear quark Lagrangian

$$\boxed{\mathcal{L}_{n\xi}^{(0)} = \bar{\xi}_n\Big(in\cdot D_n + i\not{D}_{n\perp}\frac{1}{i\bar{n}\cdot D_n}i\not{D}_{n\perp}\Big)\frac{\bar{n}\!\!\!/}{2}\,\xi_n}\,, \tag{4.64}$$

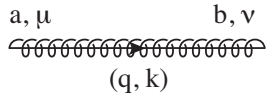

$$= \frac{-i}{\bar{n}\cdot q\, n\cdot k + q_\perp^2 + i0}\left(g_{\mu\nu} - (1-\tau)\frac{q_\mu q_\nu}{\bar{n}\cdot q\, n\cdot k + q_\perp^2}\right)\delta_{a,b}$$

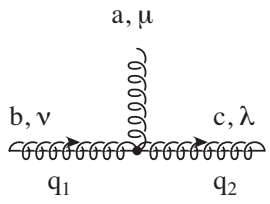

$$= g f^{abc} n_\mu \left\{\bar{n}\cdot q_1\, g_{\nu\lambda} - \tfrac{1}{2}(1-\tfrac{1}{\tau})[\bar{n}_\lambda q_{1\nu} + \bar{n}_\nu q_{2\lambda}]\right\}$$

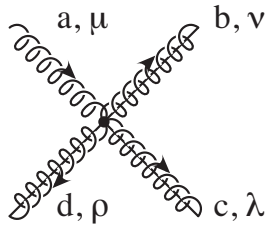

$$= -\tfrac{1}{2} i g^2 n_\mu \Big\{ f^{abe} f^{cde}(\bar{n}_\lambda g_{\nu\rho} - \bar{n}_\rho g_{\nu\lambda}) + f^{ade} f^{bce}(\bar{n}_\nu g_{\lambda\rho} - \bar{n}_\lambda g_{\nu\rho}) + f^{ace} f^{bde}(\bar{n}_\nu g_{\lambda\rho} - \bar{n}_\rho g_{\nu\lambda}) \Big\}$$

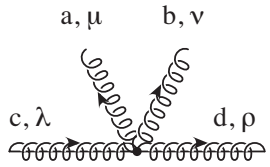

$$= \tfrac{1}{4} i g^2 n_\mu n_\nu \bar{n}_\rho \bar{n}_\lambda (1-\tfrac{1}{\alpha})\left\{ f^{ace} f^{bde} + f^{ade} f^{bce}\right\}$$

Figure 7: Collinear gluon propagator with label momentum q and residual momentum k, and the order λ^0 interactions of collinear gluons with the usoft gluon field. Here usoft gluons are springs, collinear gluons are springs with a line, and τ is the covariant gauge fixing parameter in Eq. (4.57).

while for the collinear gluon Lagrangian one finds

$$\boxed{\mathcal{L}_{ng}^{(0)} = \frac{1}{2g^2}\mathrm{Tr}\Big\{([iD_{n\,\mu}, iD_n^\nu])^2\Big\} + \tau\mathrm{Tr}\Big\{([i\partial_n^\mu, A_{n\,\mu}])^2\Big\} + 2\,\mathrm{Tr}\Big\{\bar{c}_n\,[i\partial_{n\,\mu}, [iD_n^\mu, c_n]]\Big\}}\,. \tag{4.65}$$

The soft Lagrangian is identical to the ultrasoft Lagrangian

$$\boxed{\mathcal{L}_s^{(0)} = \overline{\psi}_s i\not{D}_s \psi_s - \frac{1}{2}\mathrm{Tr}\Big\{G_s^{\mu\nu} G_{\mu\nu}^s\Big\} + \tau_s \mathrm{Tr}\Big\{(i\partial_\mu A_s^\mu)^2\Big\} + 2\mathrm{Tr}\Big\{\bar{c}_s\, i\partial_\mu i D_s^\mu c_s\Big\}}\,, \tag{4.66}$$

4.6 Rules for Combining Label and Residual Momenta in Amplitudes

In practical calculations the grid picture in Fig. 5 is not to be taken literally. Doing so would correspond to using a Wilsonian EFT with finite cutoff's (edges for the grid boxes) that distinguish the size of momenta. Instead of this, we need to use a Continuum EFT picture where the EFT modes have propagators that extend over all momenta, but integrands which obtain their key contribution from the momentum region these modes are built to describe. The terms needed to correct the (otherwise incorrect) ultraviolet contributions of the resulting Continuum EFT are included as perturbative Wilson coefficients for low energy operators. The Wilsonian and Continuum versions of EFT are really two different pictures of the same thing, in much the same way that two different renormalization schemes may represent the

physics in different ways, but in the end still do encode the same physics. Nevertheless there are many practical advantages to the Continuum EFT framework, and it makes setting up SCET much easier. In particular it allows us to use regulators like dimensional regularization which naturally preserve spacetime and gauge symmetries. To setup up SCET in this continuum framework we need to understand how the redundancy $\mathcal{I}$ in the label-residual momentum space $\mathbb{R}^{d-1} \times \mathbb{R}^d/\mathcal{I}$ (for the case with d-dimensions) is resolved, given a pair of momenta components $(p_\ell, p_r) \in \mathbb{R}^{d-1} \times \mathbb{R}^d$. The upshot is that in the simplest cases the residual momentum can simply be dropped or absorbed into a label momentum in the same direction (making it continuous), while in the most complicated cases the formalism leads to so-called 0-bin subtractions for collinear integrands. These subtractions ensure that the collinear modes do not double count an IR region that is already properly included from an ultrasoft integrand. For future convenience we list the rules in this section, but caution the reader that some parts of this section are best understood when read together with one of the one-loop examples from section 7, and also after having read the discussion of the reparameterization invariance symmetry in section 5.3 that describes the redundancy $(p_\ell^\mu) + (p_r^\mu) = (p_\ell^\mu + \beta^\mu) + (p_r^\mu - \beta^\mu)$ which specifies $\mathcal{I}$.

For an arbitrary tree level diagram in SCET we will have some set of external lines that are either ultrasoft or collinear (and either in the initial or final state), and also a set of collinear and ultrasoft propagators. For the external lines that are ultrasoft we have only residual momenta k_{us}^μ and the onshell condition $k_{us}^2 = 0$. For the external lines that are collinear it suffices to take label momenta $p_\ell^- = \bar{n} \cdot p_\ell$ and $p_{\ell\perp}^\mu$, and a single residual momentum p_r^+. This amounts to picking β^μ above to contain the full p_r^- and $p_{r\perp}^\mu$ components. The onshell condition for the collinear particles is then simply $p_\ell^- p_r^+ - \vec{p}_{\ell\perp}^{\,2} = 0$. All propagators for intermediate collinear and ultrasoft lines are then simply determined by momentum conservation as usual. At leading order in λ this perscription for tree diagrams simply amounts to the same thing as dropping any ultrasoft momentum components k_{us}^- and $k_{us}^\perp$ from collinear propagators, though of course these momenta can still appear within ultrasoft propagators. At higher orders in λ these ultrasfot momentum components can also appear from collinear propagators through Lagrangian insertions, which yield terms like the second one in Eq. (4.11).

For loop diagrams and loop integrations we need several rules for operations on the label-residual momentum space. Internal collinear lines should be considered as carrying loop momenta with two parts $q = (q_\ell, q_r)$, while ultrasoft propagators only carry loop momenta k_r. There is a seperate momentum conservation for the label and residual momenta. After using momentum conservation we have label momenta from either external collinear particles or collinear loops, and residual momenta for external ultrasoft particle, external collinear particles from p_r^+, and from collinear and ultrasoft loops.

First we note that if we integrate over all label momenta q_ℓ and residual momenta q_r that this will be equal to an integration over all of the q^μ momentum space, since it does not depend on how we divide the momentum into the two components. For notational convenience we denote the label space integration as a sum rather than an integral. In d-dimensions we have

$$\sum_{q_\ell} \int d^d q_r = \int d^d q \,, \tag{4.67}$$

where we have recombined the label and residual momenta for the minus components, and the $(d-2)$ $\perp$-components. This is relevant for combining the two collinear loop integrations back into a single d-dimensional integration. In particular at leading order in λ after having used momentum conservation there will always be one q_r^μ for each collinear loop integration, where q_r^- and $q_r^\perp$ do not appear in any collinear or ultrasoft propagator, and hence not in the integrand $F(q_\ell^-, q_\ell^\perp, q_r^+)$. We can therefore use this

residual momentum integration in Eq. (4.67) to obtain a full integration

$$1)^{\text{naive}}: \quad \sum_{q_\ell} \int d^d q_r \, F(q_\ell^-, q_\ell^\perp, q_r^+) = \sum_{q_\ell} \int d^d q_r \, F(q_\ell^- + q_r^-, q_\ell^\perp + q_r^\perp, q_r^+) = \int d^d q \, F(q^-, q^\perp, q^+) \,. \quad (4.68)$$

In the first step we use the fact that F is constant throughout each box in the grid picture of Fig. 5 so its the same with the first two arguments shifted by residual momenta. (In the continuum EFT picture its the same property, F does not depend on residual momenta in these components.) In the final equality we then combined the momenta back into a standard dimensional regularization integration as in Eq. (4.67). Essentially at leading order in λ Eq. (4.68) amounts to the same thing that would be achieved by never considering the split into label and residual momenta in the first place, and simply writing down the integrand without ultrasoft momenta appearing in the $-$ or $\perp$ components in collinear propagators, which corresponds to the lowest order term in the ultrasoft multipole expansion (and is an easy way to think about the outcome of the above formal procedure). We have called this rule $1)^{\text{naive}}$ because there is one final complication that we will have to deal with, namely that the integration on q_ℓ must avoid producing additional divergences when this collinear momentum enters the ultrasoft regime. We denote this fact by $q_\ell \neq 0$ if q is the momentum of a collinear propagator. These are referred to as 0-bin restrictions.[4] We will discuss the change needed which handles this complication below. Often the results for collinear loop integrals are called "naive" if one uses Eq. (4.68). The result from this naive result will be correct if the added terms which properly handle this complication turn out to be zero, which happens in some cases.

At higher orders in λ there will be dependence on the residual momentum components from higher order terms in the multipole expansion of the collinear propagators. If these terms correspond to the momentum components q_r^- and $q_r^\perp$ that do not appear inside any ultrasoft propagators then the resulting integration is zero

$$2): \qquad \sum_{q_\ell} \int d^d q_r \, (q_r)^j F(q_\ell^-, q_\ell^\perp, q_r^+) = 0 \,, \quad (4.69)$$

where $(q_r)^j$ denotes positive powers of the q_r^- and $q_r^\perp$ momenta, $j > 0$. Here Eq. (4.69) is like the dimensional regularization rule, $\int d^d q (q^2)^j = 0$ for $j > 0$, which is a consequence of retaining Lorentz invariance with this regulator. Eq. (4.69) is the analogous statement in the residual momentum space and ensures that we do not obtain nontrivial contributions from higher order terms in the multipole expansion, unless the residual loop momentum corresponds to a physical momentum for an ultrasoft loop integration. Both ultrasoft loop integrations and ultrasoft external particles introduce residual momenta into propagators that can not be absorbed by a rule like that in Eq. (4.67). If we consider a case with an ultrasoft loop integration, then there will be dependence on the residual momentum also in an ultrasoft propagator, so the integration will give

$$\sum_{q_\ell} \int d^d q_r \int d^d k_r \; F(q_\ell^-, q_\ell^\perp, q_r^+, k_r^\mu) = \int d^d q \int d^d k \; F(q^-, q^\perp, q^+, k^\mu) \,, \quad (4.70)$$

which in general is nonzero. This integrand corresponds to a mixed two-loop diagram with one loop momentum with collinear scaling and one with ultrasoft scaling.

Finally let us consider the implications of the zero-bin when combining label and residual momenta. Rather than Eq. (4.67) we can have

$$\sum_{q_\ell \neq 0} \int d^d q_r \,, \quad (4.71)$$

[4] After imposing momentum conservation we get a set of such restrictions, one for each collinear propagator. For example $q_\ell \neq -p_\ell$ if there is a collinear propagator carrying momentum $q + p$.

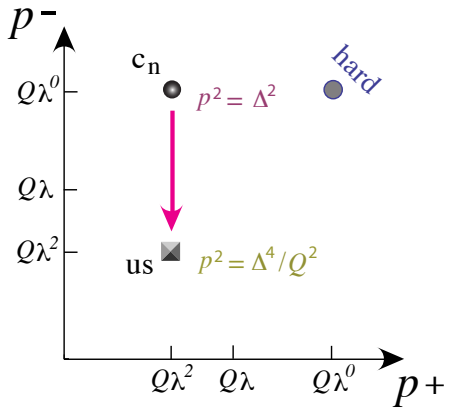

Figure 8: SCET_I zero-bin from one collinear direction scaling into the ultrasoft region.

where $q_\ell \neq 0$ is simply a label to denote the fact that the label momentum q_ℓ must be large in order to correspond to a collinear particle carrying total momentum q. If $q_\ell = 0$ then the particle would instead be ultrasoft, and we will often have included another diagram in SCET to account for the different integrand that accounts for the proper expansion in this special case. Thus these zero-bin restrictions avoid double counting between the SCET fields, which effectively means double counting from the resulting loop integrations. It is easy to determine what the set of restrictions are for any diagram, since we have one such condition for every collinear propagator. At leading order in λ only the zero-bin subtractions corresponding to collinear gluon propagators can give non-zero contributions since operators containing an ultrasoft quark together with collinear fields are power suppressed. In a continuum EFT these zerobin restrictions are implemented by subtraction terms which can be determined as follows

$$\begin{aligned}
1): \qquad \sum_{q_\ell \neq 0} \int d^d q_r \, F(q_\ell^-, q_\ell^\perp, q_r^+) &= \sum_{q_\ell \neq 0} \int d^d q_r \, F(q_\ell^- + q_r^-, q_\ell^\perp + q_r^\perp, q_r^+) \\
&= \sum_{q_\ell} \int d^d q_r \, F(q_\ell^- + q_r^-, q_\ell^\perp + q_r^\perp, q_r^+) - \int d^d q_r \, F^0(q_r^-, q_r^\perp, q_r^+) \\
&= \int d^d q \, F(q^-, q^\perp, q^+) - \int d^d q_r \, F^0(q_r^-, q_r^\perp, q_r^+) \\
&= \int d^d q \, \left[F(q^-, q^\perp, q^+) - F^0(q^-, q^\perp, q^+) \right] . \qquad (4.72)
\end{aligned}$$

Here the integrand F^0 is derived from expanding the integrand for F by taking the label momenta that appear in its first two arguments to instead scale as ultrasoft momenta $\sim \lambda^2$, expanding, and keeping the dominant and any sub-dominant scaling terms up to those that are the same order in λ as the original loop integration. If the original integrand $F \sim \lambda^{-4}$, then this corresponds to keeping just the terms up to $F^0 \sim \lambda^{-8}$, which is often the leading term. (Together with the standard scaling for the collinear measure, $d^d q \sim \lambda^4$ and for the residual measure $d^d q_r \sim \lambda^8$ these two integrands give contributions that are both the same order in λ.) In the last line we combine the subtraction term back together with the original integrand, since the integration variables are after all just dummy variables. This set of steps makes it clear that zero-bin contributions are encoded by subtractions.[5] The scaling for the subtraction is shown pictorally in Fig. 8. The F^0 term subtracts singularities from F that come from the region where the

[5] In fact, an alternate formulation of zero-bin subtractions that avoids the use of notation like $q_\ell \neq 0$ is to note that in

collinear momentum behaves like an ultrasoft momentum. In general when the subtraction integration is non-trivial there will always exist a corresponding ultrasoft diagram where the integration is ultrasoft from the start, which precisely corresponds with the contribution that the subtractions is allowing us to avoid double counting.

In general, when one has a continuum EFT with modes that live in a two dimensional space, such as those in Fig. 8, one has subtractions induced by the presence of modes at smaller (or equal) p^2. Therefore there are ultrasoft subtractions for the collinear modes, but no collinear subtractions for the ultrasoft modes.

It also should be remarked that depending on the choice of infrared regulators, the subtraction terms very often give scaleless integrations of combined dimension $d-4$ in dimensional regularization. These then just yield terms proportional to $(1/\epsilon^j_{\rm UV} - 1/\epsilon^j_{\rm IR})$, which are only important to properly interpret whether factors of $1/\epsilon$ from the naive collinear loop integration that used Eq. (4.68) are UV poles that require a counterterm, or are IR poles that correspond with physical IR singularities in QCD. In particular this is often the case for the simplest measurements with an offshellness IR regulator for collinear external lines. More complicated measurements (such as those depending on a jet algorithm) or other choices of IR regulators (like a gluon mass or a cutoff) will lead to zero-bin subtractions that are not scaleless.

We will return to this discussion when carrying out explicit examples of collinear loops in section 7.

5 Symmetries of SCET

In quantum field theory Lagrangians are often built up from symmetries and dimensional analysis. So far our leading order SCET Lagrangians were derived directly from QCD at tree level. To go further, and determine whether loops can change the form of the Lagrangians (through Wilson coefficients or additional operators) we need to exploit symmetries and power counting. In this section, we will introduce the SCET gauge symmetries and reparameterization invariance (RPI) as a way to constrain SCET operators. We will find that the gauge symmetry formalism is a simple restatement of the standard QCD picture except with two separate gauge fields. RPI is a manifestation of the Lorentz symmetry which was broken by the choice of light-cone coordinates, and which acts independently in each collinear sector. We will also examine the spin symmetries of the SCET Lagrangian, although here we will find that there are no surprises beyond what we know from QCD.

5.1 Spin Symmetry

To examine the spin symmetry of $\mathcal{L}^{(0)}_{n\xi}$ it is convenient to write the Lagrangian in a two component form. From Eq. (3.5) we can write

$$\xi_n = \frac{1}{\sqrt{2}} \begin{pmatrix} \sigma^3 \varphi_n \\ \varphi_n \end{pmatrix}, \tag{5.1}$$

a theory with both collinear and ultrasoft modes, each collinear propagator is actually a distribution, like a generalized +-function, that induces these subtraction terms. The fact that we drop higher order terms in the λ expansion when determining F^0 implies that we are making the minimal subtraction that avoids double counting IR singularities. Indeed there in principle could still be a double counting by a "constant" contribution, but such constants will be properly taken care of by the matching procedure. The minimal subtraction also ensures that the matching result remains independent of the IR regulator as desired.

where φ_n is a two-component field, dim φ_n = dim $\xi_n = 3/2$, and $\varphi_n \sim \lambda$. With this two-component field the SCET Lagrangian is

$$\mathcal{L} = \varphi_n^\dagger \left[in\cdot D + iD^\mu_{n\perp} \frac{1}{i\bar{n}\cdot D} iD^\nu_{n\perp} (g^\perp_{\mu\nu} + i\epsilon^\perp_{\mu\nu}\sigma_3) \right] \varphi_n \,. \tag{5.2}$$

Due to the σ_3 the spin symmetry is not an $SU(2)$, but rather just the $U(1)$ helicity symmetry corresponding to spin along the direction of motion n of the collinear fields. The relevant generator is

$$S_z = i\epsilon^{\mu\nu}_\perp [\gamma^\mu, \gamma^\nu] \to h = \sigma_3. \tag{5.3}$$

We can relate this symmetry to the chiral symmetry by noting that under chiral symmetry ξ_n transforms as

$$\xi_n \to \gamma^5 \xi_n = \begin{pmatrix} 0 & 1 \\ 1 & 0 \end{pmatrix} \frac{1}{\sqrt{2}} \begin{pmatrix} \phi_n \\ \sigma^3 \phi_n \end{pmatrix} \qquad \text{so} \quad \varphi_n \to \sigma_3 \varphi_n \,. \tag{5.4}$$

This $U(1)_A$ axial-symmetry is broken by fermion masses and non-perturbative instanton effects. Just like in QCD it is a useful symmetry for determining the structure of perturbation theory results. This implies that in SCET it is useful for determining the basis of operators we obtain when integrating out hard particles, and for relating Wilson coefficients.

5.2 Gauge Symmetry

The standard gauge transformation in QCD is

$$U(x) = \exp[i\alpha^A(x) T^A] \,. \tag{5.5}$$

When we go to SCET we need to have gauge transformations which do not inject large momenta into our EFT fields, that is, the transformations must leave us withing our effective field theory. For example, if we used a gauge transformation where α^A satisfied

$$i\partial_\mu \alpha^A \sim Q\alpha^A \tag{5.6}$$

then $\xi_n' = U(x)\xi_n$ would no longer have $p^2 \le Q^2\lambda^2$ and would not be described by SCET. There are two acceptable SCET gauge transformations which are defined by their momentum scale. They are

$$\text{collinear} \quad U_n(x): \quad i\partial^\mu U_n(x) \sim Q(\lambda^2, 1, \lambda) U_n(x) \tag{5.7}$$

$$\text{ultrasoft} \quad U_{us}(x): \quad i\partial^\mu U_{us}(x) \sim Q(\lambda^2, \lambda^2, \lambda^2) U_{us}(x). \tag{5.8}$$

There is also a global color transformation which for convenience we group together with the U_{us}. To avoid double counting, in the collinear transformation we fix $U_n(n\cdot x = -\infty) = 1$. We can implement a collinear gauge transformation on the collinear fields $\xi_{n,\,p_l}$ via a Fourier transform. Since $\psi(x) \to U(x)\psi(x)$ is equivalent to $\tilde{\psi}(p) \to \int dq\, \tilde{U}(p-q)\tilde{\psi}(q)$, the transformation involves a convolution in label momenta. To understand how the collinear gauge field transforms under a collinear gauge transformation, we need to recall that there is a background usoft gauge field A^μ_{us}. Consequently we must take $\partial^\mu \to \partial^\mu_{ns}$ so that A^μ_n transforms as a quantum field in an A^μ_{us} background. Therefore the collinear gauge transformations are

$$\begin{aligned} &\xi_{n,\,p}(x) \to (U_n)_{p-q}(x)\, \xi_{n,q}(x) \,, \\ &gA^\mu_{n,p}(x) \to U_{n,p-q}(x) \Big(gA^\mu_{n,q-q'}(x) + \delta_{q,q'} i\partial^\mu_{ns} \Big) U^\dagger_{n,q'}(x) \,, \end{aligned} \tag{5.9}$$

Object	Collinear $\mathcal{U}_c$	Usoft U_{us}
$\xi_n(x)$	$\hat{U}_n(x)\xi_n(x)$	$U_{us}(x)\,\xi_n(x)$
$A_n^\mu(x)$	$\hat{U}_n(x)(A_n^\mu(x)+\frac{i}{g}\partial_{ns}^\mu)\hat{U}_n^\dagger(x)$	$U_{us}(x)\,A_n^\mu(x)\,U_{us}^\dagger(x)$
$W_n(x)$	$\hat{U}_n(x)W_n$	$U_{us}(x)\,W(x)\,U_{us}^\dagger(x)$
$q_{us}(x)$	$q_{us}(x)$	$U_{us}(x)\,q_{us}(x)$
$A_{us}^\mu(x)$	$A_{us}^\mu(x)$	$U_{us}(x)(A_{us}^\mu(x)+\frac{i}{g}\partial^\mu)U_{us}^\dagger(x)$
$Y(x)$	$Y(x)$	$U_{us}(x)\,Y(x)$

Table 2: Gauge transformations for the collinear and usoft fields from Ref. [**?**], where $i\partial_{ns}^\mu \equiv \frac{n^\mu}{2}\,\bar{n}\cdot\mathcal{P} + \mathcal{P}_\perp^\mu + \frac{\bar{n}^\mu}{2}\,i\,n\cdot D_{\rm us}$. The collinear fields and transformations are understood to have momentum labels and involve convolutions, but for simplicity these indices are suppressed. The usoft transformations do not change the momentum labels of collinear fields.

Objects	Collinear $\mathcal{U}_c$	Soft U_s
$\xi_n(x)$	$\hat{U}_n(x)\;\xi_n(x)$	$\xi_n(x)$
$A_n^\mu(x)$	$\hat{U}_n(x)\,(A_n^\mu(x)+\frac{i}{g}\partial_n^\mu)\,\hat{U}_n^\dagger(x)$	$A_n^\mu(x)$
$W(x)$	$\hat{U}_n(x)\,W(x)$	$W(x)$
$q_s(x)$	$q_s(x)$	$\hat{U}_s(x)\,q_s(x)$
$A_s^\mu(x)$	$gA_s^\mu(x)$	$\hat{U}_s\,(A_n^\mu(x)+\frac{i}{g}\partial_s^\mu)\hat{U}_s^\dagger(x)$
$S(x)$	$S(x)$	$\hat{U}_s(x)\,S(x)$

Table 3: Gauge transformations for collinear and soft fields in $\text{SCET}_{\rm II}$ from Ref. [**?**]. Momentum labels are suppressed, and we have defined $i\partial_n^\mu = \frac{\bar{n}^\mu}{2}in\cdot\partial + \frac{n^\mu}{2}\bar{n}\cdot\mathcal{P} + \mathcal{P}_\perp^\mu$ and $i\partial_s^\mu = \frac{n^\mu}{2}i\bar{n}\cdot\partial + \frac{\bar{n}^\mu}{2}n\cdot\mathcal{P} + \mathcal{P}_\perp^\mu$ are defined to only pick out collinear and soft momenta respectively. Here $i\partial_c^\mu \neq i\mathcal{D}^\mu$ since usoft fields are not included in $\text{SCET}_{\rm II}$.

where we sum over repeated momentum label indices. It is convenient to setup a matrix notation for these convolutions by defining

$$(\hat{U}_n)_{p_\ell,q_\ell} \equiv (U_n)_{p_\ell - q_\ell}\,, \tag{5.10}$$

where the LHS is the (p_ℓ, q_ℓ) element of a matrix in momentum space, and the RHS is a number (both are of course also matrices in color). Then Eq. (5.9) with a sum over repeated indices becomes $\xi_{n,\,p_\ell} \to (\hat{U}_n)_{p_\ell,q_\ell}\xi_{n,q_\ell}$. And if we suppress indices then we have $\xi_n \to (\hat{U}_n)\xi_n$.

Finally the ultrasoft fields do not transform under a collinear gauge transformation, since the resulting field would have a large momentum and hence no longer be ultrasoft. Essentially this means that by definition our collinear gauge transformations do not turn ultrasoft gluons into collinear gluons.

For usoft gauge transformations, the field ξ_n and A_n^μ transform as quantum fields under a background gauge transformation, which is to say they transform as matter fields with the appropriate representation. The usoft fields have their usual gauge transformations from QCD. Since all of the fields transform, these ultrasoft gauge transformations connect fields in operators that are mixtures of collinear and ultrasoft fields. This differs from $U_n(x)$ which only connects collinear fields to each other.

For $\text{SCET}_{\rm II}$, the gauge transformation are simpler, since the virtuality of the soft fields are too large to be a background field to the collinear fields. Thus, the two gauge transformation completely decouple from one another, and both sectors transform separately as full QCD fields.

It is important to note that the gauge transformations are homogeneous in the power counting, so they do not change the order in λ for transformed operators. They are exact, there are no corrections to these transformations at higher orders in λ, and thus the power expansion will have gauge invariant operators at each order in λ.

The transformation of the fields yield transformations for objects that are built from the fields. An important case is the Wilson line W_n which is like the Fourier transform of $W(x,-\infty)$. In QCD a general Wilson line with the gauge field along a path will transform on each end as $W(x,y) \to U(x)W(x,y)U^\dagger(x)$. For the collinear gauge transformation we have fields in momentum space for labels, and position space representing residual momenta, and $U_n^\dagger(-\infty) = 1$, so the Wilson line transforms only on one side for collinear transformations. For ultrasoft transformations $W_n(x)$ is actually a local operator with all fields at x, and the product of multiple $\bar{n}\cdot A_n(x) \to U_{us}(x)\bar{n}\cdot A_n(x)U_{us}^\dagger(x)$ leads to one U_{us} and $U_{us}^\dagger$ on the left and right. Thus with the matrix notation

$$\begin{aligned} &\text{collinear}: && W_n(x) \to \hat{U}_n(x) W_n(x)\,, \\ &\text{ultrasoft}: && W_n(x) \to U_{us}(x) W_n(x) U_{us}^\dagger(x)\,. \end{aligned} \tag{5.11}$$

It is useful to consider the correspondence between the appearance of the Wilson line W_n in operators, and the collinear gauge symmetry. If we consider our example of the heavy-to-light current then without the Wilson line the operator $\bar{\xi}_n \Gamma h_v^{us}$ is not gauge invariant, transforming to $\bar{\xi}_n U_n^\dagger \Gamma h_v^{us}$. Here the ξ_n transforms because collinear gluons couple to ξ_n without taking it offshell, but h_v^{us} does not transform because this ultrasoft field can not interact with the collinear gluons while remaining near its mass shell. But recall that when the offshell collinear gluons are accounted for in matching onto the SCET operator that the $\bar{n}\cdot A_n \sim \lambda^0$ gluons generate a Wilson line W_n, so the complete result from tree level matching is

$$J_{\rm SCET} = \bar{\xi}_n W_n \Gamma h_v^{us}. \tag{5.12}$$

Now under a collinear gauge transformation $J_{\rm SCET} \to \bar{\xi}_n \hat{U}_n^\dagger \hat{U}_n W_n \Gamma h_v^{us} = \bar{\xi}_n W_n \Gamma h_v^{us}$, so the current is collinear gauge invariant. Under an ultrasoft gauge transformation $J_{\rm SCET} \to \bar{\xi}_n U_{us}^\dagger U_{us} W_n U_{us}^\dagger \Gamma U_{us} h_v^{us} = \bar{\xi}_n W_n \Gamma h_v^{us}$, so the current is also ultrasoft gauge invariant. Thus the leading order attachments of $\bar{n}\cdot A_n$ gluons that lead to the Wilson line W_n are necessary to obtain a gauge invariant result. Furthermore, by gauge symmetry the fact that the product $\bar{\xi}_n W_n$ appears in the operator will not be modified by loop corrections. We will take up what modifications can be generated by loop corrections in section 6.2 below.

Gauge symmetry forces gauge fields and derivatives to occur in the following combinations

$$\begin{aligned} in\cdot D_{ns} &= in\cdot\partial + gn\cdot A_n + gn\cdot A_{us}\,, \\ iD_{n\perp}^\mu &= \mathcal{P}_\perp^\mu + gA_{n\perp}^\mu\,, \\ i\bar{n}\cdot D_n &= \overline{\mathcal{P}} + g\bar{n}\cdot A_n\,, \\ iD_{us}^\mu &= i\partial^\mu + gA_{us}^\mu\,. \end{aligned} \tag{5.13}$$

We see that gauge symmetry is a powerful tool in determining the structure of operators. It is reasonable to ask, is power counting and gauge invariance enough to fix the leading order Lagrangian $\mathcal{L}_{n\xi}^{(0)}$ for ξ_n? Only the operators $in\cdot D$ and $(1/\overline{\mathcal{P}})D_{n\perp}D_{n\perp}$ are $\mathcal{O}(\lambda^2)$ and have the correct mass dimension. The latter will have the correct gauge transformation properties once we include W_ns. Nevertheless, nothing so far rules out the operator

$$\bar{\xi}_n iD_{n\perp}^\mu W_n \frac{1}{\overline{\mathcal{P}}} W_n^\dagger iD_{n\,\mu}^\perp \frac{\bar{n}\!\!\!/}{2}\xi_n \tag{5.14}$$

which is gauge invariant and has the correct λ scaling. To exclude this term we need to consider another symmetry prinicple, namely reparameterization invariance.

5.3 Reparamterization Invariance

Our choice of the n and $\bar{n}$ reference vectors explicitly breaks Lorentz symmetry in SCET, much like v does in HQET. Part of this breaking is natural, SCET_I is describing a collimated jet which explicitly picks out a corresponding n-collinear direction about which the field theory is describing fluctuations. There is also a part of the symmetry that is restored by the freedom we have in choosing our n and $\bar{n}$ vectors, which is a reparameterization invariance (RPI). A second attribute of the reparameterization symmetry is the freedom we have in splitting momenta between label and residual components. We will explore these two in turn.

The only required property of a set of n, $\bar{n}$ basis vectors is that they satisfy

$$n^2 = \bar{n}^2 = 0, \qquad n \cdot \bar{n} = 2. \tag{5.15}$$

Consequently a different choice for n and $\bar{n}$ can yield a valid set of light-cone coordinates as long as our result still obeys (5.15). Specifically, there are three sets of transformations which can be made on a set of light-cone coordinates to obtain another, equally valid, set.

$$\begin{array}{ccc} \underline{\textbf{I}} & \underline{\textbf{II}} & \underline{\textbf{III}} \\ n_\mu \to n_\mu + \Delta^\perp_\mu & n_\mu \to n_\mu & n_\mu \to e^\alpha n^\mu \\ \bar{n}_\mu \to \bar{n}_\mu & \bar{n}_\mu \to \bar{n}_\mu + \varepsilon^\perp_\mu & \bar{n}_\mu \to e^{-\alpha}\bar{n}_\mu \end{array} \tag{5.16}$$

where $\bar{n}\cdot\varepsilon^\perp = n\cdot\varepsilon^\perp = \bar{n}\cdot\Delta^\perp = n\cdot\Delta^\perp = 0$. The first two transformations are inifinitesimal. The third is a finite transformation (where the form is simple), but can be made infinitesimal by expansion in α. These transformations must leave a collinear momentum collinear in the same directions, so we can obtain the λ-scaling of these parameters by noting that:

$$\begin{aligned} &\lambda^2 \sim n\cdot p \to n\cdot p + \Delta^\perp \cdot p_\perp \Longrightarrow \Delta^\perp \sim \lambda^1 \\ &\lambda^0 \sim \bar{n}\cdot p \to \bar{n}\cdot p + \varepsilon^\perp \cdot p_\perp \Longrightarrow \varepsilon^\perp \sim \lambda^0 \\ &\alpha \sim \lambda^0 \end{aligned} \tag{5.17}$$

Thus only $\Delta^\perp$ is constrained by the power counting, while large changes are allowed for α and $\epsilon^\perp$. These RPI transformations are a manifestation of the Lorentz symmetry which was broken by introducing the vectors n and $\bar{n}$. The five infinitesimal parameters $\Delta^\perp_\mu$, $\varepsilon^\perp_\mu$, and α correpsond to the five generators of the Lorentz group which were broken by introducing the vectors n and $\bar{n}$. These generators are defined by $\{n_\mu M^{\mu\nu}, \bar{n}_\mu M^{\mu\nu}\}$ or in terms of our standard light-cone coordinates $Q_1^\pm = J_1 \pm K_2$, $Q_2^\pm = J_2 \pm K_1$, and K_3. Here $M^{\mu\nu}$ are the usual 6 antisymmetric SO(3,1) generators.

If we start with our canonical basis choice $n = (1,0,0,1)$ and $\bar{n} = (1,0,0,-1)$ then we can visualize the Type I and Type II transformations as changes in the directions orthogonal to the $\hat{z}$ direction

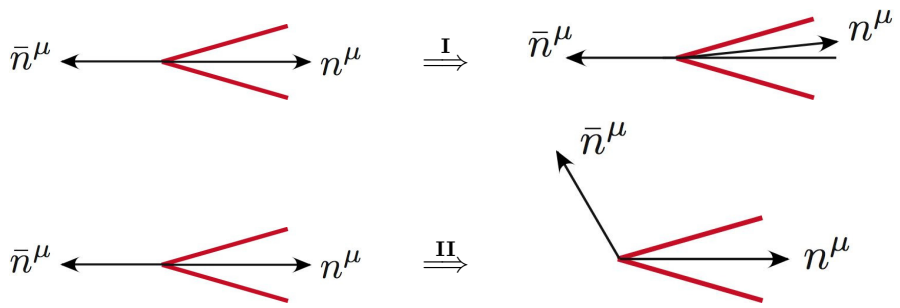

and we can visualize Type III transformations as boosts in the $\hat{z}$ direction. For Type I we can transform n by an $\mathcal{O}(\lambda)$ amount, into another vector within this collinear sector, without changing any of the physics. For Type II we recall that the auxillary vector $\bar{n}$ was chosen simply to enable us to decompose momenta, so their is a considerable freedom in its definition, and this corresponds to the freedom to make large transformations. (If we start with a more general choice for n and $\bar{n}$ that satisfies Eq. (5.15) then the picture for the Type-III transformation is more complicated than a simple boost.)

The implications of the Type III transformation for SCET operators are very simple, n and $\bar{n}$ must appear in operators either together, or with one factor of $\bar{n}/n$ in both the numerator and denominator. That is, in one of the combinations

$$(A\cdot n)(B\cdot\bar{n}), \qquad \frac{A\cdot n}{B\cdot n}, \qquad \frac{A\cdot\bar{n}}{B\cdot\bar{n}} \tag{5.18}$$

where A^μ and B^μ are arbitrary 4-vectors.

In order to derive the complete set of transformation relations we must also determine how $p_\perp^\mu$ transforms. Recall that the definition of $p_\perp$ depends on n and $\bar{n}$, since it is orthogonal to n and $\bar{n}$, satisfying $n\cdot p_\perp = 0 = \bar{n}\cdot p_\perp$. We can work out its transformation by noting that the four vector p^μ does not depend on the basis for coordinates. Using the Type-I transformation as an example

$$p^\mu = \frac{n^\mu}{2}\bar{n}\cdot p + \frac{\bar{n}^\mu}{2}n\cdot p + p_\perp^\mu \implies \frac{n^\mu}{2}\bar{n}\cdot p + \frac{\bar{n}^\mu}{2}n\cdot p + p_\perp^\mu + \frac{\Delta_\perp^\mu}{2}\bar{n}\cdot p + \frac{\bar{n}^\mu}{2}\Delta_\perp\cdot p_\perp + \delta_{\rm I}(p_\perp^\mu) = p^\mu\,. \tag{5.19}$$

Thus $p_\perp^\mu$ must transform as

$$p_\perp^\mu \overset{\mathbf{I}}{\Longrightarrow} p_\perp^\mu - \frac{\bar{n}^\mu}{2}\Delta_\perp\cdot p_\perp - \frac{\Delta_\perp^\mu}{2}\bar{n}\cdot p\,. \tag{5.20}$$

The projection relation $(\not{n}\not{\bar{n}}/4)\xi_n = \xi_n$ also implies that $\xi_n \to [1 + (\not{\Delta}^\perp\not{\bar{n}})/4]\xi_n$. Similar relations can also be worked out for type-II transformations, for example

$$p_\perp^\mu \overset{\mathbf{II}}{\Longrightarrow} p_\perp^\mu - \frac{n^\mu}{2}\varepsilon_\perp\cdot p_\perp - \frac{\varepsilon_\perp^\mu}{2}n\cdot p\,. \tag{5.21}$$

Summarizing all the type-I and type-II transformations on vectors and fields (using D^μ as a typical vector) we have

I	**II**
$n \to n + \Delta^\perp$	$n \to n$
$\bar{n} \to \bar{n}$	$\bar{n} \to \bar{n} + \varepsilon^\perp$
$n\cdot D \to n\cdot D + \Delta^\perp\cdot D^\perp$	$n\cdot D \to n\cdot D$
$D_\mu^\perp \to D_\mu^\perp - \frac{\Delta_\mu^\perp}{2}\bar{n}\cdot D - \frac{\bar{n}^\mu}{2}\Delta^\perp\cdot D$	$D_\mu^\perp \to D_\mu^\perp - \frac{\epsilon_\mu^\perp}{2}n\cdot D - \frac{n^\mu}{2}\epsilon^\perp\cdot D$
$\bar{n}\cdot D \to \bar{n}\cdot D$	$\bar{n}\cdot D \to \bar{n}\cdot D + \epsilon^\perp\cdot D^\perp$
$\xi_n \to \left(1 + \frac{1}{4}\not{\Delta}^\perp\not{\bar{n}}\right)\xi_n$	$\xi_n \to \left(1 + \frac{1}{2}\not{\epsilon}^\perp\frac{1}{i\bar{n}\cdot D}i\not{D}_\perp\right)\xi_n$
$W_n \to W_n$	$W_n \to \left(1 - \frac{1}{i\bar{n}\cdot D}\epsilon^\perp\cdot iD^\perp\right)W_n$

(5.22)

For type-III transformations $p_\perp^\mu$ does not transform, and neither does W_n.

We can show that our leading order SCET Lagrangian

$$\mathcal{L}_{n\xi}^{(0)} = \xi_n in\cdot D_{ns}\frac{\not{\bar{n}}}{2}\xi_n + \bar{\xi}_n i\not{D}_{n,\perp}\frac{1}{i\bar{n}\cdot D_n}i\not{D}_{n\perp}\frac{\not{\bar{n}}}{2}\xi_n \tag{5.23}$$

is invariant under these transformations. Under a type-I transformation we have

$$\begin{aligned}\delta_{\rm I}\mathcal{L}^{(0)}_{n\xi} &= \delta_{\rm I}\left(\xi_n in\cdot D_{ns}\frac{\bar{n}\!\!\!/}{2}\xi_n\right) + \delta_{\rm I}\left(\bar{\xi}_n i\not{D}_{n,\perp}\frac{1}{i\bar{n}\cdot D_n}i\not{D}_{n\perp}\frac{\bar{n}\!\!\!/}{2}\xi_n\right) \\ &= \bar{\xi}_n i\Delta^\perp\cdot D_n^\perp\frac{\bar{n}\!\!\!/}{2}\xi_n - \bar{\xi}_n i\Delta^\perp\cdot D_n^\perp\frac{\bar{n}\!\!\!/}{2}\xi_n \\ &= 0\end{aligned} \tag{5.24}$$

where to obtain the second line we used $\bar{n}\!\!\!/^2 = 0$, the orthogonal properties of the 4-vectors, and ignored quadratic combinations of the $\Delta^\perp$ infinitesimal. Hence the SCET quark Lagrangian obtained from tree level matching is indeed invaraiant under $\delta_{\rm I}$. However, this Lagrangian is not completely determined by invariance under $\delta_{\rm I}$. For example, the term we encountered at the end of the gauge symmetry section transforms as

$$\delta_{(I)}\left(\bar{\xi}_n iD_{n\perp\mu}\frac{1}{i\bar{n}\cdot D_n}iD^\mu_{n\perp}\frac{\bar{n}\!\!\!/}{2}\xi_n\right) = -\bar{\xi}_n i\Delta^\perp\cdot D_{n\perp}\frac{\bar{n}\!\!\!/}{2}\xi_n \tag{5.25}$$

which is the same transformation as for the second term in (5.24). Consequently, we may replace the second term with this new term with no violation of power counting, gauge symmetry, or RPI type-I. This ambiguity is only resolved by using invariance under RPI of type-II. The detailed calculation is given in [7] with the final result that our Lagrangian $\mathcal{L}^{(0)}_{n\xi}$ remains invariant under $\delta_{\rm II}$ while the term given in (5.14) does transforms in a way that can not be compensated by any other leading order term in the Lagrangian. Therefore our SCET$_{\rm I}$ Lagrangian $\mathcal{L}^{(0)}_{n\xi}$ is unique by power counting, gauge invariance, and reparameterization invariance. This also implies that its form is not modifed by loop corrections. In general type-III RPI will restrict operators at the same order in λ, type-I restricts operators at different orders in λ, and type-II will restrict operators at both the same and different orders in λ.

Reparameterization invariance also manifests itself in the ambiguity of label and residual momenta decomposition. We can separate the total momenta

$$\bar{n}\cdot p = \bar{n}\cdot(p_\ell + p_r) \qquad p^\mu_\perp = p^\mu_{l\perp} + p^\mu_{r\perp} \tag{5.26}$$

into p_ℓ and p_r in different ways as long as we maintain the power counting. Specifically, a transformation that takes

$$\mathcal{P}^\mu \to \mathcal{P}^\mu + \beta^\mu \qquad i\partial^\mu \to i\partial^\mu - \beta^\mu \tag{5.27}$$

implements this freedom. The transformation on $i\partial^\mu$ is induced by the β-transformation of the fields, for example

$$\xi_{n,p}(x) \to e^{i\beta(x)}\xi_{n,p+\beta}(x)\,. \tag{5.28}$$

The set of these β transformations also determines the space of equivalent decompositions $\mathcal{I}$ that we mod out by when constructing pairs of label and residual momenta components (p_ℓ, p_r) in $\mathbb{R}^3\times\mathbb{R}^4/\mathcal{I}$. We will refer to this as type-0 RPI to distinguish it from those discussed above. Invariance under this RPI requires the combination

$$\mathcal{P}^\mu + i\partial^\mu \tag{5.29}$$

to be grouped together for collinear fields. Since $\overline{\mathcal{P}}$ and $i\bar{n}\cdot\partial$ (and $\mathcal{P}^\mu_\perp$ and $i\partial^\mu_\perp$) appear at different orders in the power counting, this RPI connects the Wilson coefficients of operators at different orders in λ.

A natural question is how to gauge the connection between label and residual derivatives in (5.29). Recall that the gauge transformations for derivatives are

$$\begin{array}{rcc} & \text{collinear} & \text{ultrasoft} \\ iD_{n\perp} \to & \hat{U}_n iD_{n\perp}\hat{U}_n^\dagger & U_{us} iD_{n\perp} U_{us}^\dagger \\ i\bar{n}\cdot D_n \to & \hat{U}_n i\bar{n}\cdot D_n \hat{U}_n^\dagger & U_{us} i\bar{n}\cdot D_n U_{us}^\dagger m \\ in\cdot D \to & \hat{U}_n in\cdot D\hat{U}_n^\dagger & U_{us} in\cdot D U_{us}^\dagger \\ iD_{us}^\mu \to & iD_{us}^\mu & U_{us} iD_{us}^\mu U_{us}^\dagger \end{array}$$

The most natural guess for the gauging of (5.29) would be

$$iD_{n\perp}^\mu + iD_{us\perp}^\mu\,, \qquad i\bar{n}\cdot D_n + i\bar{n}\cdot D_{us}\,. \tag{5.30}$$

However, with the above transformations these combinations do not have uniform transformations under the gauge symmetries, since D_{us} does not transform under U_n. We can rectify this problem by introducing our Wilson line W_n into the combination of these derivatives. The unique result which preserves the SCET gauge symmetries without changing the power counting of the terms is

$$iD_\perp^\mu \equiv iD_{n\perp}^\mu + W_n iD_{us\perp}^\mu W_n^\dagger \tag{5.31}$$

$$i\bar{n}\cdot D \equiv i\bar{n}\cdot D_n + W_n i\bar{n}\cdot D_{us} W_n^\dagger\,, \tag{5.32}$$

where W_n transforms as $W_n \to U_n W_n$. Stripping off the regular derivative terms, the extra multi-gluon terms appearing in the formulae like $A_\perp^\mu = A_{n\perp}^\mu + A_{us\perp}^\mu + \ldots$ are the terms we denoted by ellipses in (4.9). These terms are necessary to form gauge invariant subleading operators.

Like in HQET, the RPI in SCET connects the Wilson coefficients of leading and λ-suppressed Lagrangians and external currents and operators. As an example, applying the connection to the term $\bar{\xi}_n i\not{D}_{n,\perp} W_n (1/\overline{\mathcal{P}})\, W_n^\dagger i\not{D}_{n,\perp}\xi_n$ in $\mathcal{L}_{n\xi}^{(0)}$ yields the subleading Lagrangian that couples collinear quarks to $A_\perp^{us}$ gluons,

$$\mathcal{L}_{n\xi}^{(1)} = (\bar{\xi}_n W_n) i\not{D}_\perp^{us} \frac{1}{\overline{\mathcal{P}}} (W_n^\dagger i\not{D}_{n,\perp}\xi_n) + (\bar{\xi}_n i\not{D}_{n,\perp} W_n)\frac{1}{\overline{\mathcal{P}}} i\not{D}_\perp^{us} (W_n^\dagger \xi_n). \tag{5.33}$$

The complete set of SCET_I power suppressed Lagrangians up to $\mathcal{O}(\lambda^2)$ can be found below in Sec. 8.2.

5.4 Discrete Symmetries

After considering the residual form of Lorentz symmetry encoded in reparameterization invariance it is natural to consider how our SCET fields transform under C, P, and T transformations. In this case we will satisfy ourselves with the transformations of the collinear field $\xi_{n,p}$. We have

$$\begin{aligned} C^{-1}\xi_{n,p}(x)C &= -[\bar{\xi}_{n,-p}(x)\mathcal{C}]^T \\ P^{-1}\xi_{n,p}(x)P &= \gamma_0 \xi_{\bar{n},\tilde{p}}(x_P) \\ T^{-1}\xi_{n,p}(x)T &= \mathcal{T}\xi_{\bar{n},\tilde{p}}(x_T) \end{aligned} \tag{5.34}$$

where $n = (1,0,0,1)$, $\bar{n} = (1,0,0,-1)$, $p \equiv (p^+, p^-, p^\perp)$, $x \equiv (x^+, x^-, x^\perp)$, $\mathcal{C}$ is the standard matrix induced by charge conjugation symmetry, and we have defined $\tilde{p} = (p^-, p^+, -p^\perp)$ as well as $x_P = (x^-, x^+, -x^\perp)$ and $x_T = (-x^-, -x^+, x^T)$.

5.5 Extension to Multiple Collinear Directions

For processes with more than one energetic hadron, or more than one energetic jet our list of degrees of freedom must include more than one type of collinear mode, and hence more than one type of collinear quark and collinear gluon. When two collinear modes in different directions interact, the resulting particle is offshell, and does not change the formulation of the leading order collinear Lagrangians. Therefore the Lagrangian with multiple collinear directions is

$$\mathcal{L}^{(0)}_{\rm SCET_I} = \mathcal{L}^{(0)}_{us} + \sum_n \left[\mathcal{L}^{(0)}_{n\xi} + \mathcal{L}^{(0)}_{ng}\right]. \tag{5.35}$$

for $n_1, n_2, n_3, \ldots$ collinear modes in the sum on n. The collinear modes are distinct only if

$$n_i \cdot n_j \gg \lambda^2 \quad \text{for } i \neq j\,. \tag{5.36}$$

We may understand this result by a counter argument: If a momentum $p_2 = Qn_2$, then $n_1{\cdot}p_2 = Qn_1{\cdot}n_2 \sim \lambda^2$ iff $n_1 \cdot n_2 \sim \lambda^2$. Hence p_2 is n_1-collinear, and n_2 is not a distinct collinear direction from n_1. If $n_i \cdot n_1 \sim \lambda^2$ then we say that n_i is within the RPI equivalence class $[n_1]$ defined by the member n_1. Distinct collinear directions correspond to the different equivalence classes, and we only sum over distinct directions in Eq. (5.35).

Essentially all of the things we derived with one collinear direction get repeated when we have more than one collinear direction.

- For each light-like n_i we define an auxillary light-like $\bar{n}_i$ where $n_i{\cdot}\bar{n}_i = 2$. Collinear momenta in the n_i direction are decomposed with the $\{n_i, \bar{n}_i\}$ basis vectors since the components have a definite power counting: $(n_i \cdot p, \bar{n}_i \cdot p, p_{n_i\perp}) \sim (\lambda^2, 1, \lambda)$. Note that the meaning of $\perp$ depends on which n_i-collinear sector we are discussing.

- There is a separate RPI for each n_i-collinear sector that only acts on the n_i-collinear fields, and on objects decomposed with the $\{n_i, \bar{n}_i\}$ basis vectors. Here there is no simple connection to an overall Lorentz transformation because the fields in other sectors do not transform.

- There is a collinear gauge transformation U_{n_i} for each type of collinear field. Only the fields in the n_i-collinear direction transform (fields in other collinear sectors do not transform with U_{n_i} since such transformations would yield offshell momenta that are outside the effective theory).

- Matching calculations generate multiple collinear Wilson lines $W_{n_i} = W_{n_i}[\bar{n}_i \cdot A_{n_i}]$. The definitions are identical to Eq. (4.53) with $n \to n_i$, $\bar{n} \to \bar{n}_i$, including $\overline{P} \to \bar{n}_i \cdot \mathcal{P}$. They are again always built only out of the $\mathcal{O}(\lambda^0)$ gluon fields, and correspond to straight Wilson lines. These matching calculations lead to operators in SCET that are gauge invariant under U_{n_i} transformations.

As an example of the last point consider the process $e^+e^- \to \gamma^* \to$ two-jets. The QCD current is $J^\mu = \bar{\psi}\gamma^\mu\psi$. By integrating out offshell fields to match onto $\rm SCET_I$ we obtain the leading order current

$$J^\mu_{\rm SCET} = (\bar{\xi}_{n_1} W_{n_1})\gamma^\mu (W^\dagger_{n_2}\xi_{n_2})\,. \tag{5.37}$$

Here n_1 and n_2 are the directions of the two jets. The Wilson line $W_{n_1} = W_{n_1}[\bar{n}_1 \cdot A_{n_1}]$ is generated by integrating out the attachment of $\bar{n}_1 \cdot A_{n_1}$ gluons to n_2-collinear quarks and gluons, and analogously for W_{n_2}. The resulting operator in Eq. (5.37) is invariant under n_1-collinear, n_2-collinear, and ultrasoft gauge transformations. In general one can carry out all orders tree level matching computations to derive the presence of these Wilson lines. For situations with multiple lines in different directions these calculations are greatly facilitated by using the auxillary field method (see the appendices of [6, 8]).

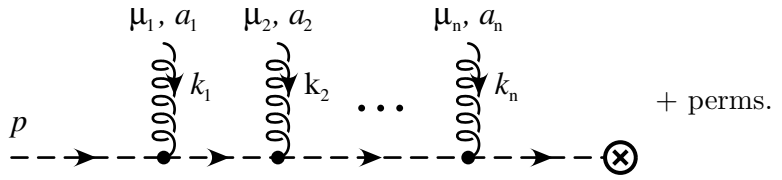

Figure 9: The attachments of ultrasoft gluons to a collinear quark line which are summed up into a path-ordered exponential.

6 Factorization from Mode Separation

One of the benefits of the SCET formalism is the clear separation of scales at the level of the Lagrangian and of operators that mediate hard interatctions. We will explore the factorization between various types of modes in this section.

6.1 Ultrasoft-Collinear Factorization

Recall that only the $n \cdot A_{us}$ component couples to n-collinear quarks and gluons at leading order in λ. This is explicit in the Feynman rules in Figs. 6 and 7 where only n_μ appears for the ultrasoft gluon with index μ. Furthermore due to the multipole expansion the collinear particles only see the $n \cdot k$ ultrasoft momentum of the $n \cdot A_{us}$ gluons. For example, if we consider Fig. 9 with only one ultrasoft gluon then the collinear quark propagator is

$$\frac{\bar{n} \cdot p}{\bar{n} \cdot p \, n \cdot (p_r + k) + p_\perp^2 + i0} = \frac{\bar{n} \cdot p}{\bar{n} \cdot p \, n \cdot k + p^2 + i0} = \frac{\bar{n} \cdot p}{\bar{n} \cdot p \, n \cdot k + i0} \,, \tag{6.1}$$

where in the last equality we used the onshell condition $p^2 = 0$ for the external collinear quark. Together with the n_μ from the vertex this result corresponds to the eikonal propagator for the coupling of soft gluons to an energetic particle. The appropriate sign for the $i0$ is determined by dividing through by $\bar{n} \cdot p$ and noting the sign of this momentum, which differs for quark and antiquarks. Accounting for attachments to incoming or outgoing particles this leads to the four eikonal propagator results summarized in Fig. 10.

Now, we consider the case of multiple usoft gluon emission. Calculating within SCET the graphs in Fig. 9 gives $\Gamma \tilde{Y}_n u_n$ where Γ is the structure at the $\otimes$ vertex, and u_n is a collinear quark spinor. Here

$$\tilde{Y}_n = \sum_{m=0}^{\infty} \sum_{\text{perms}} \frac{(-g)^m n \cdot A^{a_1}(k_1) \cdots n \cdot A^{a_m}(k_m) T^{a_m} \cdots T^{a_1}}{n \cdot k_1 \, n \cdot (k_1 + k_2) \cdots n \cdot (\sum_i k_i)} \tag{6.2}$$

where all propagators are $+i0$. These eikonal propagators come from collinear quarks with offshellness $\sim \lambda^2$, which is near their mass shell, and hence are a property of fields in the EFT itself (as opposed to the Wilson lines W_n which were generated by matching onto the EFT). This corresponds to the momentum space formula for an ultrasoft Wilson line Y_n. In position space this formula becomes

$$Y_n(x) = \text{Pexp}\left[ig \int_{-\infty}^{0} ds \, n \cdot A_{us}^a(x + ns) T^a \right] . \tag{6.3}$$

It satisfies a defining equation and unitarity condition:

$$in \cdot D_{us} \, Y_n = 0, \qquad Y_n^\dagger Y_n = 1. \tag{6.4}$$

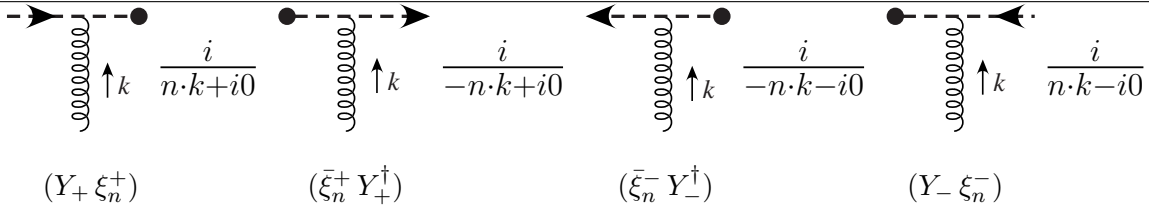

Figure 10: Eikonal $i0$ prescriptions for incoming/outgoing quarks and antiquarks and the result that reproduces this with an ultrasoft Wilson line and sterile quark field.

For the case where the Wilson line is in the fundamental representation $T^a \to T^a_{\alpha\beta}$, while for a Wilson line in the adjoint representation $T^a \to -if^{abc}$. We will assume that all Wilson lines are in the fundamental representation and reserve the notation Y_n for this case. For the adjoint Wilson line we will use $\mathcal{Y}_n$.

When we wish to be specific in the notation for our Wilson lines to show whether they extend from $-\infty$ or out to $+\infty$, and whether they are path-ordered or antipath-ordered, we will use the following notations

$$
\begin{aligned}
Y_{n+} &= \mathrm{P}\exp\left(ig\int_{-\infty}^{0} ds\; n\cdot A_{us}(x+sn)\right), \qquad & Y_{n-} &= \overline{\mathrm{P}}\exp\left(-ig\int_{0}^{\infty} ds\, n\cdot A_{us}(x+sn)\right), \\
Y_{n-}^\dagger &= \overline{\mathrm{P}}\exp\left(-ig\int_{-\infty}^{0} ds\, n\cdot A_{us}(x+sn)\right), \qquad & Y_{n+}^\dagger &= \mathrm{P}\exp\left(ig\int_{0}^{\infty} ds\; n\cdot A_{us}(x+sn)\right).
\end{aligned}
\tag{6.5}
$$

Here $(Y_{n\pm})^\dagger = Y^\dagger_{n\mp}$, and the subscript on $Y^\dagger_{n\pm}$ should be read as $(Y_n^\dagger)_\pm$ rather than $(Y_\pm)^\dagger$. The $+$ denotes Wilson lines obtained from attachments to quarks, and the $-$ denotes Wilson lines from attachments to antiquarks. The Wilson lines obtained for various situations are shown in Fig. 10.

The generation of the Wilson line Y_n from the example above motivates us to consider whether all the leading order usoft-collinear interactions within $\mathrm{SCET_I}$ (to all orders in α_s and with loop corrections) can be encoded through the non-local interactions contained in the Wilson line $Y_n(x)$. To show that this is indeed the case we consider the BPS field redefinitions [6]

$$
\xi_{n,p}(x) = Y_n(x)\xi^{(0)}_{n,p}(x), \qquad A^\mu_{n,p}(x) = Y_n(x)\, A^{(0)\mu}_{n,p}(x) Y_n^\dagger(x)\,. \tag{6.6}
$$

They include in addition $c_{n,p}(x) = Y_n(x)\, c^{(0)}_{n,p} Y_n^\dagger(x)$ for the ghost field in any general covariant gauge.

The defining equation for Y_n implies the operator equation

$$
Y_n^\dagger in\cdot D_{us} Y_n = in\cdot\partial. \tag{6.7}
$$

Also because the label operator $\overline{\mathcal{P}}$ commutes with Y_n the redefinition on $\bar n\cdot A_n$ in (6.6) implies that

$$
W_n \to Y_n W_n^{(0)} Y_n^\dagger\,, \tag{6.8}
$$

where $W_n^{(0)}$ is built from $\bar n\cdot A_n^{(0)}$ fields. Implementing these transformations into our leading collinear quark

Lagrangian we find

$$\begin{aligned}
\mathcal{L}^{(0)}_{n\xi} &= \bar{\xi}_n \left(in\cdot D + i\not{D}_{n\perp} \frac{1}{i\bar{n}\cdot D_n} i\not{D}_{n\perp} \right) \frac{\not{\bar{n}}}{2} \xi_n \\
&= \bar{\xi}_n \left(in\cdot D_{us} + gn\cdot A_{n,q} + (\not{\mathcal{P}}_\perp + g\not{\mathcal{A}}_{n,q\perp}) W \frac{1}{\overline{\mathcal{P}}} W^\dagger (\not{\mathcal{P}}_\perp + g\not{\mathcal{A}}_{n,q\perp}) \right) \frac{\not{\bar{n}}}{2} \xi_n \\
&= \bar{\xi}^{(0)}_n Y^\dagger \Big(in\cdot D_{us} + gYn\cdot A^{(0)}_{n,q} Y^\dagger \\
&\quad + (\not{\mathcal{P}}_\perp + gY\not{\mathcal{A}}^{(0)}_{n,q\perp} Y^\dagger) Y W^{(0)} Y^\dagger \frac{1}{\overline{\mathcal{P}}} Y W^{(0)\dagger} Y^\dagger (\not{\mathcal{P}}_\perp + g\not{\mathcal{A}}^{(0)}_{n,q\perp}) \Big) \frac{\not{\bar{n}}}{2} Y \xi^{(0)}_n \\
&= \bar{\xi}^{(0)}_n \left(in\cdot\partial + gn\cdot A^{(0)}_{n,q} + (\not{\mathcal{P}}_\perp + g\not{\mathcal{A}}^{(0)}_{n,q\perp}) W^{(0)} \frac{1}{\overline{\mathcal{P}}} W^{(0)\dagger} (\not{\mathcal{P}}_\perp + g\not{\mathcal{A}}^{(0)}_{n,q\perp}) \right) \frac{\not{\bar{n}}}{2} \xi^{(0)}_n \\
&= \bar{\xi}^{(0)}_n \left(in\cdot D^{(0)}_n + i\not{D}^{(0)}_{n\perp} \frac{1}{i\bar{n}\cdot D^{(0)}_n} i\not{D}^{(0)}_{n\perp} \right) \frac{\not{\bar{n}}}{2} \xi^{(0)}_n \,, \qquad (6.9)
\end{aligned}$$

where the last line is completely independent of the usoft gluon field. With similar steps we can easily show that the collinear gluon Lagrangian $\mathcal{L}^{(0)}_{ng}$ in (4.57) also completely decouples from the $n\cdot A_{us}$ usoft gluon field. In summary, we see that the usoft gluons have completely decoupled from collinear particles in the leading order collinear Lagrangian $\mathcal{L}^{(0)}_n = \mathcal{L}^{(0)}_{n\xi} + \mathcal{L}^{(0)}_{ng}$ via

$$\mathcal{L}^{(0)}_n \left[\xi_{n,p}, A^\mu_{n,q}, n\cdot A_{us} \right] = \mathcal{L}^{(0)}_n \left[\xi^{(0)}_{n,p}, A^{(0)\mu}_{n,q}, 0 \right] . \qquad (6.10)$$

However, it is important to note that the usoft interactions for our collinear field have not disappeared, but have simply moved out of the Lagrangian and into the currents. We must make the field redefinition everywhere, including external operators and currents, as well as on interpolating fields for partons and hadrons. The field redefinition on the interpolating fields that describe incoming and outgoing states will determine whether the final usoft Wilson lines are Y_+, $Y^\dagger_+$, Y_-, or $Y^\dagger_-$ since these interplolating field operators are localized either at $-\infty$ or $+\infty$.

Eg.1: Consider our standard heavy-to-light current. Performing the field redefinitions we have

$$\begin{aligned}
J^\mu &= \bar{\xi}_{n,} W \Gamma^\mu h_v = \bar{\xi}^{(0)}_n Y^\dagger_n Y_n W^{(0)} Y^\dagger_n \Gamma^\mu h_v \qquad (6.11) \\
&= \bar{\xi}^{(0)}_n W^{(0)} \Gamma^\mu Y^\dagger_n h_v \,.
\end{aligned}$$

The last line gives us our first factorization result. Since $\bar{\xi}_n$ is an outgoing quark, here $Y^\dagger_n = Y^\dagger_+$. As is necessary for effective theories, we will need to include a Wilson coefficient encoding higher energy dynamics, but we can already clearly see how different scales have separated into distinct gauge invariant quantities $(\bar{\xi}^{(0)}_{n,p} W^{(0)})$ and $(Y^\dagger_n h_v)$ at the level of operators. We can demonstrate this ultrasoft-collinear factorization diagrammatically by considering the time ordered product of two currents $TJ^\mu(x)J^{\dagger\nu}(0)$ (whose imaginary part is related to the inclusive decay rate). Rather than having diagrams with ultrasoft gluons coupling to collinear lines they decouple into distinct parts:

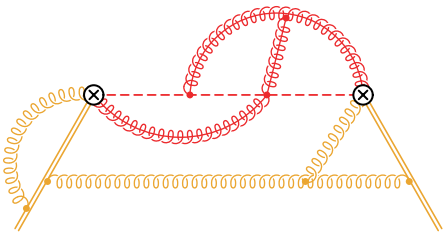

Eg.2: Consider a current that is a global color singlet within the n-collinear sector

$$J^\mu = (\bar{\xi}_n W)\Gamma^\mu W^\dagger \xi_n = (\bar{\xi}_n^{(0)} W^{(0)})\Gamma^\mu (W^{(0)\dagger}\xi_n^{(0)})\,. \tag{6.12}$$

Here all the usoft gluons have cancelled using $Y_n^\dagger Y_n = 1$, so all the usoft gluons decouple at leading order. Diagramatically we can imagine this current producing an energetic color singlet state like a collinear pion (ignoring the fact that we're in SCET_I for a moment):

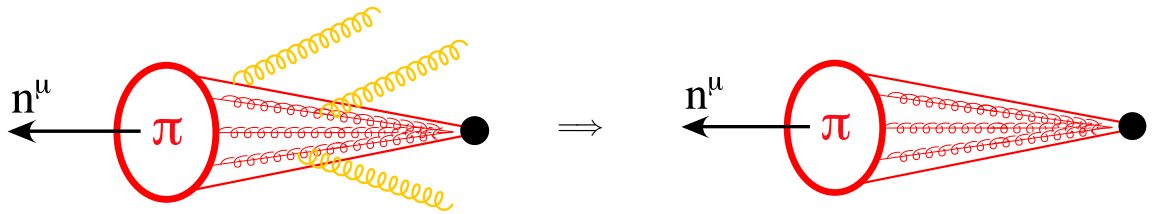

This decoupling is called color transparency, the long wavelength usoft gluons only see the overall color charge of the energetic fields in the pion, and hence cancel out for this color singlet object.

Eg.3: As a third example, consider our operator for $e^+e^- \to$ dijets. Here we have two types of collinear fields, n_1 and n_2, and the BPS field redefinitions give Y_{n_1} and Y_{n_2} ultrasoft Wilson lines:

$$J = (\bar{\xi}_{n_1} W_{n_1})\Gamma(W_{n_2}^\dagger \xi_{n_2}) = \big(\bar{\xi}_{n_1}^{(0)} W_{n_1}^{(0)}\big)\big(Y_{n_1}^\dagger Y_{n_2}\big)\Gamma\big(W_{n_2}^{(0)\dagger}\xi_{n_2}^{(0)}\big)\,. \tag{6.13}$$

This result involves the product of three factored sectors (n_1-collinear)(ultrasoft)(n_2-collinear). Here the lines are both outgoing, $Y_{n_1}^\dagger = Y_{n_1+}^\dagger$ and $Y_{n_2} = Y_{n_2-}$.

Remark: It is possible to formulate a gauge symmetry for the decoupled collinear fields via $U_n^{(0)} = Y_n^\dagger(x) U_n(x) Y_n(x)$, that then acts on the collinear (0) fields without ultrasoft components. However, there is not new content to this gauge symmetry beyond the ones we considered earlier.

6.2 Wilson Coefficients and Hard Factorization

As is standard in effective field theories, the high energy behavior of the theory is encoded in Wilson coefficients C. In SCET the Wilson coefficients can depend on the large momenta of collinear fields that are $\mathcal{O}(\lambda^0)$. Because of gauge symmetry the momenta appearing in C must be momenta for collinear gauge invariant products of fields. We can write $C(\overline{\mathcal{P}}, \mu)$ where the large momenta is picked out by the label operator $\overline{\mathcal{P}}$ which acts on these products of fields. For example, including this operator with our heavy-to-light current yields

$$(\bar{\xi}_n W_n)\Gamma^\mu h_v C(\overline{\mathcal{P}}^\dagger) = C(-\mathcal{P}, \mu)(\bar{\xi}_n W_n)\Gamma^\mu h_v \tag{6.14}$$

(noting that $\overline{\mathcal{P}}^\dagger > 0$ so we have picked a convenient sign). We have included parentheses around $\bar{\xi}_n W_n$ because $C(-\overline{P}, \mu)$ must act on this product, since only the momentum of this combination is collinear gauge invariant. It is convenient to write this result as a convolution between a real number valued Wilson coefficient and an operator depending on a new label ω

$$\begin{aligned}(\bar{\xi}_n W)\Gamma^\mu h_v C(\overline{\mathcal{P}}^\dagger) &= \int d\omega\, C(\omega,\mu)\big[(\bar{\xi}_n W_n)\delta(\omega - \overline{\mathcal{P}}^\dagger)\Gamma^\mu h_v\big] \\ &= \int d\omega\, C(\omega,\mu)\mathcal{O}(\omega,\mu)\end{aligned} \tag{6.15}$$

where $C(\omega,\mu)$ encodes the hard dynamics and $\mathcal{O}(\omega,\mu)$ encodes the collinear and ultrasoft dynamics. Thus the hard dynamics is factorized from that of collinear fields, and this in general leads to convolutions since they both have $\bar n\cdot p$ momenta that are $\mathcal{O}(\lambda^0)$.

We can show see that this hard-collinear factorization is a general result that can be applied to any SCET operator. Recall the following relations for W

$$i\bar n\cdot D_n W_n = 0\,,\qquad W_n^\dagger W_n = 1\,,\qquad i\bar n\cdot D_n = W_n\overline{\mathcal{P}}W_n^\dagger\,,\qquad 1/(i\bar n\cdot D_n) = W_n(1/\overline{\mathcal{P}})W_n^\dagger\,. \tag{6.16}$$

These conditions imply the operator equations (for any integer k)

$$(i\bar n\cdot D_n)^k = W_n(\overline{\mathcal{P}})^k W_n^\dagger\,. \tag{6.17}$$

and we have for a general function $f(\overline{\mathcal{P}})$ or $f(i\bar n\cdot D_n)$

$$\begin{aligned} f(\overline{\mathcal{P}}) &= \int d\omega\ f(\omega)\ [\delta(\omega-\overline{\mathcal{P}})]\,, \\ f(i\bar n\cdot D_n) = W_n f(\overline{\mathcal{P}})W^\dagger &= \int d\omega\ f(\omega)\ [W\delta(\omega-\overline{\mathcal{P}})W_n^\dagger]\,. \end{aligned} \tag{6.18}$$

If in general the hard dynamics leads to a function f of a large momentum $\overline{\mathcal{P}}$, then we have $f(\overline{\mathcal{P}})$ if it acts on a n-collinear gauge invariant product of fields, and this relation shows that we can always represent this by a convolution of a Wilson coefficient $f(\omega)$ which includes a $\delta(\omega-\overline{\mathcal{P}})$ as part of the collinear operator. (If we act on fields that transform under a collinear gauge transformation then the same is true but with $f(i\bar n\cdot D_n)$ and the extra Wilson lines are included in the operator.) For example, with our current for $e^+e^-\to$ dijets we have

$$\int d\omega_1\, d\omega_2\, C(\omega_1,\omega_2)\ (\bar\xi_{n_1}W_{n_1})\delta(\omega_1-\bar n_1\cdot\mathcal{P}^\dagger)\Gamma\delta(\omega_2-\bar n_2\cdot\mathcal{P})(W_{n_2}^\dagger\xi_{n_2})\,. \tag{6.19}$$

Note that since the Y_n Wilson lines commute with $\mathcal{P}^\mu$ we can perform the ultrasoft-collinear factorization by field redefinition after having determined the most general possible Wilson coefficient, and the results will be the same as we obtained prior to discussing Wilson coefficients. In general the function $C(\omega_1,\omega_2)$ will be constrained by momentum conservation for the process under consideration, and any nontrivial dependence must be determined by matching calculations.

6.3 Soft-Collinear Factorization

The factorization of soft gluons from collinear degrees of freedom is quite different than for ultrasoft gluons discussed in Sec. 6.1. This is because as discussed in Sec. 4.6, soft gluons do not couple to collinear particles in the Lagrangian. When a soft particle interacts with a collinear particle, it produces an offshell particle with momentum $p\sim Q(\lambda,1,\lambda)$. For example, a triple gluon vertex with a soft and collinear gluon has an offshell gluon with momentum $Q(\lambda,1,\lambda)$ as shown in Fig. 11. These offshell modes have $p^2\sim Q^2\lambda\gg(Q\lambda)^2$ and can therefore be integrated out of the theory. Thus, the only way that the coupling between collinear and soft particles can arise in $\mathrm{SCET_{II}}$ is through Wilson lines present in the external operators.

At lowest order in λ soft interactions with collinear fields can only involve the $n\cdot A_s$ component. This can be understood from the scaling of the momenta, where the only the momentum component $n\cdot p_s$ survives when expanding the invariant mass of a collinear and soft momentum

$$(p_n+p_s)^2 = \bar n\cdot p_n n\cdot p_s + \dots \tag{6.20}$$

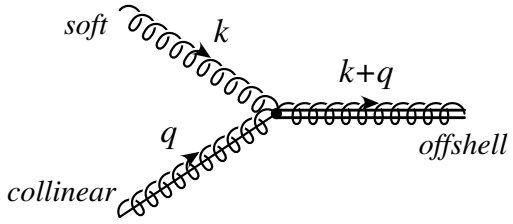

Figure 11: The interaction of a soft and collinear gluon with momenta $k \sim Q(\lambda, \lambda, \lambda)$ and $q \sim Q(\lambda^2, 1, \lambda)$ respectively, to produce an offshell gluon with momentum $k + q \sim Q(\lambda, 1, \lambda)$.

Integrating out all offshell fluctuations simply builds up factors of the Wilson line S, which is defined in position space in a very similar way to the ultrasoft Wilson line

$$S_n(x) = \mathrm{P} \exp\left[ig \int_{-\infty}^{0} ds\, n \cdot A_s^a(x + ns) T^a \right] . \tag{6.21}$$

which in momentum space becomes

$$S_n \;=\; \left[\sum_{\text{perms}} \exp\left(-g \, \frac{1}{n\cdot\mathcal{P}} \; n\cdot A_{s,q} \right) \right] . \tag{6.22}$$

Thus, much like W_n, S_n turns out to be a fundamental object in the SCET.

One can also understand the appearance of the soft Wilson lines by considering gauge invariance. Take the example of a soft-collinear heavy-to-light current. Under soft and collinear gauge transformations (suppressing the soft field labels) the fermions transform as

$$\begin{aligned} &\text{soft:} && h_v \to V_s h_v \,, && \xi_n \to \xi \\ &\text{collinear:} && h_v \to h_v \,, && \xi_{n,p} \to \hat{U}_n \xi_n \,. \end{aligned} \tag{6.23}$$

Thus, the simplest current $J = \bar{\xi}_{n,p} \Gamma h_v$ (where Γ is the spin structure) is not invariant under the gauge symmetries. To construct a gauge invariant current requires the addition of soft and collinear Wilson lines. Using the transformation properties

$$W_n \to \hat{U}_n W_n \,, \qquad S \to V_s \, S \,, \tag{6.24}$$

it is easy to see that the gauge invariant current is

$$J = \left[\bar{\xi}_n \, W_n \right] \, \Gamma \, \left[S^\dagger \, h_v \right] . \tag{6.25}$$

Thus, we see that soft gauge invariance determines how S appears. However, gauge invariance tells us nothing about the direction of the Wilson line S, and this information can only be obtained through a matching calculation.

There are three properties of Eq. (6.25) that need to be reproduced by this calculation, namely that only $\bar{n} \cdot A_{n,q}$ gluons appear to give W_n, that only the $n \cdot A_s$ component of the soft gluons appear to build up $S_n^\dagger$, and that W_n and $S_n^\dagger$ appear in the gauge invariant combination shown.

Consider the order g^2 graphs which match onto Eq. (6.25) and which contain one soft and one collinear gluon. The necessary graphs are shown in Fig. 12. Expanding the diagram in Fig. 12a to leading order gives

$$\text{Fig. 12a} = -g^2 \frac{n^\mu}{n\cdot q_s} \, \frac{\bar{n}^\nu}{\bar{n}\cdot q_c} \, \bar{\xi}_{n,p} \, T^a \, \Gamma \, T^b \, h_v \,. \tag{6.26}$$

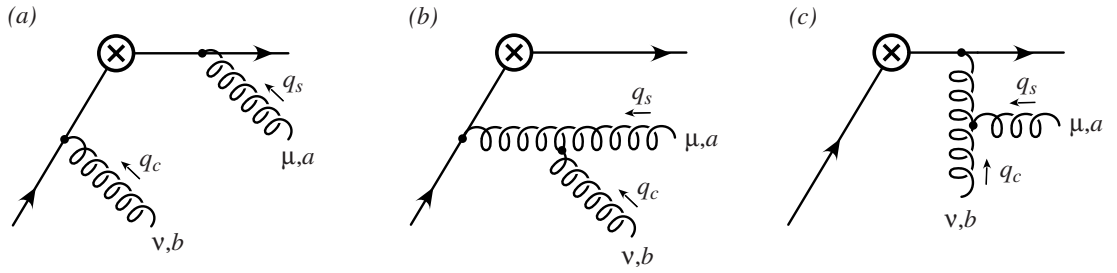

Figure 12: QCD graphs for the current $\bar{q}\,\Gamma\, b$ with offshell propagators induced by a soft gluon with momentum q_s, and a collinear gluon with momentum q_c.

We see that as expected, the leading contribution contains only the $\bar{n}\cdot A_n \sim \lambda^0$ collinear gluon by power counting, and only the $n\cdot A_s$ gluon because the γ^ν for this vertex is sandwiched between a $\bar{\xi}_{n,p}$ and an $\not{n}$ from the offshell light quark propagator. However, the two color factors T^a and T^b are in the opposite order to those in Eq. (6.25). At leading order the remaining two non-Abelian graphs are equal and give

$$\text{Fig. 12b} = \text{Fig. 12c} = \frac{g^2}{2} i f^{abc} T^c \frac{n^\mu}{n\cdot q_s}\,\frac{\bar{n}^\nu}{\bar{n}\cdot q_c}\bar{\xi}_{n,p}\Gamma h_v\,. \tag{6.27}$$

Adding the three graphs together reverses the order of the color matrices in Eq. (6.26) to give

$$\text{Figs. 12a + 12b + 12c} = -g^2 \frac{n^\mu}{n\cdot q_s}\,\frac{\bar{n}^\nu}{\bar{n}\cdot q_c}\,\bar{\xi}_{n,p}\,T^b\,\Gamma\,T^a h_v\,. \tag{6.28}$$

This is the desired result and is in agreement with Eq. (6.25). In Appendix **??** we extend this matching calculation to all orders in perturbation theory. In the next section we derive this to all orders in perturbation theory.

6.4 Mixed, hard, collinear and soft factorization [Strong overlap]

In this section we discuss the simultaneous factorization of the soft $(\lambda,\lambda,\lambda)$ modes, n-collinear $(\lambda^2,1,\lambda)$ modes, and $\bar{n}$-collinear $(1,\lambda^2,\lambda)$ modes. As discussed before, these three classes of modes can not interact with each other in a local manner and therefore do not couple through the SCET Lagrangian. However, they can couple in a gauge invariant way through external operators and currents. These interactions are built up by integrating out fluctuations with offshellness $p^2 \gg (Q\lambda)^2$. For the special case of a single collinear and soft field, this was shown to first order in Sec. 6.3. In this section, we show this to all orders in perturbation theory, and for a case where two different colliner directions are present. Much of this section is taken varbatim from Appendix A of [8].

The basic idea is to first match onto a theory which contains explicit degrees of freedom for the off-shell fluctuations. The Lagrangian of this theory describes the couplings between onshell and offshell modes that give all order λ^0 diagrams. The offshell modes (having $p^2 \gg (Q\lambda)^2$) can then be explicitly integrated out, so that all operators are expressed entirely in terms of the onshell degrees of freedom. In table 4 a summary is given of the three types of offshell momenta that are induced by adding soft, n-collinear, and $\bar{n}$-collinear momenta. For each type auxillary quark and gluon fields are defined, and for convenience momentum labels are suppressed in this section. For example, the ψ_Q quarks are created by the interaction of a n-collinear quark with an $\bar{n}$-collinear gluon. The ψ_n^L quarks are created when a collinear quark ξ_n is knocked offshell by a soft gluon, whereas the $\psi_{\bar{n}}^M$ quarks are created when a soft quark q_s is knocked offshell

Type		Momenta $(+,-,\perp)$	Fields	Wilson lines
onshell	collinear-n	$p_1^\mu \sim (\lambda^2, 1, \lambda)$	ξ_n, A_n^μ	W_n
	collinear-$\bar{n}$	$p_2^\mu \sim (1, \lambda^2, \lambda)$	$\xi_{\bar{n}}$, $A_{\bar{n}}^\mu$	$W_{\bar{n}}$
	soft	$q^\mu \sim (\lambda, \lambda, \lambda)$	q_s, A_s^μ	S_n, $S_{\bar{n}}$
	usoft	$k^\mu \sim (\lambda^2, \lambda^2, \lambda^2)$	q_{us}, A_{us}^μ	Y_n, $Y_{\bar{n}}$
offshell	$p = p_1 + p_2$	$p^\mu \sim (1, 1, \lambda)$	ψ_Q, A_Q^μ	X_n, $X_{\bar{n}}$
	$p = p_1 + q$	$p^\mu \sim (\lambda, 1, \lambda)$	ψ_n^L, $\psi_{\bar{n}}^M$, $A_n^{X\mu}$	W_n^X, S_n^X
	$p = p_2 + q$	$p^\mu \sim (1, \lambda, \lambda)$	$\psi_{\bar{n}}^M$, ψ_n^L, $A_{\bar{n}}^{X\mu}$	$W_{\bar{n}}^X$, $S_{\bar{n}}^X$

Table 4: Summary of the onshell modes discussed in section **??**, and the auxillary fields introduced to represent the offshell fluctuations that are integrated out in this appendix.

by a collinear gluon A_n. For the field ψ_Q we write $\psi_Q = \psi_n^Q + \psi_{\bar{n}}^Q$, where $\psi_n^Q = \frac{1}{4}\not{n}\not{\bar{n}}\,\psi_Q$ and $\psi_{\bar{n}}^Q = \frac{1}{4}\not{\bar{n}}\not{n}\,\psi_Q$. Then we have $\not{n}\psi_n^Q = \not{\bar{n}}\psi_{\bar{n}}^Q = 0$, $\not{n}\psi_n^L = \not{\bar{n}}\psi_{\bar{n}}^L = 0$, and $\not{n}\psi_n^M = \not{\bar{n}}\psi_{\bar{n}}^M = 0$. Various Wilson lines are also required and are listed in the table. It is convenient to define a generic Wilson line $L[a, A]$ along direction a with field A by the solution of

$$\big(a\cdot\mathcal{P} + g\,a\cdot A\big)L[a, A] = 0\,. \tag{6.29}$$

With this notation the on-shell Wilson lines are $W_n = L[\bar{n}, A_n]$, $W_{\bar{n}} = L[n, A_{\bar{n}}]$, $S_n = L[n, A_s]$, and $S_{\bar{n}} = L[\bar{n}, A_s]$. (Recall that the subscripts on W and S mean different things.) The Wilson lines involving offshell fields that we will require are

$$\begin{aligned} X_n &= L[\bar{n}, A_Q + A_n^X + A_n]\,, & X_{\bar{n}} &= L[n, A_Q + A_{\bar{n}}^X + A_{\bar{n}}]\,, \\ W_n^X &= L[\bar{n}, A_n^X + A_n]\,, & W_{\bar{n}}^X &= L[n, A_{\bar{n}}^X + A_{\bar{n}}]\,, \\ S_n^X &= L[n, A_n^X + A_s]\,, & S_{\bar{n}}^X &= L[\bar{n}, A_{\bar{n}}^X + A_s]\,. \end{aligned} \tag{6.30}$$

Below we discuss the results which allow us to integrate out offshell fluctuations. The structure of the auxiliary Lagrangians and construction of their solutions are very similar to the case presented in Ref. [**?**], to which we refer for a more detailed presentation.

From Table 4 we see that adding n and $\bar{n}$-collinear momenta gives $p^2 \sim Q^2$, whereas adding soft and collinear momenta gives $p^2 \sim Q^2\lambda$. Loops that are dominated by these offshell momenta only modify Wilson coefficients and not the infrared structure of the operators. Therefore, to determine the structure of SCET fields in an operator it sufficient to integrate out the offshell fields at tree level. For convenience we can integrate out the fluctuations starting with those with the largest offshellness. Recall that we only wish to consider offshell propagators connected to external operators. A subtelety for quarks is that distinct auxillary fields are needed for the incoming and outgoing offshell propagators. However, the solution for the outgoing field turns out to be the conjugate of the incoming field, so to avoid a proliferation of notation we simply denote the outgoing terms in the Lagrangian by +h.c., and present a solution for the incoming fields. Finally, note that for the gluon field A_Q the fields A_n, $A_{\bar{n}}$, A_n^X, $A_{\bar{n}}^X$, and A_s appear as background fields while for the fields A_n^X and $A_{\bar{n}}^X$ it is A_n, $A_{\bar{n}}$, and A_s that appear as background fields.

The terms in the auxillary Lagrangian involving the $p^2 \sim Q^2$ fields are

$$\begin{aligned} \mathcal{L}_{\rm aux}^Q &= \bar{\psi}_n^Q g n\cdot(A_Q + A_{\bar{n}}^X + A_{\bar{n}})\frac{\not{\bar{n}}}{2}(\psi_n^L + \xi_n) + \bar{\psi}_n^Q\big[n\cdot\mathcal{P} + g n\cdot(A_Q + A_{\bar{n}}^X + A_{\bar{n}})\big]\frac{\not{\bar{n}}}{2}\psi_n^Q \\ &\quad + (n \leftrightarrow \bar{n}) + \text{h.c.} \\ &\quad + \frac{1}{2g^2}\mathrm{tr}\left\{[iD_Q^\mu + gA_Q^\mu\,, iD_Q^\nu + gA_Q^\nu]^2\right\} + \frac{1}{\alpha_Q}\mathrm{tr}\{[iD_Q^\mu, A_{Q\mu}]^2\}\,. \end{aligned} \tag{6.31}$$

where $iD^\mu_Q = \frac{1}{2}n^\mu[\bar n\cdot\mathcal{P} + g\bar n\cdot(A^X_n + A_n)] + \frac{1}{2}\bar n^\mu[\mathcal{P} + gn\cdot(A^X_{\bar n} + A_{\bar n})]$. The solution of the equations of motion for these modes are

$$\begin{aligned} &\psi^Q_n = (X_{\bar n}-1)(\psi^L_n + \xi_n)\,, \qquad \psi^Q_{\bar n} = (X_n-1)(\psi^L_{\bar n} + \xi_{\bar n})\,, \\ &X^\dagger_{\bar n}X_n = W^X_n W^{X\dagger}_{\bar n}\,. \end{aligned} \tag{6.32}$$

(In addition to the last equation a constraint on the components $n\cdot A_Q$ and $\bar n\cdot A_Q$ also comes from the gauge fixing term, but will not be needed.) The terms in the auxillary Lagrangian involving the $p^2 \sim Q^2\lambda$ fields are [**?**]

$$\begin{aligned} \mathcal{L}^X_{\rm aux} &= \bar\psi^L_n gn\cdot(A^X_n + A_s)\frac{\bar n\!\!\!/}{2}\xi_n + \bar\psi^L_n\big[n\cdot\mathcal{P} + gn\cdot(A^X_n + A_s)\big]\frac{\bar n\!\!\!/}{2}\psi^L_n + (n\leftrightarrow\bar n) + \text{h.c.} \\ &+ \bar\psi^M_{\bar n} g\bar n\cdot(A^X_n + A_n)\frac{n\!\!\!/}{2}q_s + \bar\psi^M_{\bar n}\big[\bar n\cdot\mathcal{P} + g\bar n\cdot(A^X_n + A_n)\big]\frac{n\!\!\!/}{2}\psi^M_{\bar n} + (n\leftrightarrow\bar n) + \text{h.c.} \\ &+ \frac{1}{2g^2}\text{tr}\Big\{[iD^\mu_{nX} + gA^{X\mu}_n\,, iD^\nu_{nX} + gA^{X\nu}_n]^2\Big\} + \frac{1}{\alpha_n}\text{tr}\Big\{[iD^\mu_{nX}, A^X_{n\mu}]^2\Big\} + (n\leftrightarrow\bar n)\,, \end{aligned} \tag{6.33}$$

where $iD^\mu_{nX} = \frac{1}{2}n^\mu[\bar n\cdot\mathcal{P} + g\bar n\cdot A_n] + \frac{1}{2}\bar n^\mu[n\cdot\mathcal{P} + gn\cdot A_s]$. The solutions for these modes are

$$\begin{aligned} &\psi^L_n = (S^X_n - 1)\xi_n\,, \qquad \psi^M_{\bar n} = (W^X_n - 1)q_s\,, \qquad S^{X\dagger}_n W^X_n = W_n S^\dagger_n\,, \\ &\psi^L_{\bar n} = (S^X_{\bar n} - 1)\xi_{\bar n}\,, \qquad \psi^M_n = (W^X_{\bar n} - 1)q_s\,, \qquad S^{X\dagger}_{\bar n} W^X_{\bar n} = W_{\bar n} S^\dagger_{\bar n}\,. \end{aligned} \tag{6.34}$$

Together Eqs. (6.32) and (6.34) can be used at leading order to elliminate the fields representing offshell fluctutations with $p^2 \gg (Q\lambda)^2$.

As an illustration of these results we discuss the soft-collinear factorization for the production of a $q_n\bar q_{\bar n}$ pair with a large invariant mass Q^2. This process is mediated in the full theory by the electromagnetic current $J = \bar\psi\Gamma\psi$ (Γ a color singlet). This current will match onto a current in SCET that is built entirely out of onshell fields. Using the results in this section this current can be systematically derived. To start the quark field in J matches onto ξ_n plus all possible fields which the auxillary Lagrangian can create starting from ξ_n, so

$$J \to (\bar\xi_n + \bar\psi^L_n + \bar\psi^Q_n)\,\Gamma\,(\xi_{\bar n} + \psi^L_{\bar n} + \psi^Q_{\bar n})\,. \tag{6.35}$$

Integrating out the $p^2 \sim Q^2$ fluctuations with Eq. (6.32) and inserting a hard Wilson coefficient C which depends on label operators turns Eq. (6.35) into

$$(\bar\xi_n + \bar\psi^L_n)X^\dagger_{\bar n}\,C\Gamma\,X_n(\xi_{\bar n} + \psi^L_{\bar n}) = (\bar\xi_n + \bar\psi^L_n)W^X_n\,C\Gamma\,W^{X\dagger}_{\bar n}(\xi_{\bar n} + \psi^L_{\bar n})\,. \tag{6.36}$$

To construct the first operator we used the equations of motion for ψ^Q_n and $\psi^Q_{\bar n}$, and in the second operator we used the equation of motion identity for the gluons in X_n and $X_{\bar n}$. In a similar fashion we can now integrate out the $p^2 \sim Q^2\lambda$ fluctuations with Eq. (6.34) to give

$$\bar\xi_n S^{X\dagger}_n W^X_n\,C\Gamma\,W^{X\dagger}_{\bar n} S^X_{\bar n}\xi_{\bar n} = \bar\xi_n W_n S^\dagger_n\,C\Gamma\,S_{\bar n}W^\dagger_{\bar n}\xi_{\bar n}\,. \tag{6.37}$$

The operator on the right is the final result used in Eq. (**??**), and is soft, collinear, and usoft gauge invariant. It should be obvious from this example how the equations of motion in Eqs. (6.32) and (6.34) can be used to determine the factorized form of a general leading order operator.

6.5 Operator Building Blocks

Our discussion of hard-collinear factorization in SCET in the previous section motivates setting up a more convenient notation for building operators out of products that are collinear gauge invariant. For the collinear quark field we define a "quark jet field" (SCET_I) or "quark parton field" (SCET_II)

$$\begin{aligned} \chi_n &\equiv W_n^\dagger \xi_n \,, \\ \chi_{n,\omega} &\equiv \delta(\omega - \bar{n}\cdot\mathcal{P})(W_n^\dagger \xi_n) \,, \end{aligned} \tag{6.38}$$

where the last expression has a definite $\mathcal{O}(\lambda^0)$ momentum. With this notation our $e^+e^- \to$ dijets operator becomes

$$\int d\omega_1\, d\omega_2\, C(\omega_1,\omega_2)\; \bar{\chi}_{n,\omega_1} \Gamma \chi_{\bar{n},\omega_2}. \tag{6.39}$$

For the gluon field we define a "gluon jet field" (SCET_I) or "gluon parton field" (SCET_II) as

$$\begin{aligned} \mathcal{B}_{n\perp}^\mu &\equiv \frac{1}{g}\big[W_n^\dagger i D_{n\perp}^\mu W_n\big], \\ \mathcal{B}_{n\perp,\,\omega}^\mu &\equiv \big[\mathcal{B}_{n\perp}^\mu \delta(\omega - \bar{\mathcal{P}}^\dagger)\big] \,, \end{aligned} \tag{6.40}$$

where the label operators and derivatives act only on the fields inside the outer square brackets. The gluon jet field can also be written as a commutator via

$$\begin{aligned} g\mathcal{B}_{n\perp}^\mu &= \big[W_n^\dagger i D_{n\perp}^\mu W_n\big] = \Big[\frac{1}{\bar{n}\cdot\mathcal{P}}\,\bar{n}\cdot\mathcal{P} W_n^\dagger i D_{n\perp}^\mu W_n\Big] = \Big[\frac{1}{\bar{n}\cdot\mathcal{P}}\, W_n^\dagger i\bar{n}\cdot D_n i D_{n\perp}^\mu W_n\Big] \\ &= \Big[\frac{1}{\bar{n}\cdot\mathcal{P}}\, W_n^\dagger [i\bar{n}\cdot D_n, i D_{n\perp}^\mu] W_n\Big] \,. \end{aligned} \tag{6.41}$$

The outer square brackets indicate that deriviatives act only on objects inside. In the third equality we used $\bar{n}\cdot\mathcal{P} = W_n^\dagger i\bar{n}\cdot D_n W_n$, and in the last line we used that fact that within the square brackets $[i\bar{n}\cdot D_n W_n] = 0$ to write the result as a commutator. Equation (6.41) allows the gluon jet field to be written in terms of a field strength via $\mathcal{B}_{n\perp}^\mu = T^A \mathcal{B}_{n\perp}^{A\mu}$ where

$$\mathcal{B}_{n\perp}^{A\mu} = \frac{1}{\bar{n}\cdot\mathcal{P}}\,\bar{n}_\nu i G_n^{B\nu\mu_\perp} \mathcal{W}_n^{BA} \,, \tag{6.42}$$

where $\mathcal{W}_n^{BA} = \mathcal{W}_n^{BA}[\bar{n}\cdot A_n]$ is the adjoint representation collinear Wilson line and the collinear gluon field strength obeys $igG_n^{A\mu\nu}T^A = [iD_n^\mu, iD_n^\nu]$.

We can show that a complete basis of objects for building collinear operators at any order in λ is given by the three objects [15]

$$\chi_n \,, \qquad \mathcal{B}_{n\perp}^\mu \,, \qquad \mathcal{P}_{n\perp}^\mu \,. \tag{6.43}$$

Any other operators can be expressed in terms of these three objects. This basis is nice because the two gluon degrees of freedom in $\mathcal{B}_{n\perp}^\mu$ can be taken as the physical polarizations. Indeed the expansion of $\mathcal{B}_{n\perp}^\mu$ in terms of gluon fields yields

$$\mathcal{B}_{n\perp}^\mu = A_{n\perp}^\mu - \frac{q_\perp^\mu}{\bar{n}\cdot q}\,\bar{n}\cdot A_{n,q} + \ldots \,, \tag{6.44}$$

where the ellipses denote terms with ≥ 2 collinear gluon fields. In addition to the building blocks in Eq. (6.43), operators will also of course involve functions of $\overline{\mathcal{P}} = \bar{n}\cdot\mathcal{P}$ that appear as Wilson coefficients.

To see that Eq. (6.43) gives a complete basis we start by noting that the $\perp$ covariant derivative is redundant. If we consider it sandwiched by Wilson lines, then

$$i\mathcal{D}_n^{\perp\mu} \equiv W_n^\dagger i D_{n\perp}^\mu W_n = \mathcal{P}_{n\perp}^\mu + \left[W_n^\dagger i D_{n\perp}^\mu W_n\right] = \mathcal{P}_{n\perp}^\mu + g\mathcal{B}_{n\perp}^\mu \,. \tag{6.45}$$

We can also remove $in\cdot\partial$ derivatives by using the equations of motion for quarks and gluons. For instance the collinear quark equations of motion can be written as

$$in\cdot\partial\chi_n = -(gn\cdot\mathcal{B}_n)\chi_n - (i\not{\mathcal{D}}_n^\perp)\frac{1}{\bar n\cdot\mathcal{P}}(i\not{\mathcal{D}}_n^\perp)\chi_n \,, \tag{6.46}$$

where $\mathcal{D}_{n\perp}^\mu$ is given in terms of basis objects by (6.45), and where

$$n\cdot\mathcal{B}_n \equiv \frac{1}{g}\left[\frac{1}{\mathcal{P}} W_n^\dagger [i\bar n\cdot D_n, in\cdot D_n] W_n\right] . \tag{6.47}$$

The gluon equations motion allow us to elliminate $n\cdot\mathcal{B}_n$ in terms of basis objects as

$$n\cdot\mathcal{B}_n = -\frac{2\mathcal{P}_{n\perp}^\nu}{\bar n\cdot\mathcal{P}}\mathcal{B}_\nu^{n\perp} + \frac{2}{\bar n\cdot\mathcal{P}} g^2 T^A \sum_f \left[\bar\chi_n^f T^A \frac{\not{\bar n}}{2}\chi_n^f\right] + \ldots , \tag{6.48}$$

where the ellipses denote a term that involves two $\mathcal{B}_{n\perp}$s. The gluon equation of motion also allow us to eliminate $in\cdot\partial\mathcal{B}_{n\perp}^\mu$ in terms of the basic building blocks, much like for the quark term. Finally, objects like $g\mathcal{B}_{\perp\perp}^{\mu\nu} \equiv [1/(\bar n\cdot\mathcal{P})\, W^\dagger [iD_{n\perp}^\mu, iD_{n\perp}^\nu] W]$ and $g\mathcal{B}_{\perp 2}^\mu \equiv [1/(\bar n\cdot\mathcal{P})\, W^\dagger [iD_{n\perp}^\mu, in\cdot D_n] W]$ can again be eliminated in terms of the building blocks with manipulations similar to those in (6.41), and with the use of (6.48).

The standard building blocks for ultrasoft fields and operators are the same as those in QCD, namely ultrasoft quark fields ψ_{us} and ultrasoft covariant derivatives D_{us} (from which we also obtain field strengths). The ultrasoft equations of motion (equivalent to the QCD equations of motion) can be used to reduce the basis for these operators. Since at leading power the $n\cdot A_{us}$ field appears inside iD_{ns}^μ we also introduce for latter convenience the notation

$$i\mathcal{D}_{ns}^\mu = W_n^\dagger i D_{ns}^\mu W_n \,. \tag{6.49}$$

The other components of the ultrasoft gauge field are power suppressed relative to the corresponding components of the collinear gauge field, but do appear in collinear operators at subleading power (and of course in the purely ultrasoft leading power Lagrangian). It is worth remarking about the connections between our building blocks in Eq. (6.43) and the ultrasoft operators that come from RPI and gauge covariance. Multiplying the identities in (5.32) with Wilson lines on both sides we find

$$\begin{aligned} iW_n^\dagger i D_\perp^\mu\, W_n &= i\mathcal{D}_{n\,\perp}^\mu + iD_{\mathrm{us}\,\perp}^\mu = \mathcal{P}_{n\perp}^\mu + g\mathcal{B}_{n\perp}^\mu + iD_{\mathrm{us}\,\perp}^\mu \,, \\ iW_n^\dagger i\bar n\cdot D\, W_n &= \bar n\cdot\mathcal{P} + i\bar n\cdot D_{\mathrm{us}}^\mu \,. \end{aligned} \tag{6.50}$$

Thus factors of $\mathcal{P}_{n\perp}^\mu$ and $\bar n\cdot\mathcal{P}$ that appear in operators will be connected to higher order operators with these ultrasoft covariant derivatives.

For constructing operators in $\mathrm{SCET_{II}}$ at any order in the power expansion we have the same three collinear building blocks in Eq. (6.43). Since the sum of soft and collinear momenta gives an offshell momentum, we here do not need any analog of the mixed derivative in Eq. (6.49). As explained in Sec. 6.3, integrating out these offshell particles leads to soft Wilson lines S_n that appear along with soft quark and gluon fields in an analogous manner to how the collinear Wilson lines appear with collinear fields. Therefore we have direct soft analogs of the building blocks in Eq. (6.43),

$$\psi_{s(n)} \,, \qquad \mathcal{B}_{s\perp(n)}^\mu \,, \qquad \mathcal{B}_{s0(n)} \,, \qquad \mathcal{P}_\perp \,, \tag{6.51}$$

where we define the quark and gluon soft building block operators by

$$\psi_{s(n)} = S_n^\dagger \psi_s \,, \qquad \mathcal{B}_{s\perp(n)}^\mu = \frac{1}{g}\left[S_n^\dagger i D_{s\perp}^\mu S_n\right] , \qquad \mathcal{B}_{s0(n)} = \frac{1}{g}\left[S_n^\dagger i\bar n\cdot D_s S_n\right] . \tag{6.52}$$

Building Block:	$\mathcal{B}^\mu_{n_i\perp}$	χ_{n_i}	$\mathcal{P}^\mu_\perp$	ψ_{us}	D^μ_{us}	$\psi_{s(n)}$	$\mathcal{B}^\mu_{s\perp(n)}$	$\mathcal{B}^\mu_{s0(n)}$
Power Counting:	λ	λ	λ	λ^3	λ^2	$\lambda^{3/2}$	λ	λ

Table 5: Summary of building block operators for $\mathrm{SCET_I}$ and $\mathrm{SCET_{II}}$ and their power counting.

6.6 Helicity Operator Building Blocks

When building operators with many collinear directions or when building operators beyond leading power, it is useful to work with building blocks that are scalars under the Lorentz group. This can be done by projecting the building blocks from Sec. 6.5 onto objects with definite helicity, and our discussion in this section follows that of Refs. [16, **?**].

We define a collinear gluon field of definite helicity as

$$\text{h}=\pm\,1\text{:} \qquad \mathcal{B}^a_{i\pm} = -\varepsilon_{\mp\mu}(n_i,\bar n_i)\,\mathcal{B}^{a\mu}_{n_i\perp,\omega_i}\,, \tag{6.53}$$

where a is an adjoint color index and the polarization vectors are defined by

$$\varepsilon^\mu_+(n,\bar n) = \frac{\langle n+|\gamma^\mu|\bar n+\rangle}{\sqrt{2}\langle \bar n n\rangle}\,, \qquad \varepsilon^\mu_-(n,\bar n) = -\frac{\langle n-|\gamma^\mu|\bar n-\rangle}{\sqrt{2}[\bar n n]}\,. \tag{6.54}$$

The objects $\mathcal{B}^a_{i\pm}$ are the desired scalar gluon building block fields. For this discussion of objects with definite helicity, we will adopt standard spinor-helicity notations (see eg. [14, **?**, **?**]). For instance, we have

$$\begin{aligned} |p\rangle \equiv |p+\rangle &= \frac{1+\gamma_5}{2}\,u(p)\,, & |p] \equiv |p-\rangle &= \frac{1-\gamma_5}{2}\,u(p)\,,\\ \langle p| \equiv \langle p-| &= \mathrm{sgn}(p^0)\,\bar u(p)\,\frac{1+\gamma_5}{2}\,, & [p| \equiv \langle p+| &= \mathrm{sgn}(p^0)\,\bar u(p)\,\frac{1-\gamma_5}{2}\,, \end{aligned} \tag{6.55}$$

with light-like momentum p, and we choose a representation where the spinors for quarks and antiquarks are related, $u(p) = v(p)$.[6] With this definition, for an outgoing gluon with polarization $\pm$, momentum p, $p^0 > 0$ (or an incoming gluon with polarization $\mp$, momentum $-p$, $p_0 < 0$), and color a, the nonzero tree-level Feynman rules are

$$\langle g^a_\pm(p)|\mathcal{B}^b_{i\pm}|0\rangle = \delta^{ab}\tilde\delta(\tilde p_i - p)\,, \qquad \langle 0|\mathcal{B}^b_{i\pm}|g^a_\mp(-p)\rangle = \delta^{ab}\tilde\delta(\tilde p_i - p). \tag{6.56}$$

Here the $\tilde\delta$-function ensures that the momentum p is n_i-collinear and that the label momentum ω_i of the $\mathcal{B}^b_{i\pm}$ field is set equal to that of the external gluon,

$$\tilde\delta(\tilde p_i - p) \equiv \delta_{\{n_i\},p}\,\delta(\omega_i - \bar n_i\cdot p)\,, \qquad \delta_{\{n_i\},p} = \begin{cases} 1 & n_i\cdot p = \mathcal{O}(\lambda^2)\,,\\ 0 & \text{otherwise}\,. \end{cases} \tag{6.57}$$

The Kronecker delta is nonzero if the collinear momentum p is in the $\{n_i\}$ collinear equivalence class (recalling that if $n_i\cdot p\sim\lambda^2$ and $\bar n_i\cdot p\sim\lambda^0$, that by the onshell condition $p^2=0$ we automatically have $p^\mu_{n_i\perp}\sim\lambda$). The corresponding measure for this $\tilde\delta$-function is

$$\int \mathrm{d}\tilde p \equiv \sum_{\{n_i\}}\int \mathrm{d}\omega_i\,, \qquad \int \mathrm{d}\tilde p_i\;\tilde\delta(\tilde p_i - p) = 1\,. \tag{6.58}$$

[6] Note that the spinor products $\langle \bar n n\rangle$ and $[\bar n n]$, in Eq. (6.54) depend on the choice of quantization axis for the spinors, and hence are not automatically trivial even though $n\cdot\bar n = 2$ (they become trivial only if the quantization axis is taken to be $\hat n$).

The sum here runs over the distinct collinear equivalence classes.

We also define quark building block fields with definite helicity by

$$\chi^{\alpha}_{i\pm} = \frac{1 \pm \gamma_5}{2}\chi^{\alpha}_{n_i,-\omega_i}\,, \qquad \bar\chi^{\bar\alpha}_{i\pm} = \bar\chi^{\bar\alpha}_{n_i,-\omega_i}\frac{1 \mp \gamma_5}{2}\,. \tag{6.59}$$

For external quarks of definite helicity, with n_i-collinear momentum p, the spinor appearing in SCET Feynman rules is,

$$\frac{1 \pm \gamma_5}{2}\frac{\not{n}_i\bar{\not{n}}_i}{4}u(p) = \frac{\not{n}_i\bar{\not{n}}_i}{4}|p\pm\rangle = \frac{1 \pm \gamma_5}{2}u_n \equiv |p\pm\rangle_{n_i}, \tag{6.60}$$

where $|p\pm\rangle_{n_i}$ is a convenient short-hand spinor-helicity style notation for the projected spinor, and is proportional to $|n_i\pm\rangle$. Using this, we get the nonzero tree-level Feynman rules for incoming ($p^0 < 0$) and outgoing ($p^0 > 0$) quarks with definite helicity $\pm$ and color α (or $\bar\alpha$),

$$\begin{aligned}
&\big\langle 0\big|\chi^{\beta}_{i\pm}\big|q^{\bar\alpha}_{\pm}(-p)\big\rangle = \delta^{\beta\bar\alpha}\,\tilde\delta(\tilde p_i - p)\;|(-p_i)\pm\rangle_{n_i}\,, \qquad &&\big\langle q^{\alpha}_{\pm}(p)\big|\bar\chi^{\bar\beta}_{i\pm}\big|0\big\rangle = \delta^{\alpha\bar\beta}\,\tilde\delta(\tilde p_i - p)\,{}_{n_i}\langle p_i\pm|\,,\\
&\big\langle 0\big|\bar\chi^{\bar\beta}_{i\pm}\big|\bar q^{\alpha}_{\mp}(-p)\big\rangle = \delta^{\alpha\bar\beta}\,\tilde\delta(\tilde p_i - p)\,{}_{n_i}\langle(-p_i)\pm|\,, \qquad &&\big\langle \bar q^{\bar\alpha}_{\mp}(p)\big|\chi^{\beta}_{i\pm}\big|0\big\rangle = \delta^{\beta\bar\alpha}\,\tilde\delta(\tilde p_i - p)\;|p_i\pm\rangle_{n_i}\,.
\end{aligned} \tag{6.61}$$

Unlike $\mathcal{B}_{i\pm}$, the quark building blocks $\chi^{\alpha}_{i\pm}$ still carry an (implicit) spinor Lorentz index, and hence are not scalars. This can be rectified by grouping the quark building blocks into contracted pairs in currents of definite helicity. The appropriate currents include those that involve quark building block fields in distinct collinear sectors, $n_i \neq n_j$,

$$\text{h}=\pm 1\text{:} \qquad J^{\bar\alpha\beta}_{ij\pm} = \mp\sqrt{\frac{2}{\omega_i\,\omega_j}}\,\frac{\varepsilon^{\mu}_{\mp}(n_i,n_j)}{\langle n_j \mp|n_i\pm\rangle}\,\bar\chi^{\bar\alpha}_{i\pm}\,\gamma_\mu\chi^{\beta}_{j\pm}\,, \tag{6.62}$$

$$\text{h}=0\text{:} \qquad J^{\bar\alpha\beta}_{ij0} = \frac{2}{\sqrt{\omega_i\,\omega_j}\,[n_in_j]}\bar\chi^{\bar\alpha}_{i+}\chi^{\beta}_{j-}\,, \qquad (J^\dagger)^{\bar\alpha\beta}_{ij0} = \frac{2}{\sqrt{\omega_i\,\omega_j}\langle n_in_j\rangle}\bar\chi^{\bar\alpha}_{i-}\chi^{\beta}_{j+}.$$

and those involving two collinear quark building blocks in the same collinear sector,

$$\text{h}=0\text{:} \qquad J^{\bar\alpha\beta}_{i0} = \frac{1}{2\sqrt{\omega_{\bar\chi}\,\omega_\chi}}\,\bar\chi^{\bar\alpha}_{i+}\,\bar{\not{n}}_i\,\chi^{\beta}_{i+}\,, \qquad J^{\bar\alpha\beta}_{i\bar 0} = \frac{1}{2\sqrt{\omega_{\bar\chi}\,\omega_\chi}}\,\bar\chi^{\bar\alpha}_{i-}\,\bar{\not{n}}_i\,\chi^{\beta}_{i-}\,, \tag{6.63}$$

$$\text{h}=\pm 1\text{:} \qquad J^{\bar\alpha\beta}_{i\pm} = \mp\sqrt{\frac{2}{\omega_{\bar\chi}\,\omega_\chi}}\,\frac{\epsilon^{\mu}_{\mp}(n_i,\bar n_i)}{\big(\langle n_i \mp|\bar n_i\pm\rangle\big)^2}\,\bar\chi^{\bar\alpha}_{i\pm}\,\gamma_\mu\bar{\not{n}}_i\,\chi^{\beta}_{i\mp}\,.$$

Together, the currents in Eqs. (6.62) and (6.63) are sufficient to construct any operator that has multiple collinear quarks. The choice of spinor factors in these currents is such that the tree-level Feynman rules for these currents are all trivial. For example,

$$\langle q^{\alpha_1}_{+}(p_1)\bar q^{\bar\alpha_2}_{-}(p_2)|J^{\bar\beta_1\beta_2}_{12+}|0\rangle = e^{i\Phi(J_{12+})}\;\delta^{\alpha_1\bar\beta_1}\delta^{\beta_2\bar\alpha_2}\tilde\delta(\tilde p_1 - p_1)\tilde\delta(\tilde p_2 - p_2)\,, \tag{6.64}$$

where for generic momenta the phase is nontrivial, $e^{i\Phi(J_{12+})} \neq 1$, for the common situation where $p_{1\perp} = p_{2\perp} = 0$ one does have $e^{\Phi(J_{12+})} = 1$. The complete set of Feynman rules for the quark currents can be found in Refs. [16, **?**].

Finally we can also decompose $\mathcal{P}^{\mu}_{\perp}$ into scalar operators of definite helicity

$$\begin{aligned}
h = \pm 1\text{:} \qquad &\mathcal{P}^{+}_{\perp} = \mathcal{P}^{+}_{i\perp}(n_i,\bar n_i) = -\epsilon^{-}(n_i,\bar n_i)\cdot\mathcal{P}_{i\perp}\,,\\
&\mathcal{P}^{-}_{\perp} = \mathcal{P}^{-}_{i\perp}(n_i,\bar n_i) = -\epsilon^{+}(n_i,\bar n_i)\cdot\mathcal{P}_{i\perp}\,.
\end{aligned} \tag{6.65}$$

$\mathcal{B}^a_{i\pm}$	$J^{\bar\alpha\beta}_{ij\pm}$	$J^{\bar\alpha\beta}_{ij0}$	$\mathcal{P}^\pm_\perp$	$J^{\bar\alpha\beta}_{i\pm}$	$J^{\bar\alpha\beta}_{i0}$	$J^{\bar\alpha\beta}_{i\bar 0}$	$\mathcal{B}^a_{us(i)\pm}$	$\mathcal{B}^a_{us(i)0}$	$\partial_{us(i)\pm}$	$\partial_{us(i)0}$
λ	λ^2	λ^2	λ	λ^2	λ^2	λ^2	λ^2	λ^2	λ^2	λ^2

$J^{\bar\alpha\beta}_{i(us)\pm}$	$J^{\bar\alpha\beta}_{i(\overline{us})\pm}$	$J^{\bar\alpha\beta}_{i(us)0}$	$J^{\bar\alpha\beta}_{i(\overline{us})0}$	$J_{(us)^2ij\pm}$	$J_{(us)^2ij0}$
λ^4	λ^4	λ^4	λ^4	λ^6	λ^6

Table 6: Complete set of helicity building block operators in $\mathrm{SCET_I}$ and their power counting. The complete set of ultrasoft currents shown here are not all defined in the text, but can be found in Ref. [**?**].

It will always be clear from the other field content which collinear sector i the operators $\mathcal{P}^\pm_{i\perp}$ are acting on, so we can freely suppress this index. It is important to emphasize that the subscripts $\pm$ here refers to the helicity about the $\hat n_i$ axis, and not the lightcone components of the momenta.

In addition to the collinear building blocks, it is also desirable to have scalar building blocks for the ultrasoft (and soft) fields. For scalar ultrasoft gluon and derivative building blocks we define

$$\begin{aligned} h=\pm1\text{:}\qquad & \mathcal{B}^a_{us(i)\pm} = -\varepsilon_{\mp\mu}(n_i,\bar n_i)\,\mathcal{B}^{a\mu}_{us(i)}, && \partial_{us(i)\pm} = -\varepsilon_{\mp\mu}(n_i,\bar n_i)\,\partial^\mu_{us},\ , \\ h=0\text{:}\qquad & \mathcal{B}^a_{us(i)0} = \bar n_\mu \mathcal{B}^{a\mu}_{us(i)}, && \partial_{us(i)0} = \bar n_{i\mu}\partial^\mu_{us}\,, \end{aligned} \tag{6.66}$$

Note that we allow $\mathcal{B}^a_{us(i)0}$ as a building block because removing it by the gluon equations of motion would come at the expense of allowing inverse ultrasoft derivatives in our operators. On the other hand $in\cdot\partial_{us}$ can always be removed from operators beyond the leading power Lagrangian by using the equation of motion, and without introducing inverse derivatives. Examples of quark currents with ultrasoft quark building blocks include

$$\begin{aligned} h=\pm1\text{:}\quad & J^{\bar\alpha\beta}_{i(us)\pm} = \mp\frac{2}{\sqrt{\omega_i}}\,\frac{\varepsilon^\mu_\mp(n_i,\bar n_i)}{\langle \bar n_i \mp |n_i\pm\rangle}\,\bar\chi^{\bar\alpha}_{i\pm}\,\gamma_\mu\psi^\beta_{us(i)\pm}\,, \quad J^{\bar\alpha\beta}_{(us)^2ij\pm} = \mp\,\frac{\varepsilon^\mu_\mp(n_i,n_j)}{\langle n_j \mp |n_i\pm\rangle}\,\bar\psi^{\bar\alpha}_{us(i)\pm}\gamma_\mu\psi^\beta_{us(j)\pm}\,, \\ h=0\text{:}\quad & J^{\bar\alpha\beta}_{i(us)0} = \sqrt{\frac{2}{\omega_i}}\,\bar\chi^{\bar\alpha}_{i+}\psi^\beta_{us(i)-}\,. \end{aligned} \tag{6.67}$$

The complete set of definite helicity scalar building blocks for $\mathrm{SCET_I}$ is summarized in Table 6, including the full set of ultrasoft currents whose definitions can be found in Ref. [**?**]. Beyond leading power there are also nontrivial angular momentum selection rules that must be obeyed when constructing operators, and we refer to Ref. [**?**] for a detailed discussion. For $\mathrm{SCET_{II}}$ the building block fields for soft gluons, derivatives, and quark currents are defined in a manner that is exactly analogous to the ultrasoft building blocks discussed above.

As an example of the advantages of using the helicity operator building blocks, consider using the traditional SCET building blocks in Table 5 to build a basis of four quark operators or four gluon operators involving four distinct collinear directions,

$$\begin{aligned} O^{\bar\alpha\beta\bar\gamma\delta} &= \bar\chi^{\bar\alpha}_{n_1}\Gamma_1\chi^\beta_{n_2}\bar\chi^{\bar\gamma}_{n_3}\Gamma_2\chi^\delta_{n_4}\,, \\ O^{abcd} &= \mathcal{B}^{\mu a}_{n_1\perp}\mathcal{B}^{\nu b}_{n_2\perp}\mathcal{B}^{\sigma c}_{n_3\perp}\mathcal{B}^{\delta d}_{n_4\perp}\Gamma_{\mu\nu\sigma\delta}\,. \end{aligned} \tag{6.68}$$

Here Γ_1, Γ_2, and $\Gamma_{\mu\nu\sigma\delta}$ are shorthand for all possible Lorentz and Dirac structures, and to determine a basis we must enumerate the minimal number of such structures. In general this is a non-trivial task. On the other hand, using the helicity operators there are four independent helicity operators for the quark process at leading power [16],

$$\begin{aligned} O^{\bar\alpha\beta\bar\gamma\delta}_{(+;+)} &= J^{\bar\alpha\beta}_{12+}\,J^{\bar\gamma\delta}_{34+} \qquad O^{\bar\alpha\beta\bar\gamma\delta}_{(+;-)} = J^{\bar\alpha\beta}_{12+}\,J^{\bar\gamma\delta}_{34-}\,, \\ O^{\bar\alpha\beta\bar\gamma\delta}_{(-;+)} &= J^{\bar\alpha\beta}_{12-}\,J^{\bar\gamma\delta}_{34+}\,, \qquad O^{\bar\alpha\beta\bar\gamma\delta}_{(-;-)} = J^{\bar\alpha\beta}_{12-}\,J^{\bar\gamma\delta}_{34-}\,, \end{aligned} \tag{6.69}$$

and five operators for the gluons at leading power,

$$\begin{aligned}
\mathcal{O}^{abcd}_{+++} &= \frac{1}{4!}\mathcal{B}^a_{1+}\mathcal{B}^b_{2+}\mathcal{B}^c_{3+}\mathcal{B}^d_{4+}\,, & \mathcal{O}^{abcd}_{+++-} &= \frac{1}{3!}\mathcal{B}^a_{1+}\mathcal{B}^b_{2+}\mathcal{B}^c_{3+}\mathcal{B}^d_{4-} \\
\mathcal{O}^{abcd}_{++--} &= \frac{1}{4}\mathcal{B}^a_{1+}\mathcal{B}^b_{2+}\mathcal{B}^c_{3-}\mathcal{B}^d_{4-}\,, & \mathcal{O}^{abcd}_{+---} &= \frac{1}{3!}\mathcal{B}^a_{1-}\mathcal{B}^b_{2-}\mathcal{B}^c_{3-}\mathcal{B}^d_{4+} \\
\mathcal{O}^{abcd}_{----} &= \frac{1}{4!}\mathcal{B}^a_{1-}\mathcal{B}^b_{2-}\mathcal{B}^c_{3-}\mathcal{B}^d_{4-}\,. & &
\end{aligned} \tag{6.70}$$

Thus we see that the use of helicity building blocks dramatically simplifies the necessary Lorentz algebra. The choice of traditional versus helicity building blocks does not change the difficulty of enumerating a color basis. Discussion of operator color bases and the connection to the standard bases used in the amplitude literature can be found in Ref. [16].

6.7 Convolutions in $\mathrm{SCET_I}$ and $\mathrm{SCET_{II}}$ [First Pass]

Given the factorization of hard, collinear, ultrasoft (and soft) dynamics as described in SCET, it is interesting to ask the general question of how these modes can communicate with each other. The generic picture that emerges is that modes of the same type can communicate by sharing any component of their momenta, while modes of different types can only communicate through momenta that are the same order in λ, see Table 8.1. (**TODO**) Thus, ultrasoft and n-collinear fields can communicate by exchanging $n\cdot p \sim \lambda^2$ momenta, n-collinear fields can communicate with the hard Wilson coefficients through $\bar n\cdot p \sim \lambda^0$ momenta, and soft and n-collinear fields can communicate by exchanging $p_\perp \sim \lambda$ momenta. On the other hand, if we have two collinear modes, such as n and $\bar n$, they can not directly communicate through any of their momenta components. This communication will occur between soft or collinear building block fields that are individually gauge invariant, since otherwise a gauge transformation could change the exchanged momentum.

TODO: Move this table earlier?

This communication can be illustrated graphically as shown by the example of $\mathrm{SCET_I}$ in Fig. 13, where the dashed lines indicate communication between the modes through momenta that are the same order in λ. In general, when one considers a physical observable, the factorization in SCET will lead to a factorization of squared soft and collinear matrix elements, which are individually integrated over the respective phase space of their particles. So in $\mathrm{SCET_I}$ we could expect convolutions between hard (H), collinear (C_n), and ultrasoft (U) squared matrix elements of the form

$$\sigma \sim \int \mathrm{d}p^-\mathrm{d}p^+ H(p^-)C_n(p^-,p^+)U(p^+)\,. \tag{6.71}$$

The choice of observable and its factorization properties will also influence the convolutions between functions H, C_n, and U. Several explicit examples will be explored for both $\mathrm{SCET_I}$ and $\mathrm{SCET_{II}}$ in Secs. (9,10,11,14).

7 Wilson Coefficients and Hard Dynamics

We now turn to the dynamics of SCET at one loop. An interesting aspect of loops in the effective theory is that often a full QCD loop graph has more than one counterpart with similar topology in SCET. We will compare the SCET one loop calculation for a single hard interaction current with the one loop calculation in QCD. Our goal is to understand the IR and UV divergences in SCET and the corresponding logarithms, as well as understanding how the terms not associated to divergences are treated.

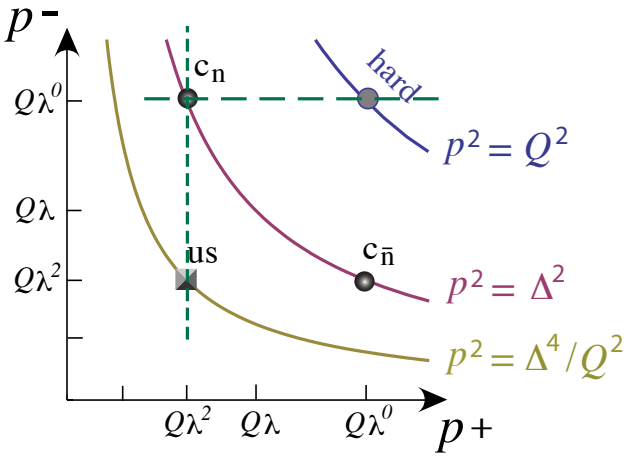

Figure 13: Convolutions that can occur between hard, n-collinear, and ultrasoft modes in $\mathrm{SCET_I}$ can only occur between momenta that are the same order in the power counting, as shown by the dashed line in this figure.

In our analysis we will use the same regulator for infrared divergences, and show that the IR divergences in QCD and SCET exactly agree, which is a validation check on the EFT. The difference determines the Wilson coefficient for the SCET operator that encodes the hard dynamics. This matching result is independent of the choice of infrared regulator as long as the same regulator is used in the full and effective theories. Finally, the SCET calculation contains additional UV divergences, beyond those in full QCD, and the renormalization and anomalous dimension determined from these divergences will sum up double Sudakov logarithms.

We will give two examples of matching QCD onto SCET, the $b \to s\gamma$ transition, and $e^+e^- \to 2$-jets. The first example has the advantage of involving only one collinear sector, but the disadvantage of requiring some familiarity with Heavy Quark Effective theory for the treatment of the b quark and involving contributions from two Dirac structures. The second example only involves jets with a single Dirac structure, but has two collinear sectors. In both cases we will use Feynman gauge for all gluons, and dimensional regularization with $d = 4 - 2\epsilon$ for all UV divergences (denoting them as $1/\epsilon$). To regulate the IR divergences we will take the strange quark offshell, $p^2 \neq 0$. For IR divergences associated purely with the heavy quark we will use dimensional regularization (denoting them $1/\epsilon_{\rm IR}$ to distinguish from the UV divergences).

7.1 $b \to s\gamma$, SCET Loops and Divergences

As a 1-loop example consider the heavy-to-light currents for $b \to s\gamma$. Although there are several operators in the full electroweak Hamiltonian, for simplicity we will just consider the dominant dipole operator $J^{\rm QCD}_{\mu\nu} F^{\mu\nu}$ where $F_{\mu\nu}$ is the photon field strength and the quark tensor current is

$$J^{\rm QCD} = \bar{s}\,\Gamma b\,, \qquad \Gamma = \sigma^{\mu\nu} P_R\,. \tag{7.1}$$

In SCET the corresponding current (for the original Lagrangian, prior to making the Y_n field redefinition) was

$$J^{\rm SCET} = (\bar{\xi}_n W)\Gamma h_v C\big(v\cdot n\,\overline{\mathcal{P}}^\dagger\big) = \int d\omega\, C(\omega)\; \bar{\chi}_{n,\omega}\Gamma h_v\,. \tag{7.2}$$

In general because of the presense of the vectors v^μ and n^μ there can be a larger basis of Dirac structures Γ for the SCET current (we will see below that at one-loop there are in fact two non-zero structures for the SCET tensor current). Note that the factor of $v \cdot n$ makes it clear that the current preserves type-III RPI. We will set $v \cdot n = 1$ in the following.

Together with the QCD and (leading order) SCET Lagrangians, we can carry out loop calculations with these two currents. First lets consider loop corrections in QCD. We have a wavefunction renormalization graph for the heavy quark denoted b, and one for the massless (strange) quark denoted q:

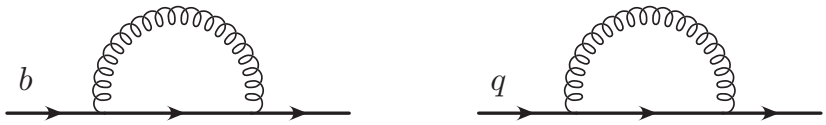

This gives the wavefunction renormalization factors Z_{ψ_b} and Z_ψ respectively. In the "on-shell" scheme which includes both the UV divergences and the finite residues these Z-factors are

$$\begin{aligned} Z_{\psi_b} &= 1 - \frac{\alpha_s C_F}{4\pi}\left[\frac{1}{\epsilon} + \frac{2}{\epsilon_{\rm IR}} + 3\ln\frac{\mu^2}{m_b^2} + 4\right], \\ Z_\psi &= 1 - \frac{\alpha_s C_F}{4\pi}\left[\frac{1}{\epsilon} - \ln\frac{-p^2}{\mu^2} + 1\right]. \end{aligned} \tag{7.3}$$

(If one instead uses $\overline{\rm MS}$ for the wavefunction renormalization factors, then the finite residues still show up in the final result for the S-matrix element due to the LSZ formula.) The remaining diagram is a vertex graph for the tensor current $J^{\rm QCD}$. At tree level the matrix element gives

$$V^0_{\rm qcd} = \bar u_s(p) P_R\, i\sigma^{\mu\nu} u_b(p_b) \tag{7.4}$$

while the one-loop diagram

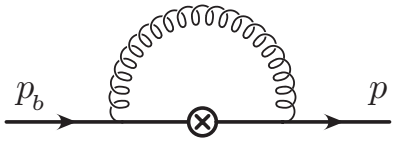

gives

$$\begin{aligned} V^1_{\rm qcd} = &-\frac{\alpha_s C_F}{4\pi}\left[\ln^2\left(\frac{-p^2}{m_b^2}\right) + 2\ln\left(\frac{-p^2}{m_b^2}\right) - \frac{2}{\epsilon} + \frac{1}{2}\ln\left(\frac{-p^2}{\mu^2}\right) + 2\ln\frac{\mu}{\omega} - 3\ln\frac{\mu}{m_b} + f_1(1-\hat q^2)\right]\bar u_s P_R\, i\sigma^{\mu\nu} u_b \\ &+ \frac{\alpha_s C_F}{4\pi} f_2(1-\hat q^2)\ \bar u_s P_R\Big(\frac{p^\mu\gamma^\nu - p^\nu\gamma^\mu}{m_b}\Big) u_b\,, \end{aligned} \tag{7.5}$$

where we have kept $p^2 \neq 0$ only for the IR singularities, and set it to zero whenever it is not needed to regulate an IR divergence. The variable $\hat q^2 = (p_b - p)^2/m_b^2 = 1 - 2p_b\cdot p/m_b^2$ and the functions appearing in Eq. (7.5) are

$$f_1(x) = \ln(x) + \frac{2}{(1-x)}\ln(x) + 2{\rm Li}_2(1-x) + \pi^2\,, \qquad f_2(x) = \frac{4}{(1-x)}\ln(x)\,. \tag{7.6}$$

Unlike for the conserved vector current, in QCD for the tensor current the sum of vertex and wavefunction graphs still contains a $1/\epsilon$ UV divergence. Hence this QCD local current operator requires an additional counterterm not related to strong coupling renormalization, and it is given by

$$Z_{\rm tensor} = 1 + \frac{\alpha_s C_F}{4\pi}\frac{1}{\epsilon}\,. \tag{7.7}$$

Adding together the QCD vertex graph and the contributions from the three Z's, and replacing the kinematic variable $\hat{q}^2 = 1 - \bar{n}\cdot p/m_b = 1 - \omega/m_b$, the sum gives

$$\begin{aligned}\text{QCD Sum} &= V^1_{\rm qcd} + \Big[\frac{1}{2}(Z_{\psi_b}-1) + \frac{1}{2}(Z_\psi - 1) + (Z^{-1}_{\rm tensor} - 1)\Big] V^0_{\rm qcd} \\ &= -\overline{u}_s \Gamma u_b \frac{\alpha_s C_F}{4\pi}\left[\ln^2\Big(\frac{-p^2}{\omega^2}\Big) + \frac{3}{2}\ln\Big(\frac{-p^2}{\omega^2}\Big) + \frac{1}{\epsilon_{\rm IR}} + \ln\Big(\frac{\mu^2}{\omega^2}\Big) + f_1\Big(\frac{\omega}{m_b}\Big) + \frac{5}{2}\right] \\ &\quad + \frac{\alpha_s C_F}{4\pi} f_2\Big(\frac{\omega}{m_b}\Big)\, \bar{u}_s P_R \Big(\frac{p^\mu\gamma^\nu - p^\nu\gamma^\mu}{m_b}\Big) u_b\,, \end{aligned} \tag{7.8}$$

Next consider the ultrasoft loops in SCET. In Feynman gauge the ultrasoft wavefunction renormalization of the collinear quark vanishes, since the couplings are both proportional to n^μ, and $n^2 = 0$. The ultrasoft wavefunction renormalization of the heavy quark is just the HQET wavefunction renormalization. We summarize these two results as:

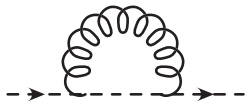

$$Z^{us}_{\xi_n} \propto n^\mu n_\mu = 0\,, \qquad$$

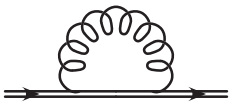

$$Z^{us}_{h_v} = 1 + \frac{\alpha_s C_F}{4\pi}\Big(\frac{2}{\epsilon} - \frac{2}{\epsilon_{\rm IR}}\Big)\,. \tag{7.9}$$

We can already note that the $1/\epsilon_{\rm IR}$ pole in $Z^{us}_{h_v}$ matches up with the IR pole in Z_{ψ_b} in full QCD (and this is the only IR divergence that we are regulating with dimensional regularization). In addition to wavefunction renormalization there is an ultrasoft vertex diagram for the SCET current. Using the on-shell condition $v\cdot p_b = 0$ for the incoming b-quark, and the SCET propagator from Eq. (4.45) for a line with injected ultrasoft momentum, we have

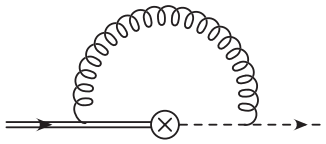

$$= V^1_{us} = (ig)^2(-i)i^2 C_F \bar{u}_n \Gamma u_v \int \frac{\bar{d}^d k \quad \mu^{2\epsilon}\iota^\epsilon \quad n\cdot v}{(v\cdot k + i0)(n\cdot k + p^2/\bar{n}\cdot p + i0)(k^2 + i0)}$$

$$V^1_{us} = -\frac{\alpha_s C_F}{4\pi}\left[\frac{1}{\epsilon^2} + \frac{2}{\epsilon}\ln\Big(\frac{\mu\bar{n}\cdot p}{-p^2 - i0}\Big) + 2\ln^2\Big(\frac{\mu\bar{n}\cdot p}{-p^2-i0}\Big) + \frac{3\pi^2}{4}\right] V^0_{\rm scet}\,, \tag{7.10}$$

where the tree level SCET amplitude is

$$V^0_{\rm scet} = \overline{u}_n \Gamma u_v\,, \tag{7.11}$$

and $\iota^\epsilon = (4\pi)^{-\epsilon} e^{\epsilon\gamma_E}$ ensures that the scale μ has the appropriate normalization for the $\overline{\rm MS}$ scheme. Note that this graph is independent of the current's Dirac structure Γ. On the heavy quark side the heavy-quark propagator gives a $P_v = (1+\not{v})/2$, but this commutes with the HQET vertex Feynman rule and hence yields a projector on the HQET spinor, $P_v u_v = u_v$. On the light quark side the propagator gives a $\not{n}/2$ and the vertex gives a $\bar{\not{n}}/2$ to yield the projector $P_n = (\not{n}\bar{\not{n}})/4$ acting on the light-quark spinor, $P_n u_n = u_n$. Hence whatever Γ is inserted at the current vertex is also the Dirac structure that appears between spinors in the answer for the loop graph. For this heavy-to-light current this feature is actually true for all loop diagrams in SCET, the spin structure of the current is preserved by loops diagrams in the EFT. For ultrasoft diagrams it happens by a simple generalization of the arguments above, while for collinear diagrams the interactions only appear on the collinear quark side of the Γ, so we just need to know that they do not induce additional Dirac matrices. (This is ensured by chirality conservation in the EFT.)

Lets finally consider the one loop diagrams with a collinear gluon. There is no wavefunction renormalization diagram for the heavy quark, since the collinear gluon does not couple to it. There is a wavefunction

renormalization graph for the light-collinear quark

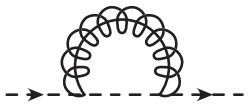

$$= \ldots = \frac{\bar{n}\!\!\!/}{2}\frac{p^2}{\bar{n}\cdot p}\frac{C_F\alpha_s}{4\pi}\Big(\frac{1}{\epsilon} - \ln\frac{-p^2}{\mu^2} + 1\Big), \quad \text{so} \quad Z_{\xi_n} = 1 - \frac{C_F\alpha_s}{4\pi}\Big(\frac{1}{\epsilon} - \ln\frac{-p^2}{\mu^2} + 1\Big). \tag{7.12}$$

We have not written out the SCET loop integrand, but it follows in a straightforward manner from using the collinear quark and gluon propagators and vertex Feynman rules from Fig. (6). Note that the result for Z_{ξ_n} is the same as the full theory Z_ψ. This occurs because for the wavefunction graph there is no connection to the ultrasoft modes or the hard production vertex, and by itself a single collinear sector is just a boosted version of full QCD (and Z_ψ is independent of this boost). There are also no subtelties related to zero-bin subtractions for this graph (the subtraction integrands are power suppressed and therefore the subtraction vanishes). There is also a diagram generated by the two-quark two-gluon Feynman rule, but this tadpole type diagram vanishes with our choice of regulators. There is also a tadpole type diagram where two gluons are taken out of the Wilson lines in the vertex, which also vanishes, ie.

$$= 0\,, \qquad\qquad$$

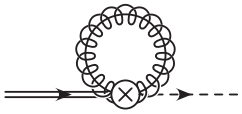

$$= 0\,. \tag{7.13}$$

The last diagram we must consider is the collinear vertex graph with an attachment from the Wilson line going to the collinear quark propagator,

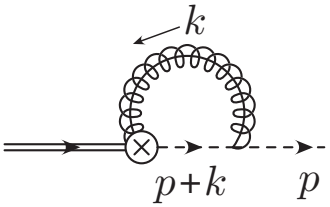

$$= V_n^1 = -ig^2 C_F \overline{u}_n \Gamma u_v\, \mu^{2\epsilon}\iota^\epsilon \sum_{\substack{k_\ell \neq 0 \\ k_\ell \neq -p_\ell}} \int\!\bar{d}^d k_r\, \frac{(n\cdot\bar{n})\,\bar{n}\cdot(p_\ell + k_\ell)}{(\bar{n}\cdot k_\ell)(k^2)(k+p)^2}$$

$$= -ig^2 C_F \overline{u}_n \Gamma u_v\, \hat{V}_n^1\,. \tag{7.14}$$

Here each momentum has been split into label and residual components $k = (k_\ell^\mu, k_r^\mu)$ and $p = (p_\ell^\mu, p_r^+)$. There are no +-momenta in the label components, and the only residual component for the external p is its +-momentum. For reasons that will soon become apparent, we have used a short hand notation for the relativistic collinear gluon and quark propagators, which in fact contain a mixture of label and residual momenta,

$$k^2 = k_r^+ k_\ell^- - \vec{k}_\ell^{\perp\,2}\,, \qquad\qquad (k+p)^2 = (k_r^+ + p_r^+)(k_\ell^- + p_\ell^-) - (\vec{k}_\ell^\perp + \vec{p}_\ell^\perp)^2\,, \tag{7.15}$$

and are homogeneous in the power counting with $k^2 \sim p^2 \sim \lambda^2$. We have also introduced the notation with a hat, $\hat{V}_n^1$, for the collinear loop integrand.

In general in collinear loop integrals there can be a nontrivial interplay between the Wilson coefficients and the large collinear loop integration, because both depend on a momentum that is the same size in the power counting, namely the large minus momenta, $k^- \sim Q$. When matching at one-loop, $\mathcal{O}(\alpha_s)$, in some cases the tree level hard matching coefficient we insert might be independent of the loop momentum k^-. In this case we can insert it back into the calculation only at the end. Even in this case it must be included when considering the renormalization group evolution, because the sharing of large momenta can lead to convolutions in the RG evolution equations. We will meet an example of this type later on when we discuss the running of parton distributions for a collinear proton. For our example of the heavy-to-light current

for $b \to s\gamma$, things are actually simple for a different reason. The SCET operator in Eq. (7.2) contains only a single gauge invariant product of collinear fields, $(\bar{\xi}_n W)$, and the Wilson coefficient only depends on the overall outgoing momentum of this product. Therefore if we include a coefficient into our diagram in Eq. (7.14) it gives only dependence on the total external momentum

$$C\big[\bar{n}\cdot(p+k)+\bar{n}\cdot(-k)\big]\big] = C\big(\bar{n}\cdot p\big)\,. \tag{7.16}$$

This result remains true for collinear loop diagrams at higher orders, so the coefficient can always be treated as multiplicative for this current, and the coefficient is always evaluated with the total $-$-momentum of the collinear jet, which in this case is $\bar{n}\cdot p = m_b$. Indeed, even when we have collinear fields for multiple directions, the large momentum are still fixed by the external kinematics *as long as we have only one(gauge invariant product of) collinear fields in each direction.* In this case the Wilson coefficient for the hard dynamics remains multiplicative in momentum space. (And we remark that this is the case that is predominantly studied for amplitudes for LHC processes with an exclusive number of jets. In general the coefficient will still be a matrix in color space once we have enough colored particles to give more than one possibility for making an overall color singlet (4 particles). There is only one possibility for the current example and hence no matrix in color space.) When we have more than one block of gauge invariant collinear fields in the same collinear direction then this will no longer be true, there will be momentum convolutions between the hard coefficient C and the collinear parts of the SCET operator.

To perform the collinear loop integration in Eq. (7.14) we should follow the rules from section 4.6 on combining label and residual momenta. As a first pass we will ignore the 0-bin restrictions $k_\ell \neq 0, -p_\ell$. In this case we can apply the simple rule from Eq. (4.68). Results following this rule in $\mathrm{SCET_I}$ are often called the naive collinear integrals. Since only momenta of external collinear particles appear in the loop integrand the multipole expansion is trivial for this integral, and this gives the same result that we would have obtained by ignoring the split into label and residual momenta from the start:

$$\begin{aligned}\hat{V}_n^{1\,\mathrm{naive}} &= \mu^{2\epsilon}\iota^\epsilon \int \frac{\bar{d}^{\,d}k\;(n\cdot\bar{n})(\bar{n}\cdot(p+k))}{(\bar{n}\cdot k)k^2(k+p)^2} \\ &= \frac{i}{(4\pi)^2}\left[\frac{2}{\epsilon^2}+\frac{2}{\epsilon}+\frac{2}{\epsilon}\ln\left(\frac{\mu^2}{-p^2}\right)+\ln^2\left(\frac{\mu^2}{-p^2}\right)+2\ln\left(\frac{\mu^2}{-p^2}\right)+4-\frac{\pi^2}{6}\right].\end{aligned} \tag{7.17}$$

This result for the loop integral can be obtained either with standard Feynman parameter rules or by contour integration in k^+ or k^-. Feynman parameter tricks and other equations that are useful for doing loop integrals in SCET are summarized in Appendix C.1.

Having assembled results for all the SCET loop graphs we can now add them up to obtain the bare SCET result

$$\text{Sum SCET} = V_{us}^1 + V_n^1 + \left[\frac{1}{2}(Z_{h_v}^{us}-1)+\frac{1}{2}(Z_{\xi_n}-1)\right]V_{\mathrm{scet}}^0\,, \tag{7.18}$$

and then compare with the full QCD calculation, setting the renormalized coupling $g^2 = 4\pi\alpha_s(\mu)$. For the moment we still will label our SCET result as naive since it ignores the 0-bin restrictions. If we examine the IR divergences encoded in the $\ln(-p^2)$ factors (and the $1/\epsilon_{\mathrm{IR}}$ from the heavy quark wavefunction renormalization) then we find for $\Gamma = P_R i\sigma^{\mu\nu}$ that at leading order $V_{\mathrm{qcd}}^0 = V_{\mathrm{scet}}^0$ and

$$\begin{aligned}(\text{Sum QCD})^{\mathrm{ren}} &= -\frac{\alpha_s C_F}{4\pi}\left[\ln^2\left(\frac{-p^2}{m_b^2}\right)+\frac{3}{2}\ln\left(\frac{-p^2}{m_b^2}\right)+\frac{1}{\epsilon_{\mathrm{IR}}}+\dots\right]V_{\mathrm{scet}}^0+\dots\,, \\ (\text{Sum SCET})^{\mathrm{naive}} &= -\frac{\alpha_s C_F}{4\pi}\left[\ln^2\left(\frac{-p^2}{m_b^2}\right)+\frac{3}{2}\ln\left(\frac{-p^2}{m_b^2}\right)+\frac{1}{\epsilon_{\mathrm{IR}}}-\frac{1}{\epsilon^2}-\frac{5}{2\epsilon}-\frac{2}{\epsilon}\ln\left(\frac{\mu}{m_b}\right)+\dots\right]V_{\mathrm{scet}}^0\,.\end{aligned} \tag{7.19}$$

Thus the results match up in the IR (as long as the remaining $1/\epsilon$ terms in the SCET result can be interpretted as UV divergences). To obtain this result for the sum of the SCET diagrams there is an important cancellation between the collinear and ultrasoft diagrams, $\ln(-p^2/\mu^2)/\epsilon - \ln[-p^2/(\mu\bar{n}\cdot p)]/\epsilon = \ln(\bar{n}\cdot p/\mu)/\epsilon = -\ln(\mu/m_b)/\epsilon$. The cancellation of the $\ln(-p^2)$ dependence in this $1/\epsilon$ pole is crucial both to match the IR divergences correctly in QCD, and in order for the remaining $1/\epsilon$ pole to possibly have an ultraviolet interpretation. The remaining dependence on $\bar{n}\cdot p = m_b$ in the $1/\epsilon$ pole is fine because this is the large momentum that the Wilson coefficient anyway depends on. This same cancellation also has a reflection in the double logarithms where the $\ln(\mu^2)$ dependence cancels out from the $\ln^2(-p^2)$ dependent term. Again this cancellation is important for the matching of IR divergences with the full theory.

The final catch is related to our use of the naive collinear integrand is the interpretation of the $1/\epsilon$ poles from the collinear loop integral. The $1/\epsilon$ divergences from the ultrasoft vertex diagram are clearly determined to be of UV origin (from large euclidean momenta or large light-like momenta). However in the collinear vertex diagram with the naive integral one of the divergences actually comes from $\bar{n}\cdot k \to 0$, and hence is of IR origin. This IR region is actually already correctly accounted for by the ultrasoft diagram where the heavy quark propagator is time-like, $v\cdot k + i0$, as it should be in the infrared region. In this region the original propagator does not behave like $\bar{n}\cdot k$. The $\bar{n}\cdot k$ term which comes from the collinear Wilson line W is instead the appropriate approximation for large $\bar{n}\cdot k$, rather than small $\bar{n}\cdot k$. Thus the issue with the naive collinear loop integral for the vertex diagram is that is double counts an IR region accounted for by the ultrasoft diagram. This double accounting is removed once we properly consider the 0-bin subtraction contributions. Therefore we apply now the rule with the 0-bin subtractions $k_\ell \neq 0, -p_\ell$ using Eq.(4.72) to obtain

$$\hat{V}_n^1 = \mu^{2\epsilon}\iota^\epsilon \int \bar{d}^d k \left[\frac{(n\cdot\bar{n})\,\bar{n}\cdot(p+k)}{(\bar{n}\cdot k)k^2(k+p)^2} - \frac{(n\cdot\bar{n})\,\bar{n}\cdot p}{(\bar{n}\cdot k)k^2(\bar{n}\cdot p\, n\cdot k + p^2)}\right] = \hat{V}_n^{1,\text{naive}} - \hat{V}_n^{1,0\text{bin}}\,. \tag{7.20}$$

It is easy to see where the 0-bin integrand comes from because it can be obtained from the appropriate ultrasoft scaling limit of the naive collinear integrand. For $k_\ell \neq 0$ we have a subtraction for the region $k_\ell \sim \lambda^2$ where we only keep terms up to those scaling as λ^{-8}, which gives precisely the integrand in Eq. (7.20) denoted as $\hat{V}_n^{1,0\text{bin}}$. The terms with $n\cdot k$ and $\bar{n}\cdot k$ in the denominator count as λ^2, while the term with $k^2 \sim \lambda^4$ to give the eight powers that compensate the $d^dk \sim \lambda^8$ for the subtraction. Note that we have kept the offshellness $0 \neq p^2 \sim \lambda^2$ since it is the same order as the $(\bar{n}\cdot p)(n\cdot k)$ term. The other subtraction is $k_\ell \neq -p_\ell$ so we have the subtraction region $k_\ell + p_\ell \sim \lambda^2$. For this case one of the factors in the denominator is $\bar{n}\cdot k \to -\bar{n}\cdot p \sim \lambda^0$ (and there is suppresion from the numerator as well) so there is no contribution at $\mathcal{O}(\lambda^{-8})$.

Being more careful about the UV ($1/\epsilon$) and IR ($1/\epsilon_{\text{IR}}$) divergences we find

$$\begin{aligned}
\hat{V}_n^{1,\text{naive}} &= \frac{i}{(4\pi)^2}\left[\frac{2}{\epsilon_{\text{IR}}\epsilon} + \frac{2}{\epsilon} + \frac{2}{\epsilon_{\text{IR}}}\ln\frac{\mu^2}{-p^2} + \Big(\frac{2}{\epsilon} - \frac{2}{\epsilon_{\text{IR}}}\Big)\ln\frac{\mu}{\bar{n}\cdot p} + \ln^2\frac{\mu^2}{-p^2} + 2\ln\frac{\mu^2}{-p^2} + 4 - \frac{\pi^2}{6}\right], \\
\hat{V}_n^{1,0\text{bin}} &= \frac{i}{(4\pi)^2}\left[\frac{2}{\epsilon} - \frac{2}{\epsilon_{\text{IR}}}\right]\left[\frac{1}{\epsilon} + \ln\frac{\mu^2}{-p^2} - \ln\frac{\mu}{\bar{n}\cdot p}\right], \\
V_n^1 &= \frac{\alpha_s C_F}{4\pi}\left[\frac{2}{\epsilon^2} + \frac{2}{\epsilon} + \frac{2}{\epsilon}\ln\left(\frac{\mu^2}{-p^2}\right) + \ln^2\left(\frac{\mu^2}{-p^2}\right) + 2\ln\left(\frac{\mu^2}{-p^2}\right) + 4 - \frac{\pi^2}{6}\right].
\end{aligned} \tag{7.21}$$

So we see that the subtraction cancels the $\bar{n}\cdot q \to 0$ IR singularities $1/\epsilon_{\text{IR}}$ in the first line. The UV divergences arising from $\bar{n}\cdot q \to \infty$ are independent of the IR regulator and just depend on the UV regulator ϵ. Since the 0-bin contribution is scaleless with our choice of regulators, taking $\epsilon_{\text{IR}} = \epsilon$ and ignoring this subtraction would give us the correct answer. Nevertheless, even with this regulator the 0-bin

contribution is still important to obtain the correct physical interpretation for the divergences. [7]

Since the final result after subtracting the 0-bin contribution is the same as in Eq. (7.17) with the $1/\epsilon$ poles all now known to be UV, we can determine the appropriate UV counterterm to renormalize the SCET current. Defining

$$C^{\rm bare}(\omega,\epsilon) = Z_C(\mu,\omega,\epsilon)C(\mu,\omega) = C + (Z_C-1)C\,, \tag{7.22}$$

and adding the counterterm graph with $(Z_C-1)C$ to cancel the $1/\epsilon$ poles in $\overline{\rm MS}$ gives

$$Z_C(\mu,\omega,\epsilon) = 1 - \frac{C_F\alpha_s(\mu)}{4\pi}\Big(\frac{1}{\epsilon^2} + \frac{1}{\epsilon}\ln\frac{\mu^2}{\omega^2} + \frac{5}{2\epsilon}\Big) + \mathcal{O}(\alpha_s^2)\,. \tag{7.23}$$

(Where by momentum conservation $\omega = m_b$.) We can now add up the collinear and ultrasoft loop graphs to obtain the final renormalized SCET result, and compare with the renormalized QCD result

$$\begin{aligned}
(\text{Sum QCD})^{\rm ren} &= -\frac{\alpha_s C_F}{4\pi}\left[\frac{1}{\epsilon_{\rm IR}} + \ln^2\Big(\frac{-p^2}{\omega^2}\Big) + \frac{3}{2}\ln\Big(\frac{-p^2}{\omega^2}\Big) + 2\ln\Big(\frac{\mu}{\omega}\Big) + f_1\Big(\frac{\omega}{m_b}\Big) + \frac{5}{2}\right] V^0_{\rm scet} \\
&\quad + \frac{\alpha_s C_F}{4\pi} f_2\Big(\frac{\omega}{m_b}\Big)\,\bar u_s P_R\Big(\frac{p^\mu\gamma^\nu - p^\nu\gamma^\mu}{m_b}\Big)u_b\,, \\
(\text{Sum SCET})^{\rm ren} &= V^1_{us} + V^1_n + \left[\frac{1}{2}(Z^{us}_{h_v}-1) + \frac{1}{2}(Z_{\xi_n}-1) + (Z_C-1)\right]V^0_{\rm scet} \\
&= -\frac{\alpha_s C_F}{4\pi}\left[\frac{1}{\epsilon_{\rm IR}} + \ln^2\Big(\frac{-p^2}{\omega^2}\Big) + \frac{3}{2}\ln\Big(\frac{-p^2}{\mu^2}\Big) - 2\ln^2\Big(\frac{\mu}{\omega}\Big) + \frac{11\pi^2}{12} - \frac{7}{2}\right] V^0_{\rm scet}\,.
\end{aligned} \tag{7.24}$$

From these two results we see that the renormalized QCD and SCET have the same infrared divergences. The difference of these results is determined by ultraviolet physics and determines the one-loop matching result for the $\overline{\rm MS}$ Wilson coefficients $C_1(\mu,\omega,m_b)$ and $C_2(\mu,\omega,m_b)$ that multiply the SCET operator in Eq. (7.2) for the Dirac structures $\Gamma = \Gamma_1 = P_R i\sigma^{\mu\nu}$ and $\Gamma = \Gamma_2 = P_R(n^\mu\gamma_\perp^\nu - n^\nu\gamma_\perp^\mu)$ respectively. Only the Dirac structure Γ_1 was present at tree-level, while Γ_2 is generated at one-loop. Taking the difference of the above two results and simplifying we find

$$\begin{aligned}
C_1(\mu,\omega,m_b) &= 1 - \frac{C_F\alpha_s(\mu)}{4\pi}\left[2\ln^2\Big(\frac{\mu}{\omega}\Big) + 5\ln\Big(\frac{\mu}{\omega}\Big) + f_1\Big(\frac{\omega}{m_b}\Big) - \frac{11\pi^2}{12} + 6\right], \\
C_2(\mu,\omega,m_b) &= \frac{C_F\alpha_s(\mu)}{4\pi}\frac{\omega}{2m_b}\,f_2\Big(\frac{\omega}{m_b}\Big)\,.
\end{aligned} \tag{7.25}$$

7.2 $e^+e^- \to$ 2-jets, SCET Loops

In this section we perform the matching from QCD onto SCET for the process $e^+e^- \to$ 2-jets. This matching will be independent of the details of the kinematical constraints that are used to enforce that we really are restricting ourselves to have only 2 jets in the final state, which will all be contained in the long distance dynamics of the effective theory. Indeed, the fact that we can successfully carry out this matching at the amplitude level makes it clear that it does not depend on which constraints we put on the phase space of the 2-jet final state. Once again, it will also be independent of the choice of IR regulator as long as the same regulator is used in both the QCD and SCET calculations. We will use Feynman gauge in both QCD and SCET, and take $d = 4-2\epsilon$ to regulate UV divergences and offshellness for the quark and antiquark, $p_q^2 = p_{\bar q}^2 = p^2 \neq 0$, to regulate all IR divergences.

[7] For other less inclusive calculations or for other choices of regulators (such as $\Omega_\perp^2 \le \vec k_\perp^2 \le \Lambda_\perp^2$, $\Omega_-^2 \le (k^-)^2 \le \Lambda_-^2$) the subtractions are even more crucial to obtain the correct result and have the UV divergences independent of the IR regulator.

In full QCD, the production of hadrons in e^+e^- collisions occurs via an s-channel exchange of a virtual photon or a Z boson. The coupling is either via a vector or an axial vector current and is therefore given by

$$J^{\rm QCD} = \bar{q}\,\Gamma_i\,q\,, \qquad \Gamma_V = g_V\gamma^\mu\,,\ \Gamma_A = g_A\gamma^\mu\gamma^5\,, \tag{7.26}$$

where $g_{V,A}$ contain the electroweak couplings for the photon or Z-boson (for a virtual photon $g_V = e_q$ the electromagnetic charge of the quark q, and $g_A = 0$). In SCET the current involves collinear quarks in the back-to-back n and $\bar{n}$ directions

$$J^{\rm SCET} = (\bar{\xi}_{\bar{n}}W_{\bar{n}})\Gamma_i C\big(\mathcal{P}^\dagger_{\bar{n}},\mathcal{P}_n,\mu\big)(W_n^\dagger\xi_n) = \int d\omega\,d\omega'\;C(\omega,\omega')\,\overline{\chi}_{\bar{n},\omega'}\Gamma_i\,\chi_{n,\omega}\,. \tag{7.27}$$

By reparametrization invariance of type-III the dependence on the label operators can only be in the combination $\omega\omega'$ inside C, so

$$C\big(\omega,\omega'\big) = C\big(\omega\omega'\big)\,. \tag{7.28}$$

Finally in the CM frame momentum conservation fixes $\omega = \omega' = Q$, the CM energy of the e^+e^- pair, so we can write

$$J^{\rm SCET} = C(Q^2)\,(\bar{\xi}_{\bar{n}}W_{\bar{n}})\,\Gamma_i\,(W_n^\dagger\xi_n)\,, \tag{7.29}$$

and the matching calculation in this section will determine the renormalized $\overline{\rm MS}$ Wilson coefficient $C(Q^2,\mu^2)$. In this case there is only one relevant Dirac structure Γ_i in SCET for each of the vector and axial-vector currents.

We again begin by calculating the full theory diagrams. As in the case of $B \to X_s\gamma$ we need the wave function contributions for the light quarks, in this case one for the quark and one for the anti-quark. Both wave function contributions are the same as the results obtained before

$$Z_\psi = 1 - \frac{\alpha_s C_F}{4\pi}\left[\frac{1}{\epsilon} - \ln\frac{-p^2}{\mu^2} + 1\right]. \tag{7.30}$$

The remaining vertex graph can again be calculated in a straightforward manner. At tree level we find

$$V^0_{\rm qcd} = \bar{u}(p_n)\Gamma_i v_{\bar{n}}(p_{\bar{n}}) \tag{7.31}$$

while the one loop vertex diagram

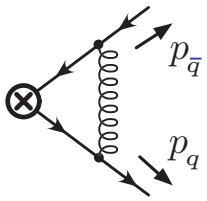

gives

$$\begin{aligned}
V^1_{\rm qcd} &= \mu^{2\epsilon}\iota^\epsilon\int\frac{d^dk}{(2\pi)^d}\,ig\,\bar{u}(p_q)\gamma^\alpha T^A\,\frac{i(\not{k}+\not{p}_q)}{(k+p_q)^2}\,\Gamma_i\,\frac{i(\not{k}-\not{p}_{\bar{q}})}{(k-p_{\bar{q}})^2}\,ig\gamma_\alpha T^A\,v(p_{\bar{q}})\,\frac{-i}{k^2}\\
&= -ig^2C_F\,\mu^{2\epsilon}\int\frac{d^dk}{(2\pi)^d}\,\bar{u}(p_q)\frac{\gamma^\alpha\,(\not{k}+\not{p}_q)\Gamma_i\,(\not{k}-\not{p}_{\bar{q}})\,\gamma_\alpha}{(k+p_q)^2\,(k-p_{\bar{q}})^2\,k^2}\,v(p_{\bar{q}})\\
&= \frac{\alpha_s C_F}{4\pi}\left[\frac{1}{\epsilon} - 2\ln^2\frac{p^2}{Q^2} - 4\ln\frac{p^2}{Q^2} - \ln\frac{(-Q^2-i0)}{\mu^2} - \frac{2\pi^2}{3}\right]\bar{u}(p_q)\,\Gamma_i\,v(p_{\bar{q}})\,.
\end{aligned} \tag{7.32}$$

Here $\iota^\epsilon = (4\pi)^{-\epsilon} e^{\epsilon\gamma_E}$ ensures that the scale μ has the appropriate normalization for the $\overline{\rm MS}$ scheme. Adding the QCD diagrams we find

$$\begin{aligned}\text{QCD Sum} &= V^1_{\rm qcd} + 2\Big[\frac{1}{2}(Z_\psi - 1)\Big] V^0_{\rm qcd} \\ &= \frac{\alpha_s C_F}{4\pi}\left[-2\ln^2\frac{p^2}{Q^2} - 3\ln\frac{p^2}{Q^2} - 1 - \frac{2\pi^2}{3}\right]\bar u(p_q)\,\Gamma_i\,v(p_{\bar q})\,. \end{aligned} \tag{7.33}$$

As before, we next consider the loops in SCET. The wave function renormalization for the collinear quark is the same as in the previous section, and we find

$$Z^{us}_\xi = 0\,, \qquad Z_\xi = 1 - \frac{C_F\alpha_s}{4\pi}\Big(\frac{1}{\epsilon} - \ln\frac{-p^2}{\mu^2} + 1\Big)\,. \tag{7.34}$$

The tree level amplitude in SCET is $V^0_{\rm scet} = \bar u_n(p_q)\Gamma_i\, v_{\bar n}(p_{\bar q})$, and to leading order $V^0_{\rm qcd} = V^0_{\rm scet}$. The ultrasoft vertex graph in SCET involves an exchange between the n-collinear and $\bar n$-collinear quarks,

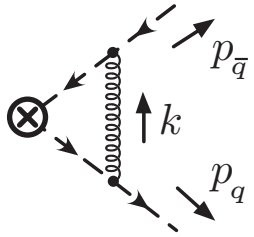

and is given by

$$\begin{aligned} V^1_{\rm usoft} &= \mu^{2\epsilon}\iota^\epsilon\int\frac{d^dk}{(2\pi)^d}\,\bar u_n\Big(ig\,\frac{\bar n\!\!\!/}{2}n^\alpha T^A\Big)\,\frac{i n\!\!\!/}{2}\frac{\bar n\cdot p_q}{\bar n\cdot p_q\; n\cdot k + p_q^2}\,\Gamma_i\,\frac{i\bar n\!\!\!/}{2}\frac{(-n\cdot p_{\bar q})}{n\cdot p_{\bar q}\;\bar n\cdot k + p_{\bar q}^2}\Big(ig\frac{n\!\!\!/}{2}\bar n_\alpha T^A\Big)\,v_{\bar n}\,\frac{(-i)}{k^2} \\ &= ig^2C_F\mu^{2\epsilon}\iota^\epsilon\Big(\bar u_n\frac{n\!\!\!/\bar n\!\!\!/}{4}\Gamma_i\frac{\bar n\!\!\!/ n\!\!\!/}{4}v_{\bar n}\Big)\int\frac{d^dk}{(2\pi)^d}\,\frac{n\cdot\bar n}{\Big(n\cdot k + \frac{p_q^2}{\bar n\cdot p_q}\Big)\Big(\bar n\cdot k + \frac{p_{\bar q}^2}{n\cdot p_{\bar q}}\Big)k^2} \\ &= \frac{\alpha_s C_F}{4\pi}\left[-\frac{2}{\epsilon^2} + \frac{2}{\epsilon}\ln\frac{-p^4}{\mu^2Q^2} - \ln^2\frac{-p^4}{\mu^2Q^2} - \frac{\pi^2}{2}\right]\bar u_n(p_q)\Gamma_i v_{\bar n}(p_{\bar q})\,. \end{aligned} \tag{7.35}$$

There are two possible collinear vertex graphs which involve a contraction between the $W_n[\bar n\cdot A_n]$ Wilson line and a n-collinear quark, and another between the $W_{\bar n}[n\cdot A_{\bar n}]$ Wilson line and the $\bar n$-collinear quark

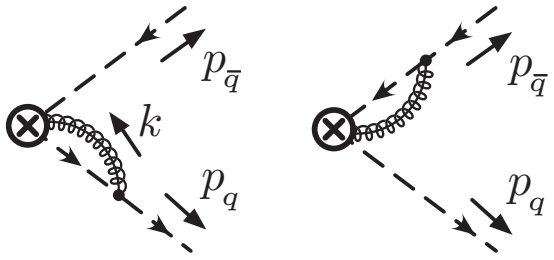

For the first diagram, we find

$$\begin{aligned} V_{\rm coll}^1 &= \mu^{2\epsilon}\iota^\epsilon \int \frac{d^dk}{(2\pi)^d}\, ig\,\bar u_n \left[n^\alpha + \frac{\not p_\perp \gamma_\perp^\alpha}{\bar n\cdot p} + \frac{\gamma_\perp^\alpha(\not p_\perp + \not k_\perp)}{\bar n\cdot(p+k)} - \frac{\not p_\perp(\not p_\perp + \not k_\perp)}{\bar n\cdot p\,\bar n\cdot(p+k)}\right]\frac{\not{\bar n}}{2} T^A \\ &\quad \times i\frac{\not n}{2}\frac{\bar n\cdot(p+k)}{(p+k)^2}\left(-g\frac{\bar n_\alpha}{\bar n\cdot k}T^A\right)\Gamma_i\, v_{\bar n}\,\frac{(-i)}{k^2} \\ &= -ig^2 C_F\mu^{2\epsilon}\iota^\epsilon \int\frac{d^dk}{(2\pi)^d}\,\frac{(n\cdot\bar n)\;\bar n\cdot(p+k)}{\bar n\cdot k\;(p+k)^2\,k^2}\,\bar u_n\Gamma_i v_{\bar n} \\ &= \frac{\alpha_s C_F}{4\pi}\left[\frac{2}{\epsilon^2}+\frac{2}{\epsilon}-\frac{2}{\epsilon}\ln\frac{-p^2}{\mu^2}+\ln^2\frac{-p^2}{\mu^2}-2\ln\frac{-p^2}{\mu^2}+4-\frac{\pi^2}{6}\right]\bar u_n(p_q)\,\Gamma_i\, v_{\bar n}(p_{\bar q})\,. \end{aligned} \tag{7.36}$$

One can easily show that the second collinear vertex diagram gives the same result as the first diagram. Furthermore the collinear integral here is identical to the one for $b\to s\gamma$ in Eq. (7.14). The result in Eq. (7.36) is for the naive integrand, since it does not include the 0-bin subtraction contribution. But the 0-bin subtraction terms here are scaleless as in Eq. (7.21), and hence the final result in Eq. (7.36) is correct with the interpretation of the $1/\epsilon$ divergences as UV.

Adding the SCET diagrams we find after some straightforward manipulations

$$\begin{aligned} \text{SCET Sum} &= V_{\rm usoft}^1 + 2V_{\rm coll}^1 + 2\Big[\frac{1}{2}(Z_\xi-1)\Big]V_{\rm scet}^0 \\ &= \frac{\alpha_s C_F}{4\pi}\left[\frac{2}{\epsilon^2}+\frac{3}{\epsilon}-\frac{2}{\epsilon}\ln\frac{-Q^2}{\mu^2}+2\ln^2\frac{\mu^2}{-p^2}-\ln^2\frac{\mu^2Q^2}{-p^4}+3\ln\frac{\mu^2}{-p^2}+7-\frac{5\pi^2}{6}\right]\bar u_n\Gamma_i v_{\bar n} \\ &= \frac{\alpha_s C_F}{4\pi}\left[\frac{2}{\epsilon^2}+\frac{3}{\epsilon}-\frac{2}{\epsilon}\ln\frac{-Q^2}{\mu^2}-2\ln^2\frac{p^2}{Q^2}+\ln^2\frac{-Q^2}{\mu^2}-3\ln\frac{p^2}{Q^2}-3\ln\frac{-Q^2}{\mu^2}+7-\frac{5\pi^2}{6}\right]\bar u_n\Gamma_i v_{\bar n}\,. \end{aligned} \tag{7.37}$$

Comparing the $\ln(p^2)$ dependence in the final line to the QCD amplitude in Eq. (7.33) We can see that SCET reproduces all IR divergences of the form $\ln p^2/Q^2$, and that the matching coefficient is therefore independent of IR divergences as it should. However, while the matrix element of the full QCD current is UV finite (since it is a conserved current), the matrix element in the effective theory is UV divergent and therefore needs to be renormalized. Defining a renormalized coupling by

$$C(Q,\epsilon) = Z_C(Q,\mu,\epsilon)C(Q,\mu) = C(Q,\mu) + \big[Z_C(Q,\mu,\epsilon)-1\big]C(Q,\mu) \tag{7.38}$$

the renormalization constant that cancels the divergences in Eq. (7.37) is

$$Z_C = 1 + \frac{C_F\alpha_s(\mu)}{4\pi}\left[-\frac{2}{\epsilon^2}-\frac{3}{\epsilon}+\frac{2}{\epsilon}\ln\left(\frac{-Q^2-i0}{\mu^2}\right)\right]. \tag{7.39}$$

Taking the difference between the renormalized matrix elements in full QCD and SCET,

$$\begin{aligned} (\text{QCD sum})^{\rm ren} &= \frac{\alpha_s(\mu)C_F}{4\pi}\left[-2\ln^2\frac{p^2}{Q^2}-3\ln\frac{p^2}{Q^2}-1-\frac{2\pi^2}{3}\right]\bar u(p_n)\,\Gamma_i\, v(p_{\bar n})\,, \\ (\text{SCET sum})^{\rm ren} &= \frac{\alpha_s(\mu)C_F}{4\pi}\left[-2\ln^2\frac{p^2}{Q^2}+\ln^2\frac{-Q^2}{\mu^2}-3\ln\frac{p^2}{Q^2}-3\ln\frac{-Q^2}{\mu^2}+7-\frac{5\pi^2}{6}\right]\bar u_n\Gamma_i v_{\bar n}\,, \end{aligned} \tag{7.40}$$

we obtain the matching result for Wilson coefficient of the operator in Eq. (5.37) at one-loop order

$$C(Q,\mu) = 1 + \frac{C_F\alpha_s(\mu)}{4\pi}\left[-\ln^2\left(\frac{-Q^2-i0}{\mu^2}\right)+3\ln\left(\frac{-Q^2-i0}{\mu^2}\right)-8+\frac{\pi^2}{6}\right]. \tag{7.41}$$

If we choose the renormalization scale to be equal to Q, we find that all logarithms vanish

$$C(Q,Q) = 1 + \frac{C_F\alpha_s(Q)}{4\pi}\left[-8+\frac{7\pi^2}{6}-3i\pi\right]. \tag{7.42}$$

7.3 Summing Sudakov Logarithms

As all perturbative objects that require renormalization, the Wilson coefficient in Eq. (7.41) depends on the renormalization scale μ. Since the Wilson coefficient depends dynamicallly only on a single scale Q, the only dependence on μ is through logarithms of the ratio of the renormalization scale to the hard scale Q. This dependence signals that it captures offshell physics from the hard scale Q that we are integrating out. One can show that for each order in perturbation theory two extra powers of logarithms of μ/Q arise. If we were to choose a renormalization scale that was very different from the hard scale Q, the logarithms would become numerically very large and could destroy the convergence of the perturbative expansion.

As already seen, by choosing $\mu = Q$, all logarithmic dependence vanishes, making the perturabative expansion at this scale choice well behaved. To obtain the Wilson coefficient at a different scale, one can now use renormalization group evolution, which sums the logarithms to all orders in perturbation theory.

With the information from either of the last two sections, we can calculate the anomalous dimensions of the opertors or Wilson coefficients. Taking

$$0 = \mu\frac{d}{d\mu}C^{\rm bare}(\epsilon) = \mu\frac{d}{d\mu}\big[Z_C(\mu,\epsilon)C(\mu)\big] = \Big[\mu\frac{d}{d\mu}Z_C(\mu,\epsilon)\Big]C(\mu) + Z_C(\mu,\epsilon)\Big[\mu\frac{d}{d\mu}C(\mu)\Big]\,, \tag{7.43}$$

we see that the anomalous dimension is defined by a derivative of the counterterm

$$\mu\frac{d}{d\mu}C(\mu) = -Z_C^{-1}(\mu,\epsilon)\Big[\mu\frac{d}{d\mu}Z_C(\mu,\epsilon)\Big]C(\mu) \equiv \gamma_C(\mu)C(\mu)\,. \tag{7.44}$$

To calculate the μ derivative we should recall the result for the derivative of the strong coupling in d dimensions

$$\mu\frac{d}{d\mu}\alpha_s(\mu,\epsilon) = -2\epsilon\,\alpha_s(\mu,\epsilon) + \beta[\alpha_s]\,, \tag{7.45}$$

where $\beta[\alpha_s]$ is the standard $d = 4$ QCD beta function written in terms of $\alpha_s(\mu,\epsilon)$.

Lets apply this to our two examples in turn. The counterterm for the $b \to s\gamma$ current is

$$Z_C^\gamma = 1 - \frac{\alpha_s(\mu)C_F}{4\pi}\left(\frac{1}{\epsilon^2} + \frac{2}{\epsilon}\ln\frac{\mu}{\omega} + \frac{5}{2\epsilon}\right). \tag{7.46}$$

Using the definition of γ_C in Eq. (7.44) we find

$$\begin{aligned}
\gamma_C^\gamma(\mu,\omega,\epsilon) &= \mu\frac{d}{d\mu}\frac{C_F\alpha_s(\mu,\epsilon)}{4\pi}\left(\frac{1}{\epsilon^2} + \frac{2}{\epsilon}\ln\frac{\mu}{\omega} + \frac{5}{2\epsilon}\right) \\
&= \frac{C_F\alpha_s(\mu,\epsilon)}{4\pi}\left(-\frac{2}{\epsilon} - 4\ln\frac{\mu}{\omega} - 5 + \frac{2}{\epsilon}\right) + \mathcal{O}(\alpha_s^2)\,, \\
&= -\frac{\alpha_s(\mu)}{4\pi}\left(2C_F\ln\frac{\mu^2}{\omega^2} + 5C_F\right),
\end{aligned} \tag{7.47}$$

where we differentiated both $\alpha_s(\mu)$ and the explicit $\ln(\mu)$, noting that the $1/\epsilon$ terms cancel to yield a well defined anomalous dimension in the $\epsilon \to 0$ limit which is given on the last line.

Similarly, the counterterm for the $e^+e^- \to$ dijets current is

$$Z_C^{\rm 2jet} = 1 + \frac{C_F\alpha_s(\mu)}{4\pi}\Big[-\frac{2}{\epsilon^2} - \frac{3}{\epsilon} + \frac{2}{\epsilon}\ln\Big(\frac{-Q^2 - i0}{\mu^2}\Big)\Big]\,, \tag{7.48}$$

so the anomalous dimension is obtained by

$$\begin{aligned}\gamma_C^{\rm 2jet}(\mu,Q,\epsilon) &= \mu\frac{d}{d\mu}\frac{C_F\alpha_s(\mu,\epsilon)}{4\pi}\left[\frac{2}{\epsilon^2}+\frac{3}{\epsilon}+\frac{2}{\epsilon}\ln\Big(\frac{\mu^2}{-Q^2-i0}\Big)\right]\\ &= \frac{C_F\alpha_s(\mu,\epsilon)}{4\pi}\left[\frac{-4}{\epsilon}-6-4\ln\Big(\frac{\mu^2}{-Q^2-i0}\Big)+\frac{4}{\epsilon}\right]+\mathcal{O}(\alpha_s^2)\,,\\ &= -\frac{\alpha_s(\mu)}{4\pi}\left[4C_F\ln\Big(\frac{\mu^2}{-Q^2-i0}\Big)+6C_F\right].\end{aligned} \tag{7.49}$$

Again in the last line we have taken the $\epsilon\to 0$ limit. Note the similarity in the form of the anomalous dimensions for our two examples of Wilson coefficients. Both anomalous dimension equations for $C(\mu)$ are homogeneous linear differential equations because in both cases the operator mixes back into itself. They both take the form

$$\mu\frac{d}{d\mu}\ln C(\omega_C,\mu) = \frac{\alpha_s(\mu)}{4\pi}\left[\frac{\rho_C}{2}\,\Gamma_0^q\,\ln\Big(\frac{\mu^2}{\omega_C^2}\Big)+\gamma_{C0}\right], \tag{7.50}$$

where $\Gamma_0^q = 4\,C_F$. For $b\to s\gamma$ we have

$$\rho_C^\gamma = -1\,, \qquad \gamma_{C0}^\gamma = -5C_F\,, \qquad \omega_C^\gamma = \omega \tag{7.51}$$

while for $e^+e^-\to$ 2jets we have

$$\rho_C^{\rm 2jet} = -2\,, \qquad \gamma_{C0}^{\rm 2jet} = -6C_F\,, \qquad \omega_C^{\rm 2jet} = \sqrt{-Q^2-i0} \tag{7.52}$$

An interesting feature of the anomalous dimensions in Eq. (7.50) is the presence of a single logarithm, $\ln(\mu^2)$, and we will show in Sec. 9 that no terms with more than a single logarithm can appear in the hard anomalous dimensions. The coefficient of this single logarithm is related to the cusp anomalous dimension that governs the renormalization of Wilson lines that meet at a cusp angle β_{ij} between lines along the four vectors n_i and n_j, where $\cosh\beta_{ij} = n_i\cdot n_j/[|n_i||n_j|]$. In the light-like limit $n_i^2, n_j^2\to 0$ we have $\beta_{ij}\to\infty$. The cusp anomalous dimension is linear in β_{ij} in this limit, which yields a logarithmic dependence on $2n_i\cdot n_j/[|n_i||n_j|]$ since $\cosh\beta_{ij}\simeq e^{\beta_{ij}}/2$. In SCET, this divergence has been handled by the renormalization procedure, and hence has become a $\ln(\mu^2)$. Indeed, if we consider making the BPS field redefinition for the dijet current we get $Y_n^\dagger Y_{\bar n}$, so it is clear that our ultrasoft diagrams involve two light-like Wilson lines meeting at a cusp. In the case of the collinear diagrams we have a Wilson line W_n that meets up with a collinear quark ξ_n, and in doing so also effectively forms a cusp. Due to this relationship of the single logarithm in the anomalous dimension to the cusp of two Wilson lines we have made the coefficient of this logarithm proportional to Γ_0^q, which is the cusp anomalous dimension of two fundamental Wilson lines at leading order.

We begin by solving the generic anomalous dimension with only the logarithmic term (in other words where $\gamma^C = 0$. Ignoring the running of the coupling constant, this equation is trivial to solve and one finds

$$C(\omega_C,\mu) = \exp\left[\frac{\alpha_s}{4\pi}\,\frac{\rho_C}{8}\,\Gamma_0^q\ln^2\left(\frac{\mu^2}{\omega_C^2}\right)\right]. \tag{7.53}$$

This result involves an exponential of a double logarithm, and is often referred to as the Sudakov form factor. Since ρ_C is negative, this amounts to a suppression that is related to the restrictions in phase space that are intrinsic for the allowed types of radiation that our operators can emit. The Sudakov form

factor also gives the probability of evolving without branching in a parton shower. For QCD we must also account for the running of the coupling, and at LL order we can use the LL β-function,

$$\mu\frac{d}{d\mu}\alpha_s(\mu) = -\frac{\beta_0}{2\pi}\,\alpha_s^2(\mu)\,, \qquad \beta_0 = \frac{11}{3}C_A - \frac{4}{3}\,T_F\,n_f\,. \tag{7.54}$$

Together Eqs. (7.50) and (7.54) are a coupled set of differential equations. The easiest way to solve these two equations is to use Eq. (7.54) to write

$$d\ln\mu = \frac{d\alpha_s}{\beta[\alpha_s]} = -\frac{2\pi}{\beta_0}\,\frac{d\alpha_s}{\alpha_s^2}\,, \qquad \ln\Big(\frac{\mu}{\omega_C}\Big) = -\frac{2\pi}{\beta_0}\int_{\alpha_s(\omega_C)}^{\alpha_s(\mu)}\frac{d\alpha}{\alpha^2}\,. \tag{7.55}$$

and to use this result in Eq. (7.50). Using the boundary condition $C(\mu_0,\omega_C) = 1 + \mathcal{O}(\alpha_s)$ we then have

$$\begin{aligned}
\ln C(\omega_C,\mu) &= \Big(\frac{2\pi}{\beta_0}\Big)^2\frac{\Gamma_0^q\,\rho_C}{4\pi}\int_{\alpha_s(\mu_0)}^{\alpha_s(\mu)}\frac{d\alpha_s}{\alpha_s}\int_{\alpha_s(\omega_C)}^{\alpha_s}\frac{d\alpha}{\alpha^2} \\
&= \frac{\Gamma_0^q\,\rho_C\,\pi}{\beta_0^2}\int_{\alpha_s(\mu_0)}^{\alpha_s(\mu)}\frac{d\alpha_s}{\alpha_s}\bigg[-\frac{1}{\alpha_s} + \frac{1}{\alpha_s(\omega_C)}\bigg] \\
&= \frac{\Gamma_0^q\,\rho_C\,\pi}{\beta_0^2}\bigg[\frac{1}{\alpha_s(\mu)} - \frac{1}{\alpha_s(\mu_0)} + \frac{1}{\alpha_s(\omega_C)}\ln\Big(\frac{\alpha_s(\mu)}{\alpha_s(\mu_0)}\Big)\bigg] \\
&= \frac{\Gamma_0^q\,\rho_C\,\pi}{\beta_0^2\,\alpha_s(\mu_0)}\Big(\frac{1}{r} - 1 + \ln r\Big) + \frac{\Gamma_0^q\,\rho_C}{2\,\beta_0}\,\ln\Big(\frac{\omega_C}{\mu_0}\Big)\ln r\,,
\end{aligned} \tag{7.56}$$

where we used $1/\alpha_s(\omega_C) = 1/\alpha_s(\mu_0) + \frac{\beta_0}{2\pi}\ln(\omega_C/\mu_0)$, and defined

$$r \equiv \frac{\alpha_s(\mu)}{\alpha_s(\mu_0)}\,. \tag{7.57}$$

The solution is therefore

$$C(\omega_C,\mu) = \exp\bigg[\frac{\Gamma_0^q\,\rho_C\,\pi}{\beta_0^2\,\alpha_s(\mu_0)}\Big(\frac{1}{r} - 1 + \ln r\Big)\bigg]\Big(\frac{\omega_C}{\mu_0}\Big)^{\Gamma_0^q\,\rho_C\ln r/(2\beta_0)}\,. \tag{7.58}$$

This result sums the infinite tower of leading-logarithms in the exponent which are of the form, $C \sim \exp(-\alpha_s L^2 - \alpha_s^2 L^3 - \alpha_s^3 L^4 - \ldots)$, where the coefficients here are schematic and $L = \ln(\mu/\mu_0)$ is a potentially large logarithm. Again this result is called the Sudakov form factor with a running coupling. Note that the form of the series obtained by expanding in the argument of the exponent is much simpler than what we would obtain by expanding the exponent itself. At each order in resummed perturbation theory the terms that are determined by solving the anomalous dimension equation can be classified by the simpler series that appears in the exponential as follows

$$\ln C \sim \Big[-L\sum_k(\alpha_s L)^k\Big]_{\rm LL} + \Big[\sum_k(\alpha_s L)^k\Big]_{\rm NLL} + \Big[\sum_k\alpha_s(\alpha_s L)^k\Big]_{\rm NNLL} + \ldots \tag{7.59}$$

Including the γ_{C0} term modifies the above equation to give

$$C(\omega_C,\mu) = \exp\bigg[\frac{\Gamma_0^q\,\rho_C\,\pi}{\beta_0^2\,\alpha_s(\mu_0)}\Big(\frac{1}{r} - 1 + \ln r\Big) + \frac{\gamma^C}{2\beta_0}\ln r\bigg]\Big(\frac{\omega_C}{\mu_0}\Big)^{\Gamma_0^q\,\rho_C\ln r/(2\beta_0)}\,. \tag{7.60}$$

This term contributes to the NLL series, but in order to get the full NLL series one needs to include the 2-loop coefficient to the term multiplying the logarithm of μ in the anomalous dimension. In the next subsection we give the general result for the solution to the renormalizaton group equation.

A natural question to ask is how generic are the two examples treated so far in this section? It turns out that much of the structure here is quite generic for cases like our examples, where the ω variables are fixed by external kinematics. This will occur for any operator that involves only one building block, χ_n or $\mathcal{B}^\mu_{n\perp}$, for each collinear direction n. For example, with four collinear directions we have the operator

$$\int d\omega_1\, d\omega_2\, d\omega_3\, d\omega_4\; C(\omega_1,\omega_2,\omega_3,\omega_4)\; \big[\overline{\chi}_{n_1,\omega_1}\Gamma_{\mu\nu}\; \mathcal{B}^\mu_{n_2\perp,\omega_2}\mathcal{B}^\nu_{n_3\perp,\omega_3}\; \chi_{n_4,\omega_4}\big] \tag{7.61}$$

and again the ω_i's will be fixed by momenta that are external to collinear loops. An example where this would not be true is if we had the same collinear direction n in two or more of our building blocks, such as

$$\int d\omega_1\, d\omega_2\; C(\omega_1,\omega_2)\big[\overline{\chi}_{n,\omega_1}\bar{\not{n}}\,\chi_{n,\omega_2}\big]\,. \tag{7.62}$$

For this operator one combination of ω_1 and ω_2 will be fixed by momentum conservation, while the other combination will involve collinear loop momenta. This will lead to anomalous dimension equations of a more complicated form, involving convolutions such as

$$\mu\frac{d}{d\mu}C(\mu,\omega) = \int d\omega'\gamma(\mu,\omega,\omega')C(\mu,\omega')\,. \tag{7.63}$$

Indeed, the operator in Eq. (7.63) is responsible for several classic evolution equations: i) DIS where we have DGLAP evolution for the parton distribution functions $f_{i/p}(\xi)$, ii) hard exclusive processes like $\gamma^*\pi^0\to\pi^0$ where we have Brodsky-Lepage evolution for the light-cone meson distributions $\phi_\pi(x)$, and iii) the deeply virtual Compton scattering process $\gamma^*p\to\gamma p'$ where the evolution is a combination of both of theses. It is interesting that all of these processes are sensitive to different projections of the evolution of the single operator given in Eq. (7.63). We will carry out an example of an evolution equation with a convolution in the Sec. 10, where we consider DIS and the DGLAP equation.

7.4 RGE solution to higher orders

The all orders form for the anomalous dimension of our two example currents of the previous section can be written as

$$\begin{aligned}
\gamma_C(s_C,\mu) &= \frac{\rho_C}{j}\,\Gamma_{\rm cusp}[\alpha_s(\mu)]\ln\Big(\frac{\mu^j}{s_C}\Big) - \gamma_C[\alpha_s(\mu)]\,,\\
\Gamma^i_{\rm cusp}[\alpha_s] &= \sum_{k=1}^\infty\Big(\frac{\alpha_s}{4\pi}\Big)^k\Gamma^i_k\,,\qquad \gamma_C[\alpha_s] = \sum_{k=1}^\infty\Big(\frac{\alpha_s}{4\pi}\Big)^k\gamma_{Ck}\,,
\end{aligned} \tag{7.64}$$

where $\Gamma^i_{\rm cups}[\alpha_s]$ is the cusp-anomalous dimension for quarks ($i=q$) or gluons ($i=g$), and the one-loop result has $\Gamma^q_1 = 4C_F$ and $\Gamma^g_1 = 4C_A$. The constant prefactor ρ_C, the variable s_C with dimension j, and the non-cusp anomalous dimension $\gamma_C[\alpha_s]$ all depend on the particular current under consideration. In order to solve the anomalous dimension equation we should decide what terms must be kept at each order in perturbation theory that we would like to consider. Counting $\alpha_s\ln(\mu)\sim 1$, the correct grouping for obtaining the leading-log (LL), next-to-leading log (NLL), etc., results is

$$\gamma_C(s_C,\mu)\sim\big[\alpha_s\ln(\mu)\big]_{\rm LL} + \big[\alpha_s+\alpha_s^2\ln(\mu)\big]_{\rm NLL} + \big[\alpha_s^2+\alpha_s^3\ln(\mu)\big]_{\rm NNLL} + \ldots\,. \tag{7.65}$$

This confirms the statement already made in the prevoius section, namely that the cusp-anomalous dimension with the $\ln(\mu)$ is required at one-higher order than the non-cusp anomalous dimension. (Typically

this is not a problem due to the universal form of the cusp contribution, and the fact that its coefficients are known to 3-loop order for QCD) To solve the first order differential equation involving γ_C we also must specify a boundary condition for $C(\mu,\omega)$. At both LL and NLL order the tree-level boundary condition suffices, while at NNLL we need the one-loop boundary condition, etc.

The general solution is given by

$$C(s_C,\mu) = C(s_C,\mu_0)\, e^{K_C(\mu,\mu_0)} \left(\frac{\mu_0^j}{s_C}\right)^{\omega_C(\mu,\mu_C)} \tag{7.66}$$

with

$$\omega_C(\mu,\mu_0) = \frac{\rho_C}{j}\int_{\alpha_s(\mu_0)}^{\alpha_s(\mu)} \frac{\mathrm{d}\,\alpha}{\beta[\alpha]}\,\Gamma_{\rm cusp}[\alpha]$$

$$K_C(\mu,\mu_0) = \int_{\alpha_s(\mu_0)}^{\alpha_s(\mu)} \frac{\mathrm{d}\,\alpha}{\beta[\alpha]}\,\gamma_C[\alpha_s] + \rho_F \int_{\alpha_s(\mu_0)}^{\alpha_s(\mu)} \frac{\mathrm{d}\,\alpha}{\beta[\alpha_s]}\,\Gamma_{\rm cusp}[\alpha_s] \int_{\alpha_s(\mu_0)}^{\alpha_s} \frac{\mathrm{d}\alpha_s'}{\beta[\alpha_s']} \tag{7.67}$$

The logarithmic counting of the solution to this RGE is usually performed for $\ln C$, such that it is helpful to write

$$\ln C(s_C,\mu) = \ln C(s_C,\mu_0) + K_C(\mu,\mu_0) + \omega_C \ln\left(\frac{\mu_0}{s_C}\right) \tag{7.68}$$

One now expands $\ln C$ in powers of α_s, but holding $\alpha_s \ln(\mu/\mu_0)$ fixed. This gives

$$\ln C(s_C,\mu) = \ln\frac{\mu}{\mu_0}\, f_{\rm LL}\left[\alpha_s(\mu_0)\ln\frac{\mu}{\mu_0}\right] + f_{\rm NLL}\left[\alpha_s(\mu_0)\ln\frac{\mu}{\mu_0}\right] + \alpha_s(\mu_0)\, f_{\rm NNLL}\left[\alpha_s(\mu_0)\ln\frac{\mu}{\mu_0}\right] \tag{7.69}$$

To NLL accuracy, one can therefore write

$$\omega_C(\mu,\mu_0) = -\frac{\rho_C\,\Gamma_0}{2\,j\,\beta_0}\left\{ [\ln r]_{\rm LL} + \left[\frac{\alpha_s(\mu_0)}{4\pi}\left(\frac{\Gamma_1}{\Gamma_0} - \frac{\beta_1}{\beta_0}\right)(r-1)\right]_{\rm NLL} + \dots \right\}, \tag{7.70}$$

and

$$\begin{aligned} K_C(\mu,\mu_0) = -\frac{\rho_F\,\Gamma_0}{4\beta_0^2}\Bigg\{ & \left[\frac{4\pi}{\alpha_s(\mu_0)}\Big(\ln r + \frac{1}{r} - 1\Big)\right]_{\rm LL} \\ & + \left[\Big(\frac{\Gamma_1}{\Gamma_0} - \frac{\beta_1}{\beta_0}\Big)(r - 1 - \ln r) - \frac{\beta_1}{2\beta_0}\ln^2 r - \frac{\gamma_{C0}}{2\beta_0}\,\ln r\right]_{\rm NLL} + \dots \Bigg\}. \end{aligned} \tag{7.71}$$

Here $r = \alpha_s(\mu)/\alpha_s(\mu_0)$ and the results are expressed in terms of series expansion coefficients of the QCD β function $\beta[\alpha_s]$, of $\Gamma[\alpha_s]$ which is given by a constant of proportionality times the QCD cusp anomalous dimension, and of a non-cusp anomalous dimension $\gamma[\alpha_s]$,

$$\beta[\alpha_s] = -2\,\alpha_s \sum_{n=0}^{\infty} \beta_n \Big(\frac{\alpha_s}{4\pi}\Big)^{n+1}, \tag{7.72}$$

$$\Gamma[\alpha_s] = \sum_{n=0}^{\infty} \Gamma_n \Big(\frac{\alpha_s}{4\pi}\Big)^{n+1},\ \gamma[x\alpha_s] = \sum_{n=0}^{\infty} \gamma_n \Big(\frac{\alpha_s}{4\pi}\Big)^{n+1}.$$

Their values can be found in Appendix **??**.

Type	Momenta $p^\mu = (+,-,\perp)$	Fields (f)	Scaling (e^f)	Operator	Scaling
collinear	$p^\mu \sim (\lambda^2, 1, \lambda)$	$\xi_{n,p}$	λ	$\bar{n}\cdot\mathcal{P}$, W_n	λ^0
		$(A^+_{n,p}, A^-_{n,p}, A^\perp_{n,p})$	$(\lambda^2,1,\lambda)$	$\mathcal{P}^\mu_\perp$	λ
soft	$p^\mu \sim (\lambda, \lambda, \lambda)$	$q_{s,p}$	$\lambda^{3/2}$	S_n	λ^0
		$A^\mu_{s,p}$	λ	$\mathcal{P}^\mu$	λ
usoft	$k^\mu \sim (\lambda^2, \lambda^2, \lambda^2)$	q_{us}	λ^3	Y_n	λ^0
		A^μ_{us}	λ^2		

Table 7: Power counting for SCET momenta and fields as well as momentum label operators and Wilson lines.

8 Power correction in SCET

In this section, we explain how power corrections to SCET can be included. Power corrections can arise from two sources: power suppressed terms in the SCET Lagrangian, and power corrections to the external operators mediating a given transition. In this section we derive the power suppressed Lagrangian in SCET, and also describe how power corrections to the external operators can be constructed. Before that, however, we derive a general power counting formula, which estimates the size of the contribution to a given process.

8.1 Power Counting Formula for $\mathrm{SCET_I}$ [Needs Cutting down]

In this section, we will derive a general power counting formula for an aribtirary graph in SCET. This is a shortened discussion of what can be found in [**?**], and we refer the reader to that paper for more details. We begin by summarizing the scaling of the fields, momenta, label operators and Wilson lines in SCET in Table 8.1. Interactions in SCET appear either in the effective theory action or in external operators (which are often operators or currents generated by electromagnetic or weak interactions). The full action of SCET can be divided into four pieces

$$S = S^U + S^S + S^C + S^{UC}\,, \tag{8.1}$$

where S^U has purely usoft interactions, S^S contains interactions with one or more soft fields, S^C contains interactions with one or more collinear fields, and S^{UC} contain possible mixed usoft-collinear terms. Mixed interactions between soft and collinear fields or usoft and soft fields do not appear in the Lagrangian at any order. After the BPS field redefinition, interactions that mix ultrasoft and collinear fields do not appear in the leading order Lagrangian, such that to that order S^{UC} vanishes and S^U, S^S, and S^C are the order λ^0 kinetic terms for the usoft, soft, and collinear fields. For any external operator, a scaling λ^k can be immediately assigned by adding up the factors of λ associated with the scaling of its fields, derivatives, and label operators.

Both interactions from the action and as well as from external operators appear in Feynman diagrams as vertices. To derive a power counting of a given Feynman diagram, one needs to know how many vertices of a given power counting are included. Thus, we introduce indexes V^i_k which count operators in a graph. Here V^i_k counts the number of operators that scale as λ^k and are of type i, where the type depends on the field content. The four vertex indexes we require are:

V^C_k for vertices involving only collinear and usoft fields ,

V_k^S for vertices involving only soft and usoft fields ,

V_k^{SC} for vertices with both soft and collinear fields ,

V_k^U for vertices with *only* usoft fields.

Note the important point that the mixed soft-collinear operators require a separate index. As an example of how these indexes work consider the purely collinear DIS operator [**?**]

$$\mathcal{O}_1 = \frac{1}{Q}\,\bar\xi_{n,p'} W_n\,\frac{\bar n\!\!\!/}{2}\,C(\bar n\cdot\mathcal{P}_+,\bar n\cdot\mathcal{P}_-,Q,\mu)\,W_n^\dagger\,\xi_{n,p}\,. \tag{8.2}$$

where $\bar n\cdot\mathcal{P}_\pm = \bar n\cdot\mathcal{P}^\dagger \pm \bar n\cdot\mathcal{P}$ and C a Wilson coefficient. It is the proton matrix element of $\mathcal{O}_1$ that leads to a convolution involving the quark or antiquark parton distribution functions. Since $\xi\sim\lambda$ and $W_n\sim\lambda^0$ this operator scales as λ^2. Thus $k=2$, and since the operator only involves collinear fields a single insertion of $\mathcal{O}_1$ makes the index $V_2^C=1$. Note that all vertices arising from the SCET action always have $k\geq 4$.

Now consider an arbitrary loop graph built out of insertions of external operators along with propagators and interactions from S. We show that such a graph scales as λ^δ, where

$$\delta = 4u + 4 + \sum_k (k-4)\big(V_k^C + V_k^S + V_k^{SC}\big) + (k-8)V_k^U\,. \tag{8.3}$$

Here $u=1$ if the graph is purely usoft and $u=0$ otherwise. We will refer to Eq. (8.3) as the *vertex power counting formula*. This result applies to any physical process whose infrared structure can be described by the fields in Table 8.1. Eq. (8.3) expresses the important result that the power of λ associated with an arbitrary diagram can be determined entirely by the scaling of operators at its vertices.

Direct Power Counting and the Derivation of Eq.(5)

An intuitive method of power counting diagrams involves counting powers of λ for the loop measures, propagators, vertices, and external lines. We will refer to this as the "direct" method of power counting and use it as our starting point. For this method it it is more intuitive to begin with indexes $\tilde V_{k'}^j$ which are analogous to the V_k^j, but do not include the scaling for the fields. Thus, $\tilde V_{k'}^j$ directly count the scaling of the vertex Feynman rules. For example, an operator $\bar\xi_n\,\partial_\perp^2\,\xi_n$ would be $\tilde V_2^C=1$, whereas $\bar\xi_n\,A_{n,q}^{\perp\,2}\,\xi_n$ is $\tilde V_0^C=1$.

Consider an arbitrary graph containing L^i loops and I^i propagators of type i with $i\in\{C,S,U\}$, $\tilde V_k^j$ vertices of type j, and E^f external lines of type f, where f runs over the fields in Table 8.1 and d^f denotes the scaling of a given field from the table. Counting the powers of λ associated with the vertices, loop measures, propagators, and external lines we find that the graph scales as λ^δ with

$$\delta = \sum_{k'} k'\big(\tilde V_{k'}^C + \tilde V_{k'}^S + \tilde V_{k'}^{SC} + \tilde V_{k'}^U\big) + 4L^C + 4L^S + 8L^U - \eta_\alpha I^C - 2I^S - 4I^U + \sum_f e^f E^f\,, \tag{8.4}$$

which we refer to as the *direct power counting formula*. Note that we have included a factor η_α, which encodes that the scaling of the gluon propagator is gauge dependent. In Feynman gauge $\eta_\alpha=2$ for all collinear particles, however in a general covariant gauge $\eta_\alpha=2$ for fermions, but the gluon propagator

$$A_n^\mu\;A_n^\nu \quad\Longrightarrow\quad \frac{-i}{p^2}\Big(g^{\mu\nu} + \alpha\frac{p^\mu p^\nu}{p^2}\Big)\,, \tag{8.5}$$

gives $\eta_\alpha=\{0,1,2,2,3,4\}$ for the $\{++,+\perp,+-,\perp\perp,-\perp,--\}$ components. We will see that the η_α gauge dependence in Eq. (8.4) is cancelled by a similar dependence in $\tilde V_{k'}^C$.

To proceed we switch to the V_k^i indexes. The difference between the two types of vertex indexes is the powers of λ associated with the fields in an operator. For example, both $\bar{\xi}_n\, \partial_\perp^2\, \xi_n$ and $\bar{\xi}_n\, A_{n,q}^{\perp\,2}\, \xi_n$ count as $V_4^C = 1$. Since the fields in a vertex are either contracted with another field or correspond to an external line we have

$$\sum_{k,i} k\, V_k^i = \sum_{k',i} k'\, \tilde{V}_{k'}^i + (4-\eta_\alpha) I^C + 2I^S + 4I^U + \sum_f e^f E^f \,. \tag{8.6}$$

For each internal line two fields are contracted and eliminated for a momentum space propagator. The difference in scaling of the two fields and the propagator induces the I^i correction terms in Eq. (8.6). For instance two collinear fermion fields scale as λ^2 on the LHS. If they are contracted then a $(4-\eta_c)I^C = (4-2)I^C = 2I^C$ term accounts for them on the RHS. The E^f terms account for them if they are not contracted. In a similar way, each soft propagator or external line is also accounted for. The most non-trivial contraction is that of two collinear gluon fields $A_n^\mu\, A_n^\nu$ since their scaling is inhomogeneous. However, it is straightforward to see, for example in a general covariant gauge, that these contractions are correctly encoded by the $(4-\eta_\alpha)I^C$ term in Eq. (8.6). Using Eq. (8.6) to eliminate the $\tilde{V}_{k'}^i$'s from Eq. (8.4) leaves

$$\delta = \sum_k k\big(V_k^C + V_k^S + V_k^{SC} + V_k^U\big) + 4L^C + 4L^S + 8L^U - 4I^C - 4I^S - 8I^U \,, \tag{8.7}$$

whose terms are now explicitly gauge independent. Eq. (8.7) can be further simplified by using Euler topological identities, which connect the number of loops, lines and vertices in an arbitrary graph. For the complete graph we have

$$\text{(E1):} \qquad \sum_k (V_k^C + V_k^S + V_k^{SC} + V_k^U) + (L^S + L^C + L^U) - (I^S + I^C + I^U) = 1 \,. \tag{8.8}$$

Using this result to remove the $L^U - I^U$ factor from Eq. (8.7) leaves

$$\delta = 8 + \sum_k (k-8)\big(V_k^C + V_k^S + V_k^{SC} + V_k^U\big) - 4L^C - 4L^S + 4I^C + 4I^S \,. \tag{8.9}$$

To proceed further we consider two cases, i) graphs with purely usoft fields, and ii) graphs with ≥ 1 soft or collinear field. In case i) $L^C = L^S = I^C = I^S = V_k^C = V_k^S = V_k^{SC} = 0$ and Eq. (8.9) gives the final result which is $\delta = 8 + \sum_k (k-8) V_k^U$. In case ii) we can use the hierarchy in p^2 of the modes in Table I to derive additional Euler relations by removing modes one at a time, starting with those propagating over the longest distance [**?**]. This is possible since the graph must stay connected when probed at the shorter distance scales. Thus, by removing all the usoft lines in the graph one can draw a reduced graph containing only soft and collinear modes, also of course keeping vertices that are not purely usoft. The Euler identity for this reduced graph reads

$$\text{(E2):} \qquad \sum_k (V_k^C + V_k^S + V_k^{SC}) + (L^S + L^C) - (I^S + I^C) = 1 \,. \tag{8.10}$$

It is easy to see that (E2) can be used to eliminate the remaining terms in Eq. (8.9) that depend on the loop measures and internal lines. Using (E2) in Eq. (8.9) leaves the final result (for graphs with at least one soft and/or collinear field, ie. case ii),

$$\delta = 4 + \sum_k (k-4)\big(V_k^C + V_k^S + V_k^{SC}\big) + (k-8) V_k^U \,. \tag{8.11}$$

Together cases i) and ii) reproduce Eq. (8.3) which is the main result of this paper. It should be noted that the derivation of Eq. (8.3) would not be possible if offshell degrees of freedom had been retained since the power counting for fields generating offshell fluctuations is ambiguous [**?**].

The power of this power counting formula is that one can immediately determine what contributions need to be included to obtain an answer at a given order in the power counting. First, vertices with only collinear or only soft fields contribute with strength $k-4$, while vertices with only usoft fields contribute with $k-8$. The interactions in the leading order collinear, soft and usoft Lagrangian have scaling $k=4$, $k=4$ and $k=8$, respectively, such that one immediately finds the sensible result that one can insert an arbitrary number of such vertices without changing the power counting of a diagram. Each interaction of a subleading Lagrangian, which has larger values of k, will lead to a suppression of the overall result, so only a finite number of such insertions are required to a given order. Only external operators can have $k<4$, such as in the DIS operator in Eq. (8.2). Furthermore, physical considerations always limit the number of external operator insertions (usually to just 1). For example, in DIS multiple insertions of $\mathcal{O}_1$ would require multiple electromagnetic interactions. Thus, at leading order in λ only graphs built out of a fixed number of external operators plus V_4^C, V_4^S, V_4^{SC}, and V_8^U vertices need to be included. These vertices are exactly those described by the interactions contained in the leading order Lagranginans. At one higher order in λ we only need to add a *single* vertex with a higher power of k to the vertices included above. For instance, a single V_5^C. From this discussion the utility of Eq. (8.3) for describing higher and higher orders in λ should be fairly evident.

8.2 Power Suppressed SCET$_{\rm I}$ Lagrangians [Check Words, Add Ghosts]

Starting at $\mathcal{O}(\lambda)$ we have several contributions to the subleading SCET Lagrangian

$$\mathcal{L}^{(1)} = \mathcal{L}^{(1)}_{\xi_n} + \mathcal{L}^{(1)}_{A_n} + \mathcal{L}^{(1)}_{\xi_n\psi_{us}}\,. \tag{8.12}$$

The operators that contribute to these Lagrangians scale as λ^5. The collinear fermion and gluon Lagrangians at $\mathcal{O}(\lambda)$ in our notation are [17, 7, 18] (**TODO**)

TODO: Add ghost terms from Appendi into this same notation here

$$\begin{aligned}
\mathcal{L}^{(1)}_{\xi_n} &= \bar\chi_n\Big(i\not{\mathcal{D}}_{us\perp}\frac{1}{i\bar n\cdot\partial_n}i\not{\mathcal{D}}_{n\perp} + i\not{\mathcal{D}}_{n\perp}\frac{1}{i\bar n\cdot\partial_n}i\not{\mathcal{D}}_{us\perp}\Big)\frac{\not{\bar n}}{2}\chi_n\,,\\
\mathcal{L}^{(1)}_{A_n} &= \frac{2}{g^2}\mathrm{Tr}\Big(\big[i\mathcal{D}^\mu_{ns}, i\mathcal{D}^\nu_{n\perp}\big]\big[i\mathcal{D}_{ns\mu}, iD_{us\perp\nu}\big]\Big) + \mathcal{L}^{(1)}_{A_n,\rm gf}\,.
\end{aligned} \tag{8.13}$$

In a covariant gauge, the gauge fixing terms at subleading power are [19]

$$\mathcal{L}^{(1)}_{A_n,\rm gf} = \frac{2}{\alpha}\mathrm{Tr}\Big(\big[iD^\mu_{us\perp}, A_{n\perp\mu}\big]\big[i\partial^\nu_{ns}, A_{n\nu}\big]\Big) + \text{ghosts}\,. \tag{8.14}$$

Here, the covariant derivative $iD^\mu_{s\perp} = i\partial^\mu_{s\perp} + gA^\mu_{s\perp}$ and the other covariant derivatives contain Wilson lines that ensure collinear gauge invariance, and were defined in Eq. (**??**). The complete subleading SCET Lagrangian at $\mathcal{O}(\lambda)$ for fermions, gauge bosons and scalars also contains an additional Lagrangian that permits soft fermion emission,

$$\mathcal{L}^{(1)}_{\xi_n\psi_s} = (\bar\xi_n W_n)\frac{1}{i\bar n\cdot\partial_n}g\not{\mathcal{B}}_{n\perp}\psi_{us} + \text{h.c.}, \tag{8.15}$$

where $\psi_{us}\sim\lambda^3$ is the ultrasoft fermion field.

At $\mathcal{O}(\lambda^2)$ the sub-subleading SCET Lagrangian contains the terms,

$$\mathcal{L}^{(2)} = \mathcal{L}^{(2)}_{\xi_n} + \mathcal{L}^{(2)}_{A_n} + \mathcal{L}^{(2)}_{\xi_n\psi_{us}}\,. \tag{8.16}$$

The operators that contribute to these Lagrangians scale as λ^6. At this order the collinear fermion and gluon Lagrangians in our notation are [7, 18]

$$\mathcal{L}^{(2)}_{\xi_n} = \bar\chi_n \left(i\not{D}_{us\perp} \frac{1}{i\bar n\cdot\partial_n} i\not{D}_{us\perp} - i\not{\mathcal{D}}_{n\perp} \frac{i\bar n\cdot D_{us}}{(i\bar n\cdot\partial_n)^2} i\not{\mathcal{D}}_{n\perp} \right) \frac{\not{\bar n}}{2}\chi_n \,, \tag{8.17}$$

$$\begin{aligned}
\mathcal{L}^{(2)}_{A_n} &= \frac{1}{g^2}\mathrm{Tr}\Big(\big[i\mathcal{D}^\mu_{ns}, iD^{\perp\nu}_{us}\big]\big[i\mathcal{D}_{ns\mu}, iD^\perp_{s\nu}\big]\Big) + \frac{1}{g^2}\mathrm{Tr}\Big(\big[iD^\mu_{us\perp}, iD^\nu_{us\perp}\big]\big[i\mathcal{D}^\perp_{n\mu}, i\mathcal{D}^\perp_{n\nu}\big]\Big) \\
&\quad + \frac{1}{g^2}\mathrm{Tr}\Big(\big[i\mathcal{D}^\mu_{ns}, in\cdot\mathcal{D}_{ns}\big]\big[i\mathcal{D}_{ns\mu}, i\bar n\cdot D_{us}\big]\Big) + \frac{1}{g^2}\mathrm{Tr}\Big(\big[iD^\mu_{us\perp}, i\mathcal{D}^\nu_{n\perp}\big]\big[i\mathcal{D}^\perp_{n\mu}, iD^\perp_{us\nu}\big]\Big) \\
&\quad + \mathcal{L}^{(2)}_{A_n,\mathrm{gf}} \,.
\end{aligned}$$

In a covariant gauge, the gauge fixing terms at sub-subleading power are [19]

$$\mathcal{L}^{(2)}_{A_n,\mathrm{gf}} = \frac{1}{\alpha}\mathrm{Tr}\Big(\big[iD^\mu_{us\perp}, A_{n\perp\mu}\big]\big[iD^\nu_{us\perp}, A_{n\perp\nu}\big]\Big) + \frac{1}{\alpha}\mathrm{Tr}\Big(\big[i\bar n\cdot D_{us}, n\cdot A_n\big]\big[i\partial^\mu_{ns}, A_{n\mu}\big]\Big) + \text{ ghosts} \,. \tag{8.18}$$

At this order there are also $\mathcal{O}(\lambda^2)$ Lagrangians involving soft fermions, which is the higher order version of Eq. (8.15)

$$\mathcal{L}^{(2)}_{\xi_n\psi_s} = \tag{8.19}$$

For later purposes it will also be useful to consider the form that the subleading Lagrangians take after the BPS field redefinition in Eq. (**??**). The field redefinition introduces Wilson lines Y_n which factor from the collinear fields in a manner so that they always sandwich the soft covariant derivatives, $Y_n^\dagger D_s^\mu Y_n$. In the process use of $in\cdot D_s Y_n = 0$ causes soft gauge fields to drop out of the mixed covariant derivatives, $iD^\mu_{ns} \to iD^\mu_n$ and $i\mathcal{D}^\mu_{ns} \to i\mathcal{D}^\mu_n$. In order to fully factor the soft and collinear fields we also want to separate out terms where the derivative in D^μ_{us} acts on collinear fields, which we can do with the identity

$$Y_n^\dagger iD^\mu_{us} Y_n = i\partial^\mu_{us} + \big[Y_n^\dagger iD^\mu_{us} Y_n\big] = i\partial^\mu_{us} + T^A g B^{A\mu}_{us(n)} \,, \tag{8.20}$$

where the covariant derivative acts only on terms within the square brackets, and

$$gB^{A\mu}_{us(n)} = \Big[\frac{1}{in\cdot\partial_{us}} n_\nu i F^{B\nu\mu}_{us} \mathcal{Y}^{BA}_n \Big] \,. \tag{8.21}$$

Here $F^{B\nu\mu}_{us}$ is the soft field strength, and $\mathcal{Y}_n$ is the soft Wilson line in the adjoint representation. This allows us to write the sum of all subleading Lagrangians in a factorized form as

$$\begin{aligned}
\mathcal{L}^{(1)} &= \sum_n \Big[\hat K^{(1)}_n + \hat K^{(1)\kappa}_{n\mu} T^{\kappa A} g B^{A\mu}_{us(n)} \Big] \,, \\
\mathcal{L}^{(2)} &= \sum_n \Big[\hat K^{(2)}_n + \hat K^{(2)\kappa}_{n\mu} T^{\kappa A} g B^{A\mu}_{us(n)} + \hat K^{(2)\kappa\kappa'}_{n\mu\nu} T^{\kappa A} T^{\kappa' B} g B^{A\mu}_{us(n)} g B^{B\nu}_{us(n)} \Big] \,.
\end{aligned} \tag{8.22}$$

Here $T^{\kappa A}$ is the A'th component of the color generator in the κ representation upon which the iD^μ_s acted. The various $\hat K^{(1)}_n$ and $\hat K^{(2)}_n$ terms contain only n-collinear quark and gauge bosons, plus $i\partial^\mu_u$ derivatives, and can be written down explicitly with the results given above. All terms involving ultrasoft fields have been made explicit in the $gB^{A\mu}_{us(n)}$ factors.[8]

[8] Note that here the superscripts (1) or (2) on the $\hat K_n$s denote the Lagrangian that these terms came from rather than their power of λ.

8.3 Power Counting Formula for SCET$_{\rm II}$ [Empty]

Need to explain why there is only a single power of log in the anomalous dimensions.

9 SCET for e^+e^- Collider Observables

One of the most important applications for SCET is to describe observables at lepton or hadron colliders is the production of jets. In this section, we will discuss the production of jets at an e^+e^- collider. The production of leptons and jets at a hadron collider will be discussed in Sec. 11.

The production of jets at an e^+e^- collider has historically been very important. Measurements of various jets in e^+e^- collisions were used to validate QCD as the correct theory of the strong interaction, and to this day, even 10 years after the LEP has been turned off, measurements of event shape distributions are being used to study the nature of the strong interaction and to determine fundamental constants of nature such as the coupling constant of the strong interaction.

The dominant kinematical situation in $e^+e^- \to$ jets is to produce two jets, but of course a larger number of jets can be obtained by the emission of additional hard strongly interacting particles. In this section we will discuss the production of two jets in e^+e^- collisions, which is to say the production of energetic particles in two back-to-back directions, accompanied only by usoft radiation in arbitrary regions of phase space.

Clearly, the question whether we have 2 or more jets has to be determined on an event by event basis, and there are many possible observables which can distinguish 2-jet events from events with more than 2 jets. The most natural definition might be to use a jet finding algorithm, and select those events with exactly two hard jets as defined by this algorithm. However, there is another set of observables which can be used to identify 2-jet events, and which are much easier to analyze theoretically. This class of observables are called event shapes, with the most well known event shape variable being thrust. In this section, we will only discuss the thrust distribution in e^+e^- collisions, but it should be clear from the discussion how one can extend the results to other event shape variables or other 2-jet observables.

9.1 Kinematics, Expansions, and Regions

The thrust of an event is defined as follows:

$$T = \max_{\vec{n}_T} \frac{\sum_i |\vec{p}_i \cdot \vec{n}_T|}{\sum_i |\vec{p}_i|} \tag{9.1}$$

The sum over i runs over all particles in the final state, and the direction $\vec{n}_T$ is called the thrust axis. To fully understand this equation, let's first ignore the $\max_{\vec{n}_T}$ and pick a fixed direction $\vec{n}_T$.Thrust is then defined by summing the absolute value of the projections of the momenta of all particles onto the thrust axis, and divide by the sum over the magnitude of all momenta. In the situation where the momenta of all particles are aligned (or anti-aligned) exactly with the thrust axis, the magnitude of the projection onto the thrust axis is exactly equal to the magnitude of the momentum itself, such that one obtains $T = 1$. Thus, energetic particles that are collinear or anti-collinear to the thrust axis give $T \approx 1$. Soft particles with vanishing momentum do not contribute to the the thrust, since their contributions vanish in the numerator and denominators. Thus, events with $T \approx 1$ only contain particles which are either collinear or anti-collinear to the thrust axis, or are usoft, and are therefore 2-jet like and can be described by SCET$_{\rm I}$. For later convenience we will often choose the variable

$$\tau = 1 - T \tag{9.2}$$

instead of T itself. In this case the 2-jet case corresponds to $\tau \to 0$, while τ away from zero corresponds to three or more jets.

To make the connection of thrust with SCET even more obvious, we will define the two four-vectors

$$n^\mu = (1, \vec{n}_T)\,, \qquad \bar{n}^\mu = (1, -\vec{n}_T) \tag{9.3}$$

Using this definition, we can write for T

$$T \;=\; \frac{Q - \sum_{i\in R} n\cdot p_i - \sum_{i\in L} \bar{n}\cdot p_i}{Q} \tag{9.4}$$

or alternatively for τ

$$\tau = \frac{\sum_{i\in R} n\cdot p_i + \sum_{i\in L} \bar{n}\cdot p_i}{Q} \tag{9.5}$$

9.2 Factorization: Hard, Jet and Soft functions [fix notation]

The thrust distribution in the full theory is given by summing over all final states in the event, and projecting each event onto its value of thrust, defined by (9.1)

$$\frac{d\sigma}{d\tau} = \frac{1}{2Q^2}\sum_X \left|M(e^+e^-\to X)\right|^2 (2\pi)^4\delta^4(q-p_X)\delta(\tau-\tau(X))\,. \tag{9.6}$$

Here $M(e^+e^-\to X)$ is the full QCD matrix element to produce the final state X from the collisions of an e^+e^- pair.

$$\left|\mathcal{M}(e^+e^-\to X)\right|^2 = \sum_{i=V,A} L^i_{\mu\nu}\,\langle 0|\, j_i^{\mu\dagger}\,|X\rangle\,\langle X|\, j_i^{\nu}\,|0\rangle\;, \tag{9.7}$$

where we have defined the vector and axial currents,

$$j_i^\mu = \bar{q}_f^a \Gamma_i^\mu q_f^a\,, \tag{9.8}$$

with $\Gamma_V^\mu = \gamma^\mu$ and $\Gamma_A^\mu = \gamma^\mu\gamma^5$. The leptonic tensor is given by

$$L^V_{\mu\nu} = -\frac{e^4}{3Q^2}\left(g_{\mu\nu} - \frac{q_\mu q_\nu}{Q^2}\right)\left[Q_f^2 - \frac{2Q^2 v_e v_f Q_f}{Q^2-M_Z^2} + \frac{Q^4(v_e^2+a_e^2)v_f^2}{(Q^2-M_Z^2)^2}\right] \tag{9.9a}$$

$$L^A_{\mu\nu} = -\frac{e^4}{3Q^2}\left(g_{\mu\nu} - \frac{q_\mu q_\nu}{Q^2}\right)\frac{Q^4(v_e^2+a_e^2)a_f^2}{(Q^2-M_Z^2)^2}\,, \tag{9.9b}$$

where fermion f has electric charge Q_f in units of e, and vector and axial charges v_f, a_f given by

$$v_f = \frac{1}{2\sin\theta_W\cos\theta_W}(T_f^3 - 2Q_f\sin^2\theta_W), \quad a_f = \frac{1}{2\sin\theta_W\cos\theta_W}T_f^3. \tag{9.10}$$

In Eq. (9.8) a sum over colors a and flavors f is understood.

Writing the four-momentum conserving delta function as the integral of an exponential, and using the dependence on p_X in the exponential to translate one of the two currents to the position x we can write the distribution as

$$\frac{d\sigma}{d\tau} = \frac{1}{2Q^2}\sum_X \int d^4x\, \mathrm{e}^{iq\cdot x}\sum_{i=V,A} L^i_{\mu\nu}\,\langle 0|\, j_i^{\mu\dagger}(x)\,|X\rangle\,\langle X|\, j_i^{\nu}(0)\,|0\rangle\,\delta(\tau-\tau(X))\,. \tag{9.11}$$

Following the discussion in Section 7.2 we match the full theory current onto the effective theory current given in Eq. (5.37) to obtain

$$\frac{d\sigma}{d\tau} = \frac{1}{2Q^2}\sum_n C_n(Q^2;\mu)\sum_X \int d^4x\, \mathrm{e}^{iq\cdot x}\sum_{i=V,A} L^i_{\mu\nu}\,\langle 0|\left[\bar\chi_{\bar n}\bar\Gamma^i_\mu\chi_n\right](x)\,|X\rangle\,\langle X|\left[\bar\chi_n\Gamma^i_\nu\chi_{\bar n}\right](0)\,|0\rangle\,\delta(\tau-\tau(X))\,. \tag{9.12}$$

This is the equivalent of the hard factorization discussed in Section 6.2.

As a next step in the deriving the factorization formula, one can eliminate the sum over the final state X. As was shown in [20], one can define an operator $\hat\tau$ such that

$$\hat\tau\,|X\rangle = \tau(X)\,|X\rangle \tag{9.13}$$

This allows us to write

$$\sum_X \delta(\tau-\tau(X))\,|X\rangle\,\langle X| = \delta(\tau-\hat\tau) \tag{9.14}$$

such that we obtain

$$\frac{d\sigma}{d\tau} = \frac{1}{2Q^2}\sum_n C_n(Q^2;\mu)\int d^4x\,\mathrm{e}^{iq\cdot x}\sum_{i=V,A} L^i_{\mu\nu}\,\langle 0|\left[\bar\chi_{\bar n}\bar\Gamma^i_\mu\chi_n\right](x)\delta(\tau-\hat\tau)\left[\bar\chi_n\Gamma^i_\nu\chi_{\bar n}\right](0)\,|0\rangle\,. \tag{9.15}$$

To complete the factorization of the differential cross section, we use the ultrasoft-collinear factorization introduced in Section 6.1 and the fact that the operator $\hat\tau$ is linear in the energy momentum tensor, which allows us to write [20]

$$\hat\tau = \hat\tau_n + \hat\tau_{\bar n} + \hat\tau_s\,, \tag{9.16}$$

which allows us to write

$$\delta(\tau-\hat\tau) = \int d\tau_n d\tau_{\bar n} d\tau_s \delta(\tau-\tau_n-\tau_{\bar n}-\tau_s)\delta(\tau_n-\hat\tau_n)\delta(\tau_{\bar n}-\hat\tau_{\bar n})\delta(\tau_s-\hat\tau_s)\,. \tag{9.17}$$

Inserting these results into Eq. (9.15) one finds

$$\begin{aligned}\frac{d\sigma}{d\tau} &= \frac{1}{6Q^2}\sum_{\hat n}\left|C_n(Q^2;\mu)\right|^2\int d^4x\int d\tau_n\, d\tau_{\bar n}\, d\tau_s\,\delta(\tau-\tau_n-\tau_{\bar n}-\tau_s) \\ &\quad\times\frac{1}{N_C^2}\mathrm{Tr}\,\langle 0|\,\chi_n(x)_\beta\delta(\tau_n-\hat\tau_n)\bar\chi_n(0)_\gamma\,|0\rangle\,\mathrm{Tr}\,\langle 0|\,\bar\chi_{\bar n}(x)_\alpha\delta(\tau_{\bar n}-\hat\tau_{\bar n})\chi_{\bar n}(0)_\delta\,|0\rangle \\ &\quad\times\mathrm{Tr}\,\langle 0|\,\overline{Y}^\dagger_{\bar n}(x)Y_n^\dagger(x)\delta(\tau_s-\hat\tau_s)Y_n(0)\overline{Y}_{\bar n}(0)\,|0\rangle\sum_{i=V,A}L^i(\bar\Gamma^\mu_i)_{\alpha\beta}(\Gamma_{i\mu})_{\gamma\delta}\,,\end{aligned} \tag{9.18}$$

where $L^i = g^{\mu\nu}L^i_{\mu\nu}$, the traces are over colors, and we now make the spin indices explicit.

The collinear matrix elements define jet functions $\mathcal{J}_{n,\bar n}$ according to

$$\frac{1}{N_C}\mathrm{Tr}\,\langle 0|\,\chi_n(x)_\beta\delta(\tau_n-\hat\tau_n)\bar\chi_n(0)_\gamma\,|0\rangle \;\equiv\; \int\frac{dk^+dk^-d^2k_\perp}{2(2\pi)^4}e^{-ik\cdot x}\mathcal{J}_n(\tau_n,k^+;\mu)\left(\frac{\bar n\!\!\!/}{2}\right)_{\beta\gamma} \tag{9.19a}$$

$$\frac{1}{N_C}\mathrm{Tr}\,\langle 0|\,\bar\chi_{\bar n}(x)_\alpha\delta(\tau_{\bar n}-\hat\tau_{\bar n})\chi_{\bar n}(0)_\delta\,|0\rangle \;\equiv\; \int\frac{dl^+dl^-d^2l_\perp}{2(2\pi)^4}e^{-il\cdot x}\mathcal{J}_{\bar n}(\tau_{\bar n},l^-;\mu)\left(\frac{n\!\!\!/}{2}\right)_{\delta\alpha}\,, \tag{9.19b}$$

while the usoft matrix element defines a soft function

$$\frac{1}{N_C}\mathrm{Tr}\,\langle 0|\,\overline{Y}_{\bar{n}}(x)Y_n^\dagger(x)\delta(\tau_s-\hat{\tau}_s)Y_n(0)\overline{Y}_{\bar{n}}(0)\,|0\rangle \equiv \int \frac{d^4r}{(2\pi)^4}e^{-ir\cdot x}S(\tau_s,r;\mu)\,. \tag{9.20}$$

Furthermore, we can use that $\mathcal{J}_n(\tau_n,k^+;\mu)$ depends only on single light-cone component $k^+\equiv n\cdot k$ of the residual momentum, as only $in\cdot\partial$ appears in the n-collinear SCET Lagrangian [2] at leading-order in λ. Similarly $\mathcal{J}_{\bar{n}}(\tau_{\bar{n}},l^-;\mu)$ depends only on $l^-\equiv\bar{n}\cdot l$.

Because the jet functions are independent of the residual transverse momenta, it is natural to change variables to their sum and difference: $K_\perp\equiv k_\perp+l_\perp$, $\kappa_\perp=(1/2)(k_\perp-l_\perp)$. The integral over the sum gives $(2\pi)^2\delta^2(x_\perp)$. In this notation, the formula (9.18) for the event shape distribution can now be written as

$$\begin{aligned}\frac{d\sigma}{d\tau} &= \frac{N_C}{6Q^2}L\sum_n\int d^2\kappa_\perp\ \left|C_n(Q^2;\mu)\right|^2\int d^4x\int d\tau_n\,d\tau_{\bar{n}}\,d\tau_s\,\delta(\tau-\tau_n-\tau_{\bar{n}}-\tau_s)\\ &\quad\times\delta\left(\frac{x^+}{2}\right)\delta\left(\frac{x^-}{2}\right)\delta^2(x_\perp)\int\frac{dk^+dl^-}{4(2\pi)^4}\int\frac{d^4r}{(2\pi)^4}\mathrm{e}^{-i(r^++k^+)x^-/2-i(r^-+l^-)x^+/2-ir_\perp\cdot x_\perp}\\ &\quad\times\mathcal{J}_n(\tau_n,k^+;\mu)\mathcal{J}_{\bar{n}}(\tau_{\bar{n}},l^-;\mu)S(\tau_s,r;\mu)\,,\end{aligned} \tag{9.21}$$

where the factor L is defined

$$L\equiv L^V\mathrm{Tr}\left(\frac{\bar{n}\!\!\!/}{2}\gamma_\perp^\mu\frac{n\!\!\!/}{2}\gamma_\mu^\perp\right)+L^A\mathrm{Tr}\left(\frac{\bar{n}\!\!\!/}{2}\gamma_\perp^\mu\gamma_5\frac{n\!\!\!/}{2}\gamma_\mu^\perp\gamma_5\right)\,. \tag{9.22}$$

In Eq. (9.21) we have integrated over k^-,l^+, and $K_\perp$ to generate delta functions setting all components of x to zero. This allows us to perform the integrals over x.

There remains a sum over label directions n and an integral over the residual momenta $\kappa_\perp$, which combined are simply an integral over total solid angle [21],

$$\sum_{\vec{n}}d^2\kappa_\perp=\frac{Q^2}{4}d\Omega\,, \tag{9.23}$$

where the overall factor arises from the magnitude of the label three-momentum of the jet in direction $\vec{n}$, which is $\left|\vec{\bar{p}}\right|=Q/2$.

As a final step, we define jet and soft functions integrated over all momenta

$$J_n(\tau_n;\mu) \equiv \int\frac{dk^+}{2\pi}\mathcal{J}_n(\tau_n,k^+;\mu) \tag{9.24a}$$

$$J_{\bar{n}}(\tau_{\bar{n}};\mu) \equiv \int\frac{dl^-}{2\pi}\mathcal{J}_{\bar{n}}(\tau_{\bar{n}},l^-;\mu) \tag{9.24b}$$

$$S(\tau_s;\mu) \equiv \int\frac{d^4r}{(2\pi)^4}S(\tau_s,r;\mu)\,. \tag{9.24c}$$

as well as a hard function, which is simply the square of the absolute value of the matching coefficient

$$H_2(Q;\mu)\equiv\left|C_2(Q;\mu)\right|^2\,. \tag{9.25}$$

This gives the final formula

$$\frac{d\sigma}{d\Omega d\tau}=\frac{d\sigma_B}{d\Omega}\,H_2(Q;\mu)\int d\tau_n\,d\tau_{\bar{n}}\,d\tau_s\,\delta(\tau-\tau_n-\tau_{\bar{n}}-\tau_s)J_n(\tau_n;\mu)J_{\bar{n}}(\tau_{\bar{n}};\mu)S(\tau_s;\mu)\,. \tag{9.26}$$

where the differential Born cross section, including the full $\gamma-Z$ interference is given by

$$\frac{d\sigma_B}{d\Omega}=\frac{\alpha_{\mathrm{em}}^2}{4Q^2}(1+\cos\theta^2)N_C\sum_f\left[Q_f^2-\frac{2Q^2v_ev_fQ_f}{Q^2-M_Z^2}+\frac{Q^4(v_e^2+a_e^2)(v_f^2+a_f^2)}{(Q^2-M_Z^2)^2}\right]\,, \tag{9.27}$$

9.3 Perturbative Results [fix notation]

The hard function can immediately be obtained from the result of the Wilson coefficient given in Eq. (7.41). One finds

$$H_2(Q;\mu) = 1 + \frac{\alpha_s C_F}{2\pi}\left[-4\log^2\frac{Q}{\mu} + 6\log\frac{Q}{\mu} - 8 + \frac{7\pi^2}{6}\right] \tag{9.28}$$

The jet and soft functions can be calculated from its definition as the vacuum matrix element of a two-point collinear function. Using Eqs. (9.24) and (9.19) together with the fact that $\tau = l^{\pm}/Q$, one can show that the jet-function can be written as

$$\begin{aligned} J_n(\tau_n;\mu) &= Q\int d^4x e^{ix\cdot r}\mathrm{Tr}\,\langle 0|\,\chi_n(x)\frac{\bar{\not{n}}}{4N_C}\bar{\chi}_n(0)\,|0\rangle \\ &= \frac{Q}{2\pi}\,\mathrm{Disc}\left[\int d^4x e^{ix\cdot r}\mathrm{Tr}\,\langle 0|\,\mathrm{T}\,\chi_n(x)\frac{\bar{\not{n}}}{4N_C}\bar{\chi}_n(0)\,|0\rangle\right] \end{aligned} \tag{9.29}$$

where we have used the optical theorem in the last line to write the jet function in terms of the discontinuity of a forward matrix element of a time ordered product. The soft function is given by

$$S(\tau_s;\mu) = \frac{1}{N_C}\mathrm{Disc}\left[\int d^4x e^{ix\cdot r}\mathrm{Tr}\,\langle 0|\,\mathrm{T}\overline{Y}_{\bar{n}}(x)Y_n^\dagger(x)\,Y_n(0)\overline{Y}_{\bar{n}}(0)\,|0\rangle\right] \tag{9.30}$$

At leading order in perturbation theory both are equal to a delta function of τ. At next to leading order, one needs to include both the virtual and real contributions. Adding everything together one finds for the renormalized jet and soft functions

$$\begin{aligned} J(\tau;\mu) &= \delta(\tau) + \frac{\alpha_s C_F}{4\pi}\left[\left(2\log^2\frac{Q\xi}{\mu^2} - 3\log\frac{Q\xi}{\mu^2} + 7 - \pi^2\right)\delta(\tau) + \left(4\log\frac{Q\xi}{\mu^2} - 3\right)\frac{1}{\xi}\mathcal{L}_0\left(\frac{\tau}{\xi}\right) + 4\frac{1}{\xi}\mathcal{L}_1\left(\frac{\tau}{\xi}\right)\right] \\ S(\tau,\mu) &= \delta(\tau) + \frac{\alpha_s C_F}{4\pi}\left[\left(-8\log^2\frac{\xi}{\mu} + \frac{\pi^2}{3}\right)\delta(\tau) - 16\log\frac{\xi}{\mu}\frac{1}{\xi}\mathcal{L}_0\left(\frac{\tau}{\xi}\right) - 16\frac{1}{\xi}\mathcal{L}_1\left(\frac{\tau}{\xi}\right)\right], \end{aligned} \tag{9.31}$$

where ξ is a dummy dimensionful variable and we have defined

$$\mathcal{L}_{-1}(x) = \delta(x) \tag{9.32}$$

and for $n \geq 0$

$$\mathcal{L}_{n>-1}(x) = \left(\frac{\theta(x)\log^{n-1}x}{x}\right)_+ \tag{9.33}$$

One can easily check that the dependence on ξ cancels for both the jet and the soft function.

As for any renormalized quanity, one can derive a renormalization group equation and for the jet and soft funtions they are given by

$$\begin{aligned} \mu\frac{d}{d\mu}J(\tau,\mu) &= \int d\tau'\,\gamma_J(\tau-\tau',\mu)\,J(\tau',\mu) \\ \mu\frac{d}{d\mu}S(\tau,\mu) &= \int d\tau'\,\gamma_S(\tau-\tau',\mu)\,S(\tau',\mu) \end{aligned} \tag{9.34}$$

Inserting these expressions, and choosing $\xi = Q$, one reproduces the well known expression for the differential thrust spectrum

$$\frac{d\sigma}{d\Omega d\tau} = \delta(\tau) + \frac{\alpha_s C_F}{2\pi}\left[\left(-1-\frac{\pi^2}{3}\right)\delta(\tau) - 3\left(\frac{1}{\tau}\right)_+ - 4\left(\frac{\log\tau/Q}{\tau}\right)_+\right]. \tag{9.35}$$

The cumulative distribution, defined as

$$\frac{d\sigma}{d\Omega}(\tau) \equiv \int_0^\tau d\tau' \frac{d\sigma}{d\Omega d\tau'} \tag{9.36}$$

is given by

$$\frac{d\sigma}{d\Omega}(\tau) = 1 + \frac{\alpha_s C_F}{2\pi}\left[1 - \frac{\pi^2}{3} - 3\log\frac{\tau}{Q} - 2\log\frac{\tau}{Q}\right] \tag{9.37}$$

Examining the differential thrust spectrum and the cumulative thrust distribution one immediately notices the presence of the logarithmic terms which depend on the ratio τ/Q. For small values of this ratio, these logarithms become large, increasing the numerical size of the α_s correction. By calculating to higher orders in perturbative theory, one finds that each additional order in perturbation theory brings two extra powers of $\log\tau/Q$, such that the entire perturbative series stops converging for small enough values of τ. As discussed in Sections **??**, these logarithms can be resummed using the renormalization group evolution of the hard, jet and soft functions.

9.4 Results with Resummation

From the NLO expressions of the hard, jet and soft functions given in Eqs (9.28) and (**??**), one can see the presence of logarithmic terms. In Appendix **??**, where these functions are given to NNLO, one can cearly see that two extra powers of such logarithms occur at each order in perturbation theory. An important point, however, is that each of these functions, besides the renormalization scale, depend on a single scale only. The hard function for example only depends on μ, such that all logarithms are of the form $\log Q/\mu$. Choosing $\xi \sim \tau$, all logarithms in jet function are of the form $\log Q\tau/\mu^2$, and those in the soft function of the form $\log\tau/\mu$. Thus, by evaluating each of these functions at the respective scales

$$\mu_H \sim Q\,, \qquad \mu_J \sim \sqrt{Q\tau}\,, \qquad \mu_S \sim \tau\,, \tag{9.38}$$

the perturbative expressions contain no large logarithms. One can then use the renormalization group evolution to evolve each of these functions to the common scale μ.

Which logarithms are important and which are not, depends on the relative size of $\log\tau/Q$ relative to the size of α_s. One typically uses the scaling $\alpha_s \log^2\tau/Q \sim 1$ for which **add more**.

The running of the hard function can be obtained from the result in Eq. (7.58)

$$H_2(Q;\mu) = \exp\left[-\frac{16\pi C_F}{\beta_0^2\alpha_s(\mu_0)}\Big(\frac{1}{z} - 1 + \ln z\Big) - \frac{6C_F}{\beta_0}\ln z\right]\Big(\frac{Q}{\mu}\Big)^{-8C_F\ln z/\beta_0}. \tag{9.39}$$

where $z = \alpha_s(\mu^{\rm FO})/\alpha_s(\mu)$. Solving the renormalization group equation for the jet and soft functions, the functions at one scale are given by a convolution between the functions at a different scale and an evoultion kernel that sums the logariths of the ratio of scales.

The renormalization group equation for the jet and soft funtions are given by

$$J(s_1,\mu) = \int ds_1'\, J_1(s_1 - s_1', \mu_{J_1})\, U_{J_1}(s_1', \mu_{J_1}, \mu) \tag{9.40}$$

	matching (singular)	nonsingular	γ_x	$\Gamma_{\rm cusp}$	β	PDF
LO	LO	LO	-	-	1-loop	LO
NLO	NLO	NLO	-	-	2-loop	NLO
NNLO	NNLO	NNLO	-	-	3-loop	NNLO
LL	LO	-	-	1-loop	1-loop	LO
NLL	LO	-	1-loop	2-loop	2-loop	LO
NNLL	NLO	-	2-loop	3-loop	3-loop	NLO
NLL$'$+NLO	NLO	NLO	1-loop	2-loop	2-loop	NLO
NNLL+NNLO	(N)NLO	NNLO	2-loop	3-loop	3-loop	NNLO
NNLL$'$+NNLO	NNLO	NNLO	2-loop	3-loop	3-loop	NNLO
N^{3}LL+NNLO	NNLO	NNLO	3-loop	4-loop	4-loop	NNLO

Table 8: The order counting we use in fixed-order and resummed perturbation theory. The last two rows are beyond the level of our calculations here, but are discussed in the text.

10 Deep Inelastic Scattering [Draft Needs Work]

DIS is a rich subject. A textbook introduction to DIS will often discuss the derivation of the leading power cross section by performing an operator product expansion with the infinite class of operators whose relevance is organized by twist. The leading twist operators give an operator formalism which justifies the parton model. The analysis of perturbative corrections in this OPE formalism is notational cumbersome.

We will see that in SCET the infinite set of leading twist operators is encoded in a single non-local operator: $O(\omega) = \bar{\xi}_n W_n \delta(\omega - \bar{n}\cdot\mathcal{P}) W_n^\dagger \xi_n$. The forward proton matrix element of this operator is the parton distribution function (PDF). For brevity we restrict our discussion of DIS to only those aspects related to factorization and the renormalization group evolution with SCET. In particular we will derive the factorization theorem for DIS that yields hard coefficients (partonic cross sections) convoluted with the PDF operators, $C(\omega) \otimes O(\omega)$. We will also derive the DGLAP RGE equation by renormalizing the operator $O(\omega)$.

10.1 DIS Factorization: Hard and Parton Distributions

The $e^- p \to e^- X$ DIS scattering process is depicted by the amplitude shown in Fig. 14. The hard scale Q of the process is defined by the photon momentum q^μ

$$q^2 = -Q^2 \tag{10.1}$$

and satisfies $Q^2 \gg \Lambda^2$. Our Bjorken variable x is defined in the standard way

$$x = \frac{Q^2}{2p\cdot q} \tag{10.2}$$

and with momentum conservation defined by $p^\mu + q^\mu = p_X^\mu$, we have

$$p_X^2 = \frac{Q^2}{x}(1-x) + m_p^2. \tag{10.3}$$

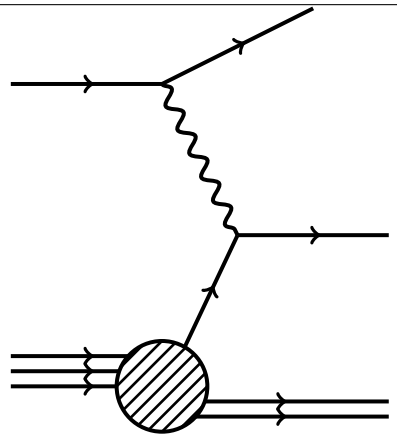

Figure 14: Deep Inelastic Scattering Amplitude

With this result we may determine the various energy regions of the process

Regions	Description
$\left(\frac{1}{x}-1\right)\sim 1 \implies p_X^2 \sim Q^2$	Standard OPE Region
$\left(\frac{1}{x}-1\right)\sim \frac{\Lambda}{Q} \implies p_X^2 \sim Q\Lambda$	Endpoint Region
$\left(\frac{1}{x}-1\right)\sim \frac{\Lambda^2}{Q^2} \implies p_X^2 \sim \Lambda^2$	Resonance Region

Describe Parton Variables

We will consider our scattering process in the standard OPE region so that the final state has p_X^2 of order Q^2 and can consequently be integrated out. Conversely, the proton with its comparatively small invariant mass $p^2 \sim \Lambda^2$ may be treated as a collinear field. We analyze the process in the **Breit Frame** in which the perpendicular momentum component of q^μ is zero with

$$q^\mu = \frac{Q}{2}(\bar{n}^\mu - n^\mu). \tag{10.4}$$

The proton and final state momentum are then

$$p^\mu = \frac{n^\mu}{2}\bar{n}\cdot p + \frac{\bar{n}^\mu}{2} n\cdot p \tag{10.5}$$

$$= \frac{n^\mu}{2}\bar{n}\cdot p + \frac{\bar{n}^\mu}{2}\frac{m_p^2}{\bar{n}\cdot p} \tag{10.6}$$

$$= \frac{n^\mu}{2}\frac{Q}{x} + \cdots \tag{10.7}$$

$$p_X^\mu = p^\mu + q^\mu \tag{10.8}$$

$$= \frac{n^\mu}{Q} + \frac{\bar{n}^\mu}{2} Q\frac{(1-x)}{x}. \tag{10.9}$$

The cross section for DIS in terms of leptonic and hadronic tensors is

$$d\sigma = \frac{d^3k'}{2|\vec{k}'|(2\pi)^3}\frac{\pi e^4}{sQ^4} L^{\mu\nu}(k,k')W_{\mu\nu}(p,q) \tag{10.10}$$

$$\tag{10.11}$$

where k and k' are the incoming and outgoing lepton momenta, respectively, and we have defined $q \equiv k' - k$, and $s \equiv (p+k)^2$. $L^{\mu\nu}(k,k')$ is the leptonic tensor computed using standard QFT methods and $W_{\mu\nu}(p,q)$ is the hadronic tensor which will occupy us in this section. $W_{\mu\nu}$ is related to the imaginary part of the DIS scattering amplitude by

$$W_{\mu\nu}(p,q) = \frac{1}{\pi}\mathrm{Im}T_{\mu\nu} \tag{10.12}$$

where

$$T_{\mu\nu}(p,q) = \frac{1}{2}\sum_{\text{spin}} \langle p|\, \hat{T}_{\mu\nu}(q)\, |p\rangle \qquad \hat{T}_{\mu\nu}(q) = i\int d^4x e^{iqx} T[J_\mu(x) J_\nu(0)]. \tag{10.13}$$

Taking J_μ to be an electromagnetic current, we may write

$$T_{\mu,\nu}(p,q) = \left(-g_{\mu\nu} + \frac{q_\mu q_\nu}{q^2}\right) T_1(x,Q^2) + \left(p_\mu + \frac{q_\mu}{2x}\right)\left(p_\nu + \frac{q_\nu}{2x}\right) T_2(x,Q^2). \tag{10.14}$$

which satisfies current conservation, P, C, and T symmetries. Matching the $\hat{T}_{\mu\nu}(q)$ onto the most general leading order SCET operator for collinear fields in the n^μ direction and satisfying current conservation $q^\mu \hat{T}_{\mu\nu}$ we have

$$\hat{T}^{\mu\nu} \;\to\; \frac{g_\perp^{\mu\nu}}{Q}\left(O_1^{(i)} + \frac{O_1^g}{Q}\right) + \frac{(n^\mu + \bar{n}^\mu)(n^\nu + \bar{n}^\nu)}{Q}\left(O_2^{(i)} + \frac{O_2^g}{Q}\right) \tag{10.15}$$

where

$$O_j^{(i)} = \overline{\xi^i_{n,p}} W \frac{\bar{n}\!\!\!/}{2} C_j^{(i)}(\overline{\mathcal{P}}_+, \overline{\mathcal{P}}_-) W^\dagger \xi^i_{n,p} \tag{10.16}$$

$$O_j^g = \mathrm{Tr}[W^\dagger B_\perp^\lambda W\, C_j^g(\overline{\mathcal{P}}_+, \overline{\mathcal{P}}_-) W^\dagger B_{\perp\,\lambda} W] \tag{10.17}$$

$$\tag{10.18}$$

with $igB_\perp^\lambda$ and $\overline{\mathcal{P}}_\pm$ defined as

$$igB_\perp^\lambda \equiv [i\bar{n}\cdot D_n,\, iD^\lambda_{n,\perp}], \qquad \overline{\mathcal{P}}_\pm = \overline{\mathcal{P}}^\dagger \pm \overline{\mathcal{P}}. \tag{10.19}$$

The subscripts j in $O_j^{(i)}$ are arbitrary labels, similar to those found in (10.14), which differentiate the two parts of of $\hat{T}_{\mu\nu}$. The superscript (i) defines the flavor $(u, d, s, \text{etc.})$ of quarks and the superscript g in O_j^g stands for a gluon. In accord with their labels, $O_j^{(i)}$ will lead to the quark and anti-quark PDF and O_j^g will lead to the gluon PDF. The placement of factors of $\frac{1}{Q}$ is done in order to yield dimensionless Wilson coefficients. The fact that these Wilson coefficients are dimensionless can be understod by realizing that according to (10.13), $\hat{T}_{\mu\nu}$ has mass dimension 2.

In (10.15) there are both quark and gluon operators. However, with $\hat{T}_{\mu\nu}$ defined in terms of an electromagnetic current we can focus on the quarks and treat the gluons as an higher order contribution so that $\hat{T}_{\mu\nu}$ becomes

$$\hat{T}^{\mu\nu} \;\to\; \frac{g_\perp^{\mu\nu}}{Q} O_1^{(i)} + \frac{(n^\mu + \bar{n}^\mu)(n^\nu + \bar{n}^\nu)}{Q} O_2^{(i)}. \tag{10.20}$$

Returning to the quark operator $O_j^{(i)}$, we may introduce a convolution to separate the hard coefficients from the long distance operators

$$O_j^{(i)} = \int d\omega_1 d\omega_2\, C_j^{(i)}(\omega_+, \omega_-)[(\overline{\xi}_n W)_{\omega_1}\delta(\omega_1 - \overline{\mathcal{P}}^\dagger)\frac{\bar{n}\!\!\!/}{2}(W^\dagger \xi_n))_{\omega_2}\delta(\omega_2 - \mathcal{P})] \tag{10.21}$$

where $\omega_\pm = \omega_1 \pm \omega_2$. Our hope is to connect this operator to the PDF as a clear demonstration of factorization. The PDF for quarks is given by

$$f_{i/p}(\xi) = \int dy e^{-2i\xi\bar{n}\cdot py}\, \langle p|\, \overline{\xi}(y) W(y,-y)\bar{n}\!\!\!/\xi(y)\, |p\rangle \tag{10.22}$$

and the PDF for anti-quarks is simply $\overline{f}_{i/p}(\xi) = -f_{i/p}(-\xi)$. In momentum space, we can write the matrix element in (10.22) as

$$\begin{aligned}
\langle p|\, \overline{\xi}(y) W(y,-y)\bar{n}\!\!\!/\xi(y)\, |p\rangle &= \langle p|\, (\overline{\xi}_n W)_{\omega_1}\bar{n}\!\!\!/(W^\dagger\xi_n))_{\omega_2}\, |p\rangle && (10.23)\\
&= 4\bar{n}\cdot p \int_0^1 d\xi\, \delta(\omega_-) && (10.24)\\
&\times [\delta(\omega_+ - 2\xi\bar{n}\cdot p) f_{i/p}(\xi) - \delta(\omega_+ + 2\bar{n}\cdot p)\overline{f}_{i/p}(\xi)]. && (10.25)
\end{aligned}$$

The delta function over ω_- sets $\omega_1 = \omega_2$. The other set of delta functions ensure that for $\omega_+ > 0$ we use quark PDF $f_{i/p}(z)$. and for $\omega_+ < 0$ we use anti-quark PDF $\overline{f}_{i/p}(z)$. Using these results we may rewrite our operator $O_j^{(i)}$ including spin averages as

$$\begin{aligned}
\frac{1}{2}\sum_{\text{spin}} \langle p|\, O_j^{(i)}\, |p\rangle &= \frac{1}{4}\int d\omega_1 d\omega_2\, C_j^{(i)}(\omega_+, \omega_-)[(\overline{\xi}_n W)_{\omega_1}\delta(\omega_1 - \overline{\mathcal{P}}^\dagger)\bar{n}\!\!\!/(W^\dagger\xi_n))_{\omega_2}\delta(\omega_2 - \mathcal{P})] && (10.26)\\
&= \frac{1}{4}\int d\omega_1 d\omega_2 C_j^{(i)}(\omega_+, \omega_-) 4\bar{n}\cdot p && (10.27)\\
&\times \int_0^1 d\xi\, \delta(\omega_-)[\delta(\omega_+ - 2\xi\bar{n}\cdot p) f_{i/p}(\xi) - \delta(\omega_+ + 2\bar{n}\cdot p)\overline{f}_{i/p}(\xi)] && (10.28)\\
&= \bar{n}\cdot p \int_0^1 [C_j^i(2\bar{n}\cdot p\xi, 0) f_{i/p}(\xi) - C_j^i(-2\bar{n}\cdot p\xi, 0)\overline{f}_{i/p}(\xi)]. && (10.29)
\end{aligned}$$

Now, by charge conjugation invariance (reference), we have $C(-\omega_+, \omega_-) = -C(\omega_+, \omega_-)$ so that the final form of the spin averaged matrix element is

$$\frac{1}{2}\sum_{\text{spin}} \langle p|\, O_j^{(i)}\, |p\rangle = \bar{n}\cdot p \int_0^1 C_j^i(2\bar{n}\cdot p\xi, 0)[f_{i/p}(z\xi) + \overline{f}_{i/p}(z\xi)]. \tag{10.30}$$

We note that although we are using SCET_{II} no soft gluons have appeared in our analysis. This fact can be understood by observing that our original operator

$$O_j^{(i)} = \overline{\xi_{n,p}^i} W \frac{\bar{n}\!\!\!/}{2} C_j^{(i)}(\overline{\mathcal{P}}_+, \overline{\mathcal{P}}_-) W^\dagger \xi_{n,p}^i$$

is a color singlet and therefore decouples from any color-charge changing (i.e. gluon) interactions. With (10.30) we have the necessary result for a demonstration of factorization. Now all that is left to do is

perform the matching of the full field theoretic operators $T_1(x,Q^2)$ and $T_2(x,Q^2)$ onto the operators $O_j^{(i)}$. Recalling our formula for $T_{\mu\nu}$ in terms of $\hat{T}_{\mu\nu}$, we have

$$T^{\mu\nu} = \frac{1}{2}\sum_{\text{spin}} \langle p|\, \hat{T}^{\mu\nu}\, |p\rangle \tag{10.31}$$

$$= \frac{g_\perp^{\mu\nu}}{Q}\frac{1}{2}\sum_{\text{spin}} \langle p|\, O_j^{(i)}\, |p\rangle + \frac{4n^\mu n^\nu}{Q}\frac{1}{2}\sum_{\text{spin}} \langle p|\, O_j^{(i)}\, |p\rangle\ . \tag{10.32}$$

This is the SCET amplitude. The QCD amplitude is

$$T^{SCET}_{\mu,\nu}(p,q) = \left(-g_{\mu\nu} + \frac{q_\mu q_\nu}{q^2}\right) T_1(x,Q^2) + \left(p_\mu + \frac{q_\mu}{2x}\right)\left(p_\nu + \frac{q_\nu}{2x}\right) T_2(x,Q^2) \tag{10.33}$$

Writing this result in light-cone coordinates and using the Ward Identity ($q_\nu L^{\mu\nu} = q_\mu L^{\mu\nu} = 0$), and the fact that all terms proportional to $(\bar{n}_\mu - n_\mu) = \frac{2q_\mu}{Q}$ become zero upon contraction with $L_{\mu\nu}$, we have

$$T^{QCD}_{\mu\nu} = -g_{\mu\nu\,\perp} T_1(x,Q^2) + n_{\mu\nu}\left(\frac{Q^2}{4x^2}T_2(x,Q^2) - T_1(x,Q^2)\right) \tag{10.34}$$

We refer the reader to [**?**] for a full derivation of this result. Matching T^{QCD} onto T^{SCET}, yields the relations

$$-\frac{1}{2Q}\sum_{\text{spin}} \langle p|\, O_j^{(i)}\, |p\rangle = T_1(x,Q^2) \tag{10.35}$$

$$\frac{2}{Q}\sum_{\text{spin}} \langle p|\, O_j^{(i)}\, |p\rangle = \left(\frac{Q^2}{4x^2}T_2(x,Q^2) - T_1(x,Q^2)\right) \tag{10.36}$$

which, upon inversion, gives

$$T_1(x,Q^2) = -\frac{1}{2Q}\sum_{\text{spin}} \langle p|\, O_j^{(i)}\, |p\rangle \tag{10.37}$$

$$= -\frac{1}{x}\int_0^1 d\xi C_1^i(2\bar{n}\cdot p\xi, 0)[f_{i/p}(\xi) + \overline{f}_{i/p}(\xi)] \tag{10.38}$$

$$T_2(x,Q^2) = \frac{8x^2}{Q^3}\sum_{\text{spin}} \langle p|\, O_j^{(i)}\, |p\rangle - \frac{2x^2}{Q^3}\sum_{\text{spin}} \langle p|\, O_j^{(i)}\, |p\rangle \tag{10.39}$$

$$= \frac{4x}{Q^2}\int_0^1 d\xi \left(4C_2^{(i)}(2\bar{n}\cdot p\xi, 0) - C_1^{(i)}(2\bar{n}\cdot p\xi, 0)\right)[f_{i/p}(\xi) + \overline{f}_{i/p}(\xi)]. \tag{10.40}$$

$$\tag{10.41}$$

where in the Breit Frame $x = \frac{Q^2}{2p\cdot q} = \frac{Q^2}{\bar{n}\cdot p n\cdot q} = \frac{Q}{\bar{n}\cdot p}$. With the definition

$$H_j(z) \equiv C_j(2Qz, 0, Q, \mu), \tag{10.42}$$

where the hard scale Q and the μ dependence has been made explicit, we have the final result

$$T_1(x,Q^2) = -\frac{1}{x}\int_0^1 d\xi\, H_1^{(i)}\left(\frac{\xi}{x}\right)[f_{i/p}(\xi) + \overline{f}_{i/p}(\xi)] \tag{10.43}$$

$$T_2(x,Q^2) = \frac{4x}{Q^2}\int_0^1 d\xi \left[4H_2^{(i)}\left(\frac{\xi}{x}\right) - H_1^{(i)}\left(\frac{\xi}{x}\right)\right][f_{i/p}(\xi) + \overline{f}_{i/p}(\xi)] \tag{10.44}$$

where the sum over i is implicit.

Remarks

- This result represents the general (to all orders in α_s) factorization for DIS. As promised we have the computable hard coefficients H_i weighted by the universal non-perturbative PDFs $f_{i/p}$ and $\overline{f}_{i/p}$.
- The coefficients C_j are dimensionless and can therefore only have $\alpha_s(\mu)\ln(\mu/Q)$ dependence on Q. This result is in accord with Bjorken Scaling.
- The μ in $H_i(\mu)$ and $f_{i/p}(\mu)$ is typically called the factorization scale $\mu = \mu_F$. There is also the renormalization scale as in $\alpha_s(\mu_R)$. In SCET μ is both the renormalization and factorization scale, since the same parameter μ is responsible for the running of the EFT coupling $\alpha_s(\mu)$ and for the EFT coupling $C_j(\mu)$.
- When we consider the tree level matching onto the wilson coefficients we find that $C_2 = 0$ implying the Callan-Gross relation

$$\frac{W_1}{W_2} = \frac{Q^2}{4x^2} \tag{10.45}$$

and that

$$C_1(\omega_+) = 2e^2Q_i^2\left[\frac{Q}{(\omega_+ - 2Q) + i\epsilon} - \frac{Q}{(-\omega_+ - 2Q) + i\epsilon}\right] \tag{10.46}$$

$$H_1 = -e^2Q_i^2\delta\left(\frac{\xi}{x} - 1\right) \tag{10.47}$$

10.2 Renormalization of PDF

(**ROUGH**) In this section we calculate the anomalous dimension of the parton distribution function. We define the PDF as

$$f_q(\xi) = \langle p_n|\,\overline{\chi}_n(0)\frac{\overline{\not{n}}}{2}\chi_{n,\omega}(0)\,|p_n\rangle \tag{10.48}$$

where $\omega = \xi\,\bar{n}\cdot p_n > 0$. Since we have a forward matrix element there is no need to consider a momentum label ω' on $\overline{\chi}_n$, by momentum conservation it would be fixed to $\omega' = \omega$. We renormalize our PDF in our EFT framework with dimensional regularization, noting that there are only collinear fields an no ultrasoft interactions for this example. Collinear loop processes can change ω (or ξ) and also the type of parton. The renormalized PDF operators are given in terms of bare operators as

$$f_i^{\text{bare}}(\xi) = \int d\xi'\, Z_{ij}(\xi,\xi')f_j(\xi',\mu). \tag{10.49}$$

The μ independence of the bare operators $f_i^{bare}(\xi)$ yields an RGE for the renormalized operators in $\overline{\text{MS}}$,

$$\mu\frac{d}{d\mu}f_i(\xi,\mu) = \int d\xi'\gamma_{ij}(\xi,\xi')f_j(\xi',\mu) \tag{10.50}$$

where

$$\gamma_{ij} = -\int d\xi'' Z^{-1}_{ii'}(\xi,\xi'')\mu\frac{d}{d\mu}Z_{i'j}(\xi'',\xi')\,. \tag{10.51}$$

At 1-loop we can take $Z^{-1}_{ii'}(\xi,\xi'') = \delta_{ii'}\delta(\xi-\xi'') + \cdots$ so that

$$\gamma_{ij}^{\text{1-loop}} = -\mu\frac{d}{d\mu}\big[Z_{ij}(\xi,\xi')\big]^{\text{1-loop}} \tag{10.52}$$

Computing the PDF at tree level, we obtain

$$= \underbrace{\overline{u}_n\frac{\not{n}}{2}u_n}_{p^-}\delta(\omega-p^-) = \delta(1-\omega/p^-) \tag{10.53}$$

At the 1-loop level there are multiple contributions the first contribution yields the computation

$$= -ig^2C_F\int d^dl\frac{p^-(d-2)l_\perp^2}{[l^2+i0]^2[(l-p)^2+i0]}\delta(l^--\omega)\frac{\mu^{2\epsilon}e^{\epsilon\gamma_E}}{(4\pi)^\epsilon} \tag{10.54}$$

$$= \frac{2g^2}{(4\pi)^2}(1-\epsilon)^2\Gamma(\epsilon)e^{\epsilon\gamma_E}(1-z)\theta(z)\theta(1-z)\left(\frac{A}{\mu^2}\right)^{-\epsilon} \tag{10.55}$$

$$= \frac{\alpha_sC_F}{\pi}(1-z)\theta(z)\theta(1-z)\left[\frac{1}{2\epsilon}-1-\frac{1}{2}\ln\left(A/\mu^2\right)\right] \tag{10.56}$$

where $A = -p^+p^-z(1-z)$ with $z=\omega/p^-$ The next contribution is given by

$$=2ig^2C_F\int\frac{d^dl\,\overline{u}_n\frac{\not{n}}{2}\frac{\not{n}}{2}\bar{n}\cdot l\not{n}u_n}{(l^- -p^-)l^2(l-p)^2}[\overbrace{\delta(l^-\omega)}^{\text{real}}-\overbrace{\delta(p^--\omega)}^{\text{virtual}}] \tag{10.57}$$

$$=\frac{C_F\alpha_s(\mu)}{\pi}e^{\epsilon\gamma_E}\Gamma(\epsilon)\left[\frac{z\theta(z)\theta(1-z)}{(1-z)^{1+\epsilon}}\left(\frac{-p^-p^+z-i0}{\mu^2}\right)^{-\epsilon}\right. \tag{10.58}$$

$$\left.-\delta(1-z)\left(\frac{-p^-p^+z-i0}{\mu^2}\right)^{-\epsilon}\frac{\Gamma(2-\epsilon)\Gamma(-\epsilon)}{\Gamma 2-2\epsilon}\right] \tag{10.59}$$

We can simplify this result with use of the distribtuion identity.

$$\frac{\theta(1-z)}{(1-z)^{1+\epsilon}} = -\frac{\delta(1-z)}{\epsilon}+\mathcal{L}_0(1-z)-\epsilon\mathcal{L}_1(1-z)+\cdots \tag{10.60}$$

where the plus function $\mathcal{L}_n(x)$ is defined as

$$\mathcal{L}_n(x) = \left[\frac{\theta(x)\ln^n(x)}{x}\right] \tag{10.61}$$

and satisfies the following identities

$$\int_0^1 dx\,\mathcal{L}_n(x) = 0, \quad \int_0^1\mathcal{L}_n(x)g(x) = \int_0^1 dx\,\frac{\ln^n x}{x}[g(x)-g(0)]. \tag{10.62}$$

With this replacement we find that the $1/\epsilon^2$ terms in the real and virtual terms cancel and the remaining $1/\epsilon$ is UV divergent. In the end the explicit contribution of this process is

$$=\frac{C_F\alpha_s(\mu)}{\pi}\left[\{\delta(1-z)+z\theta(z)\mathcal{L}_0(1-z)\}\left(\frac{1}{\epsilon}+\ln\frac{\mu^2}{-p^+p^-z-i0}\right)\right. \tag{10.63}$$

$$\left.-z\mathcal{L}_2(1-z)\theta(z)+\delta(1-z)\left(2-\frac{\pi^2}{6}\right)\right]. \tag{10.64}$$

The last conrtibution to the renormalized PDF is the wavefunction renormalization of the external fermions.

$$Fig() = \delta(1-z)(Z_\psi - 1) = \frac{\alpha_s C_F}{\pi}\left[-\frac{1}{4\epsilon} - \frac{1}{4} - \frac{1}{4}\ln\left(\frac{\mu^2}{-p^+p^- - i0}\right)\right]\delta(1-z) \tag{10.65}$$

There are additional contributions from diagrams such as those in (), but we will ignore these by assuming that the operator is not a flavor singlet. Summing the various contributions, we have

$$\begin{aligned}\text{Sum} = &\frac{C_F\alpha_s(\mu)}{\pi}\left[\left\{\frac{3}{4}\delta(1-z) + z\theta(z)\mathcal{L}_0(1-z) + \right.\right.\\ &\left.\left. + \frac{(1-z)}{2}\theta(z)\theta(1-z)\right\}\left(\frac{1}{\epsilon} + \ln\frac{\mu^2}{-p^+p^-z_i 0}\right) + \text{finite function of } z\right]\\ =&\frac{C_F\alpha_s(\mu)}{\pi}\left[\underbrace{\frac{1}{2}\left(\frac{1+z^2}{1-z}\right)_+}_{\text{Determines } Z_{qq}^{\text{1-loop}}}\left(\frac{1}{\epsilon} + \ln\frac{\mu^2}{-p^+p^-z_i 0}\right) + \cdots \text{finite function of z}\right]\end{aligned} \tag{10.66}$$

If we let the total momentum of the hadronic state be $\hat{p}^-$. Then define $p^-/\hat{p}^- = \xi^-$. So that

$$z = \frac{\omega}{p^-} = \frac{\xi\hat{p}^-}{\xi'\hat{p}^-} = \frac{\xi}{\xi'} \tag{10.67}$$

Then our $Z_{qq}^{\text{1-loop}}$ becomes

$$Z_{qq}^{\text{1-loop}} = \delta(1-z) + \frac{1}{\epsilon}\frac{\alpha_s(\mu)}{2\pi}C_F\theta z\theta(1-z)\Big(\frac{1+z^2}{1-z}\Big)_+. \tag{10.68}$$

And usng

$$\gamma_{ij} = -\mu\frac{d}{d\mu}\mathcal{Z}_{ij}(z,\mu), \quad \mu\frac{d}{d\mu}\alpha_s(\mu) = -2\epsilon\alpha_s(\mu_) + \beta[\alpha_s(\mu)] \tag{10.69}$$

we then obtain the our final result

$$\gamma_{qq}(\xi,\xi') = \frac{C_F\alpha_s\mu}{\pi}\frac{\theta(\xi'-\xi)\theta(1-\xi')}{\xi'}\left(\frac{1+z^2}{1-z}\right)_+ \tag{10.70}$$

which is the Aliterelli - Parisi (DGLAP) quark anomalous dimension at one-loop.

11 SCET for pp Collider Observables [Needs Lots of Work]

11.1 Kinematics

(**ROUGH)** Our final example will be the Drell-Yan (DY) process $p\bar{p} \to Xl^+l^-$. This is a protype LHC process. The kinematics of this process can be described by the following set of equations.

$$p_A + p_B = p_X + q \tag{11.1}$$

$$E_{cm}^2 = (p_A + p_B)^2 \quad \text{Collision Energy} \tag{11.2}$$

$$q^2 \quad : \quad \text{Hard scale of the problem} \tag{11.3}$$

$$\tau \equiv q^2/E_{cm}^2 \leq 1 \tag{11.4}$$

$$Y = \frac{1}{2}\ln\left(\frac{p_b\cdot q}{p_a\cdot q}\right) \quad \text{Total lepton rapidity (angular variable)} \tag{11.5}$$

And the analogs of the Bjorken Variables from DIS:

$$x_a \equiv \sqrt{\tau} e^{Y}, \quad x_b \equiv \sqrt{\tau} e^{-Y}, \tag{11.6}$$

where $\tau \leq x_{a,b} \leq 1$. We study this process int three distinct energy regions

$$\begin{array}{lccc} \cdot\text{Inclusive:} & \tau \sim 1 & p_x^2 \sim q^2 \sim E_{cm}^2 & x_{a,\,b} \sim 1,\ \xi_{a,\,b} \sim 1 \\ \cdot\text{Endpoint:} & \tau \to 1 & p_x^2 << q^2 \to E_{cm}^2 & x_{a,\,b} \to 1,\ \xi_{a,\,b} \to 1 \\ \cdot\text{Isolated:} & \tau \to 0 & p_x^2 >> q^2 & x_{a,\,b} \to 0,\ \xi_{a,\,b} \to 0 \end{array} \tag{11.7}$$

We now analyze these specific processes in detail.

11.2 Inclusvive Drell-Yan: $pp \to Xl^+l^-$

In this case this process represents an $SCET_I$ problem of hard-collinear factorization. we have a 4-quark operator in SCET, which after a Fierz Identity becomes,

$$[(\bar{\xi}_n W_n)\frac{\bar{n}\!\!\!/}{2}(W_n^\dagger \xi_n)][(\bar{\xi}_{\bar{n}} W_{\bar{n}})\frac{n\!\!\!/}{2}(W_{\bar{n}}^\dagger \xi_{\bar{n}})] \tag{11.8}$$

Remarks:

- $T^A \otimes T^A$ octet structure vanishes under $\langle p_n| \,|\cdot|\, |p_n\rangle$
- When we take $\xi_n \to Y_n \xi_n$ for coupling to soft gluons, the soft wilson lines cancel out.
- This operator encodes information about the PDF because both

  $$\langle p_n| \,|\chi_{n,\omega}\frac{\bar{n}\!\!\!/}{2}\chi_{n,\omega'}|\, |p_n\rangle \quad \text{and} \quad \langle p_{\bar{n}}| \,|\chi_{\bar{n},\omega}\frac{n\!\!\!/}{2}\chi_{\bar{n},\omega'}|\, |p_{\bar{n}}\rangle \tag{11.9}$$

  are defined as PDFs. These PDFs contribute to the differential cross section for this process:

  $$\frac{1}{\sigma_0}\frac{d\sigma}{dq^2 dY} = \sum_{i,j}\int_{x_a}^1 \frac{d\xi_a}{\xi_a}\int_{x_b}^1 \frac{d\xi_b}{\xi_b} H_{ij}^{\text{incl}}\left(\frac{x_a}{\xi_a}, \frac{x_b}{\xi_b}, q^2, \mu\right) f_i(\xi_a,\mu) f_j(\xi_b,\mu) \tag{11.10}$$

  $$= \left[1 + \mathcal{O}\left(\frac{\Lambda_{QCD}}{\sqrt{q^2}}\right)\right]. \tag{11.11}$$

- As a last important caveat, we not that Glauber Gluons cancel out at leadind order. However, proving this result is out of the scope of our current discussion.

11.3 Threshold Drell-Yan: $pp \to Xl^+l^-$

In the threshold limit only the terms of H_{ij}^{incl} most singular in $1-\tau$ contribute.

$$H_{ij}^{\text{incl}} \quad \to \quad S_{q\bar{q}}^{\text{thr}}\left[\sqrt{q^2}\left(1 - \frac{\tau}{q_a q_b}\right), \mu\right] H_{ij}(q^2,\mu)\left[1 + \mathcal{O}(1-\tau)\right] \tag{11.12}$$

where $i,j = u\bar{u},\ d\bar{d},\ \ldots$. The interpretation when we take $\xi_{a,b} \to 1$ is that one parton in each proton carries all the momentum. This is not the dominant LHC region.

11.4 Beam thrust in Drell-Yan: $pp \to Xl^+l^-$

The isolated case of DY allows forward jets to carry away part of E_{cm}, so $\xi_{a,b} \to 1$. It also restricts thr central region to still only have soft radiation (the signal region is background free). To guarantee this requires an experimental observation. **Observable:** $p_X = B_a + B_b$. There are two hemispheres perpendicular to the beam axis.

$$B_a^+ = n_a \cdot B_a = \sum_{k\epsilon a} n_a \cdot p_k \tag{11.13}$$

$$= \sum_{k\epsilon a} E_k(1 + \tanh Y_k)e^{-2Y_k} \tag{11.14}$$

We expect the plus momenta for n- collinear radiation to be small. We find that this is indeed the case becuase

$$B_a^+ \leq Qe^{-2Y\omega t} << Q \tag{11.15}$$

and there is an identical expression for B_b^+. For the n-collinear proton (a) and jet (a), we do not merely get a PDF from the hard-collinear-soft factorization. We get something new called a beam function. The differential cross section for this process can be written as

$$\frac{1}{\sigma_0}\frac{d\sigma}{dq^2 dY dB_a^+ dB_b^+} = \sum_{ij} H_{ij}(q^2,\mu)\int dk_a^+ dk_b^+ Q^2 B_i[\omega_a(B_a^+ - k_a^+), x_a, \mu]B_j[\omega_b(B_b^+ - k_b^+), x_b, \mu]$$
$$\times S_{i\,\mathrm{hemi}}(k_a^+, k_b^+, \mu)\left[1 + \mathcal{O}\left(\frac{\Lambda_{QCD}}{Q}, \frac{\sqrt{B_{a,b}\omega_{a,b}}}{Q}\right)\right] \tag{11.16}$$

where $\omega_{a,b} = x_{a,b}E_{cm}$ andB_i is defined as our "Beam Function."

$$B_q(\omega b^+, \omega/\hat{p}^-, \mu) = \frac{\theta(\omega)}{\omega}\int \frac{dy^-}{4\pi}e^{ib^+y/2}\left\langle p_n(\hat{p}^-)\right| |\bar{\chi}_n(y^-\frac{n}{2})\delta(\omega - \bar{\mathcal{P}})\frac{\bar{n}\!\!\!/}{2}\chi_n(0)|\left|p_n(\hat{p}^-)\right\rangle \tag{11.17}$$

We recll the definitions of jet function

$$\langle 0|\,|\bar{\chi}_{n,\omega}(y^-\frac{n}{2})\frac{\bar{n}\!\!\!/}{2}\chi_n(0)|\,|0\rangle \tag{11.18}$$

and pdf

$$\langle p|\,|\bar{\chi}_{n,\omega}(0)\frac{\bar{n}\!\!\!/}{2}\chi_n(0)|\,|p\rangle \tag{11.19}$$

We see that the Jet Function is a mix of both. The proton is a collinear field in $\mathrm{SCET_{II}}$ and the jet is collinear in $\mathrm{SCET_I}$. Matching $\mathrm{SCET_I}$ to $\mathrm{SCET_{II}}$ gives us

$$B_i(t,x,\mu) = \sum_i \int_x^1 \frac{d\xi}{\xi}\mathcal{I}_{ij}(t,\frac{x}{\xi},\mu)f_j(\xi,\mu)\left[1 + \mathcal{O}\left(\frac{\Lambda_{QCD}^2}{t}\right)\right] \tag{11.20}$$

$$b_a^\mu = (\xi - x)E_{cm}\frac{n_a}{2} + b_a^+\frac{\bar{n}_a}{s} + b_{a\,\perp} \tag{11.21}$$

At tree level the Beam Function is simply

$$B_i(t,x,\mu) = \delta(t) f_i(x,\mu) \tag{11.22}$$

as in the pdf case we can write the RGE for the beam function

$$\mu \frac{d}{d\mu} B_i(t,x,\mu) = \int dt' \gamma_i(t-t',\mu) B_i(t',x,\mu) \tag{11.23}$$

Like the jet function B_i is independent of mass evolution. The RGE sums $ln^2(t/\mu)$, is independent of x and has no mixing.

11.5 *pp* Jet Factorization:: Hard, Beam, Jet, Soft Functions

12 More SCET$_{\rm I}$ Applications (Remove)

(**ROUGH)**

In this section we will apply the SCET formalism developed in previous sections to a few additional processes that either use SCET$_{\rm I}$ or a combination of both SCET$_{\rm I}$ and SCET$_{\rm II}$ (where the more complicated part of the factorization occurs within SCET$_{\rm I}$). In particular we will consider

- $B \to X_s \gamma$
- Drell-Yan $p\overline{p} \to l^+ l^- X$: inclusive, endpoint, and isolated factorization theorems

12.1 $B \to X_s \gamma$ [Remove?]

(**ROUGH)** In this section we treat the incluzive weak radiative decay $B \to X_s \gamma$. This decay is defined by the effective Hamiltonian

$$\mathcal{H} = -\frac{4G_F}{\sqrt{2}} V_{tb} V_{ts}^* C_7 \mathcal{O}_7, \quad \mathcal{O}_7 = \frac{e}{16\pi^2} m_b \bar{s} \sigma_{\mu\nu} F^{\mu\nu} P_R b \tag{12.1}$$

with $F^{\mu\nu}$ the electromagnetic field tensor and $P_R = \frac{1}{2}(1+\gamma_5)$. The decay is defined such that the photon momentum is opposite the collinear jet i.e. $q_\mu = E_\gamma \bar{n}_\mu$.

The photon energy spectrum of the decay is

$$\frac{1}{\Gamma_0}\frac{d\Gamma}{dE_\gamma} = \frac{4E_\gamma}{m_b^3}\left(-\frac{1}{\pi}\right) \mathrm{Im} T(E_\gamma) \tag{12.2}$$

where

$$T(E_\gamma) = \frac{i}{m_b} \int d^4x \, e^{-iqx} \left\langle \overline{B}_v \right| \mathrm{T} J_\mu^\dagger(x) J^\mu(0) \left| \overline{B}_v \right\rangle \tag{12.3}$$

Is the forward scattering amplitude with EM current $J_\mu = \bar{s} i \sigma_{\mu\nu} q^\nu P_R b$.

We will consider the endpoint region of the decay in which nearly all of the final state energy is in the photon. Analyzing this process in the rest frame of B, we find that the final momentum X

$$p_X^\mu = p_B^\mu - q^\mu \tag{12.4}$$

$$= \frac{m_b}{2}(n^\mu + \bar{n}^\mu) - E_\gamma \bar{n}^\mu \tag{12.5}$$

$$= m_b \frac{\bar{n}^\mu}{2} + \frac{\bar{n}^\mu}{2}(m_b - 2E_\gamma). \tag{12.6}$$

Defining our endpoint region by

$$\frac{m_b}{2} - E_\gamma \leq \Lambda_{QCD} \tag{12.7}$$

gives us a mass squared scale of

$$p_X^2 \simeq m_b\Lambda = m_b^2\frac{\Lambda}{m_b} = m_b^2\lambda^2 \tag{12.8}$$

where in the last line we took $\lambda = \sqrt{\frac{\Lambda}{m_b}}$. Taking m_b as Q it is clear that this process is described by $\mathrm{SCET_I}$. Specifically, X will be represented by collinear gluons and quarks while B will be represented by heavy (usoft) quark. Our principal goal is to demonstrate how the effects of momentum scales are factorized in the formula for the photon energy spectrum. To this end we will prove that (12.2) can be factorized as

$$\frac{1}{\Gamma_0}\frac{d\Gamma}{dE_\gamma} = H(m_b,\mu)\int_{2E_\gamma - m_b}^{\Lambda} dk^+\, S(k^+,\mu)J(k^+ + m_b - 2E_\gamma,\mu) \tag{12.9}$$

where $H(m_b,\mu)$ is a calculable quantity arising from hard scale dynamics; $S(k^+,\mu)$ is a non-perturbative soft function; and $J(k^+)$ represents collinear gluons and quarks and is called the jet function.

We begin by matching the QCD current onto SCET to obtain

$$J_\mu = -E_\gamma e^{i(\overline{\mathcal{P}}\frac{n}{2}+\mathcal{P}_\perp - m_b v)\cdot x}C(\overline{\mathcal{P}},\mu)\overline{\xi}_{n,p}W\gamma_\mu^\perp P_L h_v \tag{12.10}$$

$$= -E_\gamma C(m_b,\mu)\overline{\xi}_{n,p}W\gamma_\mu^\perp P_L h_v \tag{12.11}$$

where in the second line we used the label momentum conservation to set $\overline{\mathcal{P}} = m_b$ and $\mathcal{P}_\perp = 0$. Inserting this result into (12.3), we may write

$$\frac{4E_\gamma}{m_b^3}T(E_\gamma) \equiv H(m_b,\mu)T_{\text{eff}}(E_\gamma,\mu) \tag{12.12}$$

where

$$T_{\text{eff}} = i\int d^4x\, e^{i(m_b\frac{\bar{n}}{2}-q)\cdot x}\left\langle \overline{B}_v\right|\mathrm{T}J^\mu_{\text{eff}}(x)J_{\mu\,\text{eff}}\left|\overline{B}_v\right\rangle. \tag{12.13}$$

This gives us a hard amplitude of

$$H(m_b,\mu) = \frac{4E_\gamma^3}{m_b^3}|C(m_b,\mu)|^2. \tag{12.14}$$

Next, we decouple usoft gluons from collinear fields by implementing the standard field redefinitions

$$\xi_{n,p} \to Y\xi^{(0)}_{n,p} \qquad W \to Y\,W^{(0)}Y^\dagger \tag{12.15}$$

thus giving us a new effective current:

$$J^\mu_{\text{eff}} = \overline{\xi}^{(0)}_n W^{(0)}\gamma_\mu^\perp P_L Y^\dagger h_v. \tag{12.16}$$

Substituting this result into (12.13) gives us

$$T_{\text{eff}} = i\int d^4x\, e^{i(m_b\frac{\bar{n}}{2}-q)\cdot x}\left\langle \overline{B}_v\right|\mathrm{T}[\overline{h}_v Y P_R\gamma_\mu^\perp W^{(0)\dagger}\xi^{(0)}_{n,p}](x)[\overline{\xi}^{(0)}_{n,p}W^{(0)}\gamma_\perp^\mu P_L Y^\dagger h_v](0)\left|\overline{B}_v\right\rangle \tag{12.17}$$

$$= -\int d^4x\int\frac{d^4k}{(2\pi)^4}e^{i(m_b\frac{\bar{n}}{2}-q-k)\cdot x}\left\langle \overline{B}_v\right|\mathrm{T}[\overline{h}_v Y](x)P_R\gamma_\mu^\perp\frac{\not{\bar{n}}}{2}\gamma_\perp^\mu P_L[Y^\dagger h_v](0)\left|\overline{B}_v\right\rangle J_P(k) \tag{12.18}$$

$$= \frac{1}{2}\int d^4x\int\frac{d^4k}{(2\pi)^4}e^{i(m_b\frac{\bar{n}}{2}-q-k)\cdot x}\left\langle \overline{B}_v\right|\mathrm{T}[\overline{h}_v Y](x)[Y^\dagger h_v](0)\left|\overline{B}_v\right\rangle J_P(k), \tag{12.19}$$

where we defined

$$i\int \frac{d^4k}{(2\pi)^4}\,\langle 0|\,\mathrm{T}[W^{(0)\dagger}\xi^{(0)}_{n,p}](x)[\bar{\xi}^{(0)}_{n,p}W^{(0)}](0)\,|0\rangle \tag{12.20}$$

with the label P representing the sum of the label momentum carried by the collinear fields. (Additional Derivation)? Now, noting that J_P only depends on the k^+ component of residual momentum k, we may do the k^- and k^+ integrals thus putting x on the light cone

$$\begin{aligned}T_{\text{eff}} &= \frac{1}{2}\int d^4x\, e^{i(m_b\frac{\bar{n}}{2}-q)\cdot x}\delta(x^+)\delta(x_\perp)\int\frac{dk_\perp}{2\pi}e^{-\frac{i}{2}k_+x_-}\left\langle\overline{B}_v\right|\mathrm{T}[\overline{h}_vY](x)[Y^\dagger h_v](0)\left|\overline{B}_v\right\rangle J_P(k^+)\\ &= \frac{1}{2}\int dk^+J_P(k^+)\int\frac{dx^-}{4\pi}e^{-\frac{i}{2}(2E_\gamma-m_b+k^+)x^-}\left\langle\overline{B}_v\right|\mathrm{T}[\overline{h}_vY]\left(\frac{n}{2}x^-\right)[Y^\dagger h_v](0)\left|\overline{B}_v\right\rangle. \end{aligned}\tag{12.21}$$

Focusing on the heavy fields, we may then define

$$\begin{aligned}S(k^+) &\equiv \frac{1}{2}\int\frac{dx^-}{4\pi}e^{-\frac{i}{2}l^+x^-}\left\langle\overline{B}_v\right|\mathrm{T}[\overline{h}_vY](\frac{n}{2}x^-)[Y^\dagger h_v](0)\left|\overline{B}_v\right\rangle &(12.22)\\ &= \frac{1}{2}\int\frac{dx^-}{4\pi}e^{-\frac{i}{2}l^+x^-}\left\langle\overline{B}_v\right|\mathrm{T}e^{x^-\frac{n}{2}\cdot\partial}[\overline{h}_vY](0)[Y^\dagger h_v](0)\left|\overline{B}_v\right\rangle\\ &= \frac{1}{2}\int\frac{dx^-}{4\pi}e^{-\frac{i}{2}l^+x^-}\left\langle\overline{B}_v\right|\mathrm{T}[\overline{h}_vY](0)e^{-x^-\frac{n}{2}\cdot\partial}[Y^\dagger h_v](0)\left|\overline{B}_v\right\rangle\\ &= \frac{1}{2}\int\frac{dx^-}{4\pi}e^{-\frac{i}{2}l^+x^-}\left\langle\overline{B}_v\right|\mathrm{T}\overline{h}_vYe^{\frac{ix^-}{2}n\cdot\partial}Y^\dagger h_v\left|\overline{B}_v\right\rangle\\ &= \frac{1}{2}\int\frac{dx^-}{4\pi}e^{-\frac{i}{2}l^+x^-}\left\langle\overline{B}_v\right|\mathrm{T}\overline{h}_ve^{i\frac{x^-}{2}(in\cdot D_{us})}h_v\left|\overline{B}_v\right\rangle\\ &= \frac{1}{2}\left\langle\overline{B}_v\right|\overline{h}_v\delta(in\cdot D_{us}-l^\dagger)h_v\left|\overline{B}_v\right\rangle. &(12.23)\end{aligned}$$

The Soft function $S(k^+)$ is non-perturbative and encodes information about the usoft dynamics of the B meson. (12.22) shows that we may interpret this result as giving the probability of finding a heavy quark b inside the $\overline{B}$ meson carrying a residual momentum of k^+. Defining $J(k^+) = -\frac{1}{\pi}\mathrm{Im}J_P(k^+)$ and using(12.12),(12.21), (12.22) in (12.2), we have the final result

$$\boxed{\frac{1}{\Gamma_0}\frac{d\Gamma}{dE_\gamma} = \underbrace{H(m_b,\mu)}_{p^2\sim m_b^2\text{ Hard}}\int_{2E_\gamma-m_b}^{\overline{\Lambda}}dl^+\ \underbrace{S(l^+)}_{p^2\sim\Lambda^2\text{ Usoft}}\ \underbrace{J(l^++m_b-2E_\gamma)}_{p^2\sim m_b\Lambda\text{ Collinear}}}\tag{12.24}$$

13 SCET II

13.1 Deriving $\mathrm{SCET_{II}}$ operators by using $\mathrm{SCET_I}$

We may construct SCET operators by another method using $\mathrm{SCET_I}$. The basis of the procedure comes from the fact that soft-modes in $\mathrm{SCET_{II}}$ and usoft modes in SCET $_I$ have the same momentum; it is only the collinear fields which have distinct momentuma. The exact procedure for obtaining $\mathrm{SCET_{II}}$ is

1. Match QCD onto $\mathrm{SCET_I}$
2. Redefine fields with the usoft wilson line Y_n so that usoft interactions are only present in currents

3. Match SCET$_{\rm I}$ onto SCET$_{II}$ by taking $Y_n \to S_n$.

As an example of the above procedure we may construct the SCET$_{\rm II}$ current postulate above.

1. Matching QCD onto SCET$_{\rm I}$

$$J = \overline{u}\Gamma^\mu b \;\to\; J_I = (\overline{\xi}_n W)\Gamma^\mu h_v \tag{13.1}$$

2. Redefining fields so that usoft interactions are only present in currents

$$J_I = (\overline{\xi}_n^{(0)} W^{(0)})\Gamma^\mu Y^\dagger h_v \tag{13.2}$$

3. Matching SCET$_{\rm I}$ onto SCET$_{II}$ by taking $Y_n \to S_n$.

$$J_{II} = (\overline{\xi}_n^{(0)} W^{(0)})\Gamma^\mu S^\dagger h_v \tag{13.3}$$

13.2 Rapidity Divergences [EMPTY]

14 SCET$_{\rm II}$ Applications

In this section we will apply SCET$_{\rm II}$ to various processes to illustrate the formalism. The examples we will treat include

- $\gamma^*\gamma \to \pi^0$
- $B \to D\pi$
- The Massive Gauge Boson Sudakov Form Factor
- p_T distribution in Higgs production
- Jet broadening

A distinguishing feature of these processes is whether they involve a new type of divergence that requires a renormalization procedure, known as rapidity divergences. The first two processes do not, while the last three do. We will discuss these divergences in detail for the massive gauge boson form factor, and then be very brief about the last two examples.

14.1 $\gamma^*\gamma \to \pi^0$ [Remove?]

14.2 $B \to D\pi$ [Needs Work]

(**ROUGH**) As another exclusive scattering process, we analyze $B \to D\pi$. We may use the SCET framework here because the hard scales $Q = \{m_b, m_c, E_\pi\} \gg \Lambda_{QCD}$. At the scale $\mu \sim m_b$ the QCD operators represented by the weak Hamiltonian are

$$H_W = \frac{4G_F}{\sqrt{2}} V_{ud}^\dagger V_{cb} [C_{\mathbf{0}}^F(\mu_0) O_{\mathbf{0}}(\mu_0) + C_{\mathbf{8}}^F(\mu_0) O_{\mathbf{8}}(\mu_0)] \tag{14.1}$$

where

$$O_{\mathbf{0}} = [\bar{c}\gamma^\mu P_L b][\bar{d}\gamma_\mu P_L u] \tag{14.2}$$
$$O_{\mathbf{8}} = [\bar{c}\gamma^\mu P_L T^a b][\bar{d}\gamma_\mu P_L T^a u]. \tag{14.3}$$

We want to factorize the matrix element $\langle D\pi|\, O_{\mathbf{0},\mathbf{8}}\, |B\rangle$. We can represent this factorization diagrammatically as (INSERT FIG) where there are no gluons between π quarks and B/D quarks. For this process we expect a $B \to D$ form factor (Isgur-Wise form factor) and a pion wavefunction/distribution. This factorization will be possible because the particles B and D have soft momentum scaling and π has collinear scalings. Specifically $p_c^2 \sim \Lambda^2$ and we therefore use SCET_{II} to describe this process.

First, matching the QCD Hamiltonian onto SCET we need the operators

$$Q_{\mathbf{0}}^{1,5} = [\bar{h}_{v'}^{(c)}\Gamma_h^{1,5} h_v^{(b)}]\,[\bar{\xi}_{n,p'}^{(d)} W\Gamma_l C_0(\overline{\mathcal{P}}_+) W^\dagger \xi_{n,p}^{(u)}] \tag{14.4}$$
$$Q_{\mathbf{8}}^{1,5} = [\bar{h}_{v'}^{(c)}\Gamma_h^{1,5} T^a h_v^{(b)}]\,[\bar{\xi}_{n,p'}^{(d)} W\Gamma_l C_8(\overline{\mathcal{P}}_+) T^a W^\dagger \xi_{n,p}^{(u)}] \tag{14.5}$$

where $\Gamma_h^1 = \frac{\not{v}}{2}$, $\Gamma_h^5 = \frac{\not{v}}{2}\gamma_5$ and $\Gamma_l = \frac{\not{\bar{n}}}{4}(1-\gamma_5)$. Note that the two operators $O_{\mathbf{0}}$ and $O_{\mathbf{8}}$ can both produce any of the $Q_{\mathbf{0},\mathbf{8}}^{1,5}$ operators. Now, implementing field redefinitions to factor usoft effects (remember we can start with SCET_{I} to derive SCET_{II} results) we have

$$\begin{aligned} \xi_{n,p} &= Y\xi_{n,p}^{(0)} \\ W &= YW^{(0)}Y^\dagger \end{aligned} \tag{14.6}$$

These redefinitions are easily implemented in $Q_{\mathbf{0}}^{1,5}$. They simply take

$$[\bar{\xi}_{n,p'}^{(d)} W\Gamma_l C_0(\overline{\mathcal{P}}_+) W^\dagger \xi_{n,p}^{(u)}] \to [\bar{\xi}_{n,p'}^{(d)(0)} W^{(0)}\Gamma_l C_0(\overline{\mathcal{P}}_+) W^{(0)\dagger} \xi_{n,p}^{(u)(0)}] \tag{14.7}$$

where we used the fact that Y commutes with the wilson coefficient $C_0(\overline{\mathcal{P}}_+)$. This argument cannot be applied to $Q_{\mathbf{8}}^{1,5}$ because Y, containing generators of its own, does not commute with T^a. However, by making use of the color identity

$$T^a \otimes Y^\dagger T^a Y = YT^aY^\dagger \otimes T^a \tag{14.8}$$

then we may move all usoft wilson lines into the usoft part of the operator yielding

$$Q_{\mathbf{8}}^{1,5} = [\bar{h}_{v'}^{(c)}\Gamma_h^{1,5} YT^aY^\dagger h_v^{(b)}]\,[\bar{\xi}_{n,p'}^{(d)} W\Gamma_l C_8(\overline{\mathcal{P}}_+) T^a W^\dagger \xi_{n,p}^{(u)}]. \tag{14.9}$$

Matching this SCET_{I} result onto SCET_{II} by the replacements $Y \to S$ and $\xi^{(0)} \to \xi$, $W^{(0)} \to W$, we have

$$Q_{\mathbf{0}}^{1,5} = [\bar{h}_{v'}^{(c)}\Gamma_h^{1,5} h_v^{(b)}]\,[\bar{\xi}_{n,p'}^{(d)} W\Gamma_l C_0(\overline{\mathcal{P}}_+) W^\dagger \xi_{n,p}^{(u)}] \tag{14.10}$$
$$Q_{\mathbf{8}}^{1,5} = [\bar{h}_{v'}^{(c)}\Gamma_h^{1,5} YT^aY^\dagger h_v^{(b)}]\,[\bar{\xi}_{n,p'}^{(d)} W\Gamma_l C_8(\overline{\mathcal{P}}_+) T^a W^\dagger \xi_{n,p}^{(u)}]. \tag{14.11}$$

Now, taking the matrix elements between the appropriate hadronic states we have

$$\left\langle \pi_n^- \right|\bar{\xi}_n W\Gamma C_0(\overline{\mathcal{P}}_+) W^\dagger \xi_n \left|0\right\rangle = \frac{i}{2} f_\pi E_\pi \int_0^1 dx C(2E_\pi(2x-1))\phi_\pi(x) \tag{14.12}$$
$$\left\langle D_{v'}\pi_n^- \right|\bar{h}_{v'}\Gamma h_v \left|B\right\rangle = N'\xi(\omega_0,\mu). \tag{14.13}$$

We are able to achieve this factorization because with B, D purely soft and π purely collinear there are no contractions between soft and collinear fields. So we find that our final factorization result is

$$\langle \pi D | \, H_W \, | B \rangle = iN\xi(\omega_0, \mu) \int_0^1 C(2E_\pi(2x-1), \mu)\phi_\pi(x, \mu) + O(\Lambda/Q) \tag{14.14}$$

where $\xi(\omega_0, \mu)$ is the Isgur-Wise function at maximum recoil and

$$\omega_0 = \frac{m_B^2 - m_D^2}{2m_B} \tag{14.15}$$

This result also applies to other B decays such as

$$\begin{array}{llll} \overline{B}^0 \to D^+\pi^-, & \overline{B}^0 \to D^{*+}\pi^-, & \overline{B}^0 \to D^+\rho^- \\ \overline{B}^- \to D^0\pi^-, & B^- \to D^{*0}\pi^-, & \overline{B}^0 \to D^+\rho^- \end{array}$$

14.3 Massive Gauge Boson Form Factor & Rapidity Divergences [Empty]

14.4 p_T Distribution for Higgs Production & Jet Broadening [Remove]

A $\mathcal{L}_{\rm SCET}$ and SCET Feynman rules

A.1 Summary of Notation for Derivatives

Various types of SCET derivatives and covariant derivatives were used in the text. We summarize them all here for easy reference:

$$
\begin{aligned}
iD_n^\mu &\equiv i\partial_n^\mu + gA_n^\mu\,, & i\partial_n^\mu &\equiv \frac{\bar n^\mu}{2} in\cdot\partial + \frac{n^\mu}{2}\overline{\mathcal{P}} + \mathcal{P}_\perp^\mu\,, \\
iD_{us}^\mu &\equiv i\partial^\mu + gA_{us}^\mu\,, & & \\
iD_{ns}^\mu &\equiv iD_n^\mu + \frac{\bar n^\mu}{2} gn\cdot A_{us}\,, & i\partial_{ns}^\mu &\equiv i\partial_n^\mu + \frac{\bar n^\mu}{2} gn\cdot A_{us}\,. \\
i\mathcal{D}_{n\perp}^\mu &= W_n^\dagger iD_{n\perp}^\mu W_n = \mathcal{P}_{n\perp}^\mu + g\mathcal{B}_{n\perp}^\mu\,, & & \\
i\mathcal{D}_{ns}^\mu &= W_n^\dagger iD_{ns}^\mu W_n\,. & &
\end{aligned}
\tag{A.1}
$$

In addition we have the combinations that are invariant under type-0 RPI and collinear gauge covariant

$$
iD_\perp^\mu \equiv iD_{n\perp}^\mu + W_n iD_{us\perp}^\mu W_n^\dagger\,, \qquad i\bar n\cdot D \equiv i\bar n\cdot D_n + W_n i\bar n\cdot D_{us} W_n^\dagger\,, \tag{A.2}
$$

as well as those that are invariant under type-0 RPI and collinear gauge invariant

$$
W_n^\dagger iD_\perp^\mu W_n = i\mathcal{D}_{n\perp}^\mu + iD_{us\perp}^\mu\,, \qquad W_n^\dagger i\bar n\cdot D W_n = \overline{\mathcal{P}} + i\bar n\cdot D_{us}\,. \tag{A.3}
$$

The terms in Eq. (A.3) act only on collinear objects that do not transform under a local collinear gauge transformation.

A.2 Massless and Massive SCET at Leading Power

With a sum over distinct collinear sectors the leading order SCET Lagrangian is

$$
\mathcal{L}^{(0)} = \mathcal{L}_{\rm us}^{(0)} + \sum_n \Big(\mathcal{L}_{n\xi}^{(0)} + \mathcal{L}_{ng}^{(0)}\Big)\,. \tag{A.4}
$$

Here $\mathcal{L}_{\rm soft}^{(0)}$ is simply the Yang-Mills Lagrangian with usoft fermion fields ψ_s and soft gluon fields A_s^μ. The leading power Lagrangians for collinear quarks and gluons are [2, 6]

$$
\begin{aligned}
\mathcal{L}_{n\xi}^{(0)} &= \bar\xi_n\Big(in\cdot D_{ns} + i\not{D}_{n\perp}\frac{1}{i\bar n\cdot D_n} i\not{D}_{n\perp}\Big)\frac{\not{\bar n}}{2}\xi_n\,, \\
\mathcal{L}_{ng}^{(0)} &= \frac{1}{2g^2}\mathrm{Tr}\Big\{([iD_{ns}^\mu, iD_{ns}^\nu])^2\Big\} + \tau\,\mathrm{Tr}\Big\{([i\partial_{ns}^\mu, A_{n\,\mu}])^2\Big\} + 2\,\mathrm{Tr}\Big\{\bar c_n[i\partial_{ns\mu}, [iD_{ns}^\mu, c_n]]\Big\}\,.
\end{aligned}
\tag{A.5}
$$

where we used a general covariant gauge for the collinear gluons with gauge fixing parameter τ. The gauge fixing terms are gauge invariant with respect to the ultrasoft field which acts like a background field. An independent gauge fixing term is specified for the ultrasoft gluons in the gluon action in $\mathcal{L}_{\rm us}^{(0)}$.

The Feynman rules that follow from the leading order collinear quark Lagrangian are shown in Fig. 15. Each collinear line carries momenta (p, p_r) with label momenta $p^\mu = \bar n\cdot p\, n^\mu/2 + p_\perp^\mu$ and residual momentum p_r^μ. Only one momentum p or p' is indicated for lines where the Feynman rule depends only on the label momentum. The Feynman rules between collinear gluons and ultrasoft gluons are shown in Fig. 16.

If we add a mass the leading power collinear quark Lagrangian becomes

$$
\mathcal{L}_{n\xi}^{(0)} = \bar\xi_n\left[in\cdot D_{ns} + (i\not{D}_{n\perp} - m)\frac{1}{i\bar n\cdot D_n}(i\not{D}_{n\perp} + m)\right]\frac{\not{\bar n}}{2}\xi_n\,, \tag{A.6}
$$

and the modified Feynman rules are shown in Fig. 17.

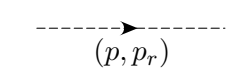

$$= \; i\,\frac{\not{\bar n}}{2}\,\frac{\bar n\cdot p}{n\cdot p_r\,\bar n\cdot p + p_\perp^2 + i0}$$

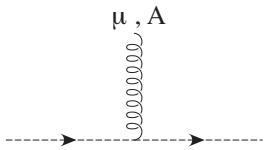

$$= ig\,T^A\,n_\mu\,\frac{\not{\bar n}}{2}$$

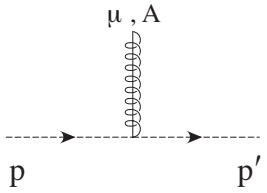

$$= ig\,T^A\left[n_\mu + \frac{\gamma_\mu^\perp \not{p}_\perp}{\bar n\cdot p} + \frac{\not{p}'_\perp \gamma_\mu^\perp}{\bar n\cdot p'} - \frac{\not{p}'_\perp \not{p}_\perp}{\bar n\cdot p\,\bar n\cdot p'}\bar n_\mu\right]\frac{\not{\bar n}}{2}$$

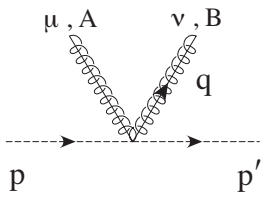

$$= \frac{ig^2\,T^A\,T^B}{\bar n\cdot(p-q)}\left[\gamma_\mu^\perp\gamma_\nu^\perp - \frac{\gamma_\mu^\perp \not{p}_\perp}{\bar n\cdot p}\bar n_\nu - \frac{\not{p}'_\perp\gamma_\nu^\perp}{\bar n\cdot p'}\bar n_\mu + \frac{\not{p}'_\perp\not{p}_\perp}{\bar n\cdot p\,\bar n\cdot p'}\bar n_\mu\bar n_\nu\right]\frac{\not{\bar n}}{2}$$

$$+ \frac{ig^2\,T^B\,T^A}{\bar n\cdot(q+p')}\left[\gamma_\nu^\perp\gamma_\mu^\perp - \frac{\gamma_\nu^\perp \not{p}_\perp}{\bar n\cdot p}\bar n_\mu - \frac{\not{p}'_\perp\gamma_\mu^\perp}{\bar n\cdot p'}\bar n_\nu + \frac{\not{p}'_\perp\not{p}_\perp}{\bar n\cdot p\,\bar n\cdot p'}\bar n_\mu\bar n_\nu\right]\frac{\not{\bar n}}{2}$$

Figure 15: Order λ^0 Feynman rules: collinear quark propagator with label p and residual momentum p_r, and collinear quark interactions with one soft gluon, one collinear gluon, and two collinear gluons respectively.

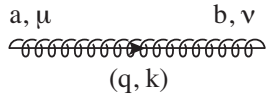

$$= \frac{-i}{\bar{n}\cdot q\, n\cdot k + q_\perp^2 + i0}\left(g_{\mu\nu} - (1-\tau)\frac{q_\mu q_\nu}{\bar{n}\cdot q\, n\cdot k + q_\perp^2}\right)\delta_{a,b}$$

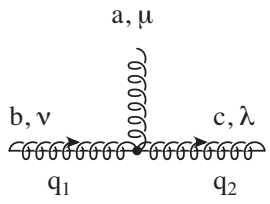

$$= g f^{abc} n_\mu \left\{\bar{n}\cdot q_1\, g_{\nu\lambda} - \tfrac{1}{2}(1-\tfrac{1}{\tau})[\bar{n}_\lambda q_{1\nu} + \bar{n}_\nu q_{2\lambda}]\right\}$$

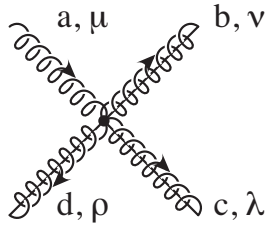

$$= -\tfrac{1}{2} i g^2 n_\mu \Big\{ f^{abe} f^{cde}(\bar{n}_\lambda g_{\nu\rho} - \bar{n}_\rho g_{\nu\lambda}) + f^{ade} f^{bce}(\bar{n}_\nu g_{\lambda\rho} - \bar{n}_\lambda g_{\nu\rho}) + f^{ace} f^{bde}(\bar{n}_\nu g_{\lambda\rho} - \bar{n}_\rho g_{\nu\lambda}) \Big\}$$

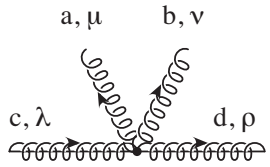

$$= \tfrac{1}{4} i g^2 n_\mu n_\nu \bar{n}_\rho \bar{n}_\lambda (1-\tfrac{1}{\alpha}) \left\{ f^{ace} f^{bde} + f^{ade} f^{bce} \right\}$$

Figure 16: Collinear gluon propagator with label momentum q and residual momentum k, and the order λ^0 interactions of collinear gluons with the usoft gluon field. Here usoft gluons are springs, collinear gluons are springs with a line, and τ is the covariant gauge fixing parameter in Eq. (4.57).

A.3 Massless SCET at Subleading Power

In this subsection Lagrangians and Feynman rules are given at subleading power in $\mathrm{SCET_I}$. There are several contributions to the subleading $\mathrm{SCET_I}$ Lagrangian at $\mathcal{O}(\lambda)$ and $\mathcal{O}(\lambda^2)$ [17, 7, 18],

$$\mathcal{L}^{(1)} = \sum_n \left(\mathcal{L}^{(1)}_{n\xi} + \mathcal{L}^{(1)}_{ng} + \mathcal{L}^{(1)}_{\xi_n q} + \mathcal{L}^{(1)}_{gf}\right), \tag{A.7}$$
$$\mathcal{L}^{(2)} = \sum_n \left(\mathcal{L}^{(2)}_{n\xi} + \mathcal{L}^{(2)}_{ng} + \mathcal{L}^{(2)}_{\xi_n q} + \mathcal{L}^{(2)}_{gf}\right).$$

For the $\mathcal{O}(\lambda)$ subleading Lagrangians we have

$$\mathcal{L}^{(1)}_{\xi_n \psi_{us}} = \bar{\chi}_n \frac{1}{\bar{n}\cdot\mathcal{P}} g \not{\mathcal{B}}_{n\perp} \psi_s + \text{h.c.}, \tag{A.8}$$
$$\mathcal{L}^{(1)}_{n\xi} = \bar{\chi}_n \Big(i\not{D}_{s\perp} \frac{1}{\bar{n}\cdot\mathcal{P}} i\not{\mathcal{D}}_{n\perp} + i\not{\mathcal{D}}_{n\perp} \frac{1}{\bar{n}\cdot\mathcal{P}} i\not{D}_{s\perp} \Big) \frac{\not{\bar{n}}}{2} \chi_n \,,$$
$$\mathcal{L}^{(1)}_{ng} = \frac{2}{g^2} \mathrm{Tr}\Big(\big[i\mathcal{D}^\mu_{ns}, i\mathcal{D}^\nu_{n\perp} \big] \big[i\mathcal{D}_{ns\mu}, iD_{s\perp\nu} \big] \Big) \,,$$
$$\mathcal{L}^{(1)}_{gf} = 2\tau\, \mathrm{Tr}\Big(\big[iD^\mu_{s\perp}, A_{n\perp\mu} \big] \big[i\partial^\nu_{ns}, A_{n\nu} \big] \Big) + 2\,\mathrm{Tr}\Big(\bar{c}_n \big[iD^\mu_{s\perp}, \big[iD^\perp_{n\mu}, c_n \big] \big] \Big) + 2\,\mathrm{Tr}\Big(\bar{c}_n \big[\mathcal{P}^\mu_\perp, \big[W_n i D^\perp_{s\mu} W_n^\dagger, c_n \big] \big] \Big) \,.$$

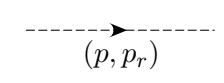

$$= \; i\,\frac{\bar{n}\!\!\!/}{2}\,\frac{\bar{n}\cdot p}{n\cdot p_r\,\bar{n}\cdot p + p_\perp^2 - m^2 + i\epsilon}$$

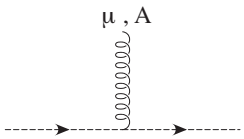

$$= ig\,T^A\,n\!\!\!/_\mu\,\frac{\bar{n}\!\!\!/}{2}$$

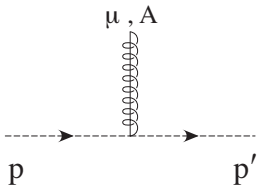

$$= ig\,T^A\left[n\!\!\!/_\mu + \frac{\gamma_\mu^\perp(p\!\!\!/_\perp + m)}{\bar{n}\cdot p} + \frac{(p\!\!\!/'_\perp - m)\gamma_\mu^\perp}{\bar{n}\cdot p'} - \frac{(p\!\!\!/'_\perp - m)(p\!\!\!/_\perp + m)}{\bar{n}\cdot p\,\bar{n}\cdot p'}\bar{n}\!\!\!/_\mu\right]\frac{\bar{n}\!\!\!/}{2}$$

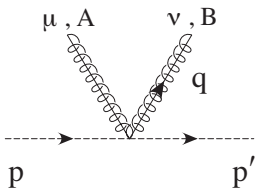

$$= \frac{ig^2\,T^A\,T^B}{\bar{n}\cdot(p-q)}\left[\gamma_\mu^\perp\gamma_\nu^\perp - \frac{\gamma_\mu^\perp(p\!\!\!/_\perp + m)}{\bar{n}\cdot p}\bar{n}\!\!\!/_\nu - \frac{(p\!\!\!/'_\perp - m)\gamma_\nu^\perp}{\bar{n}\cdot p'}\bar{n}\!\!\!/_\mu + \frac{(p\!\!\!/'_\perp - m)(p\!\!\!/_\perp + m)}{\bar{n}\cdot p\,\bar{n}\cdot p'}\bar{n}\!\!\!/_\mu\bar{n}\!\!\!/_\nu\right]\frac{\bar{n}\!\!\!/}{2}$$
$$+ \frac{ig^2\,T^B\,T^A}{\bar{n}\cdot(q+p')}\left[\gamma_\nu^\perp\gamma_\mu^\perp - \frac{\gamma_\nu^\perp(p\!\!\!/_\perp + m)}{\bar{n}\cdot p}\bar{n}\!\!\!/_\mu - \frac{(p\!\!\!/'_\perp - m)\gamma_\mu^\perp}{\bar{n}\cdot p'}\bar{n}\!\!\!/_\nu + \frac{(p\!\!\!/'_\perp - m)(p\!\!\!/_\perp + m)}{\bar{n}\cdot p\,\bar{n}\cdot p'}\bar{n}\!\!\!/_\mu\bar{n}\!\!\!/_\nu\right]\frac{\bar{n}\!\!\!/}{2}$$

Figure 17: Order λ^0 Feynman rules as in Fig. 15, but with a collinear quark mass.

For the $\mathcal{O}(\lambda^2)$ subleading Lagrangians we have

$$\begin{aligned}
\mathcal{L}^{(2a)}_{\xi_n\psi_{us}} &= \bar{\chi}_n\frac{\bar{n}\!\!\!/}{2}\left[W_n^\dagger in\cdot D\,W_n\right]\psi_{us} + \text{h.c.}\,, \qquad \text{(A.9)}\\
\mathcal{L}^{(2b)}_{\xi_n\psi_{us}} &= \bar{\chi}_n\frac{\bar{n}\!\!\!/}{2}i\mathcal{D}\!\!\!/_{n\perp}\frac{1}{\bar{n}\cdot\mathcal{P}}\,ig\mathcal{B}\!\!\!/_{n\perp}\psi_{us} + \text{h.c.}\,,\\
\mathcal{L}^{(2)}_{n\xi} &= \bar{\chi}_n\left(iD\!\!\!/_{s\perp}\frac{1}{\bar{n}\cdot\mathcal{P}}iD\!\!\!/_{s\perp} - i\mathcal{D}\!\!\!/_{n\perp}\frac{i\bar{n}\cdot D_s}{(\bar{n}\cdot\mathcal{P})^2}i\mathcal{D}\!\!\!/_{n\perp}\right)\frac{\bar{n}\!\!\!/}{2}\chi_n\,,\\
\mathcal{L}^{(2)}_{ng} &= \frac{1}{g^2}\mathrm{Tr}\Big(\big[i\mathcal{D}^\mu_{ns}, iD_s^{\perp\nu}\big]\big[i\mathcal{D}_{ns\mu}, iD^\perp_{s\nu}\big]\Big) + \frac{1}{g^2}\mathrm{Tr}\Big(\big[iD^\mu_{s\perp}, iD^\nu_{s\perp}\big]\big[i\mathcal{D}^\perp_{n\mu}, i\mathcal{D}^\perp_{n\nu}\big]\Big)\\
&\quad + \frac{1}{g^2}\mathrm{Tr}\Big(\big[i\mathcal{D}^\mu_{ns}, in\cdot\mathcal{D}_{ns}\big]\big[i\mathcal{D}_{ns\mu}, i\bar{n}\cdot D_s\big]\Big) + \frac{1}{g^2}\mathrm{Tr}\Big(\big[iD^\mu_{s\perp}, i\mathcal{D}^\nu_{n\perp}\big]\big[i\mathcal{D}^\perp_{n\mu}, iD^\perp_{s\nu}\big]\Big)\\
\mathcal{L}^{(2)}_{gf} &= \tau\,\mathrm{Tr}\Big(\big[iD^\mu_{s\perp}, A_{n\perp\mu}\big]\big[iD^\nu_{s\perp}, A_{n\perp\nu}\big]\Big) + \tau\,\mathrm{Tr}\Big(\big[i\bar{n}\cdot D_s, n\cdot A_n\big]\big[i\partial^\mu_{ns}, A_{n\mu}\big]\Big)\\
&\quad + 2\,\mathrm{Tr}\Big(\bar{c}_n\big[iD^\mu_{s\perp}, \big[W_n iD^\perp_{s\mu}W_n^\dagger, c_n\big]\big]\Big) + \mathrm{Tr}\Big(\bar{c}_n\big[i\bar{n}\cdot D_s, \big[in\cdot D, c_n\big]\big]\Big)\\
&\quad + \mathrm{Tr}\Big(\bar{c}_n\big[\bar{n}\cdot\mathcal{P}, \big[W_n i\bar{n}\cdot D_s W_n^\dagger, c_n\big]\big]\Big)\,.
\end{aligned}$$

The RPI connections for the gauge fixing and ghost terms do not follow the same rules as other contributions since they are not collinear gauge invariant. Therefore in addition to the usual connections, in the results above we use RPI and ultrasoft gauge invariance to connect $i\partial^\mu_{n\perp} + iD^\mu_{s\perp}$ and $\bar{n}\cdot\mathcal{P} + i\bar{n}\cdot D_s$. Note that all of these Lagrangians are listed prior to making the BPS field redefinition. The subleading power gauge

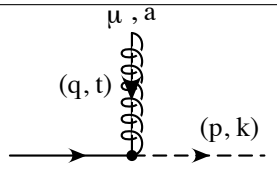

$$= \quad ig\,T^a\left[\gamma_\mu^\perp - \bar n_\mu\,\frac{\not q_\perp}{\bar n\cdot q}\right]$$

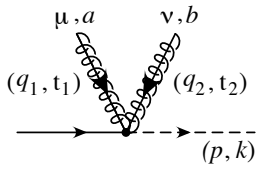

$$= \quad ig^2\,\frac{T^bT^a}{\bar n\cdot q_1}\left[\frac{\bar n_\mu \bar n_\nu\,\not p^\perp}{\bar n\cdot p} - \gamma_\nu^\perp\,\bar n_\mu\right] + ig^2\,\frac{T^aT^b}{\bar n\cdot q_2}\left[\frac{\bar n_\mu \bar n_\nu\,\not p^\perp}{\bar n\cdot p} - \gamma_\mu^\perp\,\bar n_\nu\right]$$

Figure 18: Feynman rules for the subleading usoft-collinear Lagrangian $\mathcal{L}_{\xi q}^{(1)}$ with one and two collinear gluons (springs with lines through them). The solid lines are usoft quarks while dashed lines are collinear quarks. For the collinear particles we show their (label,residual) momenta. (The fermion spinors are suppressed.)

fixing terms at subleading power were discussed in [19], but using a different organization of the subleading operators than what we use here.

All Feynman rules for $\mathcal{L}_{\xi q}^{(i)}$ involve at least one collinear gluon. From $\mathcal{L}_{\xi q}^{(1)}$ we obtain Feynman rules with zero or one $A_n^\perp$ gluons and any number of $\bar n\cdot A_n$ gluons. The one and two-gluon results are shown in Fig. 18. For $\mathcal{L}_{\xi q}^{(2a)}$ we have Feynman rules with zero or one $n\cdot A_n$ gluon and any number of $\bar n\cdot A_n$ gluons. The one and two-gluon results are shown in Fig. 19. Finally, for $\mathcal{L}_{\xi q}^{(2b)}$ one finds Feynman rules with zero, one, or two $A_n^\perp$ gluons and any number of $\bar n\cdot A_n$ gluons. In this case the one and two gluon Feynman rules are shown in Fig. 20.

For the Lagrangian $\mathcal{L}_{n\xi}^{(1,2)}$ all terms have two collinear quarks. There are terms with no gluons that yield kinematic corrections induced by the multipole expansion on soft momenta flowing through propagators. There are also terms with only usoft gluons. Finally there are are terms with one or more collinear gluons. A few of the lowest order Feynman rules are summarized in Figs. 21 and 22.

The Mixed Collinear 3-gluon vertex is:

$$\begin{aligned}
&= g\,f^{ABC}\Bigg[g_\perp^{\nu\rho}\Bigg\{\Big(1-\frac{1}{\alpha}\Big)p_n^\mu - \Big(1+\frac{1}{\alpha}\Big)\frac{\bar n^\mu}{2}n\cdot p_s - \frac{p_n^2\,\bar n^\mu}{\bar n\cdot p_n}\Bigg\} - 2g^{\mu\nu}p_{n\perp}^\rho \\
&\qquad + g_\perp^{\mu\rho}\Bigg\{\Big(1-\frac{1}{\alpha}\Big)p_n^\nu - \frac{p_n^2\,\bar n^\nu}{\bar n\cdot p_n}\Bigg\} + \Big(\bar n^\mu p_n^\nu + \bar n^\nu p_n^\mu + \frac{1}{2}\,\bar n^\mu \bar n^\nu n\cdot p_s\Big)\frac{p_{n\perp}^\rho}{\bar n\cdot p_n}\Bigg] \\
&\qquad \times \Big(g_{\rho\alpha}^\perp - \frac{n_\rho\,p_{s\alpha}^\perp}{n\cdot p_s}\Big)
\end{aligned} \tag{A.10}$$

A.4 Subleading Heavy-to-Light Currents

Here we give Feynman rules for the $\mathcal{O}(\lambda)$ heavy-to-light currents $J^{(1a)}$ and $J^{(1b)}$ in Eq. (**??**) which are valid in a frame where $v_\perp = 0$ and $v\cdot n = 1$.

For the subleading currents the zero and one gluon Feynman rules for $J^{(1a)}$ and $J^{(1b)}$ are shown in Figs. 23 and 24 respectively. (From the results in the previous sections the Feynman rules for the currents with $v_\perp \neq 0$ and $v\cdot n \neq 1$ can also be easily derived.) For $J^{(1a)}$ the Wilson coefficients depend only on the total λ^0 collinear momentum, while for $J^{(1a)}$ the coefficients depend on how the momentum is divided

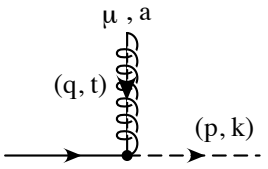

$$= \quad ig\,T^a\frac{\bar{n}\!\!\!/}{2}\Big(n_\mu - \frac{\bar{n}_\mu\, n\cdot t}{\bar{n}\cdot q}\Big)$$

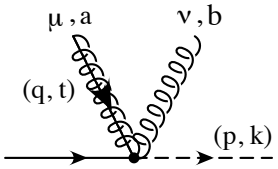

$$= \quad \frac{-g^2 f^{abc}T^c}{\bar{n}\cdot q}\,\frac{\bar{n}\!\!\!/}{2}\,\bar{n}_\mu n_\nu$$

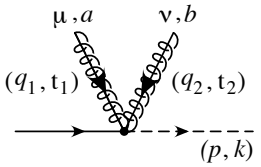

$$= \quad ig^2\,\frac{T^aT^b}{\bar{n}\cdot q_2}\Big[-n_\mu\bar{n}_\nu + \bar{n}_\mu\bar{n}_\nu\,\frac{n\cdot(t_1+t_2)}{\bar{n}\cdot p}\Big]\frac{\bar{n}\!\!\!/}{2}$$
$$+\,ig^2\,\frac{T^bT^a}{\bar{n}\cdot q_1}\Big[-n_\nu\bar{n}_\mu + \bar{n}_\mu\bar{n}_\nu\,\frac{n\cdot(t_1+t_2)}{\bar{n}\cdot p}\Big]\frac{\bar{n}\!\!\!/}{2}$$

Figure 19: Feynman rules for the $O(\lambda^2)$ usoft-collinear Lagrangian $\mathcal{L}^{(2a)}_{\xi q}$ with one and two gluons. The spring without a line through it is an usoft gluon. For the collinear particles we show their (label,residual) momenta, where label momenta are $p, q, q_i \sim \lambda^{0,1}$ and residual momenta are $k, t, t_i \sim \lambda^2$. Note that the result is after the field redefinition made in Ref. [**?**].

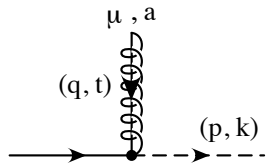

$$= \quad ig\,\frac{T^a}{\bar{n}\cdot q}\,\frac{\bar{n}\!\!\!/}{2}\Big[q\!\!\!/_\perp\gamma_\mu^\perp - \bar{n}_\mu\,\frac{q_\perp^2}{\bar{n}\cdot q}\Big]$$

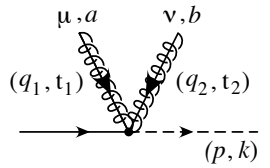

$$= \quad ig^2\,\frac{T^aT^b}{\bar{n}\cdot q_2}\,\frac{\bar{n}\!\!\!/}{2}\Big[\gamma_\mu^\perp\gamma_\nu^\perp - \frac{p\!\!\!/_\perp}{\bar{n}\cdot p}(\gamma_\mu^\perp\bar{n}_\nu + \gamma_\nu^\perp\bar{n}_\mu) - \frac{\gamma_\mu^\perp\,\bar{n}_\nu\,q\!\!\!/_{2\perp}}{\bar{n}\cdot q_2}$$
$$+\bar{n}_\mu\bar{n}_\nu\Big(\frac{p_\perp^2}{(\bar{n}\cdot p)^2} + \frac{p\!\!\!/_\perp\,q\!\!\!/_{2\perp}}{\bar{n}\cdot p\,\bar{n}\cdot q_2}\Big)\Big] + \big[(a,\mu,q_1,t_1)\leftrightarrow(b,\nu,q_2,t_2)\big]$$

Figure 20: Feynman rules for the $O(\lambda^2)$ usoft-collinear Lagrangian $\mathcal{L}^{(2b)}_{\xi q}$ with one and two gluons. For the collinear particles we show their (label,residual) momenta, where label momenta are $p, q, q_i \sim \lambda^{0,1}$ and residual momenta are $k, t, t_i \sim \lambda^2$.

between the quark and gluons. The $J^{(1a)}$ current has non-vanishing Feynman rules with zero or one $A_n^\perp$ gluon and any number of $\bar{n}\cdot A_n$ gluons. The possible gluons that appear in the $J^{(1b)}$ currents are similar, but the current vanishes unless it has one or more collinear gluons present.

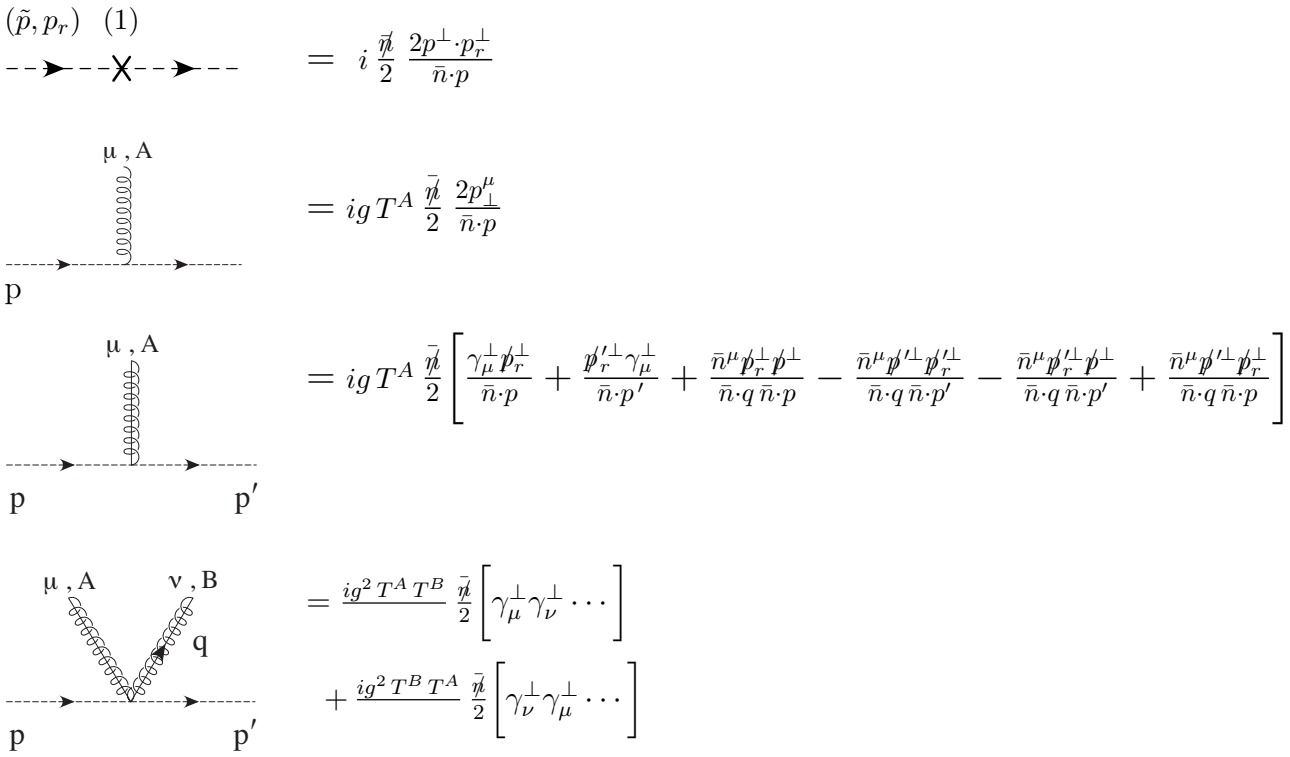

Figure 21: Order λ^1 Feynman rules with two collinear quarks from $\mathcal{L}_{\xi\xi}^{(1)}$.

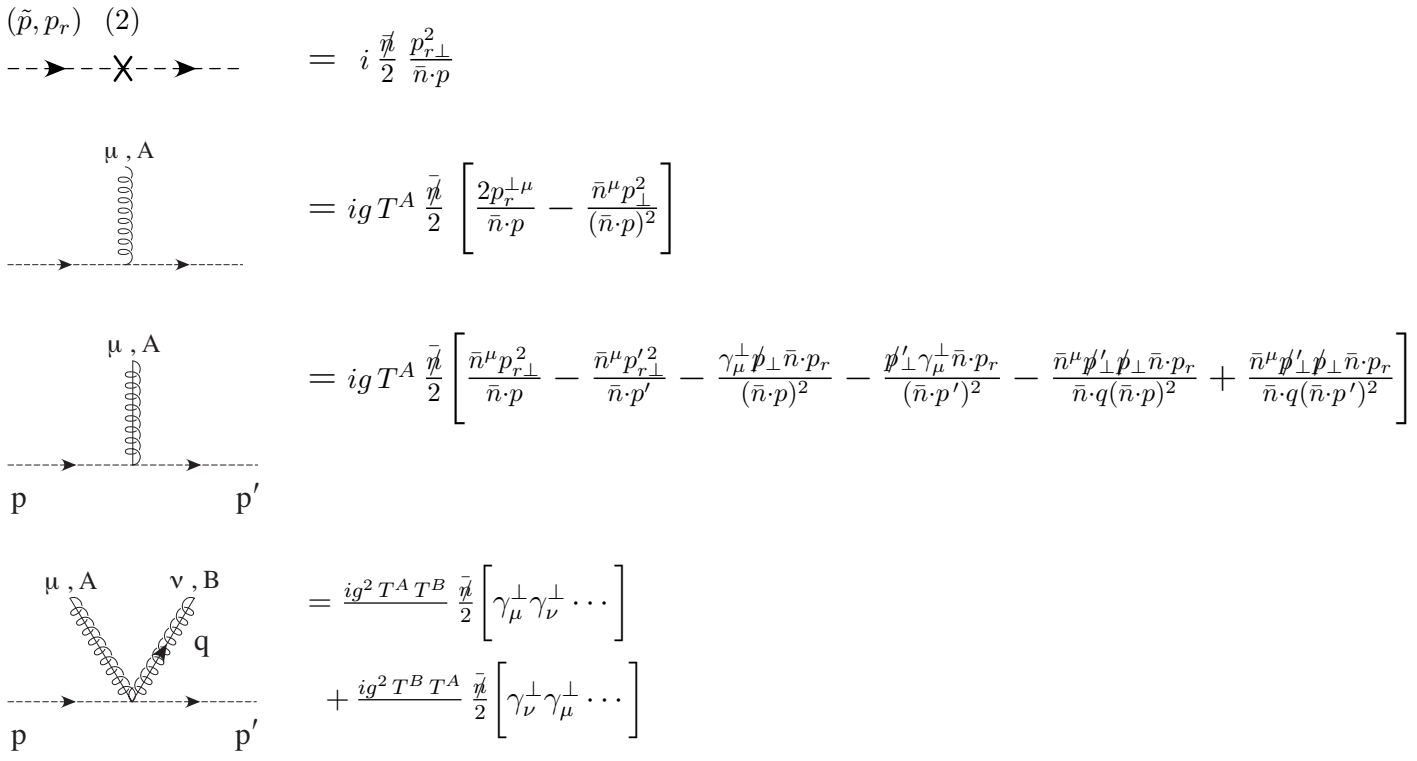

Figure 22: Order λ^2 Feynman rules with two collinear quarks from $\mathcal{L}^{(2)}_{\xi\xi}$.

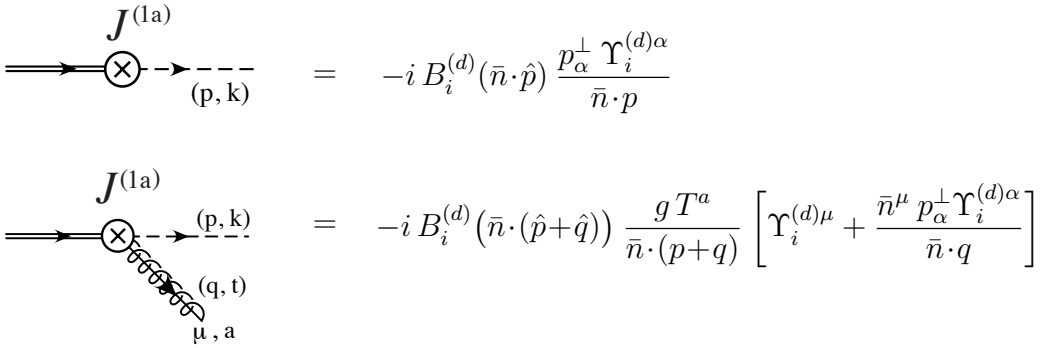

Figure 23: Feynman rules for the $O(\lambda)$ currents $J^{(1a)}$ in Eq. (**??**) with zero and one gluon (the fermion spinors are suppressed). For the collinear particles we show their (label,residual) momenta, where label momenta are $p, q \sim \lambda^{0,1}$ and residual momenta are $k, t \sim \lambda^2$. Momenta with a hat are normalized to m_b, $\hat{p} = p/m_b$ etc.

B Wilson line Identities and Feynman Rules

Some useful Wilson line identities include the connection between fundamental and adjoint lines

$$W_n^\dagger T^A W_n = \mathcal{W}_n^{AB} T^B\,, \qquad\qquad W_n T^A W_n^\dagger = T^B \mathcal{W}_n^{BA}\,, \tag{B.1}$$

where the unitary and orthogonal conditions for these lines are

$$W_n^\dagger W_n = W_n W_n^\dagger = \mathbb{1}\,, \qquad\qquad \mathcal{W}_n^{AC}\mathcal{W}_n^{BC} = \delta^{AB}\,.$$

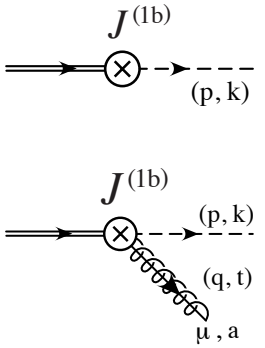

$$= \quad 0$$

$$= \quad i\, B_i^{(d)}\big(\bar n\cdot\hat p, \bar n\cdot\hat q\big)\,\frac{g\,T^a}{m_b}\left[\Theta_i^{(d)\mu} - \frac{\bar n^\mu\, q_\alpha^\perp \Theta_i^{(d)\alpha}}{\bar n\cdot q}\right]$$

Figure 24: Feynman rules for the $O(\lambda)$ currents $J^{(1b)}$ in Eq. (**??**) with zero and one gluon. For the collinear particles we show their (label,residual) momenta, where label momenta are $p, q, q_i \sim \lambda^{0,1}$ and residual momenta are $k, t \sim \lambda^2$. Momenta with a hat are normalized to m_b, $\hat p = p/m_b$ etc.

In momentum space for a gluon with incoming momentum k the Feynman rules can be read off from

$$W_n = 1 - \frac{g\,T^A\,\bar n\cdot A^A_{n,k}}{\bar n\cdot k} + \dots\,, \qquad W_n^\dagger = 1 + \frac{g\,T^A\,\bar n\cdot A^A_{n,k}}{\bar n\cdot k} + \dots\,, \tag{B.2}$$

$$\mathcal{W}_n^{AB} = \delta^{AB} + \frac{g\,if^{CAB}\,\bar n\cdot A^C_{n,k}}{\bar n\cdot k} + \dots\,, \qquad (\mathcal{W}_n^\dagger)^{AB} = \delta^{AB} - \frac{g\,if^{CAB}\,\bar n\cdot A^C_{n,k}}{\bar n\cdot k} + \dots\,,$$

by replacing the gluon field by the gluon-polarization vector ε_n^A. With the fundamental gluon building block in SCET

$$gB^\mu_{n\perp} = [W_n^\dagger i D^\mu_{n\perp} W_n] = \Big[\frac{1}{\overline{\mathcal{P}}} W_n^\dagger [i\bar n\cdot D_n, iD^\mu_{n\perp}] W_n\Big] = gB^{A\mu}_{n\perp}\,T^A\,, \tag{B.3}$$

$$gB^{A\mu}_{n\perp} = \Big[\frac{1}{\overline{\mathcal{P}}}\,\bar n_\nu i G_n^{B\nu\mu_\perp}\mathcal{W}_n^{BA}\Big]\,,$$

we have

$$W_n^\dagger i D^\mu_{n\perp} W_n = \mathcal{P}^\mu_{n\perp} + gB^\mu_{n\perp}\,. \tag{B.4}$$

For some applications it is also useful to define fields that are matrices in the color octet space which we denote with a tilde

$$\tilde B^{AB\mu}_{n\perp} = -if^{ABC} B^C_{n\perp} \tag{B.5}$$

C Mathematical Identities

C.1 Loop Integral Formula

C.1.1 Loop Integral Tricks

The following Feynman parameter tricks are useful when combining quadratic propagator denominators of loop integrals:

$$
\begin{aligned}
a^{-1}\,b^{-1} &= \int_0^1 dx\ \big[a+(b-a)x\big]^{-2}\,, \qquad\qquad (C.1)\\
a^{-m}\,b^{-n} &= \frac{\Gamma(n+m)}{\Gamma(n)\Gamma(m)}\int_0^1 dx\ \frac{x^{n-1}(1-x)^{m-1}}{[a+(b-a)x]^{n+m}}\,,\\
a^{-1}\,b^{-1}\,c^{-1} &= 2\int_0^1 dx\int_0^{1-x} dy\ \big[c+(a-c)x+(b-c)y\big]^{-3}\\
&= 2\int_0^1 dx\int_0^1 dy\ x\big[a+(c-a)x+(b-c)xy\big]^{-3}\,,\\
a_1^{-1}\cdots a_n^{-1} &= (n-1)!\int_0^1 dx_1\cdots dx_n\ \delta\Big(\sum x_i-1\Big)\ \Big(\sum x_i a_i\Big)^{-n}\,,\\
(a_1^{m_1}\cdots a_n^{m_n})^{-1} &= \frac{\Gamma(\sum m_i)}{\Gamma(m_1)\cdots\Gamma(m_n)}\int_0^1 dx_1\cdots dx_n\ \delta\Big(\sum x_i-1\Big)\ \Big(\sum x_i a_i\Big)^{-n}\prod x_i^{m_i-1}\,.
\end{aligned}
$$

To get the fourth line from the third we let $x'=1-x$ and $y'=y/x$. For integrals involving a propagator that is linear in the loop momentum, it is convenient to combine it using the Georgi parameter trick:

$$
\begin{aligned}
a^{-1}\,b^{-1} &= \int_0^\infty d\lambda\ \big[a+b\lambda\big]^{-2}\,, \qquad\qquad (C.2)\\
a^{-q}\,b^{-1} &= q\int_0^\infty d\lambda\ \big[a+b\lambda\big]^{-(q+1)} = 2q\int_0^\infty d\lambda\ \big[a+2b\lambda\big]^{-(q+1)}\,,\\
a^{-q}\,b^{-p} &= \frac{2^p\,\Gamma(p+q)}{\Gamma(p)\Gamma(q)}\int_0^\infty d\lambda\ \lambda^{p-1}\big[a+2b\lambda\big]^{-(p+q)}\,,\\
a^{-1}\,b^{-1}\,c^{-1} &= 2\int_0^\infty d\lambda\,d\lambda'\ \big[c+a\lambda'+b\lambda\big]^{-3} = 8\int_0^\infty d\lambda\,d\lambda'\ \big[c+2a\lambda'+2b\lambda\big]^{-3}\,.
\end{aligned}
$$

The Schwinger trick can also be useful, particularly for higher order loop integrals with many eikonal propagators:

$$
A^{-\nu} = \frac{(-1)^\nu}{\Gamma(\nu)}\int_0^\infty d\alpha\ \alpha^{\nu-1}\exp\big[\alpha A\big]\,. \qquad (C.3)
$$

Massive propagators can be expressed in terms of massless ones using the Melles-Barnes trick:

$$
(k^2-m^2)^{-\nu} = \frac{1}{2\pi i}\frac{1}{\Gamma(\nu)}\int_{-i\infty}^{i\infty} ds\ \frac{(-m^2)^s}{(k^2)^{\nu+s}}\Gamma(-s)\Gamma(\nu+s)\,. \qquad (C.4)
$$

Finally, for easy reference, we note the theta function identity:

$$
\theta(z) = \frac{1}{2\pi i}\int_{-\infty}^{+\infty} d\omega\ \frac{e^{iwz}}{w-i0} \qquad (C.5)
$$

C.1.2 Parameter Integrals

Useful parameter integrals include:

$$\int_0^1 dx\; x^{a-1}(1-x)^{b-1} = \frac{\Gamma(a)\Gamma(b)}{\Gamma(a+b)} \tag{C.6}$$

$$\int_0^1 \frac{dx}{ax+b} = \frac{1}{a}\ln\Big[\frac{a+b}{b}\Big] \neq \frac{1}{a}[\ln(a+b) - \ln b]$$

$$\int_0^1 dx \int_0^1 dy\; x^{c-1}(1-x)^{m-1}y^{b-1}(1-y)^{c-b-1}(1-xy)^{-a} = \frac{\Gamma(b)\Gamma(m)\Gamma(c-b)\Gamma(c+m-a-b)}{\Gamma(c+m-a)\Gamma(c+m-b)}$$

$$\int_0^\infty d\lambda\; (a\lambda+b)^{-p} = \frac{b^{1-p}}{a(p-1)}$$

$$\int_0^\infty d\lambda\; \frac{\lambda^p}{(\lambda^2+a\lambda)^q} = \int_0^\infty d\lambda\; \frac{\lambda^{p-q}}{(\lambda+a)^q} = \frac{a^{1+p-2q}\,\Gamma(1+p-q)\Gamma(-1-p+2q)}{\Gamma(q)}$$

Another useful integral for increasing the convergence:

$$\int d\lambda\,(\lambda^2+2b\lambda+a)^\alpha = \frac{(\lambda+b)(\lambda^2+2b\lambda+a)^\alpha}{1+2\alpha} + \frac{2\alpha(a-b^2)}{1+2\alpha}\int d\lambda\,(\lambda^2+2b\lambda+a)^{\alpha-1} \tag{C.7}$$

C.1.3 d-dimensional Integrals

The d-dimensional phase space can be decomposed as

$$d^n p = dp\, p^{n-1} d\Omega_n = dp\, p^{n-1} d(\cos\theta)\,(\sin\theta)^{n-3} d\Omega_{n-1}\,, \tag{C.8}$$

where $\int d\Omega_n = 2\pi^{n/2}/\Gamma(n/2)$. Including 2πs, if the integrand does not depend on some of the angular variables, then those integrals can be performed, which (progressively) gives

$$\bar{d}^n p = \frac{d^n p}{(2\pi)^n} = \frac{(2/\sqrt{\pi})}{(4\pi)^{n/2}\Gamma(\frac{n}{2}-\frac{1}{2})}\; dp\, p^{n-1} d(\cos\theta)\,(\sin\theta)^{n-3} = \frac{2}{(4\pi)^{n/2}\Gamma(\frac{n}{2})}\; dp\, p^{n-1}\,. \tag{C.9}$$

The basic Euclidean integral appearing at 1-loop is

$$\int \bar{d}^n q_e \frac{(q_e^2)^\alpha}{(q_e^2+A)^\beta} = \frac{1}{(4\pi)^{n/2}}\,\frac{\Gamma(n/2+\alpha)}{\Gamma(n/2)}\,\frac{\Gamma(\beta-\alpha-n/2)}{\Gamma(\beta)}\; A^{n/2+\alpha-\beta}\,, \tag{C.10}$$

and the Minkowski version is

$$\int \bar{d}^n q \frac{(q^2)^\alpha}{(q^2-A)^\beta} = \frac{i(-1)^{\alpha-\beta}}{(4\pi)^{n/2}}\,\frac{\Gamma(n/2+\alpha)}{\Gamma(n/2)}\,\frac{\Gamma(\beta-\alpha-n/2)}{\Gamma(\beta)}\; A^{n/2+\alpha-\beta}\,. \tag{C.11}$$

When we use the Schwinger trick we encounter the exponential integrals:

$$\int \bar{d}^n q\;\; \exp\big[Aq^2+2B\cdot q\big] = \frac{i}{(4\pi)^{d/2}}\, A^{-d/2} \exp\big[-B^2/A\big]\,, \tag{C.12}$$

$$\int \bar{d}^n q\; q^\mu \exp\big[Aq^2+2B\cdot q\big] = \frac{i}{(4\pi)^{d/2}}\Big(\frac{-B^\mu}{A}\Big) A^{-d/2} \exp\big[-B^2/A\big]\,,$$

$$\int \bar{d}^n q\; q^\mu q^\nu \exp\big[Aq^2+2B\cdot q\big] = \frac{i}{(4\pi)^{d/2}}\Big(\frac{B^\mu B^\nu}{A^2} - \frac{g^{\mu\nu}}{2A}\Big) A^{-d/2} \exp\big[-B^2/A\big]\,.$$

For massive propagators the euclidean Fourier transform is sometimes useful:

$$V(\vec{R},m) = \int \vec{d}^n k \, \frac{e^{i\vec{k}\cdot\vec{R}}}{\vec{k}^2+m^2} = \frac{2\pi^{-1/2}}{(4\pi)^{n/2}\Gamma\left(\frac{n-1}{2}\right)} \int_0^\infty dk \, \frac{k^{n-1}}{k^2+m^2} \int_{-1}^1 dx \, (1-x^2)^{\frac{n-3}{2}} e^{ikRx}$$
$$= \frac{1}{(2\pi)^{n/2}} m^{n/2-1} R^{1-n/2} K_{1-n/2}(mR). \tag{C.13}$$

where $K_\nu(x)$ is the modified Bessel function of the second kind. Note that $K_\nu(x) = K_{-\nu}(x)$. For $n = 3$, $V(\vec{R},m) = e^{-mR}/(4\pi R)$. Inverse transforms

$$\frac{1}{\vec{k}^2+m^2} = \int d^n R \, e^{-i\vec{k}\cdot\vec{R}} \, V(\vec{R},m)\,, \qquad \frac{1}{(\vec{k}^2+m^2)^\alpha} = \int d^n R \, e^{-i\vec{k}\cdot\vec{R}} \, V_\alpha(\vec{R},m)\,, \tag{C.14}$$

where the generalized transform for power α is

$$V_\alpha(\vec{R},m) = \frac{2^{1-\alpha}}{(2\pi)^{n/2}\Gamma(\alpha)} \Big(\frac{m}{R}\Big)^{n/2-\alpha} K_{n/2-\alpha}(mR). \tag{C.15}$$

C.2 One Loop SCET Integrals

C.3 Useful Function Identities

The fractional Γ identity is

$$\frac{\Gamma(\frac{x}{2})\Gamma(\frac{x+1}{2})}{\Gamma(x)} = 2^{1-x}\sqrt{\pi} \tag{C.16}$$

and conversion to trig is

$$\Gamma(x)\Gamma(1-x) = \frac{\pi}{\sin(\pi x)} \tag{C.17}$$

Polylog identities for any complex x are

$$\mathrm{Li}_2(x) = -\mathrm{Li}_2(1-x) + \frac{\pi^2}{6} - \ln(x)\ln(1-x)$$
$$\mathrm{Li}_2(x) = -\mathrm{Li}_2\Big(\frac{1}{x}\Big) - \frac{\pi^2}{6} - \frac{1}{2}\ln^2(-x) \tag{C.18}$$

Hypergeometric identites:

$${}_2F_1(a,b,c,z) = \frac{\Gamma(c)}{\Gamma(b)\Gamma(c-b)} \int_0^1 dt \, t^{b-1}(1-t)^{c-b-1}(1-tz)^{-a} \tag{C.19}$$
$${}_2F_1(a,b,c,1) = \frac{\Gamma(c)\Gamma(c-a-b)}{\Gamma(c-a)\Gamma(c-b)}$$

An identity for the incomplete Beta function:

$$\beta_z(a,b) = \int_0^z dt \, t^{a-1}(1-t)^{b-1} = \frac{z^a}{a} \, {}_2F_1(a,1-b,1+a,z) \tag{C.20}$$

Some logarithm identities

$$\ln(ab) = \ln a + \ln b + 2\pi i\big[\theta(-\Im a)\theta(-\Im b)\theta(\Im ab) - \theta(\Im a)\theta(\Im b)\theta(-\Im ab)\big]\,,$$
$$\ln(ab) = \ln a + \ln b \;\text{ if } \operatorname{sign}(\Im a) \neq \operatorname{sign}(\Im b) \text{ or } a > 0 \text{ is real}\,,$$
$$\ln\Big(\frac{z+i\lambda}{z-i\lambda}\Big) = \ln(z+i\lambda) - \ln(z-i\lambda)\,, \qquad \ln(z^2+\lambda^2) = \ln(z+i\lambda) + \ln(z-i\lambda)\,,$$
$$\arctan(w) = \frac{i}{2}\ln\Big(\frac{1-iw}{1+iw}\Big)\,, \qquad \operatorname{arctanh}(w) = \frac{1}{2}\ln\Big(\frac{1+w}{1-w}\Big) \tag{C.21}$$

C.4 Convolution identities

In calculations involving massless quarks and gluons, the +-function distribution frequently appears. Here we summarize identities for the +-function following Ref. [22]. We define a general plus distribution for some function $q(x)$, which is less singular than $1/x^2$ as $x \to 0$, as

$$\begin{aligned}\big[q(x)\big]_+^{[x_0]} &\equiv \big[\theta(x)q(x)\big]_+^{[x_0]} \\ &= \lim_{\epsilon\to 0}\frac{\mathrm{d}}{\mathrm{d}x}\big[\theta(x-\epsilon)\,Q(x,x_0)\big] \\ &= \lim_{\epsilon\to 0}\big[\theta(x-\epsilon)\,q(x) + \delta(x-\epsilon)\,Q(x,x_0)\big]\,,\end{aligned} \tag{C.22}$$

with

$$Q(x,x_0) = \int_{x_0}^{x}\mathrm{d}x'\,q(x')\,. \tag{C.23}$$

The point x_0 can be thought of as a boundary condition for the plus distribution since $Q(x_0,x_0) = 0$. Integrating the +-function against a test function $f(x)$, we have

$$\begin{aligned}&\int_{-\infty}^{x_{\max}}\mathrm{d}x\,[\theta(x)\,q(x)]_+^{[x_0]}\,f(x) \\ &\quad= \int_0^{x_{\max}}\mathrm{d}x\,q(x)\,[f(x)-f(0)] + f(0)\,Q(x_{\max},x_0)\,.\end{aligned} \tag{C.24}$$

Taking $f(x) = 1$ in Eq. (C.24) one sees that the integral of the plus distribution vanishes only when integrated over a range with $x_{\max} = x_0$,

$$\int_0^{x_0}\mathrm{d}x[\theta(x)\,q(x)]_+^{[x_0]} = 0\,. \tag{C.25}$$

Plus distributions with different boundary conditions are related to each other by

$$\big[\theta(x)\,q(x)\big]_+^{[x_0]} = \big[\theta(x)\,q(x)\big]_+^{[x_1]} + \delta(x)\,Q(x_1,x_0)\,. \tag{C.26}$$

Below and in the text we exclusively use the boundary condition $x_0 = 1$, and will always drop the superscript $[x_0]$ on the plus distributions when this default choice is used. The general discussion is included here because it is sometimes needed when comparing results in the literature.

A special case the often occurs is a power $q(x) = 1/x^{1-a}$ with $a > -1$, for which we define

$$\mathcal{L}^a(x) \equiv \left[\frac{\theta(x)}{x^{1-a}}\right]_+ = \lim_{\epsilon\to 0}\frac{\mathrm{d}}{\mathrm{d}x}\left[\theta(x-\epsilon)\,\frac{x^a-1}{a}\right]. \tag{C.27}$$

Here $\mathcal{L}^a(x)$ for $a = 0$ reduces to the standard definition of $[\theta(x)/x]_+$. Another common case is $q(x) = \ln^n x/x$ with integer $n \geq 0$, for which we define

$$\mathcal{L}_n(x) \equiv \left[\frac{\theta(x)\ln^n x}{x}\right]_+ = \lim_{\epsilon\to 0}\frac{\mathrm{d}}{\mathrm{d}x}\left[\theta(x-\epsilon)\,\frac{\ln^{n+1} x}{n+1}\right]. \tag{C.28}$$

Since both $\mathcal{L}^a(x)$ and $\mathcal{L}_n(x)$ have the same $x_0 = 1$ boundary condition, they are related by

$$\mathcal{L}_n(x) = \frac{\mathrm{d}^n}{\mathrm{d}a^n}\,\mathcal{L}^a(x)\bigg|_{a=0}. \tag{C.29}$$

Thus we can derive identities involving $\mathcal{L}_n(x)$ from identities involving $\mathcal{L}^a(x)$ by taking derivatives with respect to a. Finally, for the general case involving both powers and logarithms we define

$$\mathcal{L}^a_n(x) \equiv \left[\frac{\theta(x)\ln^n x}{x^{1-a}}\right]_+ = \frac{\mathrm{d}^n}{\mathrm{d}b^n}\,\mathcal{L}^{a+b}(x)\bigg|_{b=0}, \tag{C.30}$$

which satisfies $\mathcal{L}^0_n(x) \equiv \mathcal{L}_n(x)$ and $\mathcal{L}^a_0(x) \equiv \mathcal{L}^a(x)$. To provide continuity in various formulas it is also convenient to define

$$\mathcal{L}_{-1}(x) \equiv \mathcal{L}^a_{-1}(x) \equiv \delta(x)\,. \tag{C.31}$$

The following identities are also useful

$$\begin{aligned}
\mathcal{L}_{m+n}(x) &= \frac{\mathrm{d}^m}{\mathrm{d}a^m}\,\mathcal{L}^a_n(x)\bigg|_{a=0}, \qquad (C.32)\\
\mathcal{L}_{m+n+1}(x) &= (m+1)\frac{\mathrm{d}^m}{\mathrm{d}a^m}\,\frac{\mathcal{L}^a_n(x)-\mathcal{L}_n(x)}{a}\bigg|_{a=0},\\
\mathcal{L}^a_{m+1}(x) &= (m+1)\frac{\mathrm{d}^m}{\mathrm{d}b^m}\,\frac{\mathcal{L}^{a+b}(x)-\mathcal{L}^a(x)}{b}\bigg|_{b=0},\\
\frac{\mathrm{d}}{\mathrm{d}\ln x}\,x\mathcal{L}_n(x) &= n\;x\mathcal{L}_{n-1}(x)\,.
\end{aligned}$$

The $\mathcal{L}^a(x)$ satisfies the rescaling identity (for $\lambda > 0$)

$$\lambda\,\mathcal{L}^a(\lambda x) = \lim_{\epsilon\to 0}\frac{\mathrm{d}}{\mathrm{d}x}\left[\theta(x-\epsilon)\,\frac{(\lambda x)^a - 1}{a}\right] = \lambda^a\mathcal{L}^a(x) + \frac{\lambda^a - 1}{a}\,\delta(x)\,, \tag{C.33}$$

from which we can obtain the rescaling identity for $\mathcal{L}_n(x)$,

$$\lambda\,\mathcal{L}_n(\lambda x) = \frac{\mathrm{d}^n}{\mathrm{d}a^n}\lambda^a\mathcal{L}^a(x)\bigg|_{a=0} + \frac{\ln^{n+1}\lambda}{n+1}\,\delta(x) = \sum_{k=0}^{n}\binom{n}{k}\ln^k\lambda\,\mathcal{L}_{n-k}(x) + \frac{\ln^{n+1}\lambda}{n+1}\,\delta(x)\,. \tag{C.34}$$

We will also need convolutions of two plus distributions,

$$\begin{aligned}
\int \mathrm{d}y\,\mathcal{L}^a(x-y)\,\mathcal{L}^b(y) &= \lim_{\epsilon\to 0}\frac{\mathrm{d}}{\mathrm{d}x}\left\{\theta(x-\epsilon)\left[\frac{x^{a+b}}{a+b}V(a,b) + \frac{x^a-1}{a}\,\frac{x^b-1}{b}\right]\right\}\\
&= \Big(\mathcal{L}^{a+b}(x) + \frac{\delta(x)}{a+b}\Big)V(a,b) + \Big(\frac{1}{a}+\frac{1}{b}\Big)\mathcal{L}^{a+b}(x) - \frac{1}{b}\,\mathcal{L}^a(x) - \frac{1}{a}\,\mathcal{L}^b(x)\,. \qquad (C.35)
\end{aligned}$$

In the second step we used the definition in Eq. (C.27). Here $V(a,b)$ is defined by

$$V(a,b) = \frac{\Gamma(a)\,\Gamma(b)}{\Gamma(a+b)} - \frac{1}{a} - \frac{1}{b}\,, \tag{C.36}$$

which satisfies $V(0,0) = 0$. Taking derivatives with respect to a and b we can get the corresponding formulas for convolutions involving $\mathcal{L}_n$,

$$\begin{aligned}
\int \mathrm{d}y\, \mathcal{L}^a(x-y)\, \mathcal{L}_n(y) &= \frac{\mathrm{d}^n}{\mathrm{d}b^n}\left(\mathcal{L}^{a+b}(x) + \frac{\delta(x)}{a+b}\right) V(a,b)\bigg|_{b=0} + \frac{\mathcal{L}^a_{n+1}(x)}{n+1} + \frac{\mathcal{L}^a_n(x) - \mathcal{L}_n(x)}{a} \\
&\equiv \frac{1}{a}\sum_{k=-1}^{n+1} V_k^n(a)\, \mathcal{L}^a_k(x) \;-\; \frac{1}{a}\,\mathcal{L}_n(x)\,, \\
\int \mathrm{d}y\, \mathcal{L}_m(x-y)\, \mathcal{L}_n(y) &= \frac{\mathrm{d}^m}{\mathrm{d}a^m}\frac{\mathrm{d}^n}{\mathrm{d}b^n}\left(\mathcal{L}^{a+b}(x) + \frac{\delta(x)}{a+b}\right) V(a,b)\bigg|_{a=b=0} + \left(\frac{1}{m+1} + \frac{1}{n+1}\right)\mathcal{L}_{m+n+1}(x) \\
&\equiv \sum_{k=-1}^{m+n+1} V_k^{mn}\, \mathcal{L}_k(x)\,.
\end{aligned} \tag{C.37}$$

The coefficients $V_k^n(a)$ and V_k^{mn} are related to the Taylor series expansion of $V(a,b)$ around $a = 0$ and $a = b = 0$. The nonzero terms for $n \geq 0$ are

$$V_k^n(a) = \begin{cases} a\,\dfrac{\mathrm{d}^n}{\mathrm{d}b^n}\,\dfrac{V(a,b)}{a+b}\bigg|_{b=0}\,, & k = -1\,, \\ a\binom{n}{k}\dfrac{\mathrm{d}^{n-k}}{\mathrm{d}b^{n-k}}\,V(a,b)\bigg|_{b=0} + \delta_{kn}\,, & 0 \leq k \leq n\,, \\ \dfrac{a}{n+1}\,, & k = n+1\,. \end{cases} \tag{C.38}$$

The term δ_{kn} in $V_k^n(a)$ and the last coefficient $V_{n+1}^n(a)$ arise from the boundary terms in the convolution integral. The V_k^{mn} are symmetric in m and n, and the nonzero terms for $m, n \geq 0$ are

$$V_k^{mn} = \begin{cases} \dfrac{\mathrm{d}^m}{\mathrm{d}a^m}\,\dfrac{\mathrm{d}^n}{\mathrm{d}b^n}\,\dfrac{V(a,b)}{a+b}\bigg|_{a=b=0}\,, & k = -1\,, \\ \displaystyle\sum_{p=0}^{m}\sum_{q=0}^{n} \delta_{p+q,k}\binom{m}{p}\binom{n}{q}\frac{\mathrm{d}^{m-p}}{\mathrm{d}a^{m-p}}\,\frac{\mathrm{d}^{n-q}}{\mathrm{d}b^{n-q}}\,V(a,b)\bigg|_{a=b=0}\,, & 0 \leq k \leq m+n\,, \\ \dfrac{1}{m+1} + \dfrac{1}{n+1}\,, & k = m+n+1\,. \end{cases} \tag{C.39}$$

The last coefficient V_{m+n+1}^{mn} again contains the boundary term. Using Eq. (C.31) we can extend the results in Eq. (C.37) to include the cases $n = -1$ or $m = -1$. The relevant coefficients are

$$V_{-1}^{-1}(a) = 1\,, \qquad V_0^{-1}(a) = a\,, \qquad V_{k\geq 1}^{-1}(a) = 0\,, \qquad V_k^{-1,n} = V_k^{n,-1} = \delta_{nk}\,. \tag{C.40}$$

C.5 Laplace transform Identities

The main equation to calculate the Laplace transform of the generalized distributions introduced above is the relation

$$\left(\nu\mu^j\right)^{-\omega} = \frac{1}{\Gamma(\omega)}\int_0^\infty \mathrm{d}t\, e^{-\nu t}\left[\frac{1}{\mu^j}\mathcal{L}^\omega\left(\frac{t}{\mu^j}\right) + \frac{1}{\omega}\delta(t)\right] \tag{C.41}$$

where t is a variable of mass dimension j, while ν is a conjugate variable with mass dimension $-j$. Using the identities in Eq. (C.29) one can perform a Taylor series in ω of the right hand side of this equation to find

$$e^{\gamma_E \omega}\Gamma(\omega)(\tilde{\nu}\mu^j)^{-\omega} = \int_0^\infty \mathrm{d}t e^{-\nu t}\left[\frac{1}{\omega}\delta(t) + \sum_{k=0}^{\infty}\frac{\omega^k}{k!}\frac{1}{\mu^j}\mathcal{L}_k\Big(\frac{t}{\mu^j}\Big)\right] \tag{C.42}$$

where γ_E is Euler's constant and

$$\tilde{\nu} \equiv e^{\gamma_E}\nu \tag{C.43}$$

By also performing a Taylor series of the left hand side of this equation one can obtain the Laplace transform for any $\mathcal{L}_k$. The first few terms are

$$\begin{aligned}
\int_0^\infty \mathrm{d}t\, e^{-\nu t}\frac{1}{\mu^j}\,\mathcal{L}_{-1}\left(\frac{t}{\mu^j}\right) &= 1\,,\\
\int_0^\infty \mathrm{d}t\, e^{-\nu t}\frac{1}{\mu^j}\,\mathcal{L}_{0}\left(\frac{t}{\mu^j}\right) &= -\ln\left(\tilde{\nu}\mu^j\right)\,,\\
\int_0^\infty \mathrm{d}t\, e^{-\nu t}\frac{1}{\mu^j}\,\mathcal{L}_{1}\left(\frac{t}{\mu^j}\right) &= \frac{\log^2\left(\tilde{\nu}\mu^j\right)}{2} + \frac{\pi^2}{12}\,,\\
\int_0^\infty \mathrm{d}t\, e^{-\nu t}\frac{1}{\mu^j}\,\mathcal{L}_{2}\left(\frac{t}{\mu^j}\right) &= -\frac{\log^3\left(\tilde{\nu}\mu^j\right)}{3} - \frac{\pi^2}{6}\log\left(\tilde{\nu}\mu^j\right) - \frac{2\,\zeta_3}{3}\,,\\
\int_0^\infty \mathrm{d}t\, e^{-\nu t}\frac{1}{\mu^j}\,\mathcal{L}_{3}\left(\frac{t}{\mu^j}\right) &= \frac{\log^4\left(\tilde{\nu}\mu^j\right)}{4} + \frac{\pi^2\log^2\left(\tilde{\nu}\mu^j\right)}{4} + 2\,\zeta_3\log\left(\tilde{\nu}\mu^j\right) + \frac{3\pi^4}{80}\,.
\end{aligned} \tag{C.44}$$

One can also easily invert the Laplace transform. The relevant general identity is

$$\frac{1}{2\pi i}\int_{c-i\infty}^{c+i\infty}\mathrm{d}\nu\, e^{\nu t}\left(\nu\mu^j\right)^{-\omega} = \frac{1}{\Gamma(\omega)}\left[\frac{1}{\mu^j}\mathcal{L}^{\omega}\left(\frac{t}{\mu^j}\right) + \frac{1}{\omega}\delta(t)\right]\,, \tag{C.45}$$

where c is any constant that gives a convergent integral.

C.6 Plus functions from Imaginary parts

Sometimes it is convenient to calculate functions appearing in factorization theorems by taking the imaginary part of a forward scattering graph. An example is the inclusive hemisphere jet function. The following identities for a dimensionless variable x are useful for these calculations,

$$\mathrm{Im}\left[\frac{\ln^n(-x-i0)}{\pi(-x-i0)}\right] = \cos^2\Big(\frac{n\pi}{2}\Big)\frac{(-\pi^2)^{n/2}}{n+1}\delta(x) + \sum_{j=0}^{\left[\frac{n-1}{2}\right]}\frac{(-1)^j\, n!\,\pi^{2j}}{(2j+1)!(n-2j-1)!}\,\mathcal{L}_{n-2j-1}(x)\,, \tag{C.46}$$

where $[p]$ on the sum is the greatest integer not exceeding p, sometimes also called the Gauss bracket of p. For the first few orders this gives

$$\begin{aligned}
\frac{1}{\pi}\mathrm{Im}\left[\frac{1}{x+i0}\right] &= -\delta(x), & \frac{1}{\pi}\mathrm{Im}\left[\frac{\ln(-x-i0)}{x+i0}\right] &= -\mathcal{L}_0(x),\\
\frac{1}{\pi}\mathrm{Im}\left[\frac{1}{(x+i0)^2}\right] &= \delta'(x), & \frac{1}{\pi}\mathrm{Im}\left[\frac{\ln^2(-x-i0)}{x+i0}\right] &= \frac{\pi^2}{3}\delta(x) - 2\,\mathcal{L}_1(x).
\end{aligned} \tag{C.47}$$

D QCD Summary

D.1 Fields and Feynman Rules

The $SU(N_c)$ QCD Lagrangian without gauge fixing is

$$\mathcal{L} = \bar\psi(i\not{D} - m)\psi - \frac{1}{4}G^A_{\mu\nu}G^{\mu\nu A}\,, \qquad G^A_{\mu\nu} = \partial_\mu A^A_\nu - \partial_\nu A^A_\mu + g f^{ABC} A^B_\mu A^C_\nu \tag{D.1}$$
$$iD_\mu = i\partial_\mu + g A^A_\mu T^A\,, \qquad [iD_\mu, iD_\nu] = ig G^A_{\mu\nu} T^A\,.$$

Note our sign convention for g. The equations of motion and Bianchi identity are

$$(i\not{D} - m)\psi = 0\,, \qquad \partial^\mu G^A_{\mu\nu} = -g f^{ABC} A^{B\mu} G^C_{\mu\nu} - g\bar\psi\gamma_\nu T^A\psi\,, \qquad \epsilon^{\mu\nu\lambda\sigma}(D_\nu G_{\lambda\sigma})^A = 0. \tag{D.2}$$

Useful color identities include

$$[T^A, T^B] = i f^{ABC} T^C\,, \qquad \mathrm{Tr}\big[T^A T^B\big] = T_F\delta^{AB}\,, \qquad \bar T^A = -T^{A*} = -(T^A)^T\,,$$
$$T^A T^A = C_F \mathbf{1}\,, \qquad f^{ACD} f^{BCD} = C_A\delta^{AB}\,, \qquad f^{ABC} T^B T^C = \frac{i}{2} C_A T^A\,,$$
$$T^A T^B T^A = \Big(C_F - \frac{C_A}{2}\Big) T^B\,, \qquad d^{ABC} d^{ABC} = \frac{40}{3}\,, \qquad d^{ABC} d^{A'BC} = \frac{5}{3}\delta^{AA'}\,, \tag{D.3}$$

where $C_F = (N_c^2-1)/(2N_c)$, $C_A = N_c$, $T_F = 1/2$, and $C_F - C_A/2 = -1/(2N_c)$. The color reduction formula and Fierz formula are

$$T^A T^B = \frac{\delta^{AB}}{2N_c}\,\mathbf{1} + \frac{1}{2} d^{ABC} T^C + \frac{i}{2} f^{ABC} T^C\,, \qquad (T^A)_{ij}(T^A)_{k\ell} = \frac{1}{2}\,\delta_{i\ell}\delta_{kj} - \frac{1}{2N_c}\,\delta_{ij}\delta_{k\ell}\,. \tag{D.4}$$

The Feynman gauge Feynman rules for fermion, gluon, ghost propagators, and the Fermion-gluon vertex are

$$\frac{i(\not{p} + m)}{p^2 - m^2 + i0}\,, \qquad \frac{-ig^{\mu\nu}\delta^{AB}}{k^2 + i0}\,, \qquad \frac{i}{k^2 + i0}\,, \qquad +ig\gamma^\mu T^A\,. \tag{D.5}$$

The triple gluon and ghost Feynman rules in covariant gauge for $\{A^A_\mu(k), A^B_\nu(p), A^C_\rho(q)\}$ all with incoming momenta, and $\bar c^A(p) A^B_\mu c^C$ with outgoing momenta p are:

$$g f^{ABC}\big[g^{\mu\nu}(k-p)^\rho + g^{\nu\rho}(p-q)^\mu + g^{\rho\mu}(q-k)^\nu\big]\,, \qquad -g f^{ABC} p^\mu\,. \tag{D.6}$$

In a general covariant gauge we have the gauge fixing Lagrangian and gluon propagator

$$\mathcal{L}_{gf} = -\frac{(\partial_\mu A^\mu)^2}{2\xi}\,, \qquad D^{\mu\nu}(k) = \frac{-i}{k^2 + i0}\Big(g^{\mu\nu} - (1-\xi)\frac{k^\mu k^\nu}{k^2}\Big)\,, \tag{D.7}$$

where Feynman gauge is $\xi \to 1$ and Landau gauge is $\xi \to 0$. In background field covariant gauge $\mathcal{L}_{gf} = -(D^A_\mu Q^A_\mu)^2/(2\xi)$, where Q^A_μ is the quantum gauge field and A^A_μ in D^A_μ is a background gauge field. Here the triple gluon Feynman rule for $\{A^A_\mu(k), Q^B_\nu(p), Q^C_\rho(q)\}$ is:

$$g f^{ABC}\Big[g^{\mu\nu}\Big(k - p - \frac{q}{\xi}\Big)^\rho + g^{\nu\rho}(p-q)^\mu + g^{\rho\mu}\Big(q - k + \frac{p}{\xi}\Big)^\nu\Big]\,. \tag{D.8}$$

D.2 QCD β-Function

In $d = 4 - 2\epsilon$ dimensions the $\overline{\rm MS}$ coupling constant obeys

$$\mu \frac{d}{d\mu}\,\alpha_s(\mu) = -2\epsilon\,\alpha_s(\mu) + \beta(\alpha_s)\,, \tag{D.9}$$

where $\beta(\alpha_s)$ is the QCD β-function. Expanding it in powers of α_s we have

$$\beta(\alpha_s) = -2\alpha_s \sum_{n=0}^{\infty} \beta_n \Big(\frac{\alpha_s}{4\pi}\Big)^{n+1}\,, \tag{D.10}$$

where the coefficients to three loops are [**?**, 23]

$$\begin{aligned}
\beta_0 &= \frac{11}{3}\,C_A - \frac{4}{3}\,T_F\,n_f\,,\\
\beta_1 &= \frac{34}{3}\,C_A^2 - \Big(\frac{20}{3}\,C_A\, + 4C_F\Big)\,T_F\,n_f\,,\\
\beta_2 &= \frac{2857}{54}\,C_A^3 + \Big(C_F^2 - \frac{205}{18}\,C_F C_A - \frac{1415}{54}\,C_A^2\Big)\,2T_F\,n_f + \Big(\frac{11}{9}\,C_F + \frac{79}{54}\,C_A\Big)\,4T_F^2\,n_f^2\,.
\end{aligned} \tag{D.11}$$

Here β_2 depends on our choice of the $\overline{\rm MS}$ scheme, while $\beta_{0,1}$ are scheme independent within massless renormalization schemes. The term involving ϵ in Eq. (D.9) is needed when deriving anomalous dimensions, but we can take $\epsilon \to 0$ when defining the physical coupling constant and solving this equation for the running coupling. At leading logarithmic order we keep only the β_0 term and have the solution

$$\alpha_s(\mu) = \frac{\alpha_s(\mu_0)}{1 + \frac{\beta_0}{2\pi}\alpha_s(\mu_0)\ln\frac{\mu}{\mu_0}} = \frac{2\pi}{\beta_0 \ln\frac{\mu}{\Lambda_{\rm QCD}}}\,, \qquad\qquad \frac{1}{\alpha_s(\mu)} = \frac{1}{\alpha_s(\mu_0)} + \frac{\beta_0}{2\pi}\ln\frac{\mu}{\mu_0}\,. \tag{D.12}$$

In the first case we write the boundary condition in terms of the QCD scale parameter $\Lambda_{\rm QCD}$ (defined at this order), while in the second case we use the coupling specified at a fixed reference scale μ_0 as the boundary condition. Extending the solution to three-loops gives

$$\frac{1}{\alpha_s(\mu)} = \frac{X}{\alpha_s(\mu_0)} + \frac{\beta_1}{4\pi\beta_0}\ln X + \frac{\alpha_s(\mu_0)}{16\pi^2}\left[\frac{\beta_2}{\beta_0}\Big(1 - \frac{1}{X}\Big) + \frac{\beta_1^2}{\beta_0^2}\Big(\frac{\ln X}{X} + \frac{1}{X} - 1\Big)\right], \tag{D.13}$$

where $X \equiv 1 + \alpha_s(\mu_0)\beta_0\ln(\mu/\mu_0)/(2\pi)$. Using the analytic solution in Eq. (D.13) gives results that agree very well with numerically integrating Eq. (D.9) at 3-loops with $\epsilon = 0$.

D.3 QCD Cusp Anomalous Dimensions

Operators that involve Wilson lines that meet at an angle, where at least one line involves a light-like direction vector, will have renormalization group equations that involve the universal cusp anomalous dimension $\Gamma_{\rm cusp}$. Taking $i = q, g$ for fundamental quark induced lines or adjoint gluon induced lines respectively, we can expand the cusp anomalous dimension in powers of α_s as

$$\Gamma^i_{\rm cusp}(\alpha_s) = \sum_{n=0}^{\infty} \Gamma^i_n \Big(\frac{\alpha_s}{4\pi}\Big)^{n+1}\,. \tag{D.14}$$

Up to three loop order the cusp anomalous dimension has been proven to be universal and obey Casmir scaling, so that the difference between the quark and gluon cases is an overall color factor. The coefficients of the quark and gluon cusp anomalous dimensions in $\overline{\rm MS}$ are [**?**]

$$\begin{aligned}
\Gamma_0^q &= \frac{C_F}{C_A}\Gamma_g^0\,, \qquad \Gamma_0^g = 4C_A\,, \\
\Gamma_1^q &= \frac{C_F}{C_A}\Gamma_g^1\,, \qquad \Gamma_1^g = 4C_A\Big[\Big(\frac{67}{9}-\frac{\pi^2}{3}\Big)C_A - \frac{20}{9}T_F\,n_f\Big]\,, \\
\Gamma_2^q &= \frac{C_F}{C_A}\Gamma_g^2\,, \qquad \Gamma_2^g = 4C_A\Big[\Big(\frac{245}{6}-\frac{134\pi^2}{27}+\frac{11\pi^4}{45}+\frac{22\zeta_3}{3}\Big)C_A^2 + \Big(-\frac{418}{27}+\frac{40\pi^2}{27}-\frac{56\zeta_3}{3}\Big)C_A\,T_F\,n_f \\
&\qquad + \Big(-\frac{55}{3}+16\zeta_3\Big)C_F\,T_F\,n_f - \frac{16}{27}T_F^2\,n_f^2\Big]\,.
\end{aligned} \tag{D.15}$$

E General All-Orders Resummation Formula

E.1 Simple multiplicative RGE

In this section we give the generic solution for a simple multiplicative renormalization group equation of the form

$$\mu\frac{d}{d\mu}F(s,\mu) = \gamma_F(s,\mu)F(s,\mu)\,, \qquad \gamma_F(s,\mu) = \frac{\rho_F}{j}\,\Gamma_{\rm cusp}[\alpha_s]\,\ln\left(\frac{\mu^j}{s}\right) + \gamma_F[\alpha_s]\,. \tag{E.1}$$

Here s is a variable of mass dimension j, $\Gamma_{\rm cusp}$ is the cusp anomalous dimension given in Sec. D.3, and ρ_F is a constant that varies depends on the function F being considered.

Integrating Eq. (E.1) from μ_0 to μ by changing variables to α_s with $d\ln\mu = d\alpha_s/\beta[\alpha_s]$ gives the solution

$$\ln\left[\frac{F(s,\mu)}{F(s,\mu_0)}\right] = \omega_F(\mu,\mu_0)\,\ln\left(\frac{\mu_0^j}{s}\right) + K_F(\mu,\mu_0)\,, \tag{E.2}$$

where we define

$$\omega_F(\mu,\mu_0) = \frac{\rho_F}{j}\,\eta_\Gamma(\mu,\mu_0)\,, \qquad K_F(\mu,\mu_0) = K_{\gamma_F}(\mu,\mu_0) + \rho_F K_\Gamma(\mu,\mu_0)\,, \tag{E.3}$$

which are given in terms of

$$\begin{aligned}
\eta_\Gamma(\mu,\mu_0) &= \int_{\alpha_s(\mu_0)}^{\alpha_s(\mu)}\frac{d\alpha}{\beta[\alpha]}\,\Gamma_{\rm cusp}[\alpha]\,, \qquad K_{\gamma_F}(\mu,\mu_0) = \int_{\alpha_s(\mu_0)}^{\alpha_s(\mu)}\frac{d\alpha}{\beta[\alpha]}\,\gamma_F[\alpha]\,, \\
K_\Gamma(\mu,\mu_0) &= \int_{\alpha_s(\mu_0)}^{\alpha_s(\mu)}\frac{d\alpha}{\beta[\alpha]}\,\Gamma_{\rm cusp}[\alpha]\int_{\alpha_s(\mu_0)}^{\alpha}\frac{d\alpha'}{\beta[\alpha']}\,.
\end{aligned} \tag{E.4}$$

Thus, exponentiating Eq. (**??**), we can write the solution to the RGE in terms of the boundary condition $F(s,\mu_0)$ by

$$F(s,\mu) = \mathcal{U}_F(s,\mu,\mu_0)F(s,\mu_0)\,, \tag{E.5}$$

with the evolution kernel

$$\mathcal{U}_F(s,\mu,\mu_0) = e^{K_F(\mu,\mu_0)}\left(\frac{\mu_0^j}{s}\right)^{\omega_F(\mu,\mu_0)}\,. \tag{E.6}$$

This solution is correct to all orders in perturbation theory.

Taking the expansions for $\beta[\alpha_s]$ and $\Gamma_{\rm cusp}[\alpha_s]$ from Eqs. (D.10) and (D.14), and writing

$$\gamma_F[\alpha_s] = \sum_{n=0}^{\infty} \gamma_{Fn} \left(\frac{\alpha_s}{4\pi}\right)^{n+1}, \tag{E.7}$$

we can solve for $K_\Gamma(\mu,\mu_0)$, $\eta_\Gamma(\mu,\mu_0)$, and $K_\gamma(\mu,\mu_0)$ order by order in resumed perturbation theory in terms of the coefficients β_n, Γ_n, and γ_{Fn}. For simplicity we suppress the i superscript on Γ_n^i. Up to NNLL order the solutions are

$$\begin{aligned}
K_\Gamma(\mu,\mu_0) &= -\frac{\Gamma_0}{4\beta_0^2}\left\{\frac{4\pi}{\alpha_s(\mu_0)}\left(1-\frac{1}{r}-\ln r\right)+\left(\frac{\Gamma_1}{\Gamma_0}-\frac{\beta_1}{\beta_0}\right)(1-r+\ln r)+\frac{\beta_1}{2\beta_0}\ln^2 r\right.\\
&\quad+\frac{\alpha_s(\mu_0)}{4\pi}\left[\left(\frac{\beta_1^2}{\beta_0^2}-\frac{\beta_2}{\beta_0}\right)\left(\frac{1-r^2}{2}+\ln r\right)+\left(\frac{\beta_1\Gamma_1}{\beta_0\Gamma_0}-\frac{\beta_1^2}{\beta_0^2}\right)(1-r+r\ln r)\right.\\
&\quad\left.\left.-\left(\frac{\Gamma_2}{\Gamma_0}-\frac{\beta_1\Gamma_1}{\beta_0\Gamma_0}\right)\frac{(1-r)^2}{2}\right]\right\},\\
\eta_\Gamma(\mu,\mu_0) &= -\frac{\Gamma_0}{2\beta_0}\left[\ln r+\frac{\alpha_s(\mu_0)}{4\pi}\left(\frac{\Gamma_1}{\Gamma_0}-\frac{\beta_1}{\beta_0}\right)(r-1)+\frac{\alpha_s^2(\mu_0)}{16\pi^2}\left(\frac{\Gamma_2}{\Gamma_0}-\frac{\beta_1\Gamma_1}{\beta_0\Gamma_0}+\frac{\beta_1^2}{\beta_0^2}-\frac{\beta_2}{\beta_0}\right)\frac{r^2-1}{2}\right],\\
K_{\gamma_F}(\mu,\mu_0) &= -\frac{\gamma_0}{2\beta_0}\left[\ln r+\frac{\alpha_s(\mu_0)}{4\pi}\left(\frac{\gamma_{F1}}{\gamma_{F0}}-\frac{\beta_1}{\beta_0}\right)(r-1)\right].
\end{aligned} \tag{E.8}$$

Here $r=\alpha_s(\mu)/\alpha_s(\mu_0)$.

E.2 RGE with a Convolution

In this appendix we solve the general anomalous dimension equation

$$\mu\frac{d}{d\mu}F(t,\mu)=\int_{-\infty}^{+\infty}dt'\,\gamma_F(t-t',\mu)\,F(t',\mu)\,,\qquad \gamma_F(t,\mu)=-\frac{\rho_F\Gamma_{\rm cusp}[\alpha_s]}{j}\,\frac{1}{\mu^j}\mathcal{L}_0\Big(\frac{t}{\mu^j}\Big)+\gamma_F[\alpha_s]\,\delta(t)\,, \tag{E.9}$$

where t and t' are variables of mass-dimension j. To solve Eq. (E.9) we take the Laplace transform which yields a simple multiplicative RGE in the Laplace space variable y:

$$\mu\frac{d}{d\mu}\widetilde{F}(y,\mu)=\widetilde{\gamma}_F(y,\mu)\widetilde{F}(y,\mu)\,,\qquad \widetilde{\gamma}_F(y,\mu)=\frac{\rho_F\Gamma_{\rm cusp}[\alpha_s]}{j}\ln(y\,\mu^j\,e^{\gamma_E})+\gamma_F[\alpha_s]\,. \tag{E.10}$$

where the Laplace transforms are defined by

$$\widetilde{F}(y,\mu)=\int_0^\infty \mathrm{d}t\,e^{-y\,t}\,F(t,\mu)\,,\qquad \widetilde{\gamma}_F(y,\mu)=\int_0^\infty \mathrm{d}t\,e^{-y\,t}\,\gamma_F(t,\mu)\,. \tag{E.11}$$

The form in Eq. (E.10) matches that of Eq. (E.1) with the replacement $ye^{\gamma_E}=1/s$, so we have already obtained the solution in Eq. (E.6). To obtain the solution in t space we can take the inverse Laplace

transform, using Eq. (C.45), to find

$$\begin{aligned} F(t,\mu) &= \frac{1}{2\pi i}\int_{c-i\infty}^{c+i\infty} \mathrm{d}y\, e^{y\,t}\, \Big[e^{K_F(\mu,\mu_0)}\big(y\,\mu_0^j\, e^{\gamma_E}\big)^{\omega_F(\mu,\mu_0)} F(y,\mu_0)\Big] \\ &= e^{K_F(\mu,\mu_0)}\frac{1}{2\pi i}\int_{c-i\infty}^{c+i\infty} \mathrm{d}y\, e^{y\,t}\, \big(y\,\mu_0^j\, e^{\gamma_E}\big)^{\omega_F(\mu,\mu_0)} \int_0^\infty \mathrm{d}t'\, e^{-y\,t'} F(t',\mu_0) \\ &= e^{K_F(\mu,\mu_0)}\int_0^\infty \mathrm{d}t'\, F(t',\mu_0)\,\frac{1}{2\pi i}\int_{c-i\infty}^{c+i\infty} \mathrm{d}y\; e^{y(t-t')}\,\big(y\,\mu_0^j\, e^{\gamma_E}\big)^{\omega_F(\mu,\mu_0)} \\ &= \int_0^\infty \mathrm{d}t'\; U_F(t-t',\mu,\mu_0)\, F(t',\mu_0)\,, \end{aligned} \tag{E.12}$$

where the evolution kernel is

$$U_F(t,\mu,\mu_0) = \frac{e^{\gamma_E\omega_F(\mu,\mu_0)}\, e^{K_F(\mu,\mu_0)}}{\Gamma\big[-\omega_F(\mu,\mu_0)\big]}\,\left[\frac{1}{\mu_0^j}\mathcal{L}^{-\omega_F(\mu,\mu_0)}\left(\frac{t}{\mu_0^j}\right) - \frac{1}{\omega_F(\mu,\mu_0)}\delta(t)\right]. \tag{E.13}$$

For the cases with convolutions a few additional identities are useful. The evolution kernels obey

$$\int dr'\; U_F(r-r',\mu,\mu_I)\, U_F(r'-r'',\mu_I,\mu_0) = U_F(r-r'',\mu,\mu_0)\,, \tag{E.14}$$

which states that it is equivalent to evolve through an intermediate scale, $\mu_0 \to \mu_I \to \mu$, or directly from $\mu_0 \to \mu$. To verify Eq. (E.14) one needs

$$\begin{aligned} &\int dr''\mathcal{L}^{-\omega_1}\left(\frac{r-r''}{\mu_I^j}\right)\mathcal{L}^{-\omega_2}\left(\frac{r''-r'}{\mu_0^j}\right) = \frac{\Gamma(-\omega_1)\Gamma(-\omega_2)}{(\mu_I^{-j})\Gamma(-\omega_1-\omega_2)}\left(\frac{\mu_I^j}{\mu_0^j}\right)^{\omega_1}\mathcal{L}^{-\omega_1-\omega_2}\left(\frac{r-r'}{\mu_0^j}\right), \\ &K_F(\mu,\mu_I) + K_F(\mu_I,\mu_0) = \omega_1\,\ln\left(\frac{\mu_0^j}{\mu_I^j}\right) + K_F(\mu,\mu_0)\,, \end{aligned} \tag{E.15}$$

where here $\omega_1 = \omega_F(\mu,\mu_I)$ and $\omega_2 = \omega_F(\mu_I,\mu_0)$. The first result in Eq. (E.15) is straightforward to derive using the Fourier transform. Another useful identity simplifies the convolution of two U's that have the same renormalization scales, but variables with different mass-dimension, and different anomalous dimension coefficients

$$\begin{aligned} &\int dr'\; U_F\big(Q'(r-r'),\mu,\mu_0;j',\Gamma',\gamma',\omega_1\big)\, U_F\big(r'-r'',\mu,\mu_0;j,\Gamma,\gamma,\omega_2\big) \\ &\quad= \frac{1}{Q'}\left(\frac{(\mu_0)^{j'-j}}{Q'}\right)^{\omega_1} U_F\big(r-r'',\mu,\mu_0;j,\Gamma'+\Gamma,\gamma'+\gamma,\omega_1+\omega_2\big)\,. \end{aligned} \tag{E.16}$$

Here the variables after the semicolon denote parameter dependence, and Q' simply denotes a variable with mass dimension $j'-j$. Also here $\omega_1 = \omega(\mu,\mu_0;\Gamma'/j')$ and $\omega_2 = \omega(\mu,\mu_0;\Gamma/j)$ are simply the ω's obtained from the other parameters. The final useful identity is

$$\lim_{\omega'\to 0} U_F(r-r',\mu,\mu_0;j,\Gamma,\gamma,\omega') = e^{K_F(\mu,\mu_0;\Gamma,\gamma)}\;\delta(r-r')\,. \tag{E.17}$$

F Hard, Jet, Beam, and Soft Functions

In this section we give the expression of the inclusive collinear jet and beam functions, as well as the soft function for two Wilson lines. These are universal perturbative functions that are common ingredients appearing in factorization theorems.

F.1 Hard Functions, q and g Form Factors

In this section we discuss the hard Wilson coefficients for two-quark and two-gluon operators in SCET. These are related to the quark and gluon form factors for massless quarks in the $\overline{\rm MS}$ scheme, which are made infrared finite by converting them to Wilson coefficients in SCET.

Loop graphs generated with the QCD vector quark current $J^\mu = \bar\psi\gamma^\mu\psi$ are often referred to as the massless quark form factor, which we will consider in the time-like region. They are ultraviolet finite since this is a conserved current in QCD, but are infrared divergent. Similarly for gluons we can consider the scalar current $J = G^{\mu\nu}G_{\mu\nu}$ which appears for example when integrating out top quarks for the Higgs coupling to two gluons. Again we consider this current in the time-like region. In this case is not conserved, and has an anomalous dimension also in the full theory. By matching these form factor amplitudes onto the SCET operator with two quark or two gluon building block fields in different collinear directions, we can extract an infrared finite result for the Wilson coefficient $C^q(Q)$ and $C^g(Q)$, where the SCET operators are

$$C^q(Q)\,\bar\chi_n\gamma^\mu_\perp\chi'_n\,, \qquad\qquad C^g(Q)\,\mathcal{B}^\mu_{n\perp}\,\mathcal{B}_{n\perp\,\mu}\,. \tag{F.1}$$

The SCET diagrams have the same infrared divergences as those for the QCD currents, but are also UV divergent. These UV divergences are canceled by coefficient counterterm Z^i_C that appears when defining the renormalized Wilson coefficients $C^i(Q,\mu)$

$$C^{i\,\rm bare}(Q,\epsilon) = Z^i_C(Q,\mu,\epsilon)\,C^i(Q,\mu)\,. \tag{F.2}$$

Although displayed here, for simplicity we will almost always suppress the ϵ argument for bare coefficients and Z-factors. The Hard functions for these quark and gluon bilinear operators are then defined by the square of this renormalized Wilson coefficient

$$H^i(Q^2,\mu) = \left|C^i(Q,\mu)\right|^2. \tag{F.3}$$

While the coefficients $C^i(Q,\mu)$ are in general complex, the hard functions $H^i(Q,\mu)$ are always real. In order to provide complete information we will present complete results for the C^i and only briefly mention how the corresponding results appear for the H^i.

Since the bare coefficients in Eq. (F.2) are μ-independent, we can take $\mu{\rm d}/{\rm d}\mu$ of both sides and rearrange the result to give

$$\mu\frac{\rm d}{{\rm d}\mu}\,C^i(Q,\mu) = \gamma^i_C(Q,\mu)\,C^i(Q,\mu)\,, \tag{F.4}$$

where the anomalous dimension is defined by

$$\gamma^i_C(Q,\mu) = -(Z^i_C)^{-1}(Q,\mu)\left[\mu\frac{\rm d}{{\rm d}\mu}\,Z^i_C(Q,\mu)\right], \tag{F.5}$$

and has a finite $\epsilon\to 0$ limit. The general all orders form for this anomalous dimension is [24, 25]

$$\gamma^i_C(Q,\mu) = \Gamma^i_{\rm cusp}(\alpha_s)\,L_Q + \gamma^i_C(\alpha_s)\,. \tag{F.6}$$

where for convenience we have defined the logarithm

$$L_Q = \ln\left(\frac{-Q^2-i0}{\mu^2}\right). \tag{F.7}$$

The analogous equations for the hard functions are then

$$\mu\frac{\mathrm{d}}{\mathrm{d}\mu}\,H^i(Q,\mu) = \gamma_H^i(Q,\mu)\,H^i(Q,\mu)\,, \qquad\qquad \gamma_H^i(Q,\mu) = 2\mathrm{Re}\big[\gamma_C^i(Q,\mu)\big]\,. \tag{F.8}$$

The term multiplying L_Q in Eq. (F.6) is known as the cusp anomalous dimension, and its α_s expansion coefficients Γ_n^i to 3-loops are given in Sec. D.3. Expanding the non-cusp anomalous dimensions as a series in α_s we can write

$$\gamma_C^i(\alpha_s) = \sum_{n=0}^{\infty}\gamma_{C\,n}^i\Big(\frac{\alpha_s}{4\pi}\Big)^{n+1}\,. \tag{F.9}$$

Results for the numerical coefficients $\gamma_{C\,n}^i$ will be given below.

The results for the counterterm Z_C can be expressed as a series in $\alpha_s(\mu)$, L_Q, and $1/\epsilon$, and can be expressed entirely in terms of coefficients of the anomalous dimensions, Γ_n^i, $\gamma_{C\,n}^i$ and the β-function, β_i. Up to two loops we have

$$\begin{aligned} Z_C^i = 1 &+ \frac{\alpha_s(\mu)}{4\pi}\bigg\{-\frac{\Gamma_0^i}{2\epsilon^2} + \frac{(L_Q\Gamma_0^i+\gamma_{C\,0}^i)}{2\epsilon}\bigg\} \\ &+ \Big(\frac{\alpha_s(\mu)}{4\pi}\Big)^2\bigg\{\frac{(\Gamma_0^i)^2}{8\epsilon^4} - \frac{\big[2L_Q(\Gamma_0^i)^2 + 2\gamma_{C\,0}^i\Gamma_0^i - 3\Gamma_0^i\beta_0\big]}{8\epsilon^3} \\ &\qquad + \frac{\big[L_Q^2(\Gamma_0^i)^2 + 2L_Q\Gamma_0^i(\gamma_{C\,0}^i-\beta_0) - \Gamma_1^i + (\gamma_{C\,0}^i)^2 - 2\gamma_{C\,0}^i\beta_0\big]}{8\epsilon^2} + \frac{[L_Q\Gamma_1^i+\gamma_C^i]}{4\epsilon}\bigg\}\,. \end{aligned} \tag{F.10}$$

Since the coefficients of the L_Q dependent terms in the renormalized Wilson coefficients are related to the $1/\epsilon$ UV divergences in Z_C^i they are also determined by the anomalous dimension coefficients and lower order information. Up to two loop order from the quark vector form factor we have [**?**, **?**]

$$\begin{aligned} C^q(Q,\mu) = 1 &+ \frac{\alpha_s(\mu)}{4\pi}\bigg[-\frac{\Gamma_0^q}{4}L_Q^2 - \frac{\gamma_{C\,0}^q}{2}L_Q + c_{C\,1}^q\bigg] \\ &+ \Big(\frac{\alpha_s(\mu)}{4\pi}\Big)^2\bigg[\frac{(\Gamma_0^q)^2}{32}L_Q^4 + \frac{\Gamma_0^q(3\gamma_{C\,0}^q+2\beta_0)}{24}L_Q^3 + \frac{\big[(\gamma_{C\,0}^q)^2 + 2\beta_0\gamma_{C\,0}^q - 2\Gamma_1^q - 2\Gamma_0^q\,c_{C\,1}^q\big]}{8}L_Q^2 \\ &\qquad - \frac{[\gamma_{C\,1}^q + \gamma_{C\,0}^q\,c_{C\,1}^q + 2\beta_0 c_{C\,1}^q]}{2}L_Q + c_{C\,2}^q\bigg]\,. \end{aligned} \tag{F.11}$$

(For simplicity we have not included contributions from massive quark loops in this result.) From the gluon scalar form factor we include only the corrections from integrating out a massive top quark loop,

$$\begin{aligned} C^g(Q,\mu) = \alpha_s(\mu)F^{(0)}(q_t)\bigg[1 &+ \frac{\alpha_s(\mu)}{4\pi}\Big\{-\frac{\Gamma_0^g}{4}L_Q^2 - \frac{[\gamma_{C\,0}^g+2\beta_0]}{2}L_Q + c_{C\,1}^g(q_t)\Big\} \\ &+ \Big(\frac{\alpha_s(\mu)}{4\pi}\Big)^2\bigg\{\frac{(\Gamma_0^g)^2}{32}L_Q^4 + \frac{\Gamma_0^g(3\gamma_{C\,0}^g+8\beta_0)}{24}L_Q^3 + \frac{\big[(\gamma_{C\,0}^g)^2+6\beta_0\gamma_{C\,0}^g+8\beta_0^2-2\Gamma_1^g-2\Gamma_0^g\,c_{C\,1}^g(q_t)\big]}{8}L_Q^2 \\ &\qquad - \frac{[\gamma_{C\,1}^g + \gamma_{C\,0}^g\,c_{C\,1}^g(q_t) + 4\beta_0 c_{C\,1}^g(q_t) + 2\beta_1]}{2}L_Q + c_{C\,2}^g(q_t)\bigg\}\bigg]\,, \end{aligned} \tag{F.12}$$

where the dependence on the top quark mass appears in some coefficients through dependence on $q_t \equiv Q^2/(4m_t^2)$.

The $\overline{\rm MS}$ anomalous dimension for the hard function can be obtained [26, 27] from the IR divergences of the on-shell massless quark form factor which are known to three loops [28],

$$\begin{aligned}
\gamma^q_{C\,0} &= -6C_F\,,\\
\gamma^q_{C\,1} &= -C_F\Big[\Big(\frac{82}{9}-52\zeta_3\Big)C_A+(3-4\pi^2+48\zeta_3)C_F+\Big(\frac{65}{9}+\pi^2\Big)\beta_0\Big]\,,\\
\gamma^q_{C\,2} &= -2C_F\Big[\Big(\frac{66167}{324}-\frac{686\pi^2}{81}-\frac{302\pi^4}{135}-\frac{782\zeta_3}{9}+\frac{44\pi^2\zeta_3}{9}+136\zeta_5\Big)C_A^2\\
&\quad+\Big(\frac{151}{4}-\frac{205\pi^2}{9}-\frac{247\pi^4}{135}+\frac{844\zeta_3}{3}+\frac{8\pi^2\zeta_3}{3}+120\zeta_5\Big)C_FC_A\\
&\quad+\Big(\frac{29}{2}+3\pi^2+\frac{8\pi^4}{5}+68\zeta_3-\frac{16\pi^2\zeta_3}{3}-240\zeta_5\Big)C_F^2\\
&\quad+\Big(-\frac{10781}{108}+\frac{446\pi^2}{81}+\frac{449\pi^4}{270}-\frac{1166\zeta_3}{9}\Big)C_A\beta_0\\
&\quad+\Big(\frac{2953}{108}-\frac{13\pi^2}{18}-\frac{7\pi^4}{27}+\frac{128\zeta_3}{9}\Big)\beta_1+\Big(-\frac{2417}{324}+\frac{5\pi^2}{6}+\frac{2\zeta_3}{3}\Big)\beta_0^2\Big]\,.
\end{aligned}\tag{F.13}$$

The anomalous dimension coefficients for the gluon hard Wilson coefficient to three loops are [**?**, 29, 26]

$$\begin{aligned}
\gamma^g_{C\,0} &= -2\beta_0\,,\\
\gamma^g_{C\,1} &= \Big(-\frac{118}{9}+4\zeta_3\Big)C_A^2+\Big(-\frac{38}{9}+\frac{\pi^2}{3}\Big)C_A\,\beta_0-2\beta_1\,,\\
\gamma^g_{C\,2} &= \Big(-\frac{60875}{162}+\frac{634\pi^2}{81}+\frac{8\pi^4}{5}+\frac{1972\zeta_3}{9}-\frac{40\pi^2\zeta_3}{9}-32\zeta_5\Big)C_A^3\\
&\quad+\Big(\frac{7649}{54}+\frac{134\pi^2}{81}-\frac{61\pi^4}{45}-\frac{500\zeta_3}{9}\Big)C_A^2\,\beta_0+\Big(\frac{466}{81}+\frac{5\pi^2}{9}-\frac{28\zeta_3}{3}\Big)C_A\,\beta_0^2\\
&\quad+\Big(-\frac{1819}{54}+\frac{\pi^2}{3}+\frac{4\pi^4}{45}+\frac{152\zeta_3}{9}\Big)C_A\,\beta_1-2\beta_2\,.
\end{aligned}\tag{F.14}$$

The constants that appear in the quark Wilson coefficient in Eq. (F.11) are

$$c^q_{C\,1} = C_F\Big[-8+\frac{\pi^2}{6}\Big]\,,\tag{F.15}$$

$$\begin{aligned}
c^q_{C\,2} &= C_F^2\Big[\frac{255}{8}+\frac{7\pi^2}{2}-30\zeta_3-\frac{83\pi^4}{360}\Big]+C_FC_A\Big[-\frac{51157}{648}-\frac{337\pi^2}{108}+\frac{313\zeta_3}{9}+\frac{11\pi^4}{45}\Big]\\
&\quad+C_FT_Fn_f\Big[\frac{4085}{162}+\frac{23\pi^2}{27}+\frac{4\zeta_3}{9}\Big]\,.
\end{aligned}$$

while for the gluon Wilson coefficient in Eq. (F.12) we have the functions

$$\begin{aligned}
F^{(0)}(q_t) &= \frac{3}{2q_t}-\frac{3}{2q_t}\Big|1-\frac{1}{q_t}\Big|\begin{cases}\arcsin^2(\sqrt{q_t})\,, & 0<q_t\le 1\,,\\ \ln^2[-i(\sqrt{q_t}+\sqrt{q_t-1})]\,, & q_t>1\,,\end{cases}\\
c^g_{C\,1}(q_t) &= C_A\frac{\pi^2}{6}+F^{(1)}(q_t)\,,\qquad c^g_{C\,2}(q_t)=F^{(2)}(q_t)\,,
\end{aligned}\tag{F.16}$$

Here, $F^{(0)}(q_t)$ encodes the m_t dependence of the leading-order $gg\to H$ cross section from the virtual top-quark loop. The full analytic m_t dependence of the virtual two-loop corrections to $gg\to H$ in terms of harmonic polylogarithms were obtained in refs. [**?**, **?**]. Since the corresponding exact expression for $F^{(1)}(q_t)$ is long, we quote results expanded in Q^2/m_t^2 from ref. [**?**]. These suffice for practical purposes since the

expansion converges quickly. We also quote the first few terms in the expanded result for $F^{(2)}(q_t)$, while further terms can be obtained from the original literature [**?**, **?**],

$$\begin{aligned}
F^{(1)}(q_t) &= \Big(5 - \frac{38}{45}\,q_t - \frac{1289}{4725}\,q_t^2 - \frac{155}{1134}\,q_t^3 - \frac{5385047}{65488500}\,q_t^4\Big)C_A \\
&\quad + \Big(-3 + \frac{307}{90}\,q_t + \frac{25813}{18900}\,q_t^2 + \frac{3055907}{3969000}\,q_t^3 + \frac{659504801}{1309770000}\,q_t^4\Big)C_F + \mathcal{O}(q_t^5)\,, \\
F^{(2)}(q_t) &= \big(7C_A^2 + 11C_AC_F - 6C_F\beta_0\big)\ln(-4q_t - i0) + \Big(-\frac{419}{27} + \frac{7\pi^2}{6} + \frac{\pi^4}{72} - 44\zeta_3\Big)C_A^2 \\
&\quad + \Big(-\frac{217}{2} - \frac{\pi^2}{2} + 44\zeta_3\Big)C_AC_F + \Big(\frac{2255}{108} + \frac{5\pi^2}{12} + \frac{23\zeta_3}{3}\Big)C_A\beta_0 - \frac{5}{6}C_AT_F \\
&\quad + \frac{27}{2}C_F^2 + \Big(\frac{41}{2} - 12\zeta_3\Big)C_F\beta_0 - \frac{4}{3}C_FT_F + \mathcal{O}(q_t)\,.
\end{aligned} \tag{F.17}$$

In the $m_t \to \infty$ limit we have $F^{(0)}(0) = 1$ and $F^{(1)}(0) = 5C_A - 3C_F$, while $F^{(2)}(q_t \to 0)$ has the terms displayed in Eq. (F.17).

The solution of the RGE in Eq. (F.6) yields for the evolution of the hard function (**TODO**)

TODO: Fix this equation

$$\begin{aligned}
H^i(Q,\mu) &= H^i(Q,\mu_0)\,U_H(Q,\mu_0,\mu)\,, \qquad U_H(Q,\mu_0,\mu) = \Big|e^{K_H(\mu_0,\mu)}\Big(\frac{-Q^2-i0}{\mu_0^2}\Big)^{\eta_H(\mu_0,\mu)}\Big|^2\,, \\
K_H(\mu_0,\mu) &= -2K_\Gamma^q(\mu_0,\mu) + K_{\gamma_H^q}(\mu_0,\mu)\,, \qquad \eta_H(\mu_0,\mu) = \eta_\Gamma^q(\mu_0,\mu)\,,
\end{aligned} \tag{F.18}$$

where the functions $K_\Gamma^i(\mu_0,\mu)$, $\eta_\Gamma^i(\mu_0,\mu)$ and K_γ are given below in Eq. (**??**).

TODO: Fix this paragrapl change notations, etc

(**TODO**) To minimize the large logarithms in C_{ggH} we should evaluate Eq. (**??**) at the hard scale μ_H with $|\mu_H^2| \sim q^2 \sim m_t^2$. For the simplest choice $\mu_H^2 = q^2$ the double logarithms of $-q^2/\mu_H^2$ are not minimized since they give rise to additional π^2 terms from the analytic continuation of the form factor from spacelike to timelike argument, $\ln^2(-1-i0) = -\pi^2$, which causes rather large perturbative corrections. These π^2 terms can be summed along with the double logarithms by taking $\mu_H = -i\sqrt{q^2}$ or in our case $\mu_H = -im_H$ [**?**, 30, **?**, **?**]. For Higgs production this method was applied in Refs. [31, 32], where it was shown to improve the perturbative convergence of the hard matching coefficient. Starting at NNLO, the expansion of C_{ggH} contains single logarithms $\ln(m_t^2/\mu_H^2)$, which in Eq. (**??**) are contained as $\ln x_H$ in $C^{(2)}$ with a compensating $-\ln(-4z-i0)$ in $F^{(2)}(z)$, which are not large since $m_H/m_t \simeq 1$. In Eq. (**??**), $\alpha_s(\mu_H)$ is defined for $n_f = 5$ flavors. When written in terms of $\alpha_s(\mu_H)$ with $n_f = 6$ flavors similar $\ln(m_t^2/\mu_H^2)$ terms would already appear at NLO. The additional terms that are induced by using an imaginary scale in these logarithms are small, because the imaginary part of $\alpha_s(-im_H)$ is much smaller than its real part.

F.2 Jet Function

The operator definition of the quark jet function was already given in Eq. (9.29). For quarks and gluons the inclusive jet functions can be defined by

$$\begin{aligned}
J^q(t) &= \mathrm{Im}\left[\frac{-i}{4\pi N_C\omega}\int d^4x\, e^{ix\cdot r}\,\Big\langle 0\Big|\mathrm{T}\,\bar\chi_{n,\omega,0_\perp}(0)\bar n\!\!\!/\chi_n(x)\Big|0\Big\rangle\right]\,, \\
g_\perp^{\mu\nu}\,J^g(t) &= \mathrm{Im}\left[\frac{-i}{\pi(N_C-1)}\int d^4x\, e^{ix\cdot r}\,\Big\langle 0\Big|\mathrm{T}\,\mathcal{B}^{\mu a}_{n\perp,\omega,0_\perp}(0)\mathcal{B}^{\nu a}_{n\perp}(x)\Big|0\Big\rangle\right]\,,
\end{aligned} \tag{F.19}$$

where $r^\mu = n\cdot r\,\bar n^\mu/2$ and the invariant mass $t = \omega\, n\cdot r$. (This becomes $t = \omega\, n\cdot r - \vec\omega_\perp^{\,2}$ if $\omega_\perp$ momentum is injected.)

The renormalized jet function $J^i(s,\mu)$, for $i = q$ or g, is related to the bare jet function through the definition

$$J^{i,\text{bare}}(s) = \int \mathrm{d}s'\, Z_J^i(s-s',\mu)\, J^i(s',\mu)\,, \tag{F.20}$$

and the inverse of the Z_J^i factor is defined such that

$$\delta(s) = \int \mathrm{d}s' \left[Z_J^i\right]^{-1}(s-s',\mu)\, Z_J^i(s',\mu)\,. \tag{F.21}$$

Since $J^{i,\text{bare}}$ is μ-independent, the dependence on μ is described by the renormalization group equation

$$\mu\frac{\mathrm{d}}{\mathrm{d}\mu} J^i(s,\mu^2) = \int \mathrm{d}s'\, \gamma_J^i(s-s',\mu) J_J^i(s',\mu)\,, \tag{F.22}$$

where the μ dependence of Z_J^i appears through the UV finite anomalous dimension,

$$\gamma_J^i(s,\mu) = -\int \mathrm{d}s' \left[Z_J^i\right]^{-1}(s-s') \left[\mu\frac{\mathrm{d}}{\mathrm{d}\mu} Z_J^i(s')\right], \tag{F.23}$$

where we can take $\epsilon \to 0$.

As already discussed in Sec. E.2, a general anomalous dimension for an RGE with convolution takes the form given in Eq. (E.9). The jet function anomalous dimension can be obtained from this by using

$$j = 2\,, \qquad \rho_J = 4\,. \tag{F.24}$$

Thus, to all orders in perturbation theory, the jet function's anomalous dimension has the form

$$\gamma_J^i(s,\mu) = -2\Gamma^i_{\text{cusp}}(\alpha_s)\,\frac{1}{\mu^2}\mathcal{L}_0\Big(\frac{s}{\mu^2}\Big) + \gamma_J^i(\alpha_s)\,\delta(s)\,, \tag{F.25}$$

where the distribution $\mathcal{L}_0(s/\mu^2)$ were defined in Sec. C.4. The cusp anomalous dimension, which multiplies $\mathcal{L}_0(s/\mu^2)$ is known to three loop order, and is given in given in Sec. D.3. The non-cusp anomalous dimensions multiplying the delta function has the general expansion

$$\gamma_J^i(\alpha_s) = \sum_{n=0}^{\infty} \gamma_{J\,n}^i \Big(\frac{\alpha_s}{4\pi}\Big)^{n+1}. \tag{F.26}$$

The coefficients $\gamma_{J\,n}^i$ are known for both the quark and gluon jet functions to three loop order, and are given below.

Both the renormalized jet function and the Z_J^i factor can again be written to all orders in perturbation theory in terms of the distributions defined in Sec. D.3

$$J^i(s,\mu) = \sum_{k=-1}^{\infty} J_k^i(\alpha_s)\frac{1}{\mu^2}\mathcal{L}_k(s/\mu^2)\,, \qquad Z_J^i(s,\mu) = \sum_{k=-1}^{\infty} Z_{J,k}^i(\alpha_s)\frac{1}{\mu^2}\mathcal{L}_k(s/\mu^2)\,, \tag{F.27}$$

To a given order in perturbation theory $\mathcal{O}(\alpha_s^l)$ the coefficients $J_k^i(\alpha_s)$ with $k > 2l-1$ vanish, while the coefficients $Z_{J,k}^i$ with $k > 2l-1$ vanish. The renormalization function Z_J^i is completely determined through

its relation to the anomalous dimension. To two loop order the coefficients are given by

$$
\begin{aligned}
Z^i_{J,-1} &= 1 + \frac{\alpha_s}{4\pi}\left[\frac{\Gamma^i_{\text{cusp}\,0}}{\epsilon^2} + \frac{\gamma^i_{J0}}{2\epsilon}\right] + \left(\frac{\alpha_s}{4\pi}\right)^2\left[\frac{(\Gamma^i_{\text{cusp}\,0})^2}{2\epsilon^4} + \frac{\Gamma^i_{\text{cusp}\,0}\left(2\gamma^i_{J0} - 3\beta_0\right)}{4\epsilon^3}\right. \\
&\qquad \left. + \frac{3\gamma^i_{J0}\left(\gamma^i_{J0} - 2\beta_0\right) - 2\pi^2\,(\Gamma^i_{\text{cusp}\,0})^2 + 6\,\Gamma^i_{\text{cusp}\,1}}{24\epsilon^2} + \frac{\gamma^i_{J1}}{4\epsilon}\right], \\
Z^i_{J,0} &= \frac{\alpha_s}{4\pi}\left[-\frac{\Gamma^i_{\text{cusp}\,0}}{\epsilon}\right] + \left(\frac{\alpha_s}{4\pi}\right)^2\left[-\frac{(\Gamma^i_{\text{cusp}\,0})^2}{\epsilon^3} + \frac{\Gamma^i_{\text{cusp}\,0}\left(\beta_0 - \gamma^i_{J0}\right)}{2\epsilon^2} - \frac{\Gamma^i_{\text{cusp}\,1}}{2\epsilon}\right], \\
Z^i_{J,1} &= \left(\frac{\alpha_s}{4\pi}\right)^2\left[\frac{(\Gamma^i_{\text{cusp}\,0})^2}{\epsilon^2}\right].
\end{aligned}
\tag{F.28}
$$

For the renormalized jet function, the coefficients J^i_k for $k \geq -1$ are all related to the divergent structure and therefore again determined by the anomalous dimension coefficients. The only extra piece of information is the matching coefficient J^i_{-1}, which has to be calculated at each order in perturbation theory. To second order in perturbation theory, one finds

$$
\begin{aligned}
J^i_{-1} &= 1 + \frac{\alpha_s}{4\pi}c^i_{J1} + \left(\frac{\alpha_s}{4\pi}\right)^2 c^i_{J2}\,, \\
J^i_0 &= \frac{\alpha_s}{4\pi}\left(-\frac{\gamma^i_{J0}}{2}\right) + \left(\frac{\alpha_s}{4\pi}\right)^2\left[-c^i_{J1}\left(\beta_0 + \frac{\gamma^i_{J0}}{2}\right) - \frac{\gamma^i_{J1}}{2} + \frac{\pi^2\gamma^i_{J0}\Gamma^i_{\text{cusp}\,0}}{12} + \left(\Gamma^i_{\text{cusp}\,0}\right)^2\zeta_3\right], \\
J^i_1 &= \frac{\alpha_s}{4\pi}\left(\Gamma^i_{\text{cusp}\,0}\right) + \left(\frac{\alpha_s}{4\pi}\right)^2\left[c^i_{J1}\Gamma^i_{\text{cusp}\,0} + \frac{\beta_0\gamma^i_{J0}}{2} + \frac{(\gamma^i_{J0})^2}{4} - \frac{\pi^2(\Gamma^i_{\text{cusp}\,0})^2}{6} + \Gamma^i_{\text{cusp}\,1}\right], \\
J^i_2 &= \left(\frac{\alpha_s}{4\pi}\right)^2\left[-\Gamma^i_{\text{cusp}\,0}\,\frac{2\beta_0 - 3\gamma^i_{J0}}{4}\right], \\
J^i_3 &= \left(\frac{\alpha_s}{4\pi}\right)^2\frac{(\Gamma^i_{\text{cusp}\,0})^2}{2}\,.
\end{aligned}
\tag{F.29}
$$

To two loop order, the expressions for the non-cusp anomalous dimension γ^i_J for quarks ($i = q$) and gluons ($i = g$) are given by

$$
\begin{aligned}
\gamma^q_{J\,0} &= 6C_F\,, \\
\gamma^q_{J\,1} &= C_F\Big[\Big(\frac{146}{9} - 80\zeta_3\Big)C_A + (3 - 4\pi^2 + 48\zeta_3)C_F + \Big(\frac{121}{9} + \frac{2\pi^2}{3}\Big)\beta_0\Big], \\
\gamma^q_{J\,2} &= 2C_F\Big[\Big(\frac{52019}{162} - \frac{841\pi^2}{81} - \frac{82\pi^4}{27} - \frac{2056\zeta_3}{9} + \frac{88\pi^2\zeta_3}{9} + 232\zeta_5\Big)C_A^2 \\
&\quad + \Big(\frac{151}{4} - \frac{205\pi^2}{9} - \frac{247\pi^4}{135} + \frac{844\zeta_3}{3} + \frac{8\pi^2\zeta_3}{3} + 120\zeta_5\Big)C_AC_F \\
&\quad + \Big(\frac{29}{2} + 3\pi^2 + \frac{8\pi^4}{5} + 68\zeta_3 - \frac{16\pi^2\zeta_3}{3} - 240\zeta_5\Big)C_F^2 \\
&\quad + \Big(-\frac{7739}{54} + \frac{325}{81}\pi^2 + \frac{617\pi^4}{270} - \frac{1276\zeta_3}{9}\Big)C_A\beta_0 \\
&\quad + \Big(-\frac{3457}{324} + \frac{5\pi^2}{9} + \frac{16\zeta_3}{3}\Big)\beta_0^2 + \Big(\frac{1166}{27} - \frac{8\pi^2}{9} - \frac{41\pi^4}{135} + \frac{52\zeta_3}{9}\Big)\beta_1\Big].
\end{aligned}
\tag{F.30}
$$

and

$$\begin{aligned}
\gamma^g_{J\,0} &= 2\beta_0\,,\\
\gamma^g_{J\,1} &= \Big(\frac{182}{9} - 32\zeta_3\Big)C_A^2 + \Big(\frac{94}{9} - \frac{2\pi^2}{3}\Big)C_A\,\beta_0 + 2\beta_1\,,\\
\gamma^g_{J\,2} &= \Big(\frac{49373}{81} - \frac{944\pi^2}{81} - \frac{16\pi^4}{5} - \frac{4520\zeta_3}{9} + \frac{128\pi^2\zeta_3}{9} + 224\zeta_5\Big)C_A^3\\
&\quad + \Big(-\frac{6173}{27} - \frac{376\pi^2}{81} + \frac{13\pi^4}{5} + \frac{280\zeta_3}{9}\Big)C_A^2\,\beta_0 + \Big(-\frac{986}{81} - \frac{10\pi^2}{9} + \frac{56\zeta_3}{3}\Big)C_A\,\beta_0^2\\
&\quad + \Big(\frac{1765}{27} - \frac{2\pi^2}{3} - \frac{8\pi^4}{45} - \frac{304\zeta_3}{9}\Big)C_A\,\beta_1 + 2\beta_2\,.
\end{aligned} \tag{F.31}$$

The constant coefficients appearing in the quark jet function are given by

$$\begin{aligned}
c^q_{J\,1} &= \Big(7 - \pi^2\Big)C_F\,,\\
c^q_{J\,2} &= \Big(\frac{205}{8} - \frac{67\pi^2}{6} + \frac{14\pi^4}{15} - 18\,\zeta_3\Big)C_F^2 + \Big(\frac{53129}{648} - \frac{208\pi^2}{27} - \frac{17\pi^4}{180} - \frac{206\zeta_3}{9}\Big)C_F C_A\\
&\quad - \Big(\frac{4057}{162} - \frac{68\pi^2}{27} - \frac{16\,\zeta_3}{9}\Big)C_F T_R n_f\,,
\end{aligned} \tag{F.32}$$

while those for the gluon jet function are

$$\begin{aligned}
c^g_{J\,1} &= C_A\left(\frac{4}{3} - \pi^2\right) + \frac{5\beta_0}{3}\,,\\
c^g_{J\,2} &= C_A^2\left(\frac{4255}{108} - \frac{26\pi^2}{9} + \frac{151\pi^4}{180} - 72\zeta_3\right) - C_A\beta_0\left(\frac{115}{108} + \frac{65\pi^2}{18} - \frac{56\zeta_a}{3}\right)\\
&\quad - \beta_0^2\left(\frac{25}{9} - \frac{\pi^2}{3}\right) + \beta_1\left(\frac{55}{12} - 4\zeta_3\right)\,.
\end{aligned} \tag{F.33}$$

The solution for the RG evolved jet function can be obtained using the general convolution formula in Eq. (E.12) with the evolution kernel from Eq. (E.13). For the jet function evolution kernel one finds

$$U_J(t,\mu,\mu_0) = \frac{e^{\gamma_E\omega_J(\mu,\mu_0)}\,e^{K_J(\mu,\mu_0)}}{\Gamma[-\omega_J(\mu,\mu_0)]}\,\left[\frac{1}{\mu_0^2}\mathcal{L}^{-\omega_J(\mu,\mu_0)}\Big(\frac{t}{\mu_0^2}\Big) - \frac{1}{\omega_J(\mu,\mu_0)}\delta(t)\right]\,. \tag{F.34}$$

where

$$\omega_J(\mu,\mu_0) = 2\,\eta_\Gamma(\mu,\mu_0)\,, \qquad K_J(\mu,\mu_0) = K_{\gamma_J}(\mu,\mu_0) + 4\,K_\Gamma(\mu,\mu_0)\,, \tag{F.35}$$

and the expressions for $\eta_\Gamma(\mu,\mu_0)$, $K_J(\mu,\mu_0)$ and $K_{\gamma_J}(\mu,\mu_0)$ are given in Eq. (E.4) in general and in Eq. (E.8) up to NNLL.

F.3 b-quark Shape Function

F.3.1 Shape Function at Fixed Order

The shape function coefficients to one [33] and two loops [**?**] are

$$\begin{aligned}
S_{-1}(\alpha_s) &= 1 - \frac{\alpha_s}{\pi}\frac{\pi^2}{24}C_F - \frac{\alpha_s^2}{\pi^2}\bigg[\Big(\frac{\pi^2}{12}+\frac{3\pi^4}{640}-2\zeta_3\Big)C_F^2 + \Big(\frac{29}{108}+\frac{31\pi^2}{144}-\frac{67\pi^4}{2880}+\frac{9\zeta_3}{8}\Big)C_F C_A \\
&\quad + \Big(-\frac{1}{216}+\frac{5\pi^2}{576}-\frac{5\zeta_3}{48}\Big)C_F\beta_0\bigg], \\
S_0(\alpha_s) &= -\frac{\alpha_s}{\pi}C_F + \frac{\alpha_s^2}{\pi^2}\bigg[\Big(-\frac{7\pi^2}{24}+4\zeta_3\Big)C_F^2 \\
&\quad + \Big(\frac{11}{18}+\frac{\pi^2}{12}-\frac{9\zeta_3}{4}\Big)C_F C_A - \frac{1}{36}C_F\beta_0\bigg], \\
S_1(\alpha_s) &= -\frac{\alpha_s}{\pi}2C_F + \frac{\alpha_s^2}{\pi^2}\bigg[\Big(1-\frac{7\pi^2}{12}\Big)C_F^2 \\
&\quad + \Big(-\frac{2}{3}+\frac{\pi^2}{6}\Big)C_F C_A - \frac{1}{3}C_F\beta_0\bigg], \\
S_2(\alpha_s) &= \frac{\alpha_s^2}{\pi^2}\Big(3C_F^2 + \frac{1}{2}C_F\beta_0\Big), \\
S_3(\alpha_s) &= \frac{\alpha_s^2}{\pi^2}2C_F^2\,.
\end{aligned} \tag{F.36}$$

F.3.2 Shape Function RGE

F.4 Hemisphere Soft function

The hemisphere soft function depends on the total plus and minus component of the soft momentum in the two hemispheres, and its operator definition is given by

$$S_{\rm hemi}(\ell^+,\ell^-) \equiv \frac{1}{N_C}{\rm Tr}\left\langle 0\left|\overline{Y}_{\bar n}^T Y_n(0)\delta(\ell^+-(\hat P_a^+)^\dagger)\delta(\ell^- - \hat P_b^+))Y_n^\dagger(\overline{Y}_{\bar n}^\dagger)^T(0)\right|0\right\rangle . \tag{F.37}$$

The renormalized hemisphere soft function is related to the bare soft function by

$$S^{\rm bare}(\ell^+,\ell^-) = \int {\rm d}\ell'^+{\rm d}\ell'^- Z_S(\ell^+-\ell'^+,\ell^- - \ell'^-,\mu)\,S(\ell'^+,\ell'^-,\mu) \tag{F.38}$$

where as before the inverse of the Z factor is defined implicitly by

$$\delta(\ell^+)\delta(\ell^-) = \int {\rm d}\ell'^+{\rm d}\ell'^- [Z_S]^{-1}(\ell^+-\ell'^+,\ell^- - \ell'^-,\mu)\,Z_S(\ell'^+,\ell'^-,\mu) \tag{F.39}$$

The dependence of the renormalized soft function on μ is determined by the renormalization group equation

$$\mu\frac{\rm d}{{\rm d}\mu}S(\ell^+,\ell^-,\mu) = \int {\rm d}\ell'^+{\rm d}\ell'^- \gamma_S(\ell^+-\ell'^+,\ell^- - \ell'^-,\mu)\,S(\ell'^+,\ell'^-,\mu) \tag{F.40}$$

where the anomalous dimension is defined through the μ dependence of the Z factor

$$\gamma_S(\ell^+,\ell^-,\mu) = -\int {\rm d}\ell'^+{\rm d}\ell'^-\, Z_S^{-1}(\ell^+-\ell'^+,\ell^- - \ell'^-,\mu)\,\left[\mu\frac{\rm d}{{\rm d}\mu}Z_S(\ell'^+,\ell'^-,\mu)\right] \tag{F.41}$$

As explained in Sec. **??**, consistency between the jet and soft anomalous dimension requires that the soft anomalous dimension takes the form

$$\gamma_S(\ell^+,\ell^-,\mu) = \delta(\ell^+)\gamma_S(\ell^-,\mu) + \delta(\ell^-)\gamma_S(\ell^+,\mu) \tag{F.42}$$

This implies that the Z factor and the μ dependent part of the double differential hemisphere soft function factors into the product of two identical singly differential terms. Thus, one can write

$$Z_S(\ell^+,\ell^-,\mu) = Z_S(\ell^+,\mu)Z_S(\ell^-,\mu)\,, \qquad S(\ell^+,\ell^-,\mu) = S(\ell^+,\mu)S(\ell^-,\mu) + T(\ell^+,\ell^-) \tag{F.43}$$

The μ independent doubly differential term $T(\ell^+,\ell^-)$ contains the so-called non-global logarithms.

The general anomalous dimension can again be obtained from Eq. (E.9), using

$$j = 1\,, \qquad \rho_S = -2\,. \tag{F.44}$$

This gives

$$\gamma_S(\ell) = 2\Gamma_{\rm cusp}(\alpha_s)\frac{1}{\mu}\mathcal{L}_0\left(\frac{\ell}{\mu}\right) + \gamma_S(\alpha_s)\delta(\ell) \tag{F.45}$$

The renormalization factor $Z_S(\ell^+,\mu)$ and the renormalized function $S(\ell^+,\mu)$ can again be written as

$$S(\ell,\mu) = \sum_{k=-1}^{\infty} S_k(\alpha_s)\frac{1}{\mu}\mathcal{L}_k(\ell/\mu)\,, \qquad Z_S(\ell,\mu) = \sum_{k=-1}^{\infty} Z_{S,k}(\alpha_s)\frac{1}{\mu}\mathcal{L}_k(\ell/\mu)\,, \tag{F.46}$$

where to a given order in perturbation theory $\mathcal{O}(\alpha_s^l)$ the coefficients $S_k(\alpha_s)$ and $Z_{S,k}(\alpha_s)$ vanish for $k > 2l-1$. As always, the renormalization Z_S is completely determined through its relation to the anomalous dimension, and to two loop order the coefficients are given by

$$\begin{aligned}
Z^i_{S,-1} &= 1 + \frac{\alpha_s}{4\pi}\left[-\frac{\Gamma^i_{\rm cusp\,0}}{2\epsilon^2} + \frac{\gamma^i_{S0}}{2\epsilon}\right] + \left(\frac{\alpha_s}{4\pi}\right)^2\left[\frac{(\Gamma^i_{\rm cusp\,0})^2}{8\epsilon^4} - \frac{\Gamma^i_{\rm cusp\,0}\left(2\gamma^i_{S0}-3\beta_0\right)}{8\epsilon^3}\right.\\
&\qquad\left. + \frac{3\gamma^i_{S0}\left(\gamma^i_{S0}-2\beta_0\right) - 2\pi^2\left(\Gamma^i_{\rm cusp\,0}\right)^2 - 3\,\Gamma^i_{\rm cusp\,1}}{24\epsilon^2} + \frac{\gamma^i_{S1}}{4\epsilon}\right],\\
Z^i_{S,0} &= \frac{\alpha_s}{4\pi}\left[\frac{\Gamma^i_{\rm cusp\,0}}{\epsilon}\right] + \left(\frac{\alpha_s}{4\pi}\right)^2\left[-\frac{(\Gamma^i_{\rm cusp\,0})^2}{2\epsilon^3} - \frac{\Gamma^i_{\rm cusp\,0}\left(\beta_0-\gamma^i_{S0}\right)}{2\epsilon^2} + \frac{\Gamma^i_{\rm cusp\,1}}{2\epsilon}\right],\\
Z^i_{S,1} &= \left(\frac{\alpha_s}{4\pi}\right)^2\left[\frac{(\Gamma^i_{\rm cusp\,0})^2}{\epsilon^2}\right].
\end{aligned} \tag{F.47}$$

The coefficients $S_k(\alpha_s)$ for $k > -1$ are all related to the divergent structure and are again defined by the anomalous dimension. The only extra piece of information is the matching coefficient S_{-1}, which has be

be calculated order by order in perturbation theory. To second order in α_s one finds

$$
\begin{aligned}
S^i_{-1} &= 1 + \frac{\alpha_s}{4\pi} c^i_{S1} + \left(\frac{\alpha_s}{4\pi}\right)^2 c^i_{S2}\,, \\
S^i_0 &= \frac{\alpha_s}{4\pi}\left(-\gamma^i_{S0}\right) + \left(\frac{\alpha_s}{4\pi}\right)^2 \left[-c^i_{S1}\left(2\beta_0 + \gamma^i_{S0}\right) - \gamma^i_{S1} - \frac{\pi^2 \gamma^i_{S0}\Gamma^i_{\text{cusp}\,0}}{3} + 4\left(\Gamma^i_{\text{cusp}\,0}\right)^2 \zeta_3\right]\,, \\
S^i_1 &= \frac{\alpha_s}{4\pi}\left(-2\Gamma^i_{\text{cusp}\,0}\right) + \left(\frac{\alpha_s}{4\pi}\right)^2 \left[2\beta_0\gamma^i_{S0} + (\gamma^i_{S0})^2 - 2c^i_{S1}\Gamma^i_{\text{cusp}\,0} - \frac{2\pi^2(\Gamma^i_{\text{cusp}\,0})^2}{3} - 2\Gamma^i_{\text{cusp}\,1}\right]\,, \\
S^i_2 &= \left(\frac{\alpha_s}{4\pi}\right)^2 \left[2\beta_0\Gamma^i_{\text{cusp}\,0} + 3\gamma^i_{S0}\Gamma^i_{\text{cusp}\,0}\right]\,, \\
S^i_3 &= \left(\frac{\alpha_s}{4\pi}\right)^2 2(\Gamma^i_{\text{cusp}\,0})^2\,.
\end{aligned}
\tag{F.48}
$$

F.5 Beam Functions

The beam function is defined as

$$
B_i(t, x = \omega/P^-, \mu) \equiv \left\langle p_n(P^-)\left|\theta(\omega)\mathcal{O}_i(t,\omega,\mu)\right| p_n(P^-)\right\rangle \tag{F.49}
$$

The bare operators are defined as

$$
\begin{aligned}
\mathcal{O}^{\text{bare}}_q(t,\omega) &\equiv \bar\chi_n(0)\,\delta(t-\omega\hat p^+)\,\frac{\bar{n}\!\!\!/}{2}\,\left[\delta(\omega-\overline{\mathcal{P}}_n)\,\chi_n(0)\right] \\
\mathcal{O}^{\text{bare}}_{\bar q}(t,\omega) &\equiv \text{Tr}\,\frac{\bar{n}\!\!\!/}{2}\,\chi_n(0)\,\delta(t-\omega\hat p^+)\,\left[\delta(\omega-\overline{\mathcal{P}}_n)\,\bar\chi_n(0)\right] \\
\mathcal{O}^{\text{bare}}_q(t,\omega) &\equiv -\omega\,\mathcal{B}^c_{n\perp\mu}(0)\,\delta(t-\omega\hat p^+)\,\left[\delta(\omega-\overline{\mathcal{P}}_n)\,\mathcal{B}^{\mu c}_{n\perp}(0)\right]
\end{aligned}
\tag{F.50}
$$

The renormalized beam function $B_i(t,x,\mu)$, for $i = q$ or g, is related to the bare beam function through the definition

$$
B^{i,\text{bare}}(t,x) = \int \mathrm{d}t'\, Z^i_B(t-t',\mu)\, B^i(t',x,\mu)\,, \tag{F.51}
$$

and the inverse of the Z^i_B factor is defined such that

$$
\delta(t) = \int \mathrm{d}t'\,\left[Z^i_B\right]^{-1}(t-t',\mu)\, Z^i_B(t',\mu)\,. \tag{F.52}
$$

Since $B^{i,\text{bare}}$ is μ-independent, the dependence on μ is described by the renormalization group equation

$$
\mu\frac{\mathrm{d}}{\mathrm{d}\mu}B^i(t,x,\mu) = \int \mathrm{d}t'\,\gamma^i_B(t-t',\mu)\, B^i(t',x,\mu)\,, \tag{F.53}
$$

where

$$
\gamma^i_B(t,\mu) = -\int \mathrm{d}t'\,\left[Z^i_B\right]^{-1}(t-t',\mu)\,\left[\mu\frac{\mathrm{d}}{\mathrm{d}\mu}Z^i_B(t',\mu)\right]\,, \tag{F.54}
$$

The anomalous dimension of the beam function is identical to that of the jet function, and can therefore be obtained from the general result in Eq. (E.9) using

$$j = 2\,, \qquad \rho_B = 4 \tag{F.55}$$

Thus, to all orders in perturbation theory, the beam function anomalous dimension has the form

$$\gamma_B^i(s,\mu) = -2\Gamma^i_{\rm cusp}(\alpha_s)\,\frac{1}{\mu^2}\mathcal{L}_0\Big(\frac{s}{\mu^2}\Big) + \gamma_J^i(\alpha_s)\,\delta(s)\,, \tag{F.56}$$

Since the anomalous dimension is the same as that of the jet function, the renormalization constant of the beam function is also identical to that of the jet function

$$Z_B^i(t,\mu) = Z_J^i(t,\mu)\,, \tag{F.57}$$

where $Z_J^i(t,\mu)$ is given in Eqs. (F.27) and (F.28).

The renormalized beam function is best expressed through its OPE relating it to the PDFs

$$B_i(t,x,\mu) = \sum_j \int\frac{\mathrm{d}\xi}{\xi}\,\mathcal{I}^{ij}\Big(t,\frac{x}{\xi},\mu\Big) f_j(\xi,\mu)\Big[1+\mathcal{O}\Big(\frac{\Lambda^2_{\rm QCD}}{t}\Big)\Big]\,. \tag{F.58}$$

The matching coefficients $\mathcal{I}_{ij}(t,z,\mu)$ can be written to all orders in perturbation theory as

$$\mathcal{I}^{ij}\Big(t,z,\mu\Big) = \sum_{k=-1}^{\infty}\mathcal{I}_k^{ij}(z)(\alpha_s)\frac{1}{\mu^2}\mathcal{L}_k(t/\mu^2)\,, \tag{F.59}$$

One can write

$$\begin{aligned}
\mathcal{I}^{ij}_{-1}(z) &= \delta^{ij}\,\delta(1-z) + \frac{\alpha_s}{4\pi}c^{ij}_{I1} + \Big(\frac{\alpha_s}{4\pi}\Big)^2 c^{ij}_{I2}\\
\mathcal{I}^{ij}_{0}(z) &= \frac{\alpha_s}{4\pi}\left[-\frac{\gamma^i_{J0}\delta(1-z)-\gamma^{ij}(z)}{2}\right] + \Big(\frac{\alpha_s}{4\pi}\Big)^2\left[-c^{ij}_{I1}(z)\left(\beta_0+\frac{\gamma^i_{J0}}{2}\right) + \frac{(\hat c_{I1}\otimes\hat\gamma_0)^{ij}(z)}{2}\right.\\
&\quad\left.+\left(-\frac{\gamma^i_{J1}}{2}+\frac{\pi^2\gamma^i_{J0}\Gamma^i_{\rm cusp\,0}}{12}+\big(\Gamma^i_{\rm cusp\,0}\big)^2\zeta_3\right)\delta(1-z)+\frac{\gamma_1^{ij}(z)}{2}-\frac{\pi^2\gamma^i_{J0}(z)\Gamma^i_{\rm cusp\,0}}{12}\right]\\
\mathcal{I}^{ij}_{1}(z) &= \frac{\alpha_s}{4\pi}\left[\Gamma^i_{\rm cusp\,0}\,\delta(1-z)\right] + \Big(\frac{\alpha_s}{4\pi}\Big)^2\left[c^{ij}_{I1}(z)\,\Gamma^i_{\rm cusp\,0}+\left(\frac{\beta_0\gamma^i_{J0}}{2}+\frac{(\gamma^i_{J0})^2}{4}-\frac{\pi^2(\Gamma^i_{\rm cusp\,0})^2}{6}+\Gamma^i_{\rm cusp\,1}\right)\delta(1-z)\right.\\
&\quad\left.-\frac{\beta_0\gamma^{ij}_B(z)}{2}-\frac{\gamma^i_{J0}\,\gamma^{ij}_B(z)}{2}+\frac{(\hat\gamma_B\otimes\hat\gamma_B)^{ij}(z)}{4}\right]\\
\mathcal{I}^{ij}_{2}(z) &= \Big(\frac{\alpha_s}{4\pi}\Big)^2\left[-\Gamma^i_{\rm cusp\,0}\left(\frac{2\beta_0-3\gamma^i_{J0}}{4}\,\delta(1-z)+\frac{3\gamma^{ij}_B(z)}{4}\right)\right]\\
\mathcal{I}^{ij}_{3}(z) &= \Big(\frac{\alpha_s}{4\pi}\Big)^2\frac{(\Gamma^i_{\rm cusp\,0})^2}{2}\,\delta(1-z)
\end{aligned} \tag{F.60}$$

For the gluon beam function one finds

$$\begin{aligned}
&\mathcal{I}_{gg,-1}(z)\\
&\mathcal{I}_{gg,0}(z)\\
&\mathcal{I}_{gg,1}(z)\\
&\mathcal{I}_{gg,2}(z)\\
&\mathcal{I}_{gg,2}(z)
\end{aligned} \tag{F.61}$$

$$\begin{aligned}
&\mathcal{I}_{gq,-1}(z)\\
&\mathcal{I}_{gq,0}(z)\\
&\mathcal{I}_{gq,1}(z)\\
&\mathcal{I}_{gq,2}(z)\\
&\mathcal{I}_{gq,2}(z)
\end{aligned} \tag{F.62}$$

$$\begin{aligned}
\mathcal{I}_{qq}(t,z,\mu) &= \delta(t)\,\delta(1-z) \\
&\quad + \frac{\alpha_s(\mu)C_F}{2\pi}\,\theta(z)\bigg\{\frac{2}{\mu^2}\mathcal{L}_1\Big(\frac{t}{\mu^2}\Big)\delta(1-z) + \frac{1}{\mu^2}\mathcal{L}_0\Big(\frac{t}{\mu^2}\Big)\Big[P_{qq}(z) - \frac{3}{2}\,\delta(1-z)\Big] \\
&\quad + \delta(t)\bigg[\mathcal{L}_1(1-z)(1+z^2) - \frac{\pi^2}{6}\,\delta(1-z) + \theta(1-z)\Big(1-z-\frac{1+z^2}{1-z}\ln z\Big)\bigg]\bigg\}, \\
\mathcal{I}_{qg}(t,z,\mu) &= \frac{\alpha_s(\mu)T_F}{2\pi}\,\theta(z)\bigg\{\frac{1}{\mu^2}\mathcal{L}_0\Big(\frac{t}{\mu^2}\Big)P_{qg}(z) + \delta(t)\bigg[P_{qg}(z)\Big(\ln\frac{1-z}{z} - 1\Big) + \theta(1-z)\bigg]\bigg\}.
\end{aligned} \tag{F.63}$$

We write the matching coefficients for the gluon beam function as

$$\begin{aligned}
\mathcal{I}_{gg}(t,z,\mu_B) &= \delta(t)\,\delta(1-z) + \frac{\alpha_s(\mu_B)}{4\pi}\,\mathcal{I}_{gg}^{(1)}(t,z,\mu_B) + \frac{\alpha_s^2(\mu_B)}{(4\pi)^2}\,\mathcal{I}_{gg}^{(2)}(t,z,\mu_B)\,, \\
\mathcal{I}_{gq}(t,z,\mu_B) &= \frac{\alpha_s(\mu_B)}{4\pi}\,\mathcal{I}_{gq}^{(1)}(t,z,\mu_B) + \frac{\alpha_s^2(\mu_B)}{(4\pi)^2}\,\mathcal{I}_{gq}^{(2)}(t,z,\mu_B)\,.
\end{aligned} \tag{F.64}$$

The one-loop coefficients are given by

$$\begin{aligned}
\mathcal{I}_{gg}^{(1)}(t,z,\mu_B) &= 2C_A\,\theta(z)\bigg\{\frac{2}{\mu_B^2}\mathcal{L}_1\Big(\frac{t}{\mu_B^2}\Big)\delta(1-z) + \frac{1}{\mu_B^2}\mathcal{L}_0\Big(\frac{t}{\mu_B^2}\Big)P_{gg}(z) + \delta(t)\,\mathcal{I}_{gg}^{(1,\delta)}(z)\bigg\}, \\
\mathcal{I}_{gq}^{(1)}(t,z,\mu_B) &= 2C_F\,\theta(z)\bigg\{\frac{1}{\mu_B^2}\mathcal{L}_0\Big(\frac{t}{\mu_B^2}\Big)P_{gq}(z) + \delta(t)\,\mathcal{I}_{gq}^{(1,\delta)}(z)\bigg\},
\end{aligned} \tag{F.65}$$

where

$$\begin{aligned}
\mathcal{I}_{gg}^{(1,\delta)}(z) &= \mathcal{L}_1(1-z)\frac{2(1-z+z^2)^2}{z} - P_{gg}(z)\ln z - \frac{\pi^2}{6}\delta(1-z)\,, \\
\mathcal{I}_{gq}^{(1,\delta)}(z) &= P_{gq}(z)\ln\frac{1-z}{z} + \theta(1-z)z\,.
\end{aligned} \tag{F.66}$$

Here $P_{gg}(z)$ and $P_{gq}(z)$ are the $g \to gg$ and $q \to gq$ splitting functions given in Eq. (**??**), and the $\mathcal{L}_n(x)$ denote the standard plus distributions. At two loops we have

$$\begin{aligned}
\mathcal{I}_{gg}^{(2)}(t,z,\mu_B) &= \frac{1}{\mu_B^2}\mathcal{L}_3\Big(\frac{t}{\mu_B^2}\Big)8C_A^2\,\delta(1-z) + \frac{1}{\mu_B^2}\mathcal{L}_2\Big(\frac{t}{\mu_B^2}\Big)\big[12C_A^2 P_{gg}(z) - 2C_A\beta_0\,\delta(1-z)\big] \\
&\quad + \frac{1}{\mu_B^2}\mathcal{L}_1\Big(\frac{t}{\mu_B^2}\Big)\bigg\{4C_A^2\Big[\Big(\frac{4}{3}-\pi^2\Big)\delta(1-z) + 2\mathcal{I}_{gg}^{(1,\delta)}(z) + (P_{gg}\otimes P_{gg})(z)\Big] \\
&\quad\quad + 2C_A\beta_0\Big[\frac{10}{3}\delta(1-z) - P_{gg}(z)\Big] + 8C_F T_F n_f (P_{gq}\otimes P_{qg})(z)\bigg\} \\
&\quad + \frac{1}{\mu_B^2}\mathcal{L}_0\Big(\frac{t}{\mu_B^2}\Big)\bigg\{4C_A^2\Big[\Big(-\frac{7}{9}+8\zeta_3\Big)\delta(1-z) - \frac{\pi^2}{3}P_{gg}(z) + (\mathcal{I}_{gg}^{(1,\delta)}\otimes P_{gg})(z)\Big] \\
&\quad\quad + C_A\beta_0\Big[\Big(-\frac{92}{9}+\frac{\pi^2}{3}\Big)\delta(1-z) - 2\mathcal{I}_{gg}^{(1,\delta)}(z)\Big] \\
&\quad\quad + C_F T_F n_f\big[4\delta(1-z) + 8(\mathcal{I}_{gq}^{(1,\delta)}\otimes P_{qg})(z)\big] + 4P_{gg}^{(1)}(z)\bigg\} + 4\delta(t)\,\mathcal{I}_{gg}^{(2,\delta)}(z)\,, \\
\mathcal{I}_{gq}^{(2)}(t,z,\mu_B) &= \frac{1}{\mu_B^2}\mathcal{L}_2\Big(\frac{t}{\mu_B^2}\Big)12C_A C_F P_{gq}(z) + \frac{1}{\mu_B^2}\mathcal{L}_1\Big(\frac{t}{\mu_B^2}\Big)\bigg\{4C_F^2(P_{gq}\otimes P_{qq})(z) \\
&\quad\quad + 4C_A C_F\big[(P_{gg}\otimes P_{gq})(z) + 2\mathcal{I}_{gq}^{(1,\delta)}(z)\big] - 4C_F\beta_0 P_{gq}(z)\bigg\} \\
&\quad + \frac{1}{\mu_B^2}\mathcal{L}_0\Big(\frac{t}{\mu_B^2}\Big)\bigg\{4C_A C_F\Big[-\frac{\pi^2}{3}P_{gq}(z) + (\mathcal{I}_{gg}^{(1,\delta)}\otimes P_{gq})(z)\Big] \\
&\quad\quad + 4C_F^2(\mathcal{I}_{gq}^{(1,\delta)}\otimes P_{qq})(z) - 4C_F\beta_0\mathcal{I}_{gq}^{(1,\delta)}(z) + 4P_{gq}^{(2)}(z)\bigg\} + 4\delta(t)\,\mathcal{I}_{gq}^{(2,\delta)}(z)\,.
\end{aligned} \tag{F.67}$$

The beam function RGE is [see Eqs. (**??**) and (**??**)]

$$\begin{aligned}
\mu\frac{\mathrm{d}}{\mathrm{d}\mu}B_i(t,x,\mu) &= \int \mathrm{d}t'\,\gamma_B^i(t-t',\mu)\,B_i(t',x,\mu)\,, \\
\gamma_B^i(t,\mu) &= -2\Gamma^i_{\mathrm{cusp}}(\alpha_s)\,\frac{1}{\mu^2}\mathcal{L}_0\Big(\frac{t}{\mu^2}\Big) + \gamma_B^i(\alpha_s)\,\delta(t)\,,
\end{aligned} \tag{F.68}$$

and its solution is [**?**, 34, 35, 22] [see Eq. (**??**)]

$$\begin{aligned}
B_i(t,x,\mu) &= \int \mathrm{d}t'\,B_i(t-t',x,\mu_0)\,U_B^i(t',\mu_0,\mu)\,, \\
U_B^i(t,\mu_0,\mu) &= \frac{e^{K_B^i-\gamma_E\,\eta_B^i}}{\Gamma(1+\eta_B^i)}\left[\frac{\eta_B^i}{\mu_0^2}\mathcal{L}^{\eta_B^i}\Big(\frac{t}{\mu_0^2}\Big) + \delta(t)\right], \\
K_B^i(\mu_0,\mu) &= 4K_\Gamma^i(\mu_0,\mu) + K_{\gamma_B^i}(\mu_0,\mu)\,, \qquad \eta_B^i(\mu_0,\mu) = -2\eta_\Gamma^i(\mu_0,\mu)\,.
\end{aligned} \tag{F.69}$$

As we showed in Sec. **??**, the anomalous dimension for the beam function equals that of the jet function, $\gamma_B^q = \gamma_J^q$, so the three-loop result for γ_f^q together with Eq. (F.13) yields the non-cusp three-loop anomalous

dimension for the beam function,

$$\begin{aligned}
\gamma^q_{B\,0} &= 6C_F\,,\\
\gamma^q_{B\,1} &= C_F\Big[\Big(\frac{146}{9} - 80\zeta_3\Big)C_A + (3 - 4\pi^2 + 48\zeta_3)C_F + \Big(\frac{121}{9} + \frac{2\pi^2}{3}\Big)\beta_0\Big]\,,\\
\gamma^q_{B\,2} &= 2C_F\Big[\Big(\frac{52019}{162} - \frac{841\pi^2}{81} - \frac{82\pi^4}{27} - \frac{2056\zeta_3}{9} + \frac{88\pi^2\zeta_3}{9} + 232\zeta_5\Big)C_A^2\\
&\quad + \Big(\frac{151}{4} - \frac{205\pi^2}{9} - \frac{247\pi^4}{135} + \frac{844\zeta_3}{3} + \frac{8\pi^2\zeta_3}{3} + 120\zeta_5\Big)C_A C_F\\
&\quad + \Big(\frac{29}{2} + 3\pi^2 + \frac{8\pi^4}{5} + 68\zeta_3 - \frac{16\pi^2\zeta_3}{3} - 240\zeta_5\Big)C_F^2\\
&\quad + \Big(-\frac{7739}{54} + \frac{325}{81}\pi^2 + \frac{617\pi^4}{270} - \frac{1276\zeta_3}{9}\Big)C_A\beta_0\\
&\quad + \Big(-\frac{3457}{324} + \frac{5\pi^2}{9} + \frac{16\zeta_3}{3}\Big)\beta_0^2 + \Big(\frac{1166}{27} - \frac{8\pi^2}{9} - \frac{41\pi^4}{135} + \frac{52\zeta_3}{9}\Big)\beta_1\Big]\,.
\end{aligned} \tag{F.70}$$

The non-cusp anomalous dimension for the gluon beam function is equal to that of the gluon jet function which is given by $\gamma^g_J(\alpha_s) = -2\gamma^g_H(\alpha_s) - \gamma^g_f(\alpha_s)$. Here, $\gamma^g_f(\alpha_s)$ is the coefficient of the $\delta(1-z)$ in the gluon PDF anomalous dimension which is known to three loops [**?**]. The resulting coefficients to three loops are

$$\begin{aligned}
\gamma^g_{B\,0} &= 2\beta_0\,,\\
\gamma^g_{B\,1} &= \Big(\frac{182}{9} - 32\zeta_3\Big)C_A^2 + \Big(\frac{94}{9} - \frac{2\pi^2}{3}\Big)C_A\,\beta_0 + 2\beta_1\,,\\
\gamma^g_{B\,2} &= \Big(\frac{49373}{81} - \frac{944\pi^2}{81} - \frac{16\pi^4}{5} - \frac{4520\zeta_3}{9} + \frac{128\pi^2\zeta_3}{9} + 224\zeta_5\Big)C_A^3\\
&\quad + \Big(-\frac{6173}{27} - \frac{376\pi^2}{81} + \frac{13\pi^4}{5} + \frac{280\zeta_3}{9}\Big)C_A^2\,\beta_0 + \Big(-\frac{986}{81} - \frac{10\pi^2}{9} + \frac{56\zeta_3}{3}\Big)C_A\,\beta_0^2\\
&\quad + \Big(\frac{1765}{27} - \frac{2\pi^2}{3} - \frac{8\pi^4}{45} - \frac{304\zeta_3}{9}\Big)C_A\,\beta_1 + 2\beta_2\,.
\end{aligned} \tag{F.71}$$

At NNLL we only need γ^g_H and γ^g_B at two loops. The three-loop coefficients are given for completeness. The result in Eq. (F.71) agrees with that given in ref. [36] for the gluon jet function.[9] The non-cusp anomalous dimension of the gluon beam-thrust soft function is given by $\gamma^g_S(\alpha_s) = -2\gamma^g_H(\alpha_s) - 2\gamma^g_B(\alpha_s)$.

F.6 Parton Distribution Function

The quark and gluon splitting functions are

$$\begin{aligned}
P_{gg}(z) &= 2\mathcal{L}_0(1-z)z + 2\theta(1-z)\Big[\frac{1-z}{z} + z(1-z)\Big]\,,\\
P_{gq}(z) &= \theta(1-z)\,\frac{1+(1-z)^2}{z}\,,\\
P_{qq}(z) &= \mathcal{L}_0(1-z)(1+z^2) + \frac{3}{2}\,\delta(1-z)\,,\\
P_{qg}(z) &= \theta(1-z)\big[(1-z)^2 + z^2\big]\,.
\end{aligned} \tag{F.72}$$

[9] Apart from a typo in ref. [36] where one of the terms in the $C_A^2 n_f$ contribution is missing a π^2.

The two-loop splitting functions were calculated in refs. [**?**, **?**] and are given by [**?**]

$$
\begin{aligned}
P_{gg}^{(1)}(z) = C_A^2\Big\{&\frac{1}{3}(4-\pi^2)\mathcal{L}_0(1-z) + (-1+3\zeta_3)\delta(1-z) + \frac{-253+294z-318z^2+253z^3}{18z} \\
&+ \frac{-1+2z-z^2+z^3}{3z}\pi^2 - \frac{4}{3}(9+11z^2)\ln z + \frac{2(1+z-z^2)^2}{1-z^2}\ln^2 z \\
&- 2P_{gg}(z)\ln z\ln(1-z) - 2P_{gg}(-z)\Big[\ln z\ln(1+z) + \mathrm{Li}_2(-z) + \frac{\pi^2}{12}\Big]\Big\} \\
&+ C_A\beta_0\Big[\frac{5}{3}\mathcal{L}_0(1-z) + \delta(1-z) + \frac{23-29z+19z^2-23z^3}{6z} + (1+z)\ln z\Big] \\
&+ C_F T_F n_f\Big[-\delta(1-z) + \frac{4(1-12z+6z^2+5z^3)}{3z} - 2(1+z)\ln^2 z - 2(3+5z)\ln z\Big], \\
P_{gq}^{(1)}(z) = C_A C_F\Big\{&\frac{-101+129z-51z^2+44z^3}{9z} - \frac{1}{3}(36+15z+8z^2)\ln z + 2z\ln(1-z) \\
&+ (2+z)\ln^2 z - P_{gq}(z)\Big[2\ln z\ln(1-z) - \ln^2(1-z) + \frac{\pi^2}{6}\Big] \\
&- 2P_{gq}(-z)\Big[\ln z\ln(1+z) + \mathrm{Li}_2(-z) + \frac{\pi^2}{12}\Big]\Big\} \\
&+ C_F^2\Big[-\frac{1}{2}(5+7z) + \frac{1}{2}(4+7z)\ln z + \frac{-6+6z-5z^2}{z}\ln(1-z) - \frac{1}{2}(2-z)\ln^2 z \\
&- P_{gq}(z)\ln^2(1-z)\Big] + C_F\beta_0\Big[\frac{2(5-5z+4z^2)}{3z} + P_{gq}(z)\ln(1-z)\Big]. \qquad \text{(F.73)}
\end{aligned}
$$

The convolution of two splitting functions is defined as (the index j is not summed over)

$$
(P_{ij}\otimes P_{jk})(z) = \int_z^1 \frac{\mathrm{d}w}{w}\, P_{ij}(w)P_{jk}\Big(\frac{z}{w}\Big), \qquad \text{(F.74)}
$$

and analogously for the convolution $(\mathcal{I}_{ij}^{(1,\delta)} \otimes P_{jk})$. The necessary convolutions are

$$
\begin{aligned}
(P_{gq} \otimes P_{qg})(z) &= \frac{4+3z-3z^2-4z^3}{3z} + 2(1+z)\ln z\,, \qquad \text{(F.75)}\\
(P_{gq} \otimes P_{qq})(z) &= 2 - \frac{z}{2} + (2-z)\ln z + \frac{2(2-2z+z^2)}{z}\ln(1-z)\,,\\
(P_{gg} \otimes P_{gq})(z) &= \frac{-31+24z+3z^2+4z^3}{3z} - \frac{4(1+z+z^2)}{z}\ln z + \frac{2(2-2z+z^2)}{z}\ln(1-z)\,,\\
(P_{gg} \otimes P_{gg})(z) &= 8\mathcal{L}_1(1-z) - \frac{2\pi^2}{3}\delta(1-z) + \frac{4(-11+9z-9z^2+11z^3)}{3z}\\
&\quad + \frac{4(-1-3z^2+4z^3-z^4)}{z(1-z)}\ln z + \frac{8(1-2z+z^2-z^3)}{z}\ln(1-z)\,,\\
(\mathcal{I}_{gq}^{(1,\delta)} \otimes P_{qg})(z) &= \frac{-13+12z+6z^2-5z^3}{9z} + \pi^2\frac{1+z}{3} + \frac{-4+9z^2+4z^3}{3z}\ln z\\
&\quad + \frac{4+3z-3z^2-4z^3}{3z}\ln(1-z) - (1+z)\ln^2 z - 2(1+z)\mathrm{Li}_2(z)\,,\\
(\mathcal{I}_{gq}^{(1,\delta)} \otimes P_{qq})(z) &= \frac{5-4z+2z^2}{2z} + \pi^2\frac{-4+6z-3z^2}{6z} + \frac{-2-z}{2}\ln z + \frac{4+3z}{2}\ln(1-z)\\
&\quad + \frac{z-2}{2}\ln^2 z + \frac{2(2-2z+z^2)}{z}\ln(1-z)[\ln(1-z)-\ln z] + (z-2)\mathrm{Li}_2(z)\,,\\
(\mathcal{I}_{gg}^{(1,\delta)} \otimes P_{gq})(z) &= \frac{21-26z+5z^2}{6z} + \pi^2\frac{-2-6z-3z^2}{6z} + \frac{9-30z-9z^2-4z^3}{3z}\ln z\\
&\quad + \frac{-31+24z+3z^2+4z^3}{3z}\ln(1-z) + \frac{2(1+z+z^2)}{z}\ln^2 z\\
&\quad + \frac{2-2z+z^2}{z}\ln(1-z)[\ln(1-z)-2\ln z] + (8+2z)\mathrm{Li}_2(z)\,,\\
(\mathcal{I}_{gg}^{(1,\delta)} \otimes P_{gg})(z) &= 6\mathcal{L}_2(1-z) - \pi^2\mathcal{L}_0(1-z) + 4\zeta_3\delta(1-z) + \frac{(1-z)(67-2z+67z^2)}{9z}\\
&\quad + \pi^2\frac{-3+2z-7z^2+3z^3}{3z} + \frac{2(11-21z+6z^2-22z^3)}{3z}\ln z\\
&\quad + \frac{4(-11+9z-9z^2+11z^3)}{3z}\ln(1-z) + \frac{2(1+3z^2-4z^3+z^4)}{z(1-z)}\ln^2 z\\
&\quad + \frac{8(-1+2z-3z^2+2z^3-z^4)}{z(1-z)}\ln z\ln(1-z)\\
&\quad + \frac{6(1-2z+z^2-z^3)}{z}\ln^2(1-z) + 8(1+z)\mathrm{Li}_2(z)\,.
\end{aligned}
$$

F.7 Convolution of Soft and Jet Functions

To convolute $\mathcal{L}_n[p^-(\omega-\omega')/\mu_J^2]$ with $\mathcal{L}_m(\omega/\mu_s)$ we first rescale them to have the same dimensionless arguments. Using Eq. (C.34), J and $\bar{S}$ satisfy the rescaling identities (**TODO**)

TODO: what notation for perturbative part of S? $\bar{S}$?

$$
\begin{aligned}
J(p^-\omega,\mu) &= \frac{1}{p^-\xi}\sum_{n=-1}^{\infty} J_n\Big[\alpha_s(\mu), \frac{p^-\xi}{\mu^2}\Big]\,\mathcal{L}_n\Big(\frac{\omega}{\xi}\Big)\,,\\
\bar{S}(\omega,\mu) &= \frac{1}{\xi}\sum_{n=-1}^{\infty} S_n\Big[\alpha_s(\mu), \frac{\xi}{\mu}\Big]\,\mathcal{L}_n\Big(\frac{\omega}{\xi}\Big)\,. \qquad \text{(F.76)}
\end{aligned}
$$

where ξ is an arbitrary dimension-one parameter that we will choose at our convenience later on, and the rescaled coefficients are

$$\begin{aligned}
J_{-1}(\alpha_s, x) &= J_{-1}(\alpha_s) + \sum_{n=0}^{\infty} J_n(\alpha_s)\, \frac{\ln^{n+1} x}{n+1}\,, \\
J_n(\alpha_s, x) &= \sum_{k=0}^{\infty} \frac{(n+k)!}{n!\,k!}\, J_{n+k}(\alpha_s)\, \ln^k x\,, \\
S_{-1}(\alpha_s, x) &= S_{-1}(\alpha_s) + \sum_{n=0}^{\infty} S_n(\alpha_s)\, \frac{\ln^{n+1} x}{n+1}\,, \\
S_n(\alpha_s, x) &= \sum_{k=0}^{\infty} \frac{(n+k)!}{n!\,k!}\, S_{n+k}(\alpha_s)\, \ln^k x\,.
\end{aligned} \tag{F.77}$$

Using Eq. (F.76), the convolution of J and $\bar{S}$ becomes

$$\begin{aligned}
(J \otimes S)(\omega, \mu_i, \mu_\Lambda) &\equiv \int \mathrm{d}\omega'\, p^- J[p^-(\omega - \omega'), \mu_i]\, \bar{S}(\omega', \mu_\Lambda) \\
&= \sum_{m,n=-1}^{\infty} J_m\Big[\alpha_s(\mu_i), \frac{p^-\xi}{\mu_i^2}\Big]\, S_n\Big[\alpha_s(\mu_\Lambda), \frac{\xi}{\mu_\Lambda}\Big]\, \frac{1}{\xi} \int \mathrm{d}x\, \mathcal{L}_m\Big(\frac{\omega}{\xi} - x\Big)\, \mathcal{L}_n(x) \\
&= \sum_{\ell=-1}^{\infty} \sum_{\substack{m,n\geq -1 \\ m+n+1\geq \ell}}^{\infty} V_\ell^{mn} J_m\Big[\alpha_s(\mu_i), \frac{p^-\xi}{\mu_i^2}\Big]\, S_n\Big[\alpha_s(\mu_\Lambda), \frac{\xi}{\mu_\Lambda}\Big]\, \frac{1}{\xi}\, \mathcal{L}_\ell\Big(\frac{\omega}{\xi}\Big)\,.
\end{aligned} \tag{F.78}$$

In the last step we used Eq. (C.37) to perform the x integral, yielding a sum of plus distributions, whose coefficients V_ℓ^{mn} are given in Eq. (C.38).

G More on the Zero-Bin [Remove?]

G.1 0-bin subtractions with a 0-bin field Redefinition

G.2 0-bin subtractions for phase space integrations

H Spinor Relations with a different representation

For a collinear momentum $p^\mu = (p^0, p^1, p^2, p^3)$ we have $p^- = p^0 + p^3 \gg p_\perp^{1,2} \gg p^+ = p^0 - p^3$ so

$$\frac{\vec{\sigma}\cdot\vec{p}}{p^0} = \sigma_3 + \dots\,, \tag{H.1}$$

where the terms in the $+\dots$ are smaller. Keeping only the leading term gives us the spinors

$$\begin{aligned} u(p) &= \frac{(2p^0)^{1/2}}{\sqrt{2}}\begin{pmatrix} \mathcal{U} \\ \frac{\vec{\sigma}\cdot\vec{p}}{p^0}\mathcal{U}\end{pmatrix} \quad\Longrightarrow\quad u_n = \sqrt{\frac{p^-}{2}}\begin{pmatrix}\mathcal{U}\\ \sigma^3\mathcal{U}\end{pmatrix} \\ v(p) &= \frac{(2p^0)^{1/2}}{\sqrt{2}}\begin{pmatrix} \frac{\vec{\sigma}\cdot\vec{p}}{p^0}\mathcal{V} \\ \mathcal{V}\end{pmatrix} \quad\Longrightarrow\quad v_n = \sqrt{\frac{p^-}{2}}\begin{pmatrix}\sigma^3\mathcal{V}\\ \mathcal{V}\end{pmatrix} \end{aligned} \tag{H.2}$$

where here $\mathcal{U}$ and $\mathcal{V}$ are each either $\begin{pmatrix}1\\0\end{pmatrix}$ or $\begin{pmatrix}0\\1\end{pmatrix}$. From this analysis we see that in the collinear limit both quark and antiquarks remain as relevant degrees of freedom (and indeed, there is no suppression for pair creation from splitting). We also see that both spin components remain in each of the spinors.
Having defined $\hat{\xi}_n = P_n\psi$, the corresponding result for the spinors is $u_n = P_n u(p)$ and $v_n = P_n v(p)$, which do not precisely reproduce the lowest order expanded results in Eq. (H.2). Instead we find

$$\begin{aligned} u_n &= \frac{1}{2}\begin{pmatrix}\mathbb{1} & \sigma_3\\ \sigma_3 & \mathbb{1}\end{pmatrix}\sqrt{p^0}\begin{pmatrix}\mathcal{U}\\ \frac{\vec{\sigma}\cdot\vec{p}}{p_0}\mathcal{U}\end{pmatrix} = \frac{\sqrt{p^0}}{2}\begin{pmatrix}\left(1+\frac{p_3}{p_0}-\frac{(i\vec{\sigma}\times\vec{p}_\perp)_3}{p^0}\right)\mathcal{U}\\ \sigma_3\left(1+\frac{p_3}{p_0}-\frac{(i\vec{\sigma}\times\vec{p}_\perp)_3}{p^0}\right)\mathcal{U}\end{pmatrix} \\ &= \sqrt{\frac{p^-}{2}}\begin{pmatrix}\tilde{\mathcal{U}}\\ \sigma_3\tilde{\mathcal{U}}\end{pmatrix} \end{aligned} \tag{H.3}$$

where the two component spinor is

$$\tilde{\mathcal{U}} = \sqrt{\frac{p^0}{2p^-}}\left(1+\frac{p_3}{p_0}-\frac{(i\vec{\sigma}\times\vec{p}_\perp)_3}{p^0}\right)\mathcal{U}\,. \tag{H.4}$$

The same derivation gives

$$v_n = \sqrt{\frac{p^-}{2}}\begin{pmatrix}\sigma_3\tilde{\mathcal{V}}\\ \tilde{\mathcal{V}}\end{pmatrix} \tag{H.5}$$

where $\tilde{\mathcal{V}}$ is defined in terms of $\mathcal{V}$ by a formula analogous to Eq. (H.4). Since the spin relations in Eqs. (3.11) and (3.10) do not depend on the form of the two component spinors ($\tilde{\mathcal{U}}$ versus $\mathcal{U}$ etc), they remain true. We will see later that the results for the u_n and v_n spinors involving $\tilde{\mathcal{U}}$ and $\tilde{\mathcal{V}}$ rather than $\mathcal{U}$ and $\mathcal{V}$ are required to avoid breaking a reparameterization symmetry in SCET. The extra terms appearing in the definition of $\tilde{\mathcal{U}}$ ensure the proper structure under reparameterizations of the lightcone basis. Finally we note that

$$\sum_s \tilde{\mathcal{U}}^s\tilde{\mathcal{U}}^{\dagger\,s} = \mathbb{1}_{2\times2}\,. \tag{H.6}$$

Thus if we take the product of u_n spinors

$$u_n\bar{u}_n = \frac{p^-}{2}\begin{pmatrix}\tilde{\mathcal{U}}\tilde{\mathcal{U}}^\dagger & -\tilde{\mathcal{U}}\tilde{\mathcal{U}}^\dagger\sigma_3\\ \sigma_3\tilde{\mathcal{U}}\tilde{\mathcal{U}}^\dagger & -\sigma_3\tilde{\mathcal{U}}\tilde{\mathcal{U}}^\dagger\sigma_3\end{pmatrix}, \tag{H.7}$$

References

[1] C. W. Bauer, S. Fleming, and M. E. Luke, Phys. Rev. D **63**, 014006 (2001), [hep-ph/0005275].

[2] C. W. Bauer, S. Fleming, D. Pirjol, and I. W. Stewart, Phys. Rev. D **63**, 114020 (2001), [hep-ph/0011336].

[3] C. W. Bauer, D. Pirjol, and I. W. Stewart, Phys. Rev. **D66**, 054005 (2002), [hep-ph/0205289].

[4] C. W. Bauer and I. W. Stewart, Phys. Lett. B **516**, 134 (2001), [hep-ph/0107001].

[5] A. V. Manohar and I. W. Stewart, Phys. Rev. **D76**, 074002 (2007), [hep-ph/0605001].

[6] C. W. Bauer, D. Pirjol, and I. W. Stewart, Phys. Rev. D **65**, 054022 (2002), [hep-ph/0109045].

[7] A. V. Manohar, T. Mehen, D. Pirjol, and I. W. Stewart, Phys. Lett. **B539**, 59 (2002), [hep-ph/0204229].

[8] C. W. Bauer, S. Fleming, D. Pirjol, I. Z. Rothstein, and I. W. Stewart, Phys. Rev. D **66**, 014017 (2002), [hep-ph/0202088].

[9] I. W. Stewart, F. J. Tackmann, and W. J. Waalewijn, JHEP **1009**, 005 (2010), [1002.2213].

[10] C. W. Bauer, D. Pirjol, and I. W. Stewart, Phys. Rev. **D68**, 034021 (2003), [hep-ph/0303156].

[11] J.-Y. Chiu, A. Jain, D. Neill, and I. Z. Rothstein, JHEP **1205**, 084 (2012), [1202.0814].

[12] M. Beneke, A. P. Chapovsky, M. Diehl, and T. Feldmann, Nucl. Phys. **B643**, 431 (2002), [hep-ph/0206152].

[13] C. W. Bauer, D. Pirjol, and I. W. Stewart, Phys. Rev. D **67**, 071502 (2003), [hep-ph/0211069].

[14] L. J. Dixon, hep-ph/9601359.

[15] C. Marcantonini and I. W. Stewart, Phys.Rev. **D79**, 065028 (2009), [0809.1093].

[16] I. Moult, I. W. Stewart, F. J. Tackmann, and W. J. Waalewijn, 1508.02397.

[17] J. Chay and C. Kim, Phys. Rev. **D65**, 114016 (2002), [hep-ph/0201197].

[18] C. W. Bauer, D. Pirjol, and I. W. Stewart, Phys.Rev. **D68**, 034021 (2003), [hep-ph/0303156].

[19] D. Pirjol and I. W. Stewart, Phys. Rev. **D67**, 094005 (2003), [hep-ph/0211251].

[20] C. W. Bauer, S. P. Fleming, C. Lee, and G. F. Sterman, Phys.Rev. **D78**, 034027 (2008), [0801.4569].

[21] S. Fleming, A. H. Hoang, S. Mantry, and I. W. Stewart, Phys.Rev. **D77**, 074010 (2008), [hep-ph/0703207].

[22] Z. Ligeti, I. W. Stewart, and F. J. Tackmann, Phys. Rev. **D78**, 114014 (2008), [0807.1926].

[23] S. A. Larin and J. A. M. Vermaseren, Phys. Lett. **B303**, 334 (1993), [hep-ph/9302208].

[24] A. V. Manohar, Phys. Rev. **D68**, 114019 (2003), [hep-ph/0309176].

[25] C. W. Bauer, C. Lee, A. V. Manohar, and M. B. Wise, Phys. Rev. **D70**, 034014 (2004), [hep-ph/0309278].

[26] A. Idilbi, X.-d. Ji, and F. Yuan, Nucl. Phys. **B753**, 42 (2006), [hep-ph/0605068].

[27] T. Becher, M. Neubert, and B. D. Pecjak, JHEP **0701**, 076 (2007), [hep-ph/0607228].

[28] S. Moch, J. A. M. Vermaseren, and A. Vogt, JHEP **08**, 049 (2005), [hep-ph/0507039].

[29] A. Idilbi, X.-d. Ji, J.-P. Ma, and F. Yuan, Phys.Rev. **D73**, 077501 (2006), [hep-ph/0509294].

[30] G. Sterman, Nucl. Phys. B **281**, 310 (1987).

[31] V. Ahrens, T. Becher, M. Neubert, and L. L. Yang, Phys. Rev. D **79**, 033013 (2009), [0808.3008].

[32] V. Ahrens, T. Becher, M. Neubert, and L. L. Yang, Eur. Phys. J. C **62**, 333 (2009), [0809.4283].

[33] C. W. Bauer and A. V. Manohar, Phys. Rev. **D70**, 034024 (2004), [hep-ph/0312109].

[34] M. Neubert, hep-ph/0408179.

[35] S. Fleming, A. H. Hoang, S. Mantry, and I. W. Stewart, Phys.Rev. **D77**, 114003 (2008), [0711.2079].

[36] T. Becher and M. D. Schwartz, JHEP **1002**, 040 (2010), [0911.0681].